UNIVERSITY OF SOUTHERN QUEENSLAND

INCORPORATING SPATIAL VARIABILITY IN SOIL AND CROP PROPERTIES FOR EFFECTIVE IRRIGATION

A Dissertation Submitted by

Jyotiprakash Padhi
B.Tech., M.Tech.

for the award of

Doctor of Philosophy

2009

This thesis is dedicated to my parents.

ABSTRACT

Soil water content varies spatially and temporally on landscapes due to various processes including water loss by evapotranspiration (ET). When rainfall is not sufficient to meet water demand caused by ET losses from crop fields, irrigation becomes necessary to maintain sustainable crop productivity. More efficient use of water from rainfall and irrigation is required at the field scale through improved irrigation scheduling to improve our understanding of crop response to water deficit stress.

Most of the previous research in spatially variable crop production has focussed on variable rate fertilizer and chemical application. The research reported here is aimed at extending precision farming concepts to precision water management to ensure water is applied in the right place, in the right amount, and at the right time, to optimise production and efficiency. In order to determine the feasibility and applicability of precision water management, experiments were undertaken to:

1. test and evaluate the performance of a load-cell-based mini-lysimeter inside a glasshouse to determine evapotranspiration losses with high precision;
2. test the prospects of thermal sensing of crop plants with a thermal infrared camera (infrared thermography) to identify the relationship between canopy temperature and soil water including the physiological basis of crop water deficit stress;
3. examine the spatial variability in soil water content with electrical conductivity measurements with EM38 (based on the electromagnetic induction technique).

Field and glass house experiments were conducted with cotton (*Gossypium hirsutum* L.) and wheat (*Triticum aestivum* L.) crops using a self-mulching, black vertosol soil. All experiments consisted of four irrigation treatments (either based on irrigation when soil water content was depleted to a known percent of plant available water capacity (PAWC) or field capacity (FC). All experiments used a randomized complete block design involving 3 to 5 replications of each irrigation treatment.

Irrigation treatments (T50, T60, T70 and T85) in the field were designed to allow soil water depletion to 50%, 60%, 70% and 85% of the PAWC in the soil for both wheat and cotton crop. Irrigation treatments used for the glasshouse experiment included: T80 – 80% of FC, T70 – 70% of FC, T50 – 50% of FC and T40 – 40% of FC. Frequency of irrigation in all experiments varied over time to allow the soil water deficit to develop as required for the irrigation treatments. Two field (2007-08, 2008-09) and one glasshouse (2008) experiments were conducted for cotton, while one field (2008) and a glasshouse experiment (2009) was conducted for wheat.

Measurements in all experiments included essential weather data (rainfall, relative humidity, solar radiation, and maximum and minimum air temperature), volume of irrigation and drainage (for glasshouse experiments only), soil water content, yield and biomass of the crops. On selected occasions, thermal images were taken with an NEC TH7800 infrared camera before and/or after irrigation both in the field and glasshouse experiments. Canopy temperature was derived from processing of the thermal images. Leaf water potential was measured with a pressure chamber and stomatal conductance of leaves measured with a steady state porometer at the time of thermal imaging. All measurement positions in the field were recorded with a hand-held GPS. Images of wet (leaf covered with water on both sides of the leaf) and dry reference (leaf covered with petroleum jelly) leaves were taken for each irrigation treatment at the time of image acquisition of normal leaves. The temperatures of normal, wet and dry reference leaves were used in the calculation of crop water deficit indices such as ICWSI (Improved Crop Water Stress Index) and I_G (Index relating to stomatal conductance). For the field experiments, apparent electrical conductivity (EC_a) was measured on the same day as the other measurements with the EM38 equipment in both vertical and horizontal modes on the ground as well as 0.1 m and 0.4 m above the ground. Soil temperature within 0-25 cm depth was recorded with a resistance temperature detector (RTD) probe.

Results indicated the ability of thermal imaging to consistently distinguish water deficit in crops for the most frequently irrigated treatments (i.e. T50 in the field and T80 in the glasshouse) from the least frequently irrigated treatments (i.e. T85 treatment in the field and T40 in the glasshouse). Due to the strong dependency of canopy temperature on water relations of leaves (leaf water potential and stomatal conductance); it was possible to ascertain the extent of soil water availability within

the root zone of crops to maintain an optimum transpiration rate in leaves of the studied crops. The relationship between crop water deficit indices (i.e. ICWSI and I_G) and soil water within the root zone were also explored. Maps of spatial variations in canopy temperature for the entire field matched well with soil water maps. Due to the close correspondence between soil water deficit and canopy temperature, these maps are expected to be useful for precision irrigation. The trends between thermal data and other indicators (leaf water potential, stomatal conductance and soil water) suggest that thermography is a rapid and convenient approach to detect crop water deficit stress in the field, when soil water deficit may vary randomly due to existing variation in soil and/or landscape properties and water management.

Measurement of EC_a with EM38 equipment was also found to be useful in assessing spatial distribution of soil water content and water deficit stress in crop fields. Since EC_a is a complex function of several variables including temperature, absolute quantities of soil water can be predicted in crop fields with only moderate accuracy, however wet and dry areas within the field can be easily identified. It is clearly possible to incorporate information on spatial variability in soil water content/deficit in the field directly with EC_a maps and/or with thermal imagery (as a crop property affecting transpiration) to improve the effectiveness of irrigation by irrigating spatially variable fields at a high precision.

With the mini-lysimeter system described in this work, it is possible to measure ET losses from crops at a resolution of 0.027 mm with a time interval of approximately 10 min, which is ideal for studying spatial and temporal variability in growth and performance of irrigated crops.

An irrigation strategy is considered effective if it does not cause significant yield reduction while allowing highest possible water use efficiency to be maintained. Analysis of yield and ET data for cotton and wheat indicates that both crops should be irrigated when soil water content depletes to 60% of PAWC in the field or 70% of FC in the glasshouse. Since soil water content and its spatial distribution can be estimated in the field with thermal imagery or EM38 measurements, irrigation can be applied to maintain soil water content above these limits throughout the field.

CERTIFICATION OF DISSERTATION

I certify that the ideas, experimental work, results, analyses, software and conclusions reported in this dissertation are entirely my own effort, except where otherwise acknowledged. I also certify that the work is original and has not been previously submitted for any other award, except where otherwise acknowledged.

_____ _____

Jyotiprakash Padhi, Candidate Date

ENDORSEMENT:

_____ _____

Dr. Rabindra K. Misra, Principal Supervisor Date

_____ _____

Prof. Steven R. Raine, Associate Supervisor Date

ACKNOWLEDGEMENTS

Completion of this dissertation would not be possible without genuine support and help from a number of people to whom I wish to express my sincere gratitude.

I would like to express my sincere thanks to my principal supervisor Dr. Rabi Misra and associate supervisor Prof. Steven Raine for their invaluable guidance, patience and persistence in helping me complete this dissertation. Without their support it may not have been possible for me to complete this research project.

Without the financial support of the Cooperative Research Centre for Irrigation Futures (CRC IF) who offered me the Postgraduate Scholarship I would not have been able to undertake this study.

I would also like to thank Dr. Josè Payero and Graham Harris for allowing me to collect data from the experiments conducted at Department of Employment, Economic development and Innovation's research station and also for their valuable suggestions in my research. Thanks to Prof. Mark Sutherland for giving permission to conduct experiments inside the glasshouse and Dr. Joan Vickers for help with disease and pest control. I would also like to express my thanks to Bob Coy from the Faculty of Science with purchasing of equipment used in my experiments. I would also like to thank the staff of National Centre for Engineering in Agriculture (NCEA) for their support during my research. Sincere thanks are due to the Engineering technical staff Chris Galligan, Brian Aston, Glen Bartkowski, Mohan Trada, Daniel Eising, Adrian Blokland and Nishant Pradhan for their kind support while I was conducting experiments for this project. This research was also supported by the Queensland Government's "Growing the Smart State PhD funding program".

My thanks go to all the staff and research students of the Faculty of Engineering & Surveying and staff of the Office of Research of Higher Degrees who helped me in various ways during my stay at the University of Southern Queensland. I also can not forget my friends and their families, who are outside the university, for their kindness and support during my stay in Toowoomba.

I would like to thank my parents and sisters for their encouragement and support during my studies. Finally, my sincere thanks go to my wife Shubhasri and our son Swastik, for their love, patience and support throughout this study.

TABLE OF CONTENTS

LIST OF FIGURES

Chapter 2

Chapter 3

Chapter 4

Chapter 5

Chapter 6

Chapter 7

Appendix A1

LIST OF TABLES

Chapter 3

Chapter 4

Chapter 5

Chapter 6

Chapter 7

Appendix A1

NOTATIONS

C_p	=	Specific heat of air at constant pressure
$D_{i,i+1}$	=	Drainage
G	=	Soil heat flux
g_s	=	Stomatal conductance
H	=	Sensible heat flux
$I_{i,i+1}$	=	Irrigation
k	=	Stiffness constant of the load cell
L	=	Instantaneous latent heat of vaporization of water
LE	=	Instantaneous latent heat flux
q	=	Instantaneous specific humidity
R^2	=	Coefficient of determination
R_n	=	Net irradiance
$P_{i,i+1}$	=	Rainfall
S	=	Measured signal when the load cell is under a given load
S_{max}	=	Signal at maximum load
S_0	=	Signal at zero load
T_a	=	Air temperature
T_c	=	Canopy temperature
T_{dry}	=	Temperature of the leaf covered with petroleum jelly on both sides
T_{leaf}	=	Average temperature of normal leaf measured with infrared camera
T_{nws}	=	Canopy temperature expected for a well-watered crop
T_r	=	Transpiration rate of single leaves
T_{wet}	=	Temperature of leaf sprayed with water on both sides of the leaf
W	=	Load
w	=	Instantaneous vertical wind velocity
W_{max}	=	Maximum load
W_0	=	Zero load
W_p	=	Prediction of weight
α	=	Ratio of the turbulent transfer coefficients for sensible heat and water vapour
β	=	Bowen Ratio
Δe	=	Vapour pressure gradient
ΔT	=	Air temperature gradient between two heights above the surface

λ	=	Latent heat of vaporization
λE	=	Latent heat flux
ρ	=	Instantaneous air density
Ψ_l	=	Leaf water potential
θ	=	Stored soil water
θ_l	=	Estimation of stored soil water from lysimetric measurement
θ_{nl}	=	Estimation of stored soil water from non-lysimetric measurement
θ_z	=	Soil water within root zone

ABBREVIATIONS

CLL	-	Crop lower limit
CWSI	-	Crop water stress index
DAC	-	Digital to Analogue Converter
DAP	-	Days after planting
DUL	-	Drained upper limit
EC_a	-	Apparent soil electrical conductivity
EMI	-	Electromagnetic Induction
ET	-	Evapotranspiration
FC	-	Field capacity
GPS	-	Global positioning system
HM	-	Horizontal mode
IRT	-	Infrared thermometer
LSD	-	Least significant difference
PAWC	-	Plant Available Water Capacity
PI	-	Precision Irrigation
RTD	-	Resistance temperature detector
SDD	-	Stress degree day
SR	-	Surface renewal
SSM	-	Site specific management
TDR	-	Time domain reflectometry
TSD	-	Temperature stress day
USQ	-	University of Southern Queensland
VM	-	Vertical mode
VMC	-	Volumetric Moisture Content
VPD	-	Vapour pressure deficit
VRI	-	Variable rate irrigation
WAAS	-	Wide area augmentation system
WUE	-	Water use efficiency

Chapter 1

INTRODUCTION

1.1 Background

Agricultural fields are usually managed on the basis of average information about the soil and crop (except for crops managed under precision agriculture). This requires uniform application of all inputs despite some degree of heterogeneity in soil and other landscape characteristics that may exist causing some variation in growth and yield. In regions where rainfall is inadequate or uneven during the year, irrigation becomes a necessity for high value crops requiring optimal management of the water input. Evapotranspiration (ET) represents the major consumptive use of irrigation and rainfall water in agricultural land (Burt et al., 2005). There has been considerable research to define ET for various crops to understand the relationship between ET and crop yield (DeTar 2008; Kirda et al., 1999; Kirda 2000; Ko and Piccini, 2009; Liu et al., 2002). Due to increased competition for water, it is important to search for new ways to conserve water or to use it more efficiently (Fereres and Soriano, 2007; Hsiao et al., 2007). Irrigation scheduling is a farmer level decision process which includes when to irrigate and how much water to apply to a crop field.

Irrigation scheduling is conventionally based either on ‘soil water measurement’ or on ‘soil water balance calculations’. A potential problem with all soil-water based approaches is that many features of the plant’s physiology respond directly to changes in water status of the plant tissues, whether in the roots or in other tissues, rather than to changes in the bulk soil water content (Jones, 2004a). The plant response to a given amount of soil moisture therefore varies as a complex function of evaporative demand. As a result it has been suggested (Jones, 1990a) that greater precision in the application of irrigation can potentially be obtained by a third approach, the use of ‘plant stress sensing’.

Over decades of irrigation research (Idso et al., 1981; Yuan et al., 2004), a number of stress indices have been proposed for irrigation scheduling based on indirect measures of water stress, such as canopy temperature. Infrared thermometry and thermography are based on the fact that variations in temperature within a typical canopy, as stomatal conductance changes, would be expected to increase

approaching stomatal closure (Fuchs, 1990). Canopy temperature can be measured rapidly with non-contact, infrared sensors that allow calculation of an index (e.g. crop water stress index, CWSI, Idso et al., 1981). Such indices measured using infrared sensors appear to perform better in arid and semiarid areas than humid areas because of lack of discrimination between leaf and other plant parts during the measurement of reference temperature. Recent use of thermal imaging of crop canopies with infrared cameras has overcome the limitation of CWSI and has demonstrated its full potential as a practical tool for remote sensing of water deficit in crop fields (Fuentes et al., 2004; Jones et al., 2002). Information on a crop's water status, which is required when planning irrigation programs, is best provided by crop physiological indicators (Remorini and Massai, 2003). Thermal imaging has the potential to provide a more robust measure of the crop water status along with measurement of leaf water potential and stomatal conductance.

Spatial soil variability in the field can reduce overall efficiency of the irrigation system. Any inefficiency with water application can cause reductions in yield and quality of the crop, and contribute to inefficient use of fertilizer and other inputs lowering overall water use efficiency (Sanders et al., 2000). Water use efficiency is defined as crop yield per unit of water use (Sinclair et al., 1984). In order to increase water use efficiency, there is a need to measure spatial variability in farms and identify if it is associated with one or more soil properties. Intensive soil sampling is the most effective way to quantify spatial variability in a field (Havlin et al., 1999), but it demands considerable effort, time and cost. Therefore, there is a need to develop methods that enable rapid measurements of spatial variability in soil and/or crop properties.

As a rapid, non-invasive method, electromagnetic induction (EMI) technique is commonly used to measure apparent electrical conductivity (EC_a) to complement traditional soil surveys allowing extraction of information on spatial variation in soil moisture and texture (Dalgaard et al., 2001; Ehlert et al., 2001; King and Dampney, 2000; Waine et al., 2000). Using the EMI method with the EM38 sensor, (Sudduth et al., 1999) have demonstrated the usefulness of this technique for investigating soil variability and using the information to practice variable management of soils with a clay-pan. Use of EM38 early in the growing season allows the data to be used to

make a management decision about application of inputs, at a time when input rate influences yield.

Main causes of crop yield variability in the field are due to nutrients, soil and landscape factors (soil texture, structure, depth, salinity, organic matter, field slope and aspect), water, weather and some other factors such as competition from weeds, pesticide damage, inconsistent seed germination, lodging, and hail damage. Although there are many factors that contribute to variation in yield, the single most important factor is too much or too little water (McBride, 2003). Experience with yield maps has convinced many researchers and agriculturists that water availability could be an important factor influencing spatial yield patterns in the field.

Spatially variable management of the crop allows various agricultural inputs to be applied at spatially variable rates to improve efficiency of input use and reduce environmental impacts. However, most of the previous research and commercial developments in spatially variable crop production have been concentrated on variable rate fertilizer and chemical application (Torre-Neto et al., 2001). Thus it makes sense to use precision farming concepts for irrigation water management/scheduling (called 'precision irrigation', PI), to ensure water is applied in the right place, in the right amount, and at the right time (Sanders et al., 2000), for optimum production and efficiency. PI is still in the development stage and requires a lot of experimental work to determine its feasibility and applicability. PI is also sometimes referred to as ''variable rate irrigation'' (VRI). Both PI and VRI are excitingly new aspects of site-specific farming that is just beginning to be explored and is still very much a research issue (Al-Karadsheh et al., 2002).

1.2 Research hypotheses

- Uneven crop water deficit can be detected in the field with plant physiological measurements such as leaf water potential and stomatal conductance.
- Thermal sensing of stomatal closure to indicate water stress in crops can be used as a plant based sensing method for irrigation scheduling.

- Spatial variation in growth and yield of crop plants in a field at any given time is a function of the nature and scale of spatial variation that exists in the field.

1.3 Objectives

- Testing and evaluation of the performance of a load-cell-based lysimeter system for measurement of daily and seasonal evapotranspiration (ET) for accurate estimate of water deficit in irrigated crops inside a glasshouse.
- Evaluate the prospects of proximal thermal sensing of crop plants with a thermal infrared camera (thermography) to identify the relationship between physiological aspects of crop water stress and soil water availability.
- Identify spatial variability in crop water deficit stress and soil properties under field conditions with the help of electromagnetic induction technique.
- Quantify the impact of spatial variability in soil water deficit in the field on crop response under a range of irrigation management options.

1.4 Outcomes of the study

- Strategies and recommendations for the implementation of precision irrigation on fields with spatially variable water content.
- Evaluation of tools and technology to obtain spatial information on soil or crop properties to assist irrigation decisions.

As a result of the adoption of the above outcomes, it is expected that water use efficiency will improve and risk of contamination of the ground water from fertilizers and other agrochemicals will reduce.

1.5 Structure of the Thesis

This thesis contains seven chapters including this introduction chapter. A brief summary of each chapter is outlined below.

Chapter 1 gives a brief outline of the overall background to this research, research hypotheses and objectives. It also includes the outcomes of the research project followed by a brief overview of the structure of the dissertation.

In **Chapter 2**, a comprehensive literature review related to the broad aims of research is presented. This chapter includes a brief overview of techniques for measuring evapotranspiration (ET), an introduction on the use of infrared thermography and thermal indices to identify crop water stress and the usefulness of EM38 for the study of spatial variability in crop fields. All these are essential for improving the precision of irrigation scheduling.

In order to achieve objective 1, glasshouse experiments for cotton and wheat crop were conducted at the University of Southern Queensland, Toowoomba, Australia. **Chapter 3** includes the details of the experimental design used, the set up for a load cell based mini-lysimeter system inside the glasshouse, management of crops and irrigation treatment and procedures used for the collection of data from these experiments are explained. Sensitivity of the lysimeter and its performance in estimating ET under various irrigation treatments and crops are also discussed.

In addition to the glasshouse experiments described in Chapter 3, field experiments were conducted with cotton and wheat crops at the Queensland Primary Industries and Fisheries (Department of Employment, Economic development and Innovation) experimental station near Kingsthorpe to accomplish objective 2. These are described in two separate chapters (Chapters 4 and 5) that include the experimental set up, crop and irrigation management in the field and details of procedures used for all measurements. **Chapters 4 and 5** describe how thermal imaging can be used to determine spatial variation in canopy temperature that may exist within a crop field when plants are exposed to varying irrigation treatments. A comparison between the response of crops (cotton and wheat) to irrigation treatments are examined. These chapters also explore the relationship between canopy temperature and soil water within the root zone. In addition, thermal indices, their relationships with soil water within the root zone and implication to irrigation scheduling of crops have been also discussed in these chapters. Relative performance of plant physiological parameters (leaf water potential and stomatal conductance) in quantifying water deficit in plants and their relationships with canopy temperature are also described in these chapters. The suitability of thermal imaging for irrigation scheduling is also discussed.

The effects of variation in soil water and soil/air temperature on apparent electrical conductivity of soil (EC_a) measured with EM38 for both vertical and horizontal mode in the field is explained in **Chapter 6**. Measurement of EC_a at various heights

above the ground and the effect of height on EC_a are also discussed here along with a brief description of mapping of EC_a data for precision irrigation.

Finally, **Chapter 7** presents a discussion of results from all previous chapters to derive specific conclusions from this research project with recommendations for future research in this area. Further information on specific experimental results, material data and other information not relevant directly within a chapter is included in the **Appendices**.

Chapter 2

REVIEW OF LITERATURE

The major driving force to develop effective irrigation technology in many countries around the globe is water scarcity. For countries such as Australia, which is one of the driest continents on earth, improvement in the efficiency of crop water use is essential (Fuentes, 2005). Therefore an understanding of water needs in agriculture is critical for maintaining a stable production system and ensuring availability of water in the future since agricultural irrigation accounts for 65% of fresh water extracted (Fig. 2.1, ABS, 2006). In this chapter, information is provided on previous studies which focused on principles, methods and techniques used to increase the efficiency of crop water use to help meet the research objectives stated in Chapter 1.

2.1 Crop Water Deficit and Irrigation scheduling

Mean global temperatures is expected to rise over the next few decades, which will increase evaporation and evapotranspiration rates with the possibility of expansion of arid regions. Thus water availability will be a major limitation to plant growth in the future (Houghton et al., 2001). As a result, irrigation of crops will become an increasingly common practice. Evapotranspiration (ET) represents the major consumptive use of irrigation water and rainfall on agricultural land (Burt et al., 2005). ET from crop fields is an important factor affecting water deficit, growth and yield of crop plants. Accurate estimation of ET is an important step to manage water efficiently because it provides the information on losses of water from the system that is essential in maintaining productivity (Tyagi et al., 2000). Inaccurate estimates of ET can lead to poor assessment of water deficit in crop plants reducing our ability to interpret variation in growth and yield of crops that may lead to inefficient use of water. Efficient use of irrigation water has become very important due to the lack of adequate water resources combined with high cost of fertilizers and other farm expenses (De Azevedo et al., 2008). Thus, appropriate timing and quantity of irrigation-water application is vital for world agriculture. Various methods used to estimate water deficit and water use relating to irrigation scheduling of crop plants are discussed below.

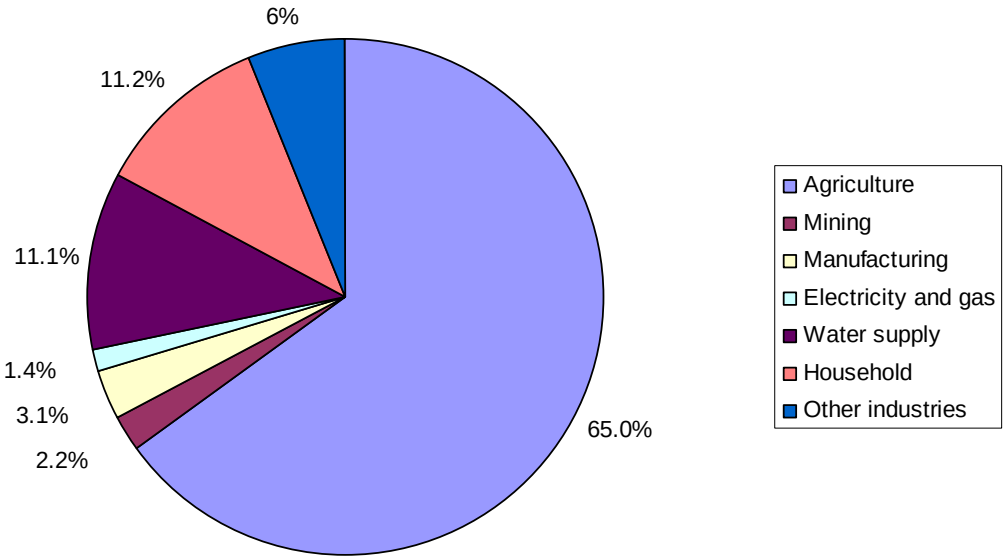

Figure 2.1 Diagram showing percentages of water used by various sectors in Australia (ABS, 2006).

2.1.1 Estimation of evapotranspiration

Evapotranspiration is the combination of two separate processes where water is lost on the one hand from the soil surface by evaporation and on the other hand from the crop by transpiration (Allen et al., 1998). Evapotranspiration (ET) is affected by various factors such as weather parameters (i.e. radiation, air temperature, humidity and wind speed), crop factors (crop type, variety and development stage) and management and environmental conditions and other factors (ground cover, plant density and soil water content). Therefore there are various methods of estimating ET, such as hydrological approaches (e.g. soil water balance and lysimeter methods), micrometeorological methods (e.g. eddy covariance, energy balance or Bowen ratio method and aerodynamic method) and plant physiological approaches (e.g. whole-plant enclosures or chambers and sap flow method) (Allen et al., 1998; Li et al., 2008; Monteith and Unsworth, 1990). Eddy covariance theory addresses the turbulent transport of an entity in a body of fluid. For the case of latent heat flux in the atmosphere (Kizer et al., 1990):

$$LE = \rho L w q, \quad (2.1)$$

where LE = instantaneous latent heat flux (W m^{-2}), ρ = instantaneous air density (kg m^{-3}), L = instantaneous latent heat of vaporization of water (J kg^{-1}), w = instantaneous vertical wind velocity (m s^{-1}) and q = instantaneous specific humidity (kg kg^{-1}). LE can be converted to water vapour flux by dividing left hand side of Eqn. 2.1 by L and then evapotranspiration rate (E) is estimated after dividing it with the density of water. Eddy covariance method is based on the assumption that the instantaneous deviation of air density and latent heat of vaporization is zero and the long term mean vertical wind velocity over a flat, uniform surface is also zero (Baldocchi et al., 2000; Kizer et al., 1990; Lee, 1998; Massman et al., 2002). This method requires accurate measurement of vapour pressure and wind speed at different levels above the surface limiting their practical application (Allen et al., 1998). Eddy covariance method is most applicable over flat terrain, when the environmental conditions are steady and when the underlying vegetation extends upwind for an extended distance (Baldocchi, 2003). Bowen ratio or energy balance method has been also used to quantify crop ET and is an indirect measuring method. Bowen ratio technique was first proposed by Bowen (1926) who defined Bowen-ratio (β) as:

$$\beta = H/\lambda E = \alpha(C_p \Delta T/\lambda \Delta e), \quad (2.2)$$

where H is sensible heat flux (W m^{-2}), λE is the latent heat flux (W m^{-2}), α is the ratio of the turbulent transfer coefficients for sensible heat and water vapour, C_p is specific heat of air at constant pressure (J kg^{-1} °C^{-1}), ΔT is the air temperature gradient (°C) between two heights above the surface, λ is latent heat of vaporization (J kg^{-1}) and Δe is the gradient of vapour pressure (kPa) at the same two heights as for T under non-advective conditions. The surface energy balance can be expressed as:

$$R_n - G - \lambda E - H = 0, \quad (2.3)$$

where R_n is the net irradiance (W m^{-2}), G is soil heat flux (W m^{-2}) and H and λE are as defined for Eqn. 2.2. Using Eqns. 2.2 and 2.3 and solving for λE yields the estimate of evaporation:

$$\lambda E = (R_n - G)/(1+ \beta) \quad (2.4)$$

Net radiation (R_n) and soil heat fluxes (G) can be measured or estimated from climatic parameters. H requires accurate measurements of the temperature gradient above the surface. As evaporation is determined by using both Bowen ratio and energy balance approach this method is termed as Bowen-ratio energy balance method. Bowen-ratio energy balance method is often used because of the simplicity of data collection. This technique has increased in popularity because of the recent improvements in portable data acquisition systems for field studies and accuracy and precision of sensors (Prueger et al., 1997). However, Bowen ratio method makes several critical assumptions which rely heavily on the precision of net radiation measurement, and has limited application when the ratio is –1.0. Surface renewal (SR) method is another method for estimation of ET. SR method is simple in design and is used for measuring sensible heat flux density (H) involving the use of fine wire thermocouples to monitor high frequency temperature fluctuations (Paw U et al., 1995). The SR method has the advantage that temperature or wind speed profiles and corrections for atmospheric stability are unnecessary. However, the major problem with the SR method is due to the need to calibrate an α factor using an independent measurement of H or LE (Snyder et al., 2008).

Lysimeter is another direct method commonly used for the measurement of ET. A lysimeter is defined as a container or tank filled with soil, with bare or vegetated soil surface for determining the ET of a growing crop or for evaporation from bare soils. Lysimeters can be classified into two categories: non-weighing and weighing lysimeters. In weighing lysimeters the change of weight provides a direct and accurate measurement of the change of soil water content over time (Aboukhaled et al., 1982). In case of non-weighing lysimeters, changes in soil water content can be determined by soil sampling or using neutron probes. The weighing lysimeter represents the best available technology for determining water use by plants as it gives additional information on soil water balance (Hatfield, 1990; Xu and Chen, 2005). Weighing lysimeters have become standard tools for ET measurements (Howell et al., 1991; Prueger et al., 1997; Young et al., 1997) within the soil-plant-atmosphere research community because these can directly measure evapotranspiration (Van Bavel, 1961). Lysimeters can be further classified into monolithic or reconstructed soil profile when combined with weighing, weighable or non-weighing and gravity or vacuum drainage lysimeters (Tolk et al., 2005). Direct

weighing lysimeters often use load cells of the beam or button type to carry the total load of the lysimeter as well as to indicate any change in load (Evett et al., 2009). With increase in availability and affordability of modern computers and data loggers, continuous monitoring of weighing lysimeters is a real possibility (Marek et al., 2006).

Measurements of ET with various approaches described above has enabled understanding of seasonal pattern of variation in ET for various crops and the relationships between ET and crop yield (Karam et al., 2007; Kirda et al., 1999; Ko and Piccini, 2009). As water is a finite source available for irrigation of agricultural crops (due to increased competition from other sectors), it is important to search for new ways to conserve water or use it more efficiently (Fereres and Soriano, 2007; Hsiao et al., 2007). Despite the constraints associated with the water economics (the cost and availability of water), irrigation scheduling remains as a farmer level decision that includes when to irrigate and how much water to apply to a crop field. Irrigation scheduling is conventionally based on either when the soil is sufficiently dry (reaching a critically low value as a 'soil water content measurement') or drawn down from a full irrigation (depleted to a low soil water content based on 'soil water balance calculations'). A potential problem with all soil-water based approaches is that many features of the plant's physiology respond directly to changes in water status of the plant tissues (either in the roots or another plant tissue), rather than to changes in the bulk soil water content (Jones, 2004a). The actual tissue water potential at any time therefore depends both on the soil moisture status and on the rate of water flow through the plant and the corresponding hydraulic flow resistances between the bulk soil and the appropriate plant tissues. Plant response to a given amount of soil water therefore varies as a complex function of the evaporative demand of the atmosphere. As a result, it has been suggested (Jones, 1990a) that greater precision in the application of irrigation can potentially be obtained by a third approach, the use of 'plant stress sensing' compared with the conventional approach of 'soil water sensing'.

2.1.2 Plant stress sensing with infrared thermography

The most established method for detecting crop water stress remotely is through the measurement of a crop's surface temperature (Jackson, 1982). The correlation

between surface temperature and water stress in a crop plant is based on the assumption that as a crop transpires, the evaporated water cools the leaves below the surrounding air temperature. When crops are experiencing water shortage, transpiration from the leaves decreases which is expected to reduce both stomatal conductance and water potential of leaves. A decrease in transpiration can also cause insufficient cooling of leaf surface which will ultimately lead to an increase in leaf temperature (Jackson et al., 1981). Although other factors (e.g. air temperature and relative humidity) affect actual water stress level in a plant, leaf temperature is one of the most important factors (Jackson, 1982). Plant canopy temperature has been used as an indicator of water stress since the availability of infrared thermometers (IRTs) that made this measurement possible without physically contacting the plant (Ehrler et al., 1978). Fig. 2.2 shows that the wavelength range of 1.3-2.6 μm (including mid and thermal infrared) are not influenced by chlorophyll or cell structure but are influenced by the amount of water present in the plant leaf because the reflection is very low at mid and thermal infrared wavelengths. Healthy plants which are actively taking up water, release this water in vapour form into the air through transpiration which cools the leaves of a plant.

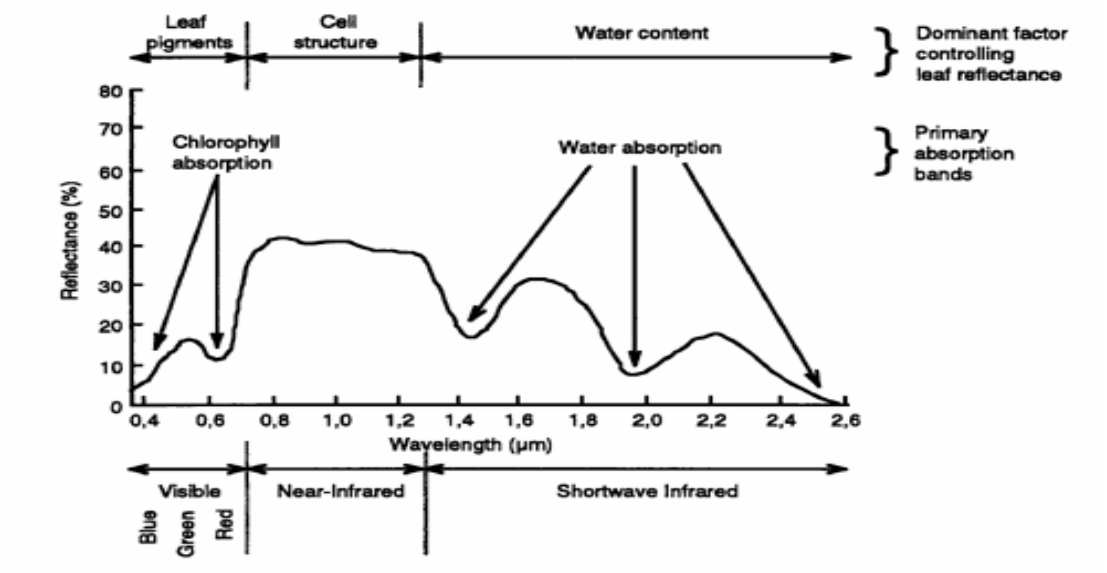

Figure 2. 2 Typical response characteristics of green vegetation (after Hoffer, 1978)**.**

Infrared thermometers have been considered ideal for the measurement of crop temperature as they are reliable and non-invasive, although the operator must

assume uniformity of soil water content and of plant canopy for large areas (Cohen et al., 2005) because crop temperature is usually based on a few point measurements. In order to map variability in water status of a crop at an adequate resolution, a network of many infrared thermometers is required (Evans et al., 2000). The technological advances in remote thermal imaging offer the potential for the mapping of canopy temperature variability over large areas (Jones and Schofield, 2008). Thermal imagery is a viable alternative to point measurements with infrared thermometers, since the canopy temperature of the whole field can be measured at once and a map of the plant water status distribution in the field can be produced (Cohen et al., 2005). The term 'thermography' that involves the process of obtaining thermal images (Jones, 2004b) theoretically overcomes the limitations of most studies on infrared thermometry. It is only relatively recently that thermography has become affordable in many laboratories with the development of a new generation of uncooled focal plan array of microbolometers as thermal detectors (e.g. Liddiard, 2004) in handheld, infrared cameras giving a thermal resolution of better than 0.1 °C (Jones and Leinonen, 2003). Microbolometers are capable of measuring energy associated with the incident electromagnetic radiation at high sensitivity as a small change in temperature causes change in electrical resistance that can be detected with these devices (Wang et al., 2004). It has also helped to propose thermal sensing of stomatal closure as an indicator of water deficit stress as a plant-based sensing method for irrigation scheduling (Leinonen et al., 2006), although most irrigation scheduling remains to be based on measurements and estimation of soil water deficit.

The advantages of infrared thermometry in studies of plant temperature measurements include: lack of the need to make a physical contact with the plant, simple automation of data collection and non-point measurements that accommodate inherent spatial variability (Mahan and Yeater, 2008). The potential advantage of thermal imagery (or its equivalent infrared thermography) over point measurements with infrared thermometers is the ability of the image to cover a large number of individual leaves and plants at one time. Infrared thermometers have a finite angle of view so that it is common for these to include background noise arising from soil or sky within the field of view in addition to plant canopy which can introduce some bias (Jones and Leinonen, 2003). The recent development and commercial availability of portable thermal imagers has greatly expanded the opportunities for

analysis of the thermal properties of plant canopies in relation to the growth and development of plants (Jones, 1999a). Although the role of other environmental factors (especially radiation and wind) on stomatal conductance remains unknown, Jones (1999a) pointed out that the mean canopy temperature not only increases as the stomata close, but, in a canopy composed of randomly oriented leaves, the variance of observed leaf temperatures also increases. These observations indicate that, it may not be practical to use conventional infrared thermometry to study the frequency distribution of temperature for large number of leaves due to lack of sensitivity of the method, but should be replaced with thermography (Jones et al., 2002).

Thermal imaging is potentially more capable than thermometery to provide a more robust measure of the crop water status. The portable thermal imagers and the associated image analysis software have overcome most of the problems experienced with infrared thermometers. Availability of equipment for digital thermal imaging provides a unique opportunity to develop instantaneous spatial canopy stress indices for use in precision agriculture (Chaerle and van der Straten, 2000). Grant et al. (2006) described experiments in which irrigation scheduling is determined by different methods, one of these being thermal imaging alone and should be tested. Earlier studies which have used infrared methods for irrigation scheduling are able to indicate stomatal closure or evaporation rate but they give no information on the amount of soil water available or needed at that time (Jones, 2004b). Rigorous testing of thermal imaging against more traditional physiological techniques under field conditions is still desirable for different types of crops due to the variation in stomatal sensitivity to water deficit (Grant et al., 2006) and extent of stomatal regulation of transpiration.

2.1.3 Thermal Indices

Major interest in the application of thermal sensing to irrigation of crops in the field was with the development of indices of crop water stress as a guiding tool for irrigation scheduling. Estimation of crop water status using thermal indices has been shown to be very robust (Idso et al., 1981; Jackson et al., 1981) and allowed mapping of plant water status in the field. An important milestone in the

development of methods for using canopy temperature information in irrigation scheduling was the stress degree day (SDD) index defined by Idso et al. (1977) as:

$$SDD_i = (T_c - T_a), \quad (2.5)$$

where T_c and T_a are midday canopy and air temperatures (°C) on day i. Significant elevation of canopy temperature above air temperature was considered as an indication of stomatal closure and crop water stress. An alternative approach based on the temperature difference between the experimental canopy and a comparable well-irrigated crop (Clawson and Blad, 1982; Fuchs and Tanner, 1966) has been also used as temperature stress day (TSD) (Gardner et al., 1981). However, both SDD and TSD approaches have been found to be somewhat unsatisfactory because the magnitude of indices such as SDD varies as a function of climatic factors, especially atmospheric humidity (Jones, 2004b). Crop water stress index (CWSI) is considered as a key step in the development of thermal sensing for irrigation management purposes as introduced by Idso and colleagues (Idso, 1982; Idso et al., 1981; Jackson et al., 1981) as it was able to account for the variation in atmospheric humidity. Idso and colleagues showed that $(T_{canopy} - T_a)$ was linearly related to atmospheric vapour pressure deficit for well-watered crops which led to the definition of CWSI as:

$$CWSI = [(T_c - T_a)_m - (T_c - T_a)_{LB}/ [(T_c - T_a)_{UB} - (T_c - T_a)_{LB}]. \quad (2.6)$$

In Eqn. 2.6, T_c = canopy temperature (°C), T_a = air temperature (°C). The subscripts m, LB and UB refer to the (T_c-T_a) values for the measured, lower baseline (non-water-stressed) and upper baseline (non-transpiring) respectively. Because it was not usually possible to have an actual, non-stressed crop adjacent to any field, a standard relationship between $(T_{canopy} - T_{air})$ and vapour pressure deficit was developed for each crop to represent the non-water-stressed baseline. Idso's CWSI has been found to work reasonably well in dry climates but still had significant limitations when applied to humid and maritime climates and in environments with substantial climatic variability (Hipps et al., 1985). In humid climates, vapour pressure deficit is usually low, which decreases the absolute difference between leaf and air temperatures causing a decline in the sensitivity of CWSI. To overcome this deficiency, substantial efforts have been directed to improve the sensitivity of water stress indices for humid environments (Jones, 1999b). The use of specific reference surfaces within the study area is probably the most powerful method to improve the

sensitivity of thermal detection of stomatal closure. An implication of this approach is that canopy temperature measurements are probably best made at the scale of individual leaves. The use of local and simultaneous reference measurements is facilitated greatly by the use of thermography and helps overcome any short term variation of equilibrium temperature (Jones, 2004b). Using single leaf measurements, Jones (1999b) defined a stress index ICWSI that is analogous to Idso's crop water stress index as:

$$ICWSI = (T_{leaf} - T_{wet}) / (T_{dry} - T_{wet}), \quad (2.7)$$

where T_{leaf} is average temperature of normal leaf measured with an infrared camera (°C), T_{dry} is the average temperature of the leaf covered with petroleum jelly on both sides (°C) and T_{wet} is the average temperature of the leaf sprayed with water on both sides of the leaf (°C). Jones (1999b) proposed several alternative formulations of indices based on combinations of T_{leaf}, T_{wet}, and T_{dry}. Of particular interest is the index I_G given by:

$$I_G = (T_{dry} - T_{leaf}) / (T_{leaf} - T_{wet}) = \alpha g_s, \quad (2.8)$$

in which α is an empirical coefficient that depends only on wind speed and to a lesser extent on air temperature. As stomata close, this form of the index has been shown to be more stable than its reciprocal ICWSI because it relates linearly to stomatal resistance (Jones, 1999b).

2.2 Identification of Spatial Variability

It is convenient to apply irrigation water to a crop field by treating the whole field as homogeneous even if the soil may not be homogeneous in the entire field. If some degree of soil heterogeneity is present in the field, some part of the field would be under irrigated while the other part would be over irrigated. If both under and over irrigated areas produce the same amount of yield then the area which is under irrigated will have higher water use efficiency than the over irrigated area. There is a need to quantify spatio-temporal variability in crop yields within a field by robust methods to explain within-field variations in physical and chemical properties of soil, considered as crucial elements of precision agriculture (Bullock and Bullock, 2000). The ability to delineate geo-referenced areas within a field that display similar behaviour with respect to crop yield potential is difficult due to the complex

combination of edaphic, anthropogenic, biological, and meteorological factors that affect crop yield (Corwin and Lesch, 2005).

There are many causes for crop yield to vary within a field that may include nutrients, soil and landscape factors (soil texture, structure, depth, salinity, organic matter, field slope and aspect), water, weather and other factors such as competition from weeds, pesticide damage, inconsistent seed germination, lodging, and hail damage. Although there are many factors that contribute to variations in yield but the single most important factor is too much or too little water (McBride, 2003). Climate and water availability have been reported to be the major factors influencing corn production (Morgan et al., 2003). Paz et al. (1998, 2001) also found water stress to be one of the greatest limiting factors in the yield of soybeans. Soil properties which affect availability of water to plants include water holding capacity, infiltration rate, texture, structure, bulk density, organic matter, soil depth, and the presence of restrictive soil layers.

Measurement of these properties is expensive and time consuming since it generally involves in-field characterization by a trained soil scientist requiring collection of soil samples from various depths and locations in the field, followed by laboratory analysis. Because of this, quantifying soil physical characteristics at the scale required for accurate mapping of within-field variations has been impractical (Sudduth et al., 2001). Yield maps alone do not provide the information necessary to differentiate edaphic (i.e. soil related), anthropogenic (e.g., compaction due to tillage or harvesting equipment), biological (e.g. incidence of disease or pests etc.) and meteorological (e.g. humidity, rainfall, wind etc.) factors affecting spatial patterns in growth and yield of crops within a field. Furthermore, yield-monitoring over space and time has not been developed for all crops (Corwin and Lesch, 2005). Therefore development of inexpensive methods for measuring spatial variability in soil properties is of great interest. One of the most recent and promising approach in quantifying spatial variability is to measure a surrogate soil property that depends on and/or correlates with other soil properties, such as measurement of apparent soil electrical conductivity (EC_a). Non invasive measurements of EC_a can provide detailed spatial information relatively rapidly and cheaply about soil-related and anthropogenic properties that influence crop yield and its spatial pattern. It has been

suggested that EC_a measurements may be a viable alternative when yield-monitoring data are not available (Corwin et al., 2003).

2.2.1 Apparent soil electrical conductivity (EC_a)

A transmitter located at one end of an electromagnetic (electrical conductivity) instrument induces circular eddy current loops in the soil. The magnitude of these loops is directly proportional to the conductivity of the soil in the vicinity of that loop. Each current loop generates a secondary electromagnetic field which is proportional to the value of the current flowing within the loop. A fraction of the secondary induced electromagnetic field from each loop is intercepted by the receiver coil and the sum of these signals is amplified and formed into an output voltage which is linearly related to depth-weighted soil EC_a (Rhoades, 1992). Apparent soil electrical conductivity (EC_a) has become one of the most frequently measured soil property to characterize field variability although it has little direct effects on crop growth and yield. Variation in EC_a has been found to be correlated with variation in several soil properties which directly affect crop productivity. In general, EC_a can be affected by a number of different soil properties, including soil water content (Kachanoski et al., 1988; Kachanoski et al., 1990), soil organic matter (Banton et al., 1997), drainage conditions (Kravchenko et al., 2002), salinity (Williams and Hoey, 1987), soil texture (Banton et al., 1997; Williams and Hoey, 1987) and depth to claypan horizons (Doolittle et al., 1994; Kitchen et al., 1999). During an evaluation of EC_a to delineate a number of physical, chemical and biological properties of soil related to yield and ecological potential, Johnson et al. (2001) found EC_a to be useful for separating distinct zones of different soil conditions. As many of these factors relate directly or indirectly to crop yield, EC_a measurements can be used for some soils as a surrogate measure of soil chemical and physical properties therefore reducing cost (Hartsock et al., 2001). It is important to understand the basic theories and principles of EC_a measurement to appreciate their application in characterizing soil spatial variability for site-specific soil and crop management.

The electrical conductivity model suggested by Rhoades et al. (1989) indicates that EC_a measurement is a function of soil physical and chemical properties such as soil salinity, saturation percentage, soil moisture content and soil bulk

density. Since soil bulk density and saturation percentage are closely associated with the soil texture and soil moisture, EC_a measurements in non-saline soils could be primarily be used as indicators of soil texture and water content (Corwin and Lesch, 2003). Both soil texture and water content of soil are the primary driving factors which affect soil water availability to crops. Because soil water is one of the essential factors affecting variation in yield, EC_a maps can often exhibit similar spatial pattern variation as yield maps. Therefore, the focus on spatial measurement of EC_a has increased as a potential measurement tool to explain spatial variability in crop production. Although ground-truth soil sampling is needed in conjunction with EC_a measurements, EC_a-directed soil sampling can reduce the number of samples to the minimum necessary to describe spatial variability in the field (Corwin and Lesch, 2003; Lesch, 2005). Thus, EC_a has become one of the most reliable and frequently used measurements to characterize field variability for application to precision agriculture due to its ease of measurement and reliability (Corwin and Lesch, 2003; Rhoades et al., 1999a, 1999b). There are two primary methods of measuring EC_a, the direct or contact method and a non contact method that utilizes electromagnetic induction (EMI). Contact methods use voltage between electrodes in contact with the soil to directly measure the resistance of the soil to the resulting current to derive EC_a as the reciprocal of electrical resistance.

2.2.2 Electromagnetic Induction (EMI)

Continuous proximal sensing, commonly referred to as electromagnetic induction sensing (EMI) of the apparent electrical conductivity of soil (EC_a), together with the measurement position with a precise global positioning system (GPS) has enabled accurate mapping of within-field soil variability (Plant, 2001). EMI is a non-invasive technique that measures soil EC_a by inducing an electrical field at the ground level. The principle of electromagnetic induction used to measure EC_a is shown in Fig. 2.3. Kachanoski et al. (1988) found that the spatial variation of soil water content in the top 0.5 m measured by time domain reflectometry at 52 sites in a 1.8 ha field in Canada was highly correlated with EMI readings. Reedy and Scanlon (2003) indicated a similar success with EMI during a detailed evaluation of spatial and temporal variability in water content (in the upper 1.5 m of the soil). These studies show that EMI could be a useful technique in soil surveying by locating boundaries between soil types more easily and accurately to identify distinct management zones

within a field. These data could be also integrated with the sequential analysis of yield map to hydrologically manage different areas in a field prone to either drought or water logging (King and Dampney, 2000; King et al., 2001).

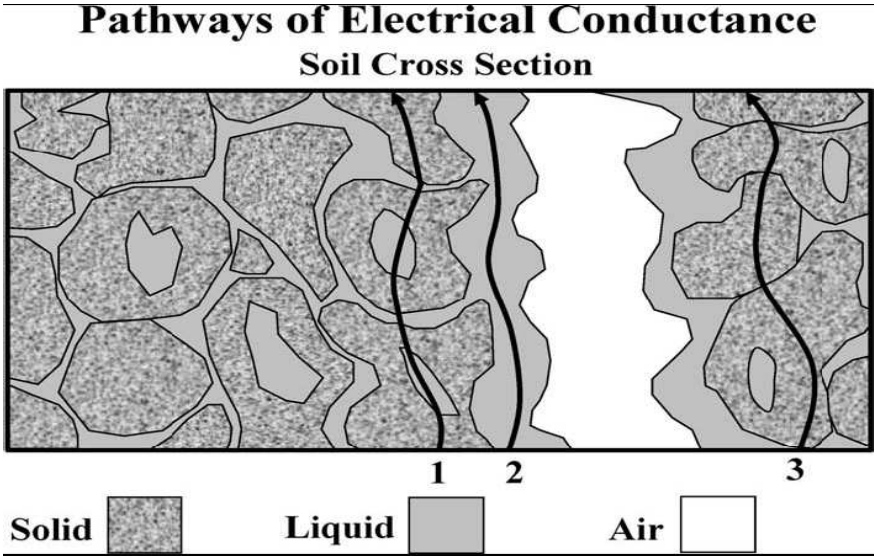

Figure 2. 3 Three conductance pathways for the EC_a measurement (Modified from Rhoades et al., 1989).

EMI technique is currently available as commercial equipment to measure EC_a directly during tillage with two soil cutting discs as Veris System (Veris Technologies, Salina, Kansas, USA), or indirectly using a non contact EMI probe as EM38 (Geonics Limited, Mississauga, Ontario, Canada). Since Veris is restricted to tillage operation, EM38 is better suited to the experiments described in the later part of this thesis. Thus, more detailed information on the range of application and sensitivity of EM38 have been sought and discussed below.

2.2.3 EM38

The EM38 instrument uses a spacing of 1 m between a transmitting coil located at one end of the instrument and a receiver coil at the other end using an electromagnetic signal frequency of 14.6 kHz. EM38 can be operated in one of the two measurement modes. The vertical dipole mode provides an effective measurement depth of 1.5 m and the horizontal dipole mode provides an effective measurement depth of 0.75 m (Sudduth et al., 2001). EM38 has considerably greater

application for agricultural purposes because the depth of measurement corresponds roughly with the root zone of most agricultural crops (i.e., 1.5 m), when the instrument is placed in the vertical coil configuration (Corwin and Lesch, 2005). Sensitivity of the equipment in the vertical dipole mode is relatively low, but increases with depth, with maximum sensitivity at about 40 cm depth below the instrument (Fig. 2.4). In the horizontal dipole mode, the sensitivity is at maximum at the soil surface and decreases exponentially with depth (McKenzie et al., 1989; McNeil, 1992). Measurement of EC_a with an EM38 provides the average response within an area that is approximately equal to the measurement depth. The principle of operation of EM38 probe is shown in Fig. 2.5. The instrument's response to soil conductivity varies as a nonlinear function of depth.

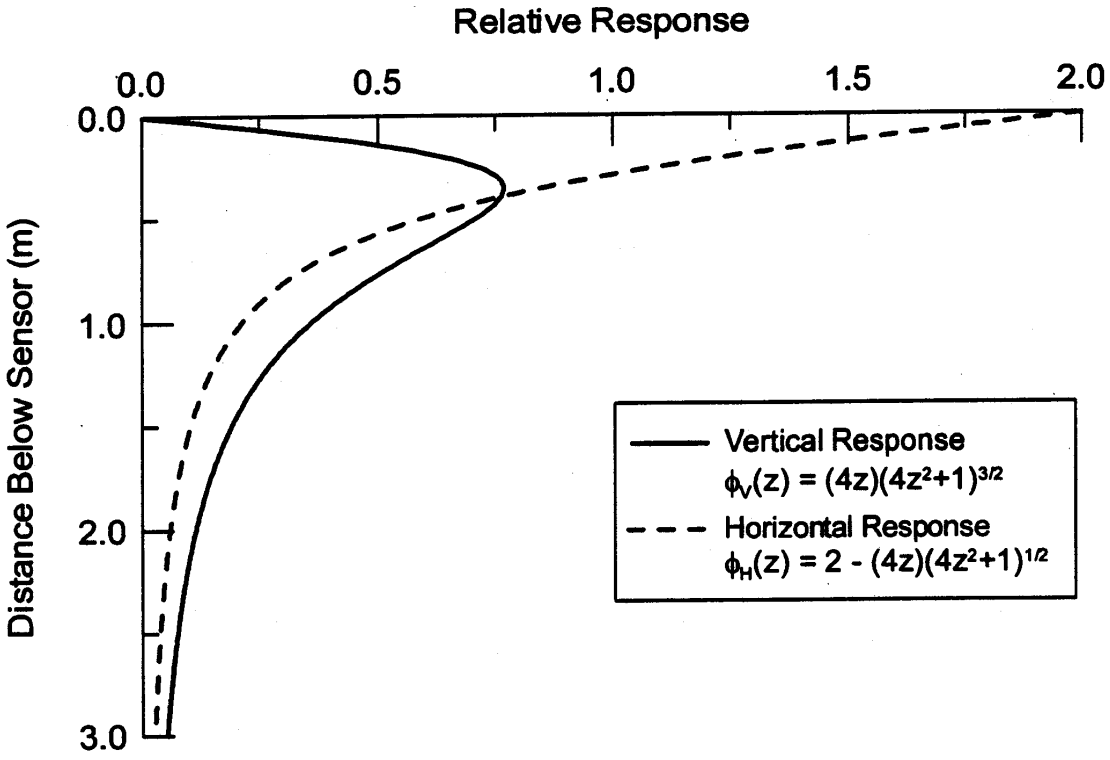

Figure 2. 4 Relative response of EM38 as a function of distance (adapted from McNeill, 1992)

Equipment similar to EM38 has been also used to detect spatial variability of salt and clay contents (e.g. Geonics EM 34/3 electromagnetic conductivity meter by Williams and Hoey, 1987). Soil water content has been reported to be the single most important of the four commonly cited factors influencing ECa (soluble salts,

clay content and mineralogy, soil water content and soil temperature) in determining EC_a (Brevik and Fenton, 2002).

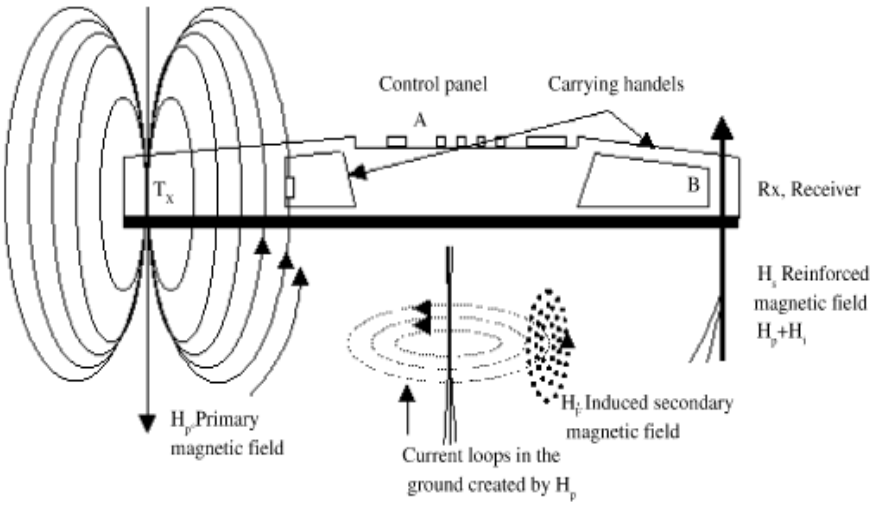

Figure 2. 5 Diagram of EM38 meter showing the principle of operation (Lesch et al., 2005).

In a 1.8 ha field near Brantford (Ontario, Canada) Kachanoski et al. (1988) found spatial variation in soil water stored within the top 0.5 m to be highly correlated with the spatial variation in bulk soil electrical conductivity measured with EMI meters (i.e. EM38 and EM31). In another study 50 km west of Saskatoon (Saskatchewan, Canada) Kachanoski et al. (1990) found that the bulk soil electrical conductivity could explain more than 80% of the variation in soil water storage in the top 1.7 m of a moderately fine-textured, moderately calcareous soil along a 660 m transect. Sheets and Hendrickx (1995) conducted a similar study that used 65 neutron probe access tubes at 30 m intervals and compared water content measurements with EC_a readings using EM31 equipment along a 1950 m transect in New Mexico for 16 monthly measurements. They found 64% of variation in soil water content to be explained by EC_a readings that was lower than the value reported by Kachanoski et al. (1988, 1990). Reduced performance of EM31 could be due to deeper penetration of the transmitted signal by the EM31 meter (4 m) relative to the depth of water content monitoring (1.5 m) and greater distance between the EC_a measurements and water content measurements with the neutron probe (~ 10 m). Reedy and Scanlon (2003) evaluated the water content predictive ability of EMI

measurements in the top 1.5 m of an engineered barrier soil profile designed as a prototype for waste containment. They monitored water content in the top 1.5 m with a neutron probe as well as a Geonics EM38 bulk soil electrical conductivity meter. They found a simple linear regression model to be adequate in predicting the average volumetric soil water content within the profile at any location at any time (with a coefficient of determination, $R^2 = 0.80$) and even for in predicting spatially averaged volumetric water content over the entire area at any time ($R^2 = 0.99$). It may be noted that the coefficient of determination for a regression indicates how well the regression equation is able to account for the variability in the data set used for regression.

EM38 has been also found useful for investigating soil variability and its application to variable management of clay-pan soils (Sudduth et al., 1999). Lesch et al. (2005)'s study demonstrated the use of EM38 survey for precise mapping of soil texture under non-saline conditions and to precisely locate the positions of buried tile drainage lines in the field. Kitchen et al. (2005) concluded that productivity zones can now be delineated by measuring EC_a and elevation data with EM38 and real time kinematic GPS, respectively due to the good agreement between EM38 data and productivity zones delineated from yield map data. Similar good results have been obtained in characterizing spatial variability of soil properties and delineation of soil management zones for site specific management of potato (Cambouris et al., 2006). These studies demonstrate that EM38 can be used in a number of ways, e.g. in reconnaissance mode to reduce cost of soil sampling, to re-define boundaries of sparsely sampled co-regional data and as a surrogate measurement for soil properties which are often expensive and time-consuming to measure.

2.3 Summary

In this chapter, the principles of various methods and techniques to measure and/or estimate evapotranspiration were discussed for the purpose of quantifying water deficit in a crop field to assist irrigation scheduling. Since evapotranspiration (ET) combines evaporation from soil surface and transpiration from plant surfaces (essentially leaves), it represents the greatest form of all losses of the applied irrigation water to a crop field. Weighing lysimeters have been considered in this work (in later chapters of this thesis) as a direct and potentially the most accurate

method to measure ET and to determine crop water use. The reviewed literature in this chapter suggests that infrared thermography could be useful for early detection of water deficit in crop plants to assist decisions on timing of irrigation. The application of this technique in detecting spatial variability of crop water deficit in the field will be shown in a later chapter of this thesis. The capability of the EM38 as a non-invasive tool to characterise spatial variability in the field has been discussed in this chapter as background information to support EM38 measurements described in a later chapter of this thesis to test the sensitivity of this technique and its usefulness to determine spatial variability in soil water content to develop precise and effective methods of irrigation scheduling.

Chapter 3

DESIGN AND PERFORMANCE EVALUATION OF A MINI-LYSIMETER SYSTEM TO MEASURE EVAPOTRANSPIRATION OF GLASSHOUSE-GROWN PLANTS

3.1 Introduction

Evapotranspiration (ET) is an important hydrological process that influences the availability of water for functioning of all vegetation on natural landscapes. It also represents the major consumptive use of irrigation water and rainfall on agricultural land (Burt et al., 2005). There has been considerable research in the past decade to define ET for various crops to establish the relationship between ET and crop yield (DeTar 2008; Karam et al., 2007; Kirda et al., 1999; Kirda 2000; Ko and Piccini, 2009; Liu et al., 2002). Due to the world-wide shortage of water in some regions and competition for water from other sectors, there is an impetus to find new ways to conserve water or use it more efficiently (Fereres and Soriano, 2007; Hsiao et al., 2007). Irrigation scheduling is a farmer level decision that requires information on crop ET in order to decide when to irrigate and how much water to apply to a crop field.

A lysimeter is essentially a container or tank in which plants are grown that allows various input and output components of the soil water balance to be measured directly. ET is an important component of the soil water balance that can be measured directly with lysimeters when other input and output terms of the soil water balance are known. Since ET can be measured and/or estimated in a number of ways, most research on crop water use tend to focus on lysimeters so that ET measured with other methods can be compared (e.g. Ashktorab et al., 1994). Lysimeters allow determination of ET by direct weighing and since 1970s; it has involved the use of load cells to determine total lysimeter mass with an accuracy of 0.05 mm of water (Malone et al., 1999).

All load-cell based lysimeters require calibration and frequent calibration may lead to excessive workload, although a sensible level of quality control is

warranted (Malone et al., 1999). In previous studies, the need for testing load cells for linearity, repeatability, thermal shift and creep have been considered as important component of measuring the performance of lysimeters (Martin et al., 2001). Since data loggers and multiplexers are often involved with the collection of lysimetric data, these can affect the accuracy and resolutions of lysimeters (Evett et al., 2009). Therefore experiments were carried out inside the glasshouse for testing and evaluation of the performance of a load-cell based mini- lysimeter system for long-term monitoring of evapotranspiration in controlled environmental conditions (i.e. glasshouse).

3.2 Materials and Methods

3.2.1 Measurements

An aluminium frame with adjustable feet (Fig. 3.1) was constructed in a mechanical workshop to mount 12 load cells (Fig. 3.2), arranged in a 4×3 grid. A circular aluminium plate (Fig. 3.1) was attached to each load cell that allowed experimental pots filled with soil to be placed over it for monitoring of pot weights at short time intervals.

Figure 3. 1 A mini-lysimeter system consisting of an aluminium frame fitted with 12 load cells (each located under a circular aluminium plate) arranged in a 4×3 grid to represent 12 weighing lysimeters.

For the mini-lysimeter system, aluminium, single point, load cells (Model PT2000, PT Limited, Australia) of 20 kg capacity with an expected resolution of 0.1 g were used (Fig. 3.2). Specification for a typical load cell from its calibration certificate is given in Table 3.1 with the indication of parameters which varied slightly with each load cell.

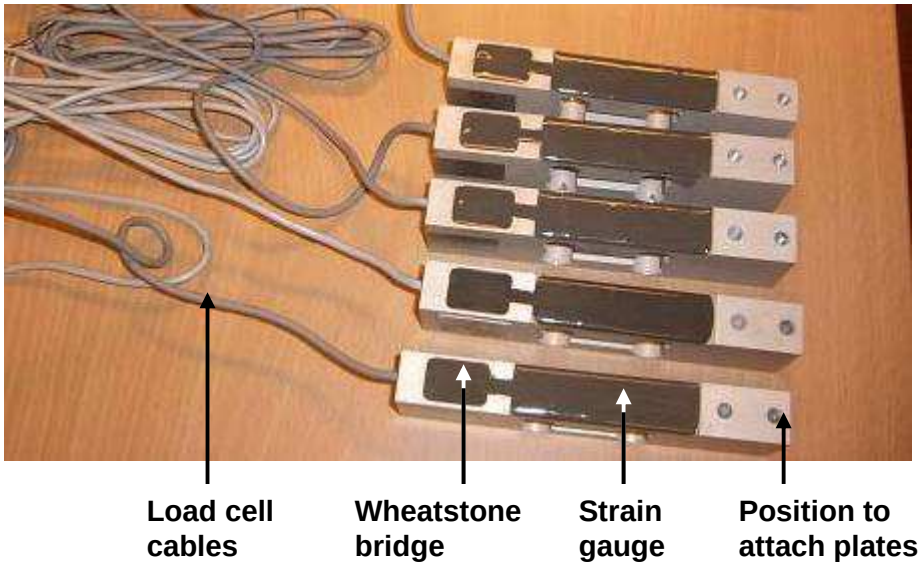

Figure 3. 2 Samples of load cells used for the min-lysimeter system.

Table 3. 1 Specification of a typical load cell used for the mini-lysimeter system. Parameters shown with an asterisk varied between load cells.

Parameters	Value
Capacity (kg)	20 kg
Serial Number*	3184042
mV/V*	1.982
Full scale output (mV/V)*	1.982
Zero load output (mV/V)*	-0.825
Non repeatability (% FS)	< 0.015
Non linearity (% FS)	< 0.025
Creep (% FS in 30 min)	< 0.05
Combined error (% FS)	< 0.03
Recommended excitation (V)	10
Operating temperature (°C)	-30 to 70
Thermal zero TC (%FS/°C)	< 0.01
Thermal span TC (%FS/°C)	< 0.003
Input resistance (Ohm)*	426.97
Output resistance (Ohm)	352.2
Insulation resistance (MOhm @50 V)	> 5000

Each load cell had 4 holes: 2 holes at the bottom and another 2 holes at the top situated at the opposite ends of the load cell. The holes at the bottom of a load cell were used to mount the load cell on the aluminium frame. A circular aluminium plate (20.5 cm in diameter) was fixed to the top of each load cell through the two holes at the top. PVC pots (with a drainage dish underneath) could be placed over a designated load cell (Fig. 3.3) so that any variation in pot weight could be monitored over time.

Figure 3. 3 An irrigation experiment with wheat in the glasshouse consisting of 4 irrigation treatments arranged in a randomised block design. The front four pots represents one replicate (block) of four irrigation treatments and the front three rows of pots represent the mini-lysimeter system used.

The Wheatstone bridge of each load cell had a single shielded cable that enclosed four individually insulated signal cables, colour coded to represent excitation voltage (+ve with red and –ve with black) and signal voltage (+ve with green and –ve with white). The cable from each load cell was connected to a differential channel of an AM16/32B analogue relay multiplexer (Campbell Scientific, Townsville, Australia). Each differential channel represented two consecutive odd and even, single ended channels that could be switched to high (H) and low (L) with a programmable delay period to provide excitation voltage to the

load cell and collect signal data from the load cell. After connecting all 12 load cells to the multiplexer, the multiplexer was connected to a CR1000 data logger (Campbell Scientific, Townsville, Australia). The data logger and multiplexer connections are shown in Fig. 3.4. The CR1000 data logger consists of a 16-bit microcontroller with 32-bit internal CPU architecture that allows 13-bit analogue to digital conversions with a single DAC (Digital to Analogue Converter) for both signal excitation and measurements essentially known as ratio-metric measurements of signal. Power to the data logger was supplied from a deep cycle, 12 V battery. A replacement battery was used when the battery voltage dropped below 12 V. Typical excitation voltage supplied to each load cell was ±2500 mV to make a full bridge measurement. On most occasions, output signal from the data logger was sampled every minute and then averaged over 10 min. Signal from the twelve load cells were sampled with a one-second delay due to the use of the relay multiplexer with a single data logger.

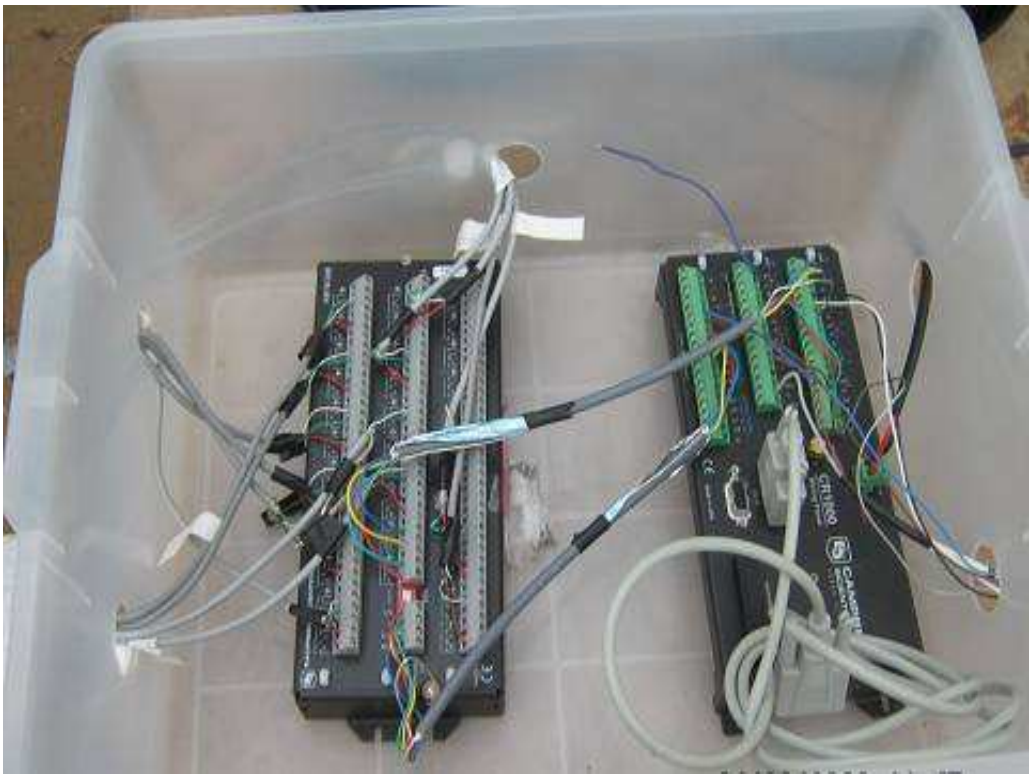

Figure 3. 4 The connections between relay multiplexer (on left) with the data logger (on right) shown for the mini-lysimeter system.

3.2.2 Sensitivity of lysimeters to operating environment

Collection of long-term data from load-cell based lysimeters requires consideration of the adequacy of the data logging system to maintain a consistent performance. It has been noted that when CR1000 data logger is used in a bridge measurement that involves switched voltage excitation, it requires a settling time for the signal to reach its stable value. Sample load cells were subject to settling times within the range of 100-2000 μs to determine appropriate settling time that could be used for signal sampling. During testing for settling time, each signal measurement was repeated 10 times at the selected settling time. The relay multiplexer used with our lysimeter system can also induce a voltage drop that may reduce the excitation voltage at the Wheatstone bridge of the load cell. In order to test if voltage drop has any effect on signal an additional AM16/32A multiplexer was used to bypass the signal relaying multiplexer to provide power for signal excitation. This setting was used to compare signal measurements with and without excitation compensation. For this measurement, unloaded load cells were used for signal collection at 1-minute interval and signal was averaged over a period of 4 min. For a given load cell, 4-min average signal was collected 14-15 times by extending the signal collection period to1 h.

Sensitivity of load cell to variation in temperature was evaluated over a period of 1 week to capture the range of temperature variation expected within the glasshouse. Since all components of the mini-lysimeter system including load cells were aluminium, there was a possibility of partial exposure of aluminium plates (with or without significant load) affecting signal stability. Thus, an experiment was conducted by randomly selecting four lysimeters (as replicates) to allocate three treatments to determine temperature sensitivity of lysimeters (Table 3.2).

Table 3. 2 Treatments used for evaluation of temperature effects on the performance of load cells. Lysimeter plates used for testing are shown by plate nos. 1…12.

Treatments	Plates used for testing	Load (kg)
Zero load + zero shade	P2, P4, P5, P11	0
Small load + full shade	P1, P7, P10, P12	0.1
Large load + full shade	P3, P6, P8, P9	7.4

Variation in air temperature during the experimental period was measured within a distance of 2 m from the lysimeter system using a HMP50-L Vaisala

Humitter temperature and relative humidity probe (Campbell Scientific, Townsville, Australia) mounted within a radiation shield. The effects of hysteresis in load-cell based lysimeters can arise if signal at a given load deviates significantly from its true value when the load cell is subjected to increasing or decreasing load. To test any effect of hysteresis, five load cells were selected randomly to measure the variation in signal to loading and unloading conditions. Hysteresis tests were conducted for a set of six loads (including a zero load) in the range of 0-15.7 kg.

3.2.3 Calibration of lysimeters

The signal measured with a load-cell based lysimeter requires calibration in order to convert signal (mV V^{-1}) data into actual load or weight. Here weight is used instead of mass because load cells need to be subject to a force to cause a variation in load cell signal. Before placing any experimental pots over the load cell plates, all load cells were calibrated using a set of four loads (including a zero load) within the range of 0-8.5 kg. Later the calibration was expanded to include a wider range of loads (0-14.9 kg) to combine with the data used for sensitivity-tests of load cells to hysteresis. During calibration of lysimeters, the weight of the desired load was first measured with a pre-calibrated electronic platform balance of 32 kg capacity (± 0.01 g). For a given load, the load cell signal (mV V^{-1}) was captured at 1 min intervals over a period of 5-10 min. Then the signals were averaged over 5-10 min and plotted against load (g).

3.2.4 Analysis of calibration data

The deflection behaviour of a proving ring as used in classical mechanics is analogous to the stretching behaviour of a strain gauge under load within the elastic range of deflection or deformation. The spring (or in case of a load cell the strain gauge) has a stiffness constant that relates to the linear deflection behaviour under a set of loads (Fig. 3.5). If S is considered as the measured signal (in mV V^{-1}) when the load cell is under a given load (W, g) and S_0 the signal (mV V^{-1}) at zero weight (W = 0 g), then

$$S = S_0 + W/\mathrm{k}, \qquad (3.1)$$

where k = stiffness constant of the load cell (mV V^{-1} g^{-1}). Rearrangement of the terms in Eq. (3.1) gives

$$W = k\,(S\text{-}S_0) \tag{3.2}$$

When a load cell is subject to zero load, including the situation when a plate is fixed to the load cell, $W = W_0 = 0$ and $S = S_0$. Similarly, at a maximum load, $W = W_{max}$ and $S = S_{max}$.

The stiffness coefficient (k, mV V^{-1} g^{-1}) is the slope of the line joining the points (W_0, S_0) and (W_{max}, S_{max}). Thus,

$$k = \frac{S_{max} - S_0}{W_{max} - W_0} = \frac{S_{max} - S_0}{W_{max}} \tag{3.3}$$

because $W_0 = 0$ g.

This is the basis of a 2-point calibration of a load cell that can be used to determine k for prediction of weight (W_p, g) within the range of W and W_{max} for unknown measured signal within the range of S and S_{max}. Although statistical fit of a linear relationship between S and W is usually good and has a coefficient of determination for the regression $R^2 \sim 1$, the fitted line describes a load-cell response to minimise the deviation (measured weight – estimated weight) at each measurement point. This deviation can be manipulated to some degree if it is not within acceptable limits of predicted weight.

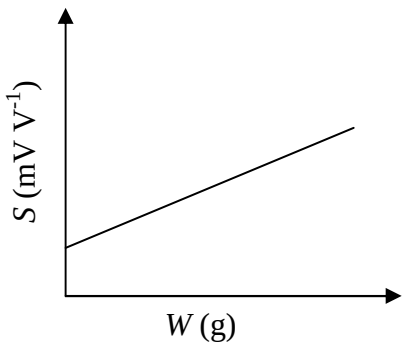

Figure 3. 5 Linear behaviour of signal (S) from a load cell as a function of increased load.

3.2.5 Experimental set up for lysimeter evaluation

Glasshouse experiments for wheat (*Triticum aestivum* L.) and cotton (*Gossypium hirsutum* L.) crops were conducted in a glasshouse of the University of Southern Queensland, Toowoomba, Australia using the soil from the top 15 cm depth of an experimental field at Kingsthorpe research station (27°30'44"S, 151°46'55"E, and 431 m elevation) of the Queensland Primary Industries and Fisheries (now referred to as Department of Employment, Economic development and Innovation). The soil at this experimental site was a haplic, self-mulching, black vertosol (Isbell, 1996). This soil is a medium to heavy, cracking clay soil with 76% clay, 14% silt and 10% sand in the surface horizons. The organic carbon content of the soil was 1.3%, pH 7.2, EC 0.35 dS m^{-1} and CEC 86 $cmol_c$ kg^{-1} (Foley & Harris, 2007; Ghadiri et al., 1999). Field bulk density of this soil was 1200 kg m^{-3}.

Sufficient soil (approx. 360 kg) was collected from the top 15 cm depth of the experimental site when the ground was moderately dry and then transported to the laboratory. Large aggregates were broken by hand and stones and other organic debris were removed. Then the soil was sieved to collect aggregates of <9.5 mm size. Soil retained over the sieve was further broken down with a wooden hammer to increase extraction of soil of <9.5 mm size. After sieving, the soil was stored in several air tight plastic containers to reduce loss of moisture and its variation over time.

3.2.6 Preparation of pots

The drainage holes of pots used for the experiment were first sealed with a porous, pot lining material to prevent soil loss from the pots during drainage. Then the weight of each pot and its drainage dish was taken with an electronic platform balance of 32 kg capacity (± 0.01 g). Soil was then removed from the plastic storage containers and mixed before being packed into several PVC pots (25.2 and 16.7 cm, top and bottom diameters respectively, and 23.2 cm height) to achieve a bulk density of 0.89 g cm^{-3}. This bulk density was close to the soil bulk density measured at the field site. Soil was compressed with a wooden platen in several layers of 4.5 cm thickness to achieve uniform compaction. The surface of each compacted layer was slightly disturbed with a spatula before packing the next layer to reduce soil layering.

The final depth of the compacted soil in each pot was 19.2 cm. During packing of each pot, a sample of soil was put aside to determine the initial moisture content of soil in each pot. Soil was compacted in 31 pots for the experiment. The weight of each pot was measured with the electronic platform balance to estimate the amount of air-dry soil in each pot. Soil samples taken for each pot during packing were dried in a convection oven for 2 days at 105 °C and subsequently weighed to estimate the moisture content of soil to estimate its oven dry mass in each pot at the time of packing. Of the 31 pots, 28 pots were used for growing plants and the remaining 3 pots to measure the field capacity (FC) of soil. All pots were placed inside a well ventilated glasshouse.

3.2.7 Irrigation treatments

Twenty eight pots were used to randomly allocate four irrigation treatments to each of seven blocks (replicates). Twenty pots were used for non-destructive measurements on plant and soil and the remaining 8 pots for destructive measurement. Irrigation treatments were based on the field capacity (FC) of soil. FC is defined as the water retained in soil on a volumetric basis when it is saturated and allowed to drain over time (in absence of evaporation) until drainage becomes negligible. In order to determine FC, soil in 3 pots was fully saturated with tap water until free drainage was visible and continued for a few minutes. Then irrigation was discontinued and each pot was kept covered on the top with cling wrap and plastic bags to minimise any exposure of soil to radiation and soil evaporation. Pots were kept inside the glass house under the same condition as the other pots to allow soil water redistribution within each pot for 2-3 days. Then the soil from each pot was removed and placed in large metal trays for drying at 105 °C over 2-3 days. The weight of oven-dry soil was measured with a balance to estimate gravimetric soil moisture content at FC at the bulk density used for the pot experiment. Other experimental pots were irrigated in the same way as the pots used for FC measurement. Irrigation treatments used for the experiment included: T80 – 80% of FC, T70 - 70% of FC, T50 - 50% of FC and T40 - 40% of FC. Irrigation was given to a pot when its weight (or volumetric soil water content) dropped to these percent of FC values.

Of the 28 experimental pots, 12 pots (representing three replicates of four irrigation treatments) were placed over the mini-lysimeter system for monitoring of pot weights over time. All experiments in the glasshouse with cotton or wheat were based on a randomised block design involving the irrigation treatments described above. Since the regression of load (g) against signal (mV/V) for all 12 load cells was linear with a coefficient of determination ($R^2 > 0.99$ and $P<0.001$), slope and intercept parameters of the regression equations were used in developing a data logger program that provided estimates of pot weight (g) at 10 min intervals each day during crop growth experiments for wheat and cotton. On a few occasions, pots were removed from the mini-lysimeter system temporarily to measure their weights with a pre-calibrated electronic balance for comparison with the mini-lysimeter output. In each experiment, 16 pots (4 treatments × 4 replicates) were placed on a bench adjacent to the mini-lysimeter system inside the glasshouse at the same height as the lysimeter pots. A portable weather station was mounted on the glasshouse bench adjacent to the pot experiment at approx. 1 m height to record air temperature (°C), relative humidity (%) and solar radiation (W m^{-2} or MJ m^{-2}). During the experimental period both air temperature and relative humidity were measured with a HMP50-L Vaisala Humitter temperature and relative humidity probe (Campbell Scientific, Townsville, Australia) mounted within a radiation shield. Solar radiation was measured with SP110 Apogee silicon-cell pyranometer levelled with AL-100 Apogee PYR-P-L pyranometer levelling base.

3.2.8 Wheat

An irrigation experiment with wheat (*Triticum aestivum* L., cv. Lang) was conducted within the glasshouse from 31st July 2008 to 5th December 2008. Daily maximum and minimum air temperature during the experimental period was in the range of 12.6–41.8 °C and relative humidity 22 – 81%. Seven uniform sized wheat seeds were planted in each pot at 4-5 cm depth of soil on 31st July 2008. After planting, each pot was brought to FC by adding tap water to help germination and seedling establishment. After irrigation each pot was fertilized with 0.94 g of Urea (equivalent to 100 kg N ha^{-1} in field) and 3 g of Super phosphate (equivalent to 60 kg P ha^{-1} in field). Additional 0.94 g of Urea was applied to all the experimental pots at 60 days after planting. About 90% of plants emerged within 8 days after planting (DAP) and

subsequently thinned on 21st August 2008 (21 DAP) to leave 3 plants per pot. Six drops of Yates product confider (active ingredient Midacloprid) was diluted to 1 litre and was applied on 6th and 8th of October to control aphids on wheat plants.

All pots remained under the same soil water deficit up to 55 DAP. The timing and frequency of irrigation for various pots varied after this time to allow a range of soil water deficit to develop in the pots. The irrigation treatment was imposed by checking the weight of pots from the load cell data and also by weighing the remaining pots with an electronic platform balance with a resolution of ± 0.01 g. Irrigation was applied to each pot when its weight reached 40 – 80% of its weight at FC. Irrigation was applied 2, 5, 10 and 15 occasions for T40, T50, T70 and T80 treatments, respectively during 56 -107 DAP. Before irrigation was applied, the weight of each pot was also measured with the balance to determine the amount of water deficit present and the amount required to irrigate each pot. During irrigation, tap water was added slowly at the centre of the pot to ensure that it was distributed through the soil in the pot while avoiding water flow along the soil-pot interface. Irrigation was suspended after 107 DAP. The volume of irrigation water applied and drainage collected in the drainage dish was measured for each pot throughout the experiment. Net amount of irrigation water retained in soil during an irrigation event was measured by weighing each pot before irrigation and 2-4 h after irrigation (when drainage ceased) with the electronic balance. 425.4, 370.2, 312.3 and 210.2 mm of irrigation was applied for T80, T70, T50 and T40 irrigation treatments, respectively for the wheat crop.

3.2.9 Cotton

An experiment similar to wheat was also conducted with cotton (*Gossypium hirsutum* L.) using the same set up inside the glass house from 12th December 2008 to 4th June 2009 (Fig. 3.6). Bollgard II cotton variety Sicala 60 BRF was used in this experiment. Daily maximum and minimum air temperature during the experimental period was in the range of 11.6 – 44.4 °C and relative humidity 20 – 85%. Three uniform sized cotton (*Gossypium hirsutum* L.) seeds were planted in each pot at 4-5 cm depth of soil on 12th December 2008. After planting, each pot was brought to field capacity by adding tap water to help germination and seedling establishment. Each pot was fertilized with 0.56 g of Urea (i.e. equivalent to 126 kg ha^{-1} of Urea in

field) on 17th December 2008 (5 DAP). All plants emerged at 5 DAP and subsequently thinned to 1 plant per pot on 30th December 2008 (18 DAP). In order to control an infestation of mite on the cotton crop during 13-23 February 2009 (63-73 DAP) a systemic insecticide ROGOR 100 (constituent - Dimethoate) was sprayed twice after mixing 1.5 ml of the insecticide with 1.5 litre of water. At 70 DAP (20th Feb 2009), an additional 0.84 g of Urea (i.e. equivalent to 190 kg ha^{-1} of Urea in field) was applied to each pot.

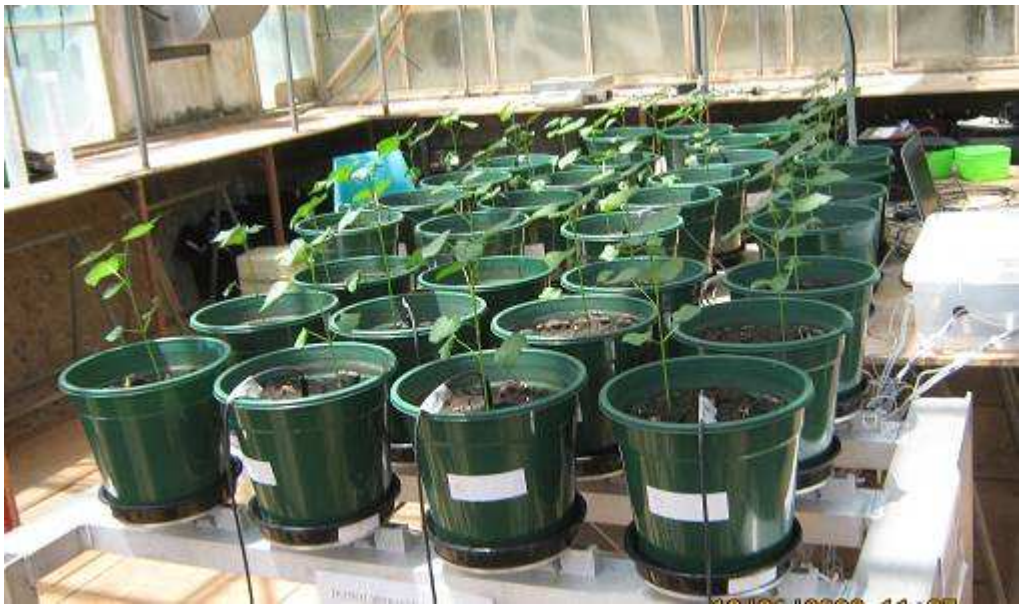

Figure 3. 6 An irrigation experiment with cotton in the glasshouse consisting of 4 irrigation treatments arranged in a randomised block design. The front four pots represents one replicate (block) of four irrigation treatments and the front three rows of pots represent the mini-lysimeter system used.

All pots were maintained under the same soil water deficit up to 100 days after planting. After 100 DAP, irrigation frequency for each pot varied over time to allow cotton plants to experience a range of soil water deficit as required for the irrigation treatments T40…T80, that was described for wheat. The weights of pots derived from the load cell data were supplemented with manual weighing of the pots with an electronic balance. Irrigation was applied 2, 4, 10 and 14 occasions for T40, T50, T70 and T80 treatments, respectively from 101 to 152 DAP. All procedures used for irrigation application and measurements of soil water deficit, volume of irrigation and drainage remained similar to that described for wheat. 614.9, 585.9, 514.3 and 417.5 mm of irrigation was applied for T80, T70, T50 and T40 irrigation

treatments, respectively for the cotton crop. Table 3.3 shows the various irrigation treatments allocated for 12 load cells (numbered as P1…P12) for wheat and cotton crop.

Table 3. 3 Irrigation treatments assigned to 12 load cells of the mini-lysimeter system used for the wheat and cotton experiments.

Irrigation treatments	Load cells
T80	P3, P6, P12
T70	P2, P5, P9
T50	P1, P8, P10
T40	P4, P7, P11

3.3 Results and Discussion

3.3.1 Effects of operational environment on lysimeter performance

Variation in load-cell signal over a range of settling time is shown for a typical load cell in Fig. 3.7. Since, the average signal varied little (small SE) at any of the settling time used and the signal did not vary much over the range of settling time used, a default settling time of 450 μs was used for all signal collections.

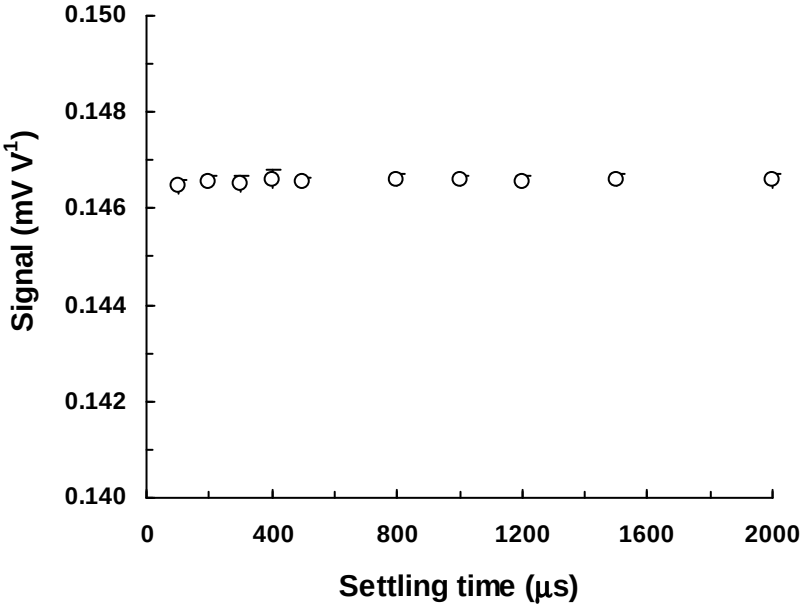

Figure 3. 7 Effects of signal settling time on load cell signal when it is loaded with a small load (~0.9 kg). Vertical bars over mean values indicate standard errors (SE, *n* = 10).

Voltage required to excite load cells may affect the measured signal when the required voltage is supplied via a multiplexer. Load cell signals measured at zero load with and without any compensation of excitation voltage were measured for each of 12 load cells. These data are presented in Fig. 3.8 which showed no significant differences arising from compensation of excitation voltage. Variation in ambient temperature may cause a thermal shift in load cell signal although it appears to be of minor importance (Martin et al., 2001). In this study, a separate experiment was conducted to study variation of signal for sample load cells over time when some of the load cells were continuously shaded with or without a significant load or remained unshaded without a significant load (Table 3.4). Variation in signal and air temperature over time is shown in Fig. 3.9. Although air temperature fluctuated within the range of 6-24 °C, signal remained more or less constant over time. This suggested that thermal shift in the load cell signal was not likely to influence long term measurements.

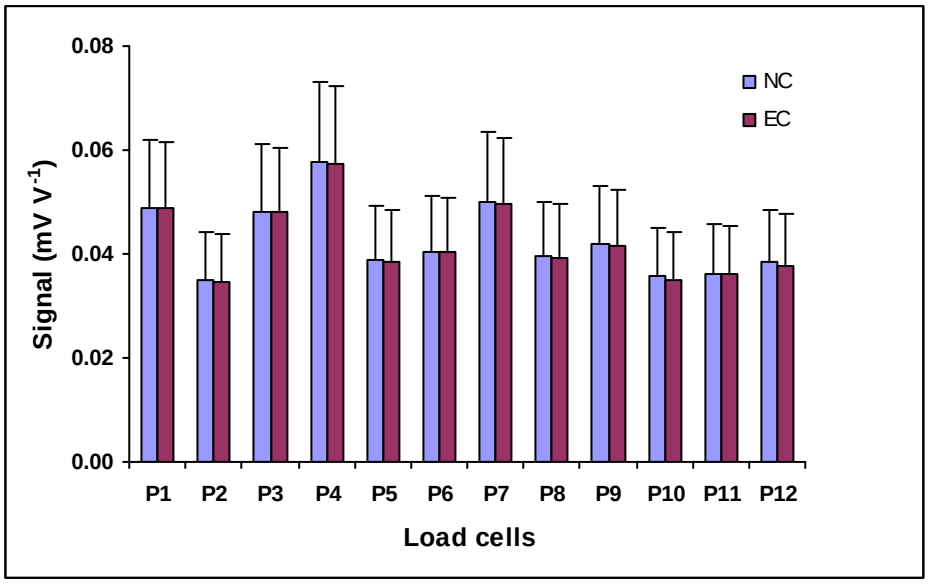

Figure 3. 8 Effects of voltage excitation compensation on measured signal from unloaded load cells. NC and EC respectively refer to uncompensated and compensated situations for the excitation voltage supplied to the load cells. Vertical bars over mean values indicate standard errors (SE) for 14-15 repeated measurements.

Performance of load cell based lysimeters can be influenced by hysteresis when these are exposed to an increase in load (for example during irrigation) or a decrease in load (as during evapotranspiration). The difference in signal measured by

a load cell at a given load due to an increase in load from a low load or a decrease in load from a high load is referred to as hysteresis.

Table 3. 4 Effects of shading and loading on load cell signal. Mean value and standard error (SE) for signal is based on four separate load cells (n = 4).

Treatments	Signal (mV V^{-1}) ± SE
Zero load + zero shade	0.0425 ± 0.000018
Small load + full shade	0.0445 ± 0.000019
Large load + full shade	0.7679 ± 0.000025

Five separate load cells were used to investigate the effects of hysteresis over six separate loads covering a load range of 0-15.7 kg. Regression lines were fitted to these data in a way similar to that shown by Payero and Irmak (2008). Since there was no significant difference in signal during loading and unloading conditions for these five load cells, there was an overlap of regression lines fitted to signal vs. load data (graph not shown). Regression coefficients (intercept and slope parameters) and other statistical parameters are presented in Table 3.5. All parameters shown in Table 3.5 were compared with a t-test that indicated no significant difference between load cells due to hysteresis.

Table 3. 5 The effects of loading and unloading of load cells on the parameters of a 6-point calibration equation $W = a_1 + b_1 S$, where W and S, respectively refer to fixed load on the load cell (g) and measured signal (mV V^{-1}). Intercept and slope parameters of the calibration equation were a_1 and b_1, respectively. Coefficient of determination (R^2) for all regression equations was 1.00 and P-value of the fitted regression was ≤0.001. Standard errors (SE) of the fitted parameters are shown (n = 6).

Load cell no.	a_1 (g)	SE of a_1	b_1 (g mV^{-1} V)	SE of b_1
Increased loading of load cells from zero load				
1	-505.46	1.49	10002.33	1.59
4	-587.01	0.84	10230.93	0.91
6	-389.59	4.92	10015.72	5.31
8	-404.84	0.87	10325.66	0.96
11	-348.33	1.45	10436.40	1.64
Decreased loading of load cells from a maximum load				
1	-521.07	2.47	10010.84	2.63
4	-593.70	0.68	10236.07	0.74
6	-384.36	1.39	10018.47	1.50
8	-413.03	0.57	10331.27	0.63
11	-343.22	1.56	10433.87	1.75

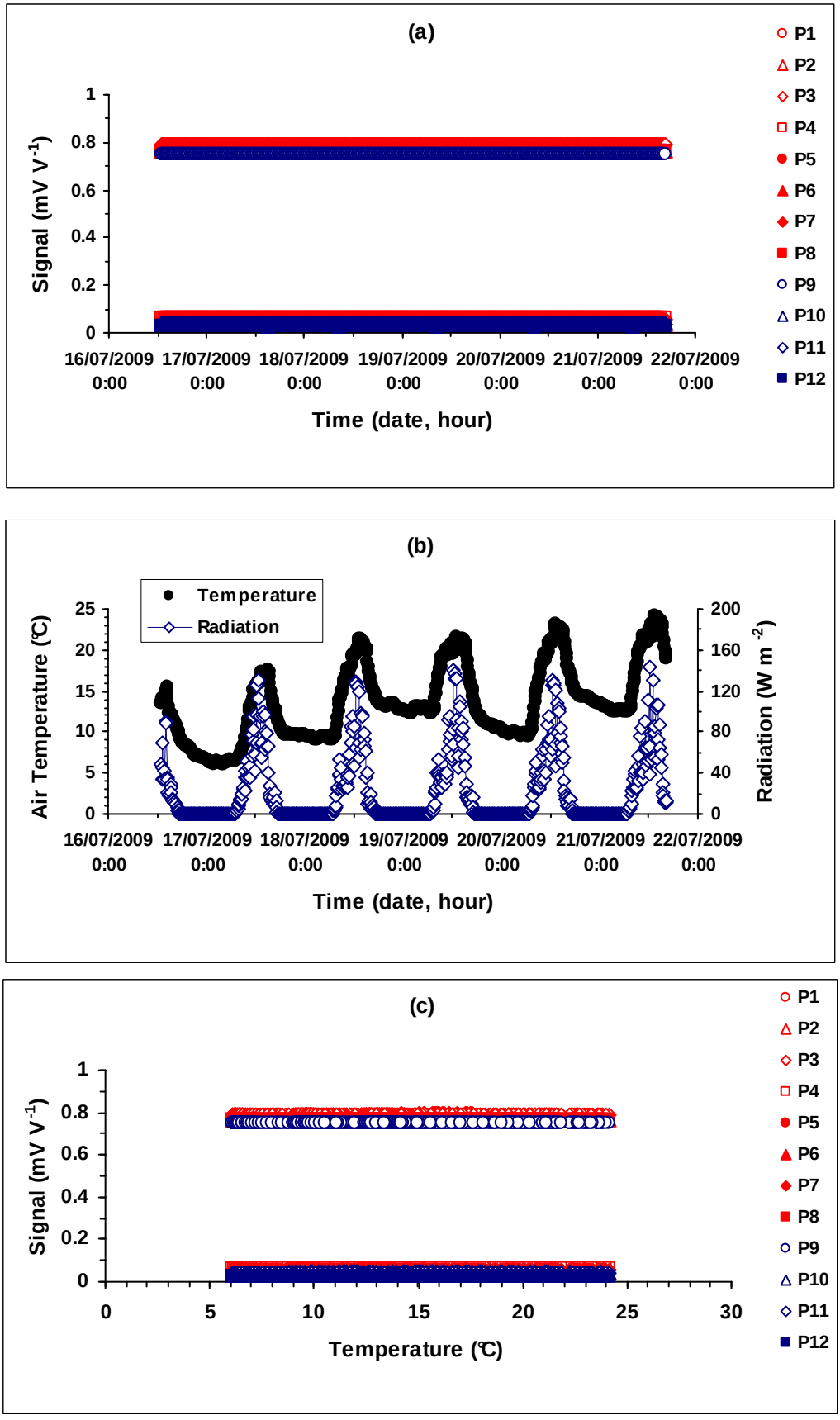

Figure 3. 9 Simultaneous variations of (a) load cell signal and (b) air temperature over time. A plot of signal against temperature is shown (c).

3.3.2 Calibration of lysimeters

Table 3.6 shows the results of a 4-point calibration equation with a linear regression used to represent the variation in signal (*S*, mV V^{-1}) with load (*W*, g). The slope and intercept parameters shown in this table indicated that all 12 load cells had a unique slope of 0.0001 mV V^{-1} g^{-1} with $R^2 = 1$, except for a limited number of load cells (numbered as 4, 5 and 6) for which R^2 was <1. Although it is relatively easier to predict *W* from *S* by rearrangement of terms in the equation $S = a_2 + b_2 W$ as $W = (S-a_2)/b_2$, the right hand side of this equation represents a ratio of two random variables (*S* and b_2) that could introduce bias and there is no exact expression for its standard error (P 171, Snedecor and Cocharan, 1989). Thus, it is useful to develop regression equation by switching the variables. Table 3.7 shows the parameters of the 4-point calibration equation assuming the dependence of *W* on *S*. Some improvements in R^2 can be seen in Table 3.7 compared to Table 3.6 although data used for both regressions were the same. It can be also seen from Table 3.7 that standard errors of both slope and intercept parameters were much larger for load cells numbered 4…6 compared with the remaining load cells.

Table 3. 6 Parameters of a 4-point calibration equation $S = a_2 + b_2 W$, where *W* and *S*, respectively refer to fixed load placed on the load cell (g) and measured load cell signal (mV V^{-1}). Intercept and slope parameters of the calibration equation are a_1 and b_1, respectively. Coefficient of determination (R^2) for the regression equation is shown. For all fitted regressions, $P \leq 0.001$.

Load cell no.	Intercept (a_2, mV V^{-1})	Slope (b_2, mV V^{-1} g^{-1})	R^2
1	0.04830	0.00010	1.00000
2	0.03593	0.00010	1.00000
3	0.04947	0.00010	1.00000
4	0.05209	0.00010	0.99932
5	0.04246	0.00010	0.99984
6	0.04526	0.00010	0.99984
7	0.04931	0.00010	1.00000
8	0.03856	0.00010	1.00000
9	0.04104	0.00010	1.00000
10	0.03446	0.00010	1.00000
11	0.03499	0.00010	1.00000
12	0.03702	0.00010	1.00000

In order to select a method of calibration that would suit most load cells used for the mini-lysimeter system, a comparison was made using 4-point calibration with

load increasing from zero (method 1), 6-point calibration with load increasing from zero (method 2) and 6-point calibration with load decreasing from 15.7 kg as the maximum load (method 3). A plot of the difference between estimated and measured load with each method is shown as a function of measured load (Fig. 3.10). It can be seen from this figure that 4-point calibration (method 1) was unsuitable since the deviation of the estimated load from true load was ±60 g that was three times the deviation achieved with methods 2 or 3. Thus, a 6-point calibration was performed for all load cells. The calibration results are shown in Fig. 3.11 and related data in Table 3.8. It can be seen that the standard errors for parameters were reasonable for all load cells except for the load cell no. 7 that caused a maximum deviation of ±80 g (Fig. 3.12). In order to minimise this deviation (D), a 4th order polynomial function ($D = 25.8 - 0.034W_1 + 1.31\times10^{-5}W_1^2 - 1.87\times10^{-9}W_1^3 + 7.79\times10^{-14}W_1^4$) was fitted as a function of estimated weight (W_1) that could be used to obtain a final estimate of weight from signal after applying correction to the first estimate of weight (using the calibration parameters shown in Table 3.8). The effect of this correction on the performance for lysimeter no. 7 is shown in Fig. 3.13 which brought deviations for all load cells to within ±12 g of the measured load. Using this calibration approach, pot weights could be predicted well with the measured weight (Fig. 3.14).

Table 3. 7 Parameters of a 4-point calibration equation $W = a_3 + b_3 S$, where S and W, as defined before in Table 3. Intercept and slope parameters of the calibration equation were a_3 and b_3, respectively. Coefficient of determination (R^2) for the regression equation is shown. Standard errors (SE) of the fitted parameters are shown (n = 4). For all fitted regressions, P≤0.001.

Load cell no.	intercept (a_3, g)	SE of a_3	Slope (b_3, g mV^{-1} V)	SE of b_3	R^2
1	-483.038	0.227	10001.236	0.471	1.000
2	-362.582	0.630	10092.370	1.350	1.000
3	-499.317	0.436	10093.380	0.918	1.000
4	-529.600	89.000	10206.000	188.000	0.999
5	-424.400	42.800	10008.300	89.600	1.000
6	-456.200	42.800	10090.200	90.200	1.000
7	-504.982	0.797	10241.650	1.690	1.000
8	-397.955	0.842	10321.350	1.830	1.000
9	-420.105	0.540	10237.240	1.150	1.000
10	-352.153	0.403	10217.709	0.874	1.000
11	-364.910	2.410	10429.410	5.340	1.000
12	-380.750	1.630	10284.230	3.540	1.000

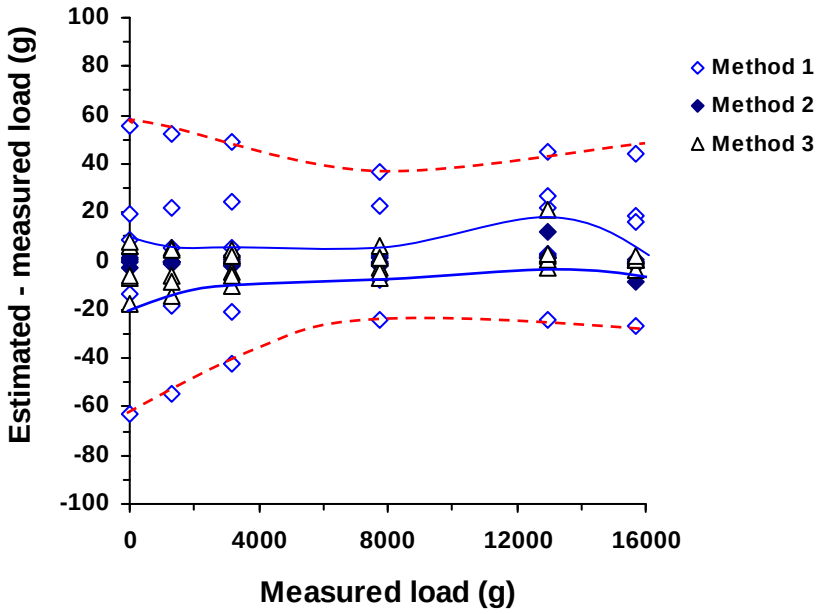

Figure 3. 10 Variation in deviation of estimated load from measured load for selected load cells as a function of measured load with three methods of estimation. Dashed line indicates the upper and lower boundaries of the deviation of load as a function of measured load for method 1 and the solid line shows the boundaries of combined deviation for methods 2 and 3.

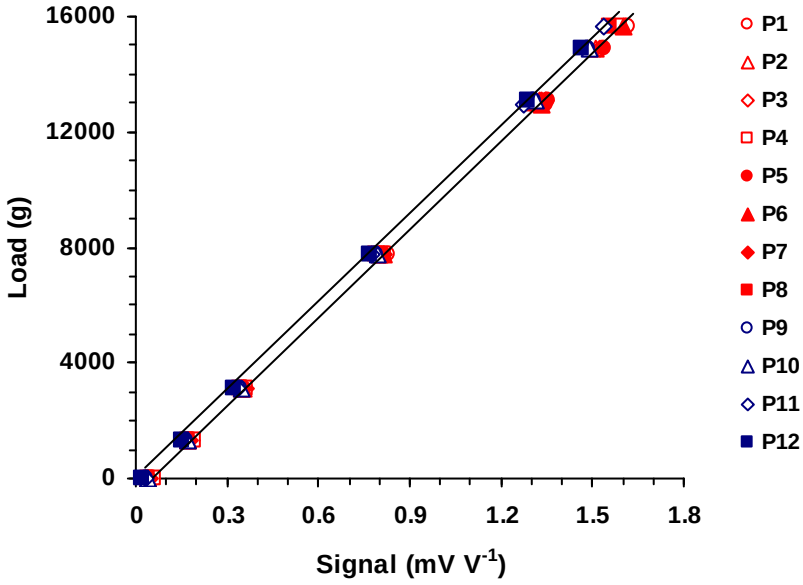

Figure 3. 11 Joint variation in load and signal measured with a 6-point calibration method for 12 load cells. Calibration equation parameters fitted to these data are given in Table 3.8.

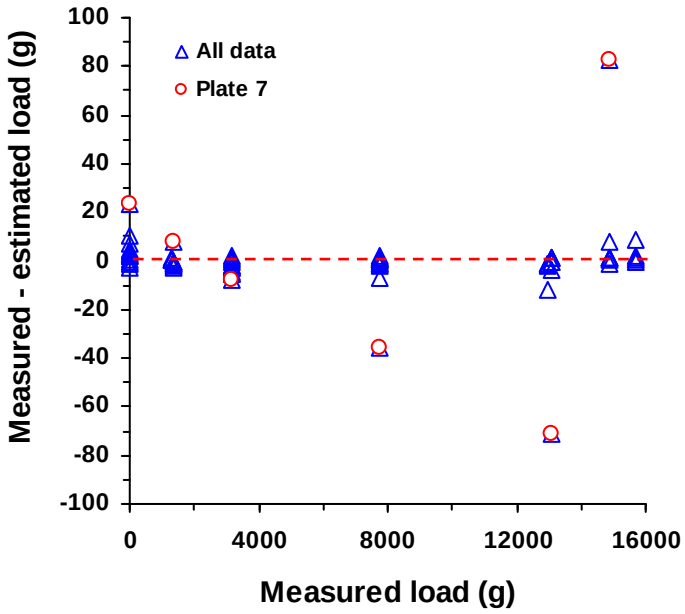

Figure 3. 12 Variation in deviation of estimated load from measured load over the range of measured loads for all load cells using a 6-point calibration equation.

For lysimeters, the resolution often indicates a minimum increment of measureable ET expressed in mm of water as loss of water and should also apply to gain of water from irrigation. On many occasions, it is an indicator of the sensitivity of the lysimeter as the interaction between lysimeter area, weighing system (mechanical or electrical device used) and data recording system can be quite complex.

Table 3. 8 Parameters of a 6-point calibration equation $W = a_4 + b_4 S$, where W and S, respectively refer to fixed loads on the load cell (g) and measured signal (mV V^{-1}). Slope and intercept parameters of the calibration equation were a_4 and b_4, respectively. Coefficient of determination (R^2) for all regression equations was 1.00 and P-value of the fitted regression was ≤0.001. Standard errors (SE) of the fitted parameters are shown (n = 6).

Load cell no.	intercept (a_4, g)	SE of a_4	Slope (b_4, g mV^{-1} V)	SE of b_4
1	-505.46	1.49	10002.33	1.59
2	-369.80	1.61	10097.97	1.79
3	-504.08	0.95	10103.12	1.04
4	-587.01	0.84	10230.93	0.91
5	-383.34	5.23	9947.36	5.72
6	-389.59	4.92	10015.72	5.31
7	-517.60	38.60	10312.50	43.30
8	-404.84	0.87	10325.66	0.96
9	-372.51	1.31	10262.97	1.48
10	-378.43	3.02	10221.60	3.40
11	-348.33	1.45	10436.40	1.64
12	-199.52	2.05	10292.36	2.36

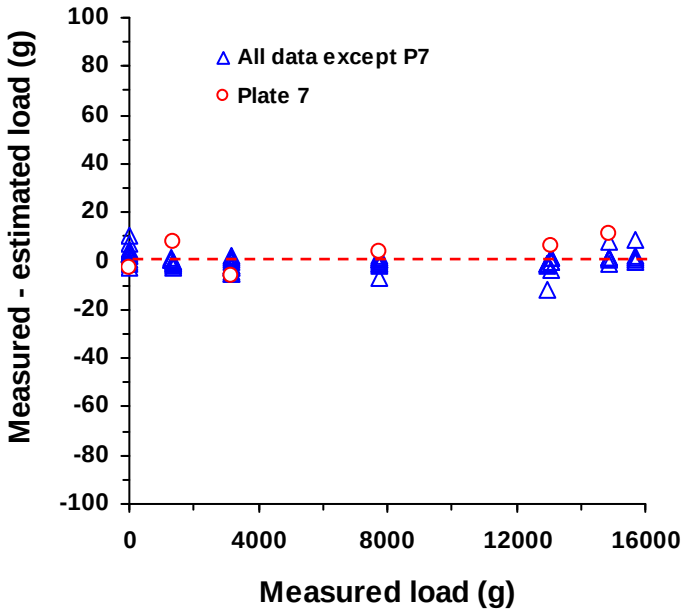

Figure 3. 13 Variation in deviation of estimated load from measured load over the range of measured load after minimisation of deviation for Plate 7.

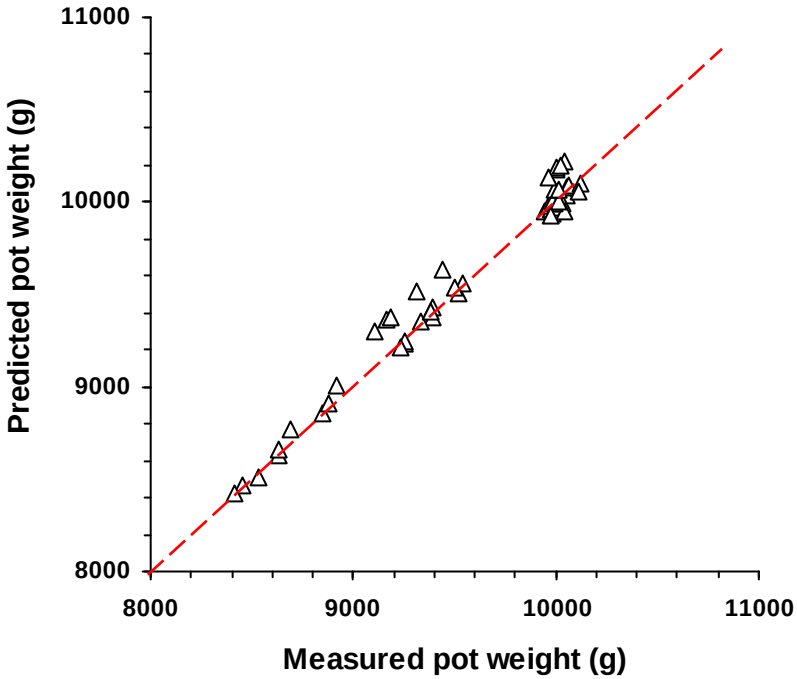

Figure 3. 14 Application of final calibration equation to new measurements of load. Variation in predicted pot weight over a range of measured pot weights is shown along with a dashed, 1:1 line.

A review of the performance of various lysimeters in terms of their sensitivity is given by Payero and Irmak (2008). Since the mini-lysimeter system described here is able to measure a weight that deviates from the measured load by

±12 g, this weight is equivalent to 0.027 mm of water based on the soil surface area of 441.3 cm^2 for the pots shown in Fig. 3.3. Although overall resolution of a lysimeter system is dependent on the capability of the data logger in terms of voltage resolution and representation of significant digits (Payero and Irmak, 2008), these are not considered further as effective calibration and deviation minimisation schemes described here incorporate these essential features of the measurement system used.

3.3.3 Estimation of daily change in soil water from lysimeter measurements

Fig. 3.15 shows plotted values of variation in stored soil water (θ, mm) as a function of time (date, hour) during the year for various irrigation treatments applied to the wheat crop during the experiment. For each replicate pot (lysimeter) of the irrigation treatments used, values of stored soil water are shown at 10 min interval for each day in Fig. 3.15. In order to calculate stored soil water, the weights of the lysimeter pots were collected from the data logger to estimate gravimetric soil water content. The gravimetric soil water content was then multiplied by the bulk density of soil in the pot to obtain an estimate of volumetric soil water content (θ, $m^3\ m^{-3}$). Finally, θ was converted to mm of water by multiplying it with the effective depth of soil in each pot (i.e. 192 mm). It can be seen from Fig. 3.15 that up to 55 days after planting (i.e. 25th September 2008), there was a steady decline in θ for all irrigation treatments as no irrigation treatment was imposed. After 55 DAP, soil water values changed over time for each irrigation treatment depending on the frequency of irrigation. Since pots under T80 irrigation treatments were more frequently irrigated than T40 irrigation treatment, changes in θ reflected the cyclic behaviour in relation to irrigation treatments imposed (Fig. 3.15). The behaviour of replicate pots (load cells) of each irrigation treatment was similar. Plotted values of variation in θ at 10 min interval for various irrigation treatments given to the cotton crop in the glasshouse are shown in Fig. 3.16. Stored soil water for cotton was calculated in the same way as described for wheat. It can be observed from Fig. 3.16 that θ fluctuated initially with time for all the irrigation treatments during 12th December 2008 to 22nd March 2009 as all pots were irrigated with the same frequency until specific irrigation treatments were imposed.

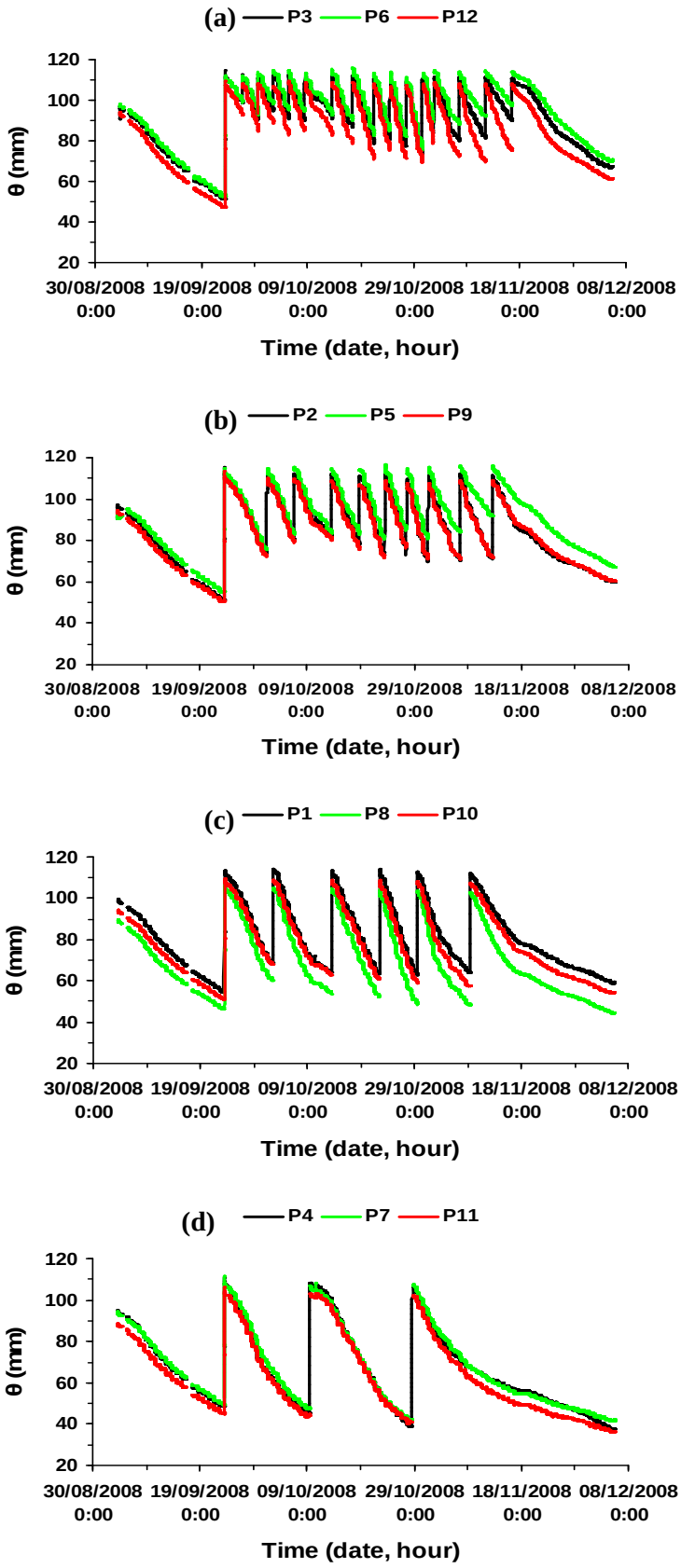

Figure 3. 15 Daily changes in stored soil water (θ, mm) for the wheat crop as a function of the time (date, hour) of the year for (a) T80, (b) T70, (c) T50 and (d) T40 irrigation treatments. Separate lines indicate replicates within irrigation treatments shown as lysimeter plates by number. Total number of data (n) plotted was 13232.

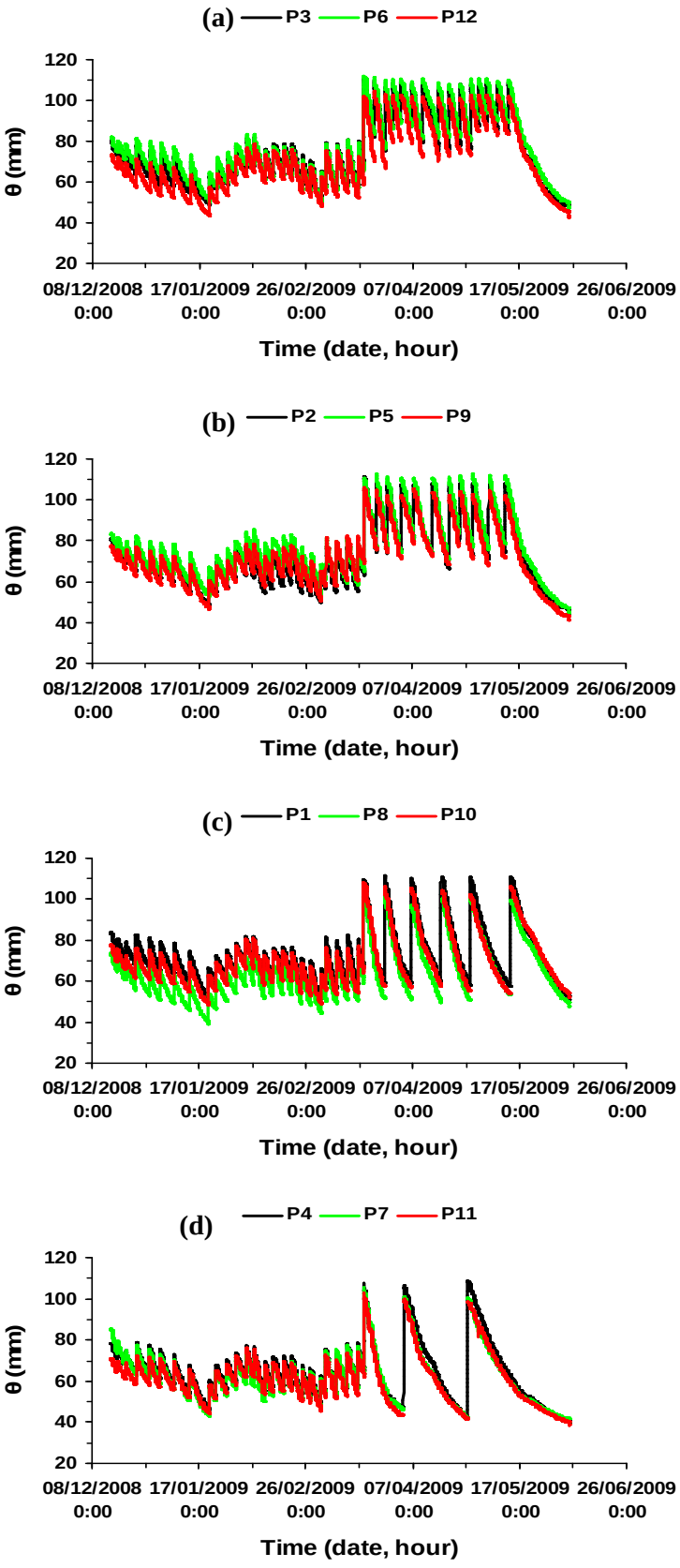

Figure 3. 16 Daily changes in stored soil water (θ, mm) for the cotton crop as a function of the time (date, hour) of the year for (a) T80, (b) T70, (c) T50 and (d) T40 irrigation treatments. Separate lines indicate replicates within irrigation treatments shown as lysimeter plates by number. Total number of data (n) plotted was 24723.

3.3.4 Comparison of stored soil water between lysimetric and nonlysimetric measurements

Stored soil water was calculated for all pots in the experiment in two ways: first, from pot weights as retrieved from the data logger (lysimeteric measurements) and second, from manual weighing of pots before and after each irrigation (nonlysimeteric measurements). All nonlysimetric measurements were made with an electronic platform balance after temporary removal of pots from the load cells used for the lysimetric measurements. Stored soil water (θ, mm) was calculated for both types of measurements. A comparison of stored soil water with these two measurements for wheat and cotton are shown in Figures 3.17 and 3.18, respectively.

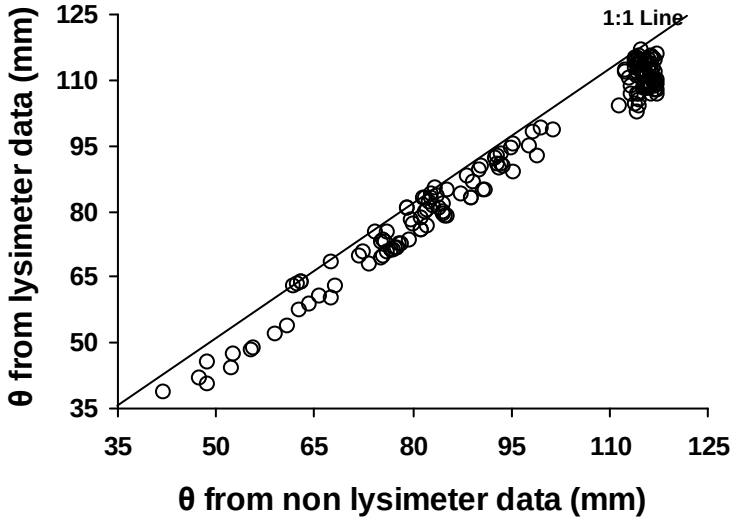

Figure 3. 17 Variation in stored soil water (θ, mm) with lysimetric measurement as a function variation in nonlysimetric measurements for wheat.

Since θ (mm) with lysimetric measurement (θ_l) was slightly below the 1:1 line, it can be concluded from these figures that overestimation of θ with nonlysimetric measurement (θ_{nl}) was due to the accumulation of biomass due to crop growth. Since nonlysimetric measurements are usually made at long time intervals, it is possible to correct ET for biomass accumulation using lysimetric measurements by using equations 3.4 and 3.5, because at short time intervals contribution to biomass via crop growth is less than water use (ET).

$$\theta_l = 0.98\ \theta_{nl} - 2.1 \qquad (3.4)$$

$$\theta_l = 0.96\ \theta_{nl} - 1.4 \qquad (3.5)$$

where, θ_l and θ_{nl} represents estimation of stored soil water (θ, mm) from lysimeteric and nonlysimetric measurements for wheat and cotton crop respectively.

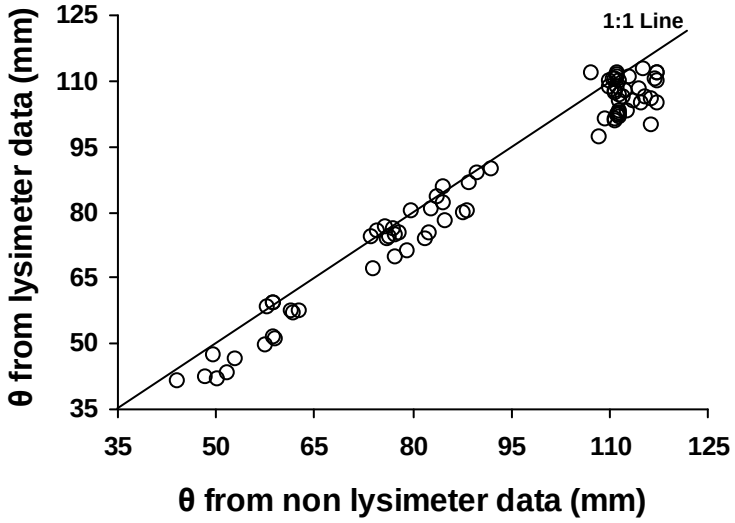

Figure 3. 18 Variation in stored soil water (θ, mm) with lysimetric measurement as a function variation in nonlysimetric measurements for cotton.

3.3.5 Estimation of evapotranspiration from lysimeter measurements

For both wheat and cotton, evapotranspiration (ET, mm) for a given day was estimated by taking the difference between stored soil water calculated from lysimeter data at 24 h interval (i.e. 12 A.M. of that day to 12 A.M of the next day) of time. Plotted values of ET (mm) against days after planting for various irrigation treatments of wheat and cotton crops are shown in Figures 3.19 and 3.20. These figures show the variation in ET for various irrigation treatments during the entire growth period for both crops. It can be seen from Fig. 3.19 that ET values gradually decreased from T80 to T40 irrigation treatments as T80 was more frequently irrigated than T40. ET values varied from 0.2-15, 0.2-12.3, 0.4-11.7 and 0.1-7.5 mm for T80, T70, T50 and T40 irrigation treatments, respectively for the wheat crop. Seasonal ET varied from 478.2, 391.8, 338.4 and 233.4 mm for T80, T70, T50 and T40 irrigation treatments, respectively for the wheat crop. Low values of ET for wheat at the early period of growth and towards the end of the crop growth period due to maturity of the crop can be observed in Fig. 3.19. High values of ET for wheat occurred during 75 to 95 days after planting for all the irrigation treatments. For the cotton crop, ET values decreased from T80 to T40 treatment, but there was greater temporal variation in ET values among the irrigation treatments than for wheat due to the longer period of crop growth (Fig. 3.20).

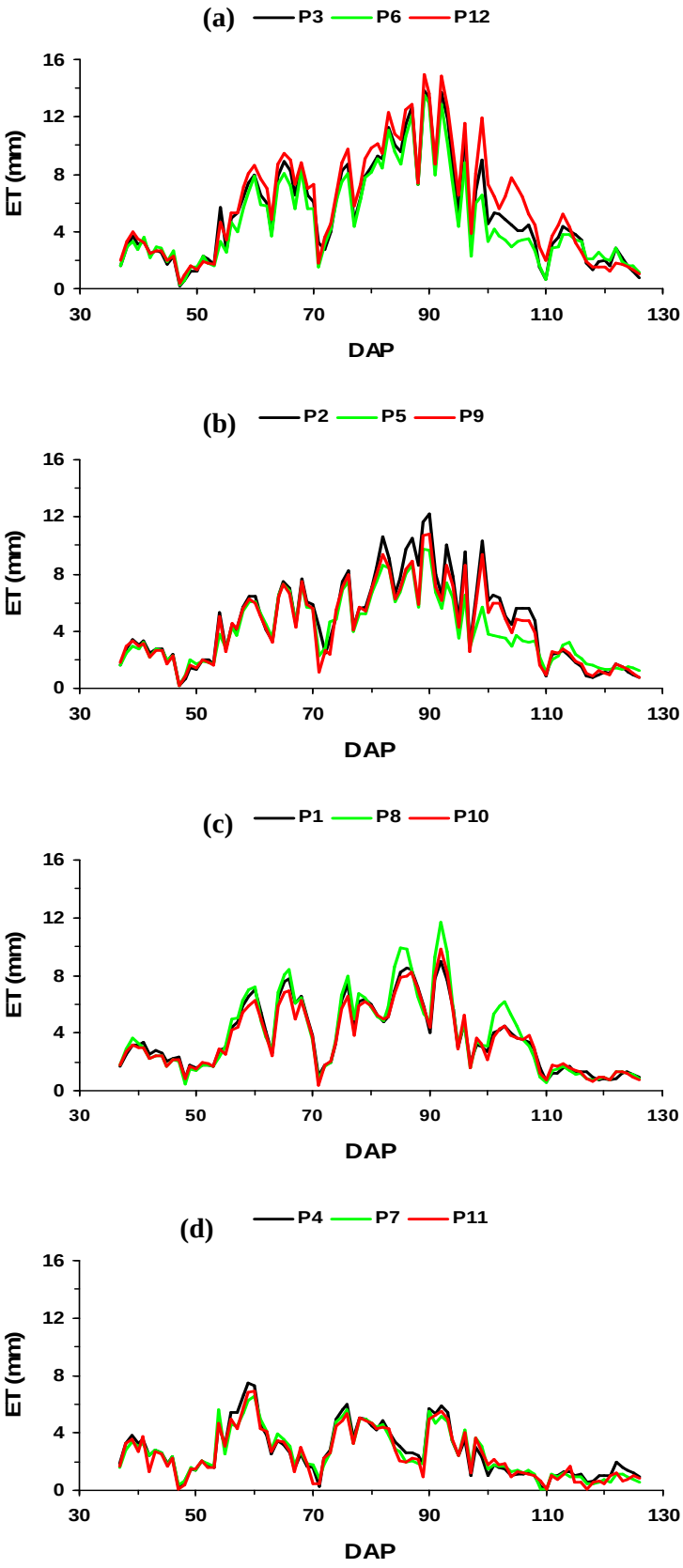

Figure 3. 19 Evapotranspiration (ET, mm) estimated from lysimeter data for (a) T80, (b) T70, (c) T50 and (d) T40 irrigation treatments given to wheat. Separate lines indicate replicates within irrigation treatments shown as lysimeter plates by number. Total number of data (n) plotted was 90.

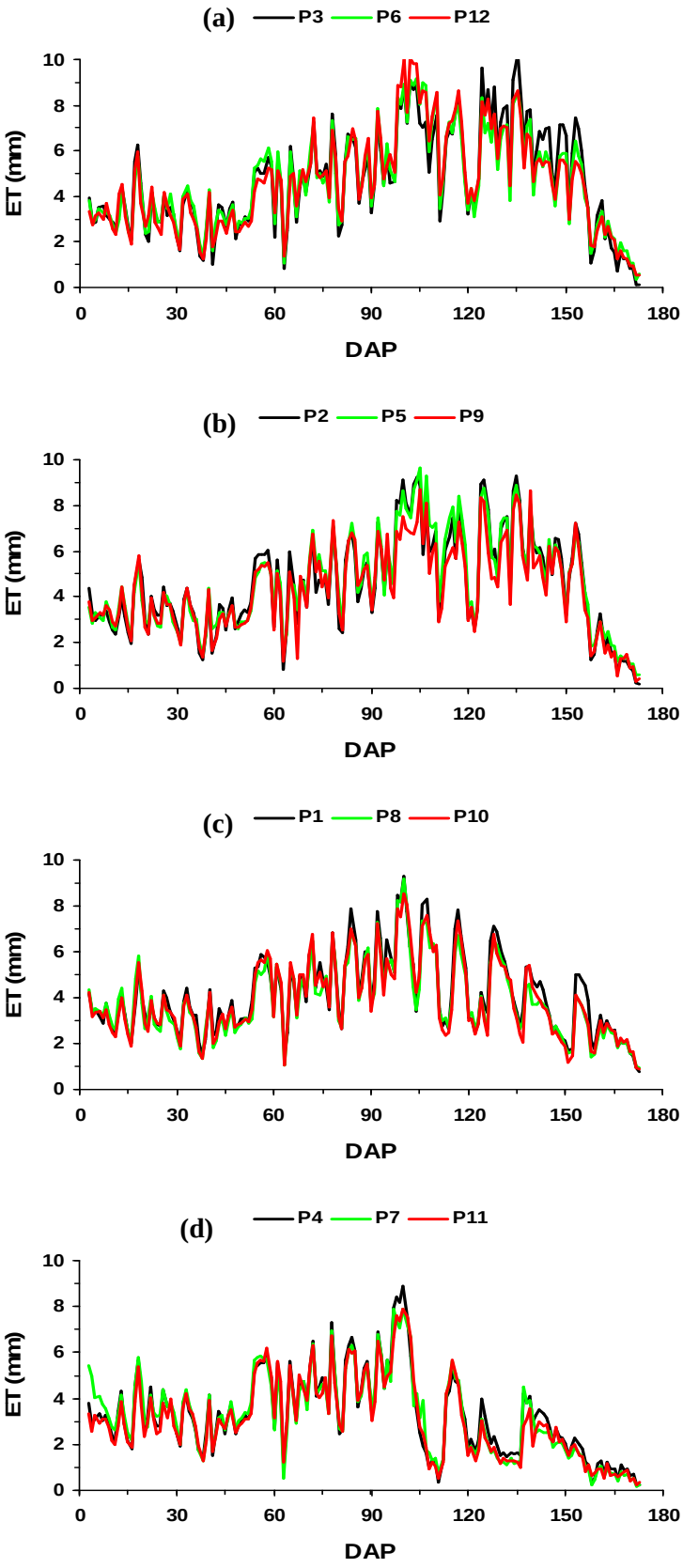

Figure 3. 20 Evapotranspiration (ET, mm) estimated from lysimeter data for (a) T80, (b) T70, (c) T50 and (d) T40 irrigation treatments given to cotton. Separate lines indicate replicates within irrigation treatments shown as lysimeter plates by number. Total number of data (n) plotted was 171.

ET values for the cotton crop varied from 0.4-10.0, 0.2-9.6, 0.8-9.3 and 0.2-8.9 mm for T80, T70, T50 and T40 treatments respectively. Seasonal ET varied from 793.4, 770.8, 677.4 and 550.5 mm for T80, T70, T50 and T40 irrigation treatments, respectively for the wheat crop. Temporal variation in ET was similar for all irrigation treatments up to 100 DAP, but thereafter ET values for T80 irrigation treatments was mostly greater than T40 treatment due to more frequent irrigation of cotton under T80 treatment.

3.3.6 Comparison of ET estimates between lysimetric and nonlysimetric measurements

Pot weights taken just before and after irrigation and drainage for each irrigation event was used to estimate ET. These are referred to as nonlysimetric measurements because of the longer time duration used for estimation of ET compared with ET estimates obtained from mini-lysimeters. For both lysimeteric and non lysimetric measurements, ET estimates were derived as differences in stored soil water (θ, mm) between consecutive irrigation events. Figures 3.21 and 3.22 show the comparison of ET values between lysimetric and non lysimetric measurements for wheat and cotton, respectively.

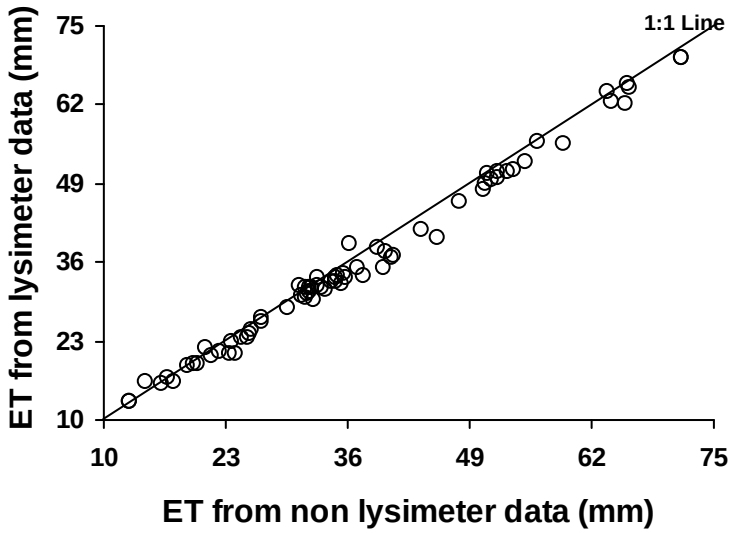

Figure 3. 21 Variation in evapotranspiration (ET, mm) with lysimetric measurement as a function of variation in nonlysimetric measurements for wheat.

It can be observed from these figures that ET measurements from these two methods fall on 1:1 line for both crops. Good agreement between both methods was due to the longer period of estimation used for ET compared to that used for estimation of θ. These results suggest that for glasshouse grown plants accurate measurements of ET over a long period is possible with load-cell based mini-lysimeters.

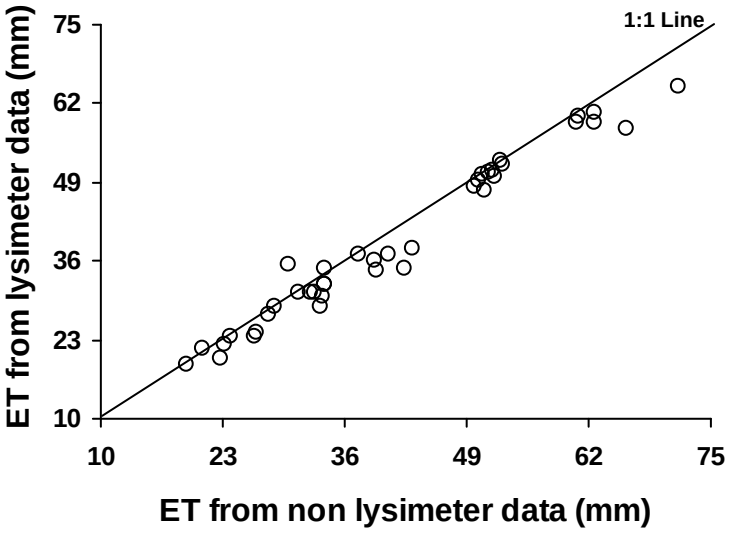

Figure 3. 22 Variation in evapotranspiration (ET, mm) with lysimetric measurement as a function of variation in nonlysimetric measurements for cotton.

3.4 Concluding remarks

The design of mini-lysimeter system based on twelve load cells (of 20 kg capacity) was found to be adequate for continuous measurement of evapotranspiration from plants growing in twelve separate pots in the glasshouse. A single data logger-multiplexer combination used to connect all load cells and collect output signal following full-bridge excitation mode of measurement provided sufficient resolution for estimation of ET via calibration. Initial testing of load cells examining the effects of signal settling time, excitation compensation, hysteresis and variation in ambient temperature suggests that the performance of all load cells were similar and satisfactory. Final calibration of load cells improved prediction of pot weights to ±12 g which is expected to provide prediction of soil water and ET over time with good accuracy and adequate resolution. Since the cost ($5450) of the mini-lysimeter system is not excessive, the results indicate that it is possible to obtain good lysimetric measurements of evapotranspiration for long-term monitoring of water use with reasonable accuracy and sufficient resolution.

Chapter 4

USE OF INFRARED THERMOGRAPHY TO DETECT PLANT RESPONSE TO SOIL WATER DEFICIT IN AN IRRIGATED COTTON CROP

4.1 Introduction

Mean global temperature is expected to rise over the next few decades which is likely to increase evaporation rate and cause an expansion of arid regions. Thus water availability will be a major limitation to plant growth in the future (Houghton et al., 2001). As a result, irrigation of crops will become an increasingly common practice. The Australian cotton crop occupies some 161,000 ha, of which around 87% of the area is irrigated (Dowling, 2009). Irrigation is essential to achieve potential yield in cotton grown in eastern Australia, as in-season precipitation is inadequate to meet crop water demand (Tennakoon & Hulugalle, 2006). The entire cotton crop in Australia consumes 1.8 million mega litres of irrigation water annually (ABS, 2006) which is around 16% of the total agricultural water use in Australia. Therefore water use is a critical issue for the Australian cotton industry. Water use is also important to the irrigator from the point of view of gaining maximum return from a limited resource.

Although many factors can reduce the yield of a crop, the major limiting factor is plant water stress caused by insufficient supply of water (Wanjura & Upchurch, 2000). Jones (1990a) suggested that greater precision in the application of irrigation can potentially be obtained by the using ‘plant stress sensing’ because crops respond to both soil and environment. Therefore it is necessary to quantify water stress levels of crops so that this information can be used in irrigation management for crops (Wanjura et al., 2006). The most established method for detecting crop water stress remotely is through the measurement of a crop’s surface temperature (Jackson, 1982). When crops are experiencing water shortage, transpiration from the leaves decreases that is expected to reduce both stomatal conductance and water potential of leaves. A decrease in transpiration can also cause insufficient cooling of the leaf surface which will ultimately lead to an increase in leaf temperature (Jackson et al., 1981). Although there are a number of factors which

affect actual level of water stress in a plant, leaf temperature is considered as one of the most important factors (Petersen et al., 1992). Canopy temperature has long been recognized as a good indicator of plant water stress and as a potential tool for irrigation scheduling (Gates, 1964). Plant canopy temperature has been used an indicator of water stress since the availability of infrared thermometers (IRTs) made this measurement possible without physically contacting the plant (Ehrler et al., 1978).

Most of the past studies on detection of water stress in plants have been based on infrared thermometry which involves acquisition of thermal signal from the plant and its surroundings (Evett et al., 1996; Pinter Jr. et al., 1983; Mahan and Yeater, 2008). Crop temperature measurements with thermal infrared thermometers are reliable and non-invasive, but they are usually based on a few point measurements and therefore depend on the assumption of uniformity of soil water content and plant density over large areas. In order to map crop water status variability at an adequate resolution, many IRTs need to be distributed over an area (Evans et al. 2000). Thermography, on the other hand, is the process of obtaining thermal image of an area controlled by the user. The potential advantage of thermal imagery (also known as infrared thermography) over point measurements with infrared thermometers, is the ability of the image to cover a large number of individual leaves and plants at one time at a high spatial resolution. Infrared thermometers usually have a finite angle of view so that it is common for the image to include plant canopy as well as some background noise arising from soil or sky within the field of view. However, the bias introduced by background noise can be easily corrected during analysis and interpretation of the image (Jones and Leinonen, 2003).

Recent development and commercial availability of portable thermal imagers and the associated image analysis software has overcome the problems associated with infrared thermometers. Thermal imaging has the potential to provide a more robust measure of the crop water status. Availability of equipment for digital thermal imaging also provides a unique opportunity to develop instantaneous spatial canopy stress indices for use in precision agriculture (Chaerle and van der Straten, 2000). Thermal and visual imagery can be combined to estimate the canopy temperature and identify plant stress in a number of crops, e.g. grape vines (Jones and Leinonen,

2004) and cotton (Cohen et al., 2005). Thermal and visible images of cotton canopies have been used to estimate and map leaf water potential (Cohen et al., 2005; Sela et al., 2007). The sensitivity of an unmanned air vehicle equipped with a thermal infrared sensor has been also tested to measure the response of cotton to irrigation and crop residue management (Sullivan et al., 2007). Plant water stress in cotton at full canopy can be detected by a number of spectral sensors including hyperspectral, multispectral and thermal infrared sensors (Detar et al., 2006).

Rigorous testing of thermal imaging against more traditional physiological techniques under field conditions is still required to determine the correspondence between thermal emission characteristics and physiological response of plants to water deficit for various types of crops (Grant et al., 2006). Earlier studies which have used infrared methods for irrigation scheduling are able to indicate stomatal closure or evaporation rate but they give no information on the amount of soil water available or that needs to be supplemented via irrigation at that time (Jones, 2004b). Grant et al. (2006) suggested that experiments in which irrigation scheduling is determined by a range of methods, one of these should include thermal imaging. Therefore, the experimental measurements reported here were carried out to test:

- Whether thermal imaging can be used to distinguish cotton crops growing under a systematic variation in deficit irrigation treatments;
- If there are any relationships between canopy or leaf temperature with the soil water within the root zone;
- The usefulness of crop water stress indices: one which corresponds closely with the stomatal conductance (I_G) and an improved crop water stress index (ICWSI, suggested by Jones, 1999b) and their relationships with soil water.
- The effects of plant physiological parameters on the canopy temperature and their relationship with thermal indices for the cotton crop.

4.2 Materials and Methods

Two field and one glass house experiments for cotton (*Gossypium hirsutum* L.) were conducted at the Queensland Primary Industries and Fisheries (now referred to as Department of Employment, Economic development and Innovation) experimental

station near Kingsthorpe (27°30'44"S, 151°46'55"E, and 431 m elevation) and at the University of Southern Queensland, Toowoomba.

4.2.1 Experimental site

Soil at the experimental site was a haplic, self-mulching, and black vertosol (Isbell, 1996). It is a self-mulching medium to heavy cracking clay soil with 76% clay, 14% silt and 10% sand in the surface horizons. It has been reported by Foley & Harris (2007) and Ghadiri et al. (1999) that the soil has an organic carbon content of 1.3%, pH 7.2, EC 35 mS m^{-1} and CEC 86 $cmol_c$ kg^{-1}. The field bulk density of the soil was 1200 kg m^{-3}.

4.2.2 Experimental lay-out

The field experiment consisted of four irrigation treatments with three replications using a randomized complete block design. Most irrigation treatments were based on plant available water capacity (PAWC) as defined below. Plant available water capacity (PAWC) is the difference between the upper water storage limit of the soil and the lower extraction limit of a crop over the depth of rooting (Godwin et al., 1984; Gardner 1985). Field determination of PAWC requires measurement of 2 parameters such as drained upper limit (DUL) as the upper water storage limit and crop lower limit (CLL) as the lower extraction limit over the depth of rooting. DUL is the volumetric water content in the field after a soil profile is thoroughly wetted and then allowed to drain to a steady state condition under the influence of gravity (Godwin et al., 1984; Ratliff et al., 1983). CLL is a measure of the extent to which a particular crop can extract water when planted in a particular type of soil. Both DUL and CLL were determined in the field at 10 cm depth increments from the soil surface down to 150 cm depth. The methods used to determine DUL and CLL were similar to those described by Ritchie (1981) and Ratliff et al. (1983). Irrigation treatments used for this experiment were: T50 – 50% depletion of PAWC, T60 – 60% depletion of PAWC, T70 – 70% of PAWC and T85 – 85% of PAWC. These treatments were used to schedule irrigation of specific plots using measured soil water for each plot with a neutron probe (details given later). All T85 treatment plots were subdivided into solid (T85-Solid) and skip (T85-Skip) row planting. Here, normal planting is referred to as solid planting while the skip row planting had one row without plants between two adjacent rows of cotton.

The layout of the experiment is shown in Fig. 4.1. There were altogether 12 experimental plots. Each replicate plot had a dimension of 20 m × 13 m, which was separated from adjacent plots with 4 m wide buffer and an additional area of 7 m × 20 m was used for planting of a refuge crop. Bollgard II cotton variety Sicala 60 BRF was selected for this experiment. Bollgard II is a genetically modified variety of cotton which is capable of reducing pesticide use by 80% compared with the conventional varieties of cotton. For refugee crop, a non-Bollgard cotton variety Sicala 41 RRF was used in this experiment. Refuge crops are usually planted in order to divert the attention of insects from the Bollgard crop.

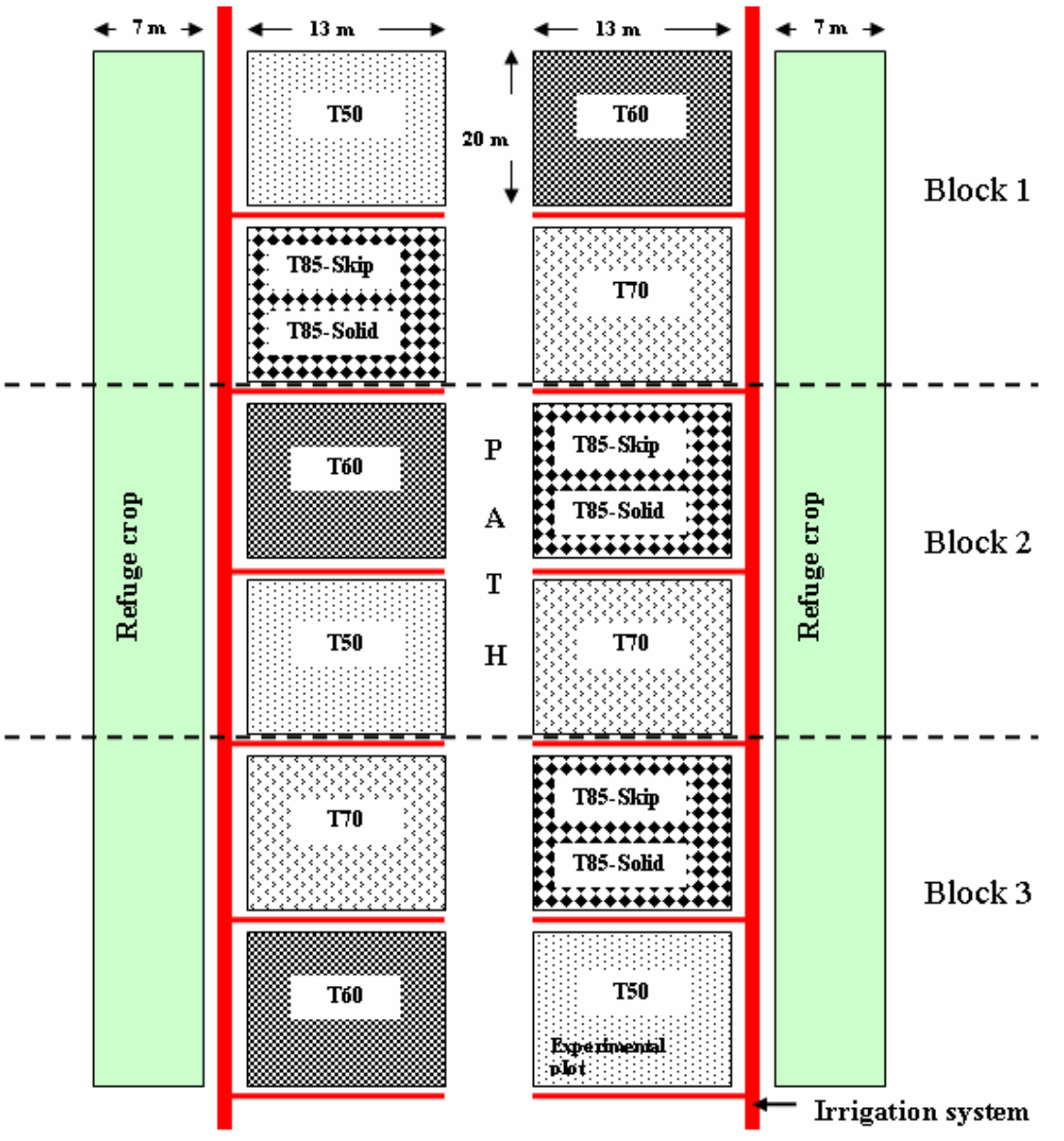

Figure 4. 1 Experimental layout for cotton crop under various irrigation treatments (T50, T60, T70 and T85) at the field experimental site at Kingsthorpe.

4.2.3 Cotton (2007-08 season)

The growth period of the cotton was from 12th November 2007 to 16th May 2008. Cotton seeds were sown at a depth of 5 cm on 12th November 2007. Row and plant spacing was maintained at 100 and 10 cm, respectively. During sowing, a starter fertilizer containing 10.5% N, 19.5% P and 2.2% S was applied at a rate of 188.4 kg ha^{-1} with further addition of 126 kg ha^{-1} of urea. The target planting density for the cotton crop was 11-12 plants m^{-1}. Most of the crop emerged within 8 days after planting (DAP) and the measured planting density after emergence was 10.9 plants m^{-1}. For weed control, 1 kg ha^{-1} of Roundup was applied with additional mechanical cultivation in all the experimental plots on 9th December 2007. Additional 190 $kgha^{-1}$ of urea was applied 68 days after sowing. In order to control the pest pale cotton stainer, the insecticide Decis (Deltamethrin as the active ingredient) was applied at a rate of 200 ml ha^{-1} on 15th March 2008. Each replicate plot was irrigated with bore water using a hand-shift solid sprinkler system (Fig. 4.2).

Figure 4. 2 Hand-shift solid sprinkler system used for application of irrigation water to the cotton crop.

Partial-circle sprinkler heads were used to avoid irrigation of adjacent plots. Three rain gauges were installed in each plot to estimate the amount of water applied during irrigation. Irrigation treatment in various plots was imposed on 75 DAP and continued up to 162 DAP. All replicates of T50, T60 and T70 treatment received 228, 82.8 and 82.3 mm irrigation water, respectively. Due to the variation in rainfall distribution over the growing season, T85 treatment did not receive any irrigation. Since many cotton farmers monitor soil water within their farm with neutron moisture meters (Tennakoon and Milroy, 2000), neutron probe access tubes were installed in each plot to monitor the soil water distribution over the growing season. For T85-Solid and skip-row irrigation treatments, 3 neutron probe access tubes were installed at the centre of each plot. For T50, T60 and T70 irrigation treatments, 1 neutron probe access tube was installed in the centre of each replicate plot. A neutron probe (503DR Hydroprobe, Campbell Pacific Nuclear Inc., Martinez, CA, USA) was used to measure soil water content from the surface to a depth of 1.33 m at 0.1 m depth increments. Standard reference count for the neutron probe was taken in water prior to field measurements. Neutron count ratio (n) was estimated by dividing each neutron count for a specific soil depth with the standard reference count taken in water. To calibrate the neutron probe, a soil core was taken from each irrigation treatment (T50-T85) during a time when there were considerable differences in water content among the treatments. The cores were divided into 10 cm sections and the moisture content and bulk density were determined gravimetrically. This information was used to develop a relationship between measured count ratios and volumetric soil content ((θ, m^3 m^{-3}). Neutron count ratio was converted to the volumetric soil water content (θ, m^3 m^{-3}) by using the calibration equation:

$$\theta = 1.36\ n - 0.44. \qquad (R^2 = 0.86,\ n=10,\ P \leq 0.001) \qquad (4.1)$$

An automatic weather station was installed on the experimental site to measure rainfall (mm), solar radiation (W m^{-2}), relative humidity (%), wind speed (km hr^{-1}) and air temperature (maximum and minimum in °C) at 1 h interval at appox. 30 m distance from the edge of the plots. During the growing season, daily maximum and minimum air temperature was in the range of 0.2 – 38.4 °C and

relative humidity 20 – 100% for the experiment. Total rainfall during the growing season was 272 mm.

4.2.3.1 Measurements

Thermal imagery

Thermal images of plants located close to the neutron access tubes were taken from each plot with a thermal infrared camera (NEC TH7800 model, NEC, Japan) which operates within the waveband of 8-14 µm with a thermal resolution of 0.1 °C to acquire thermal images with spatial resolution of 320 (V) × 240 (H) pixels, where V and H respectively refer to vertical and horizontal directions. This infrared camera also captured visible image as well as the thermal image. Thermal images were taken 2 m above the ground for all the 12 plots throughout the experiment. Canopy temperature (°C) was derived from each image with the help of Image Processor Pro II software (Version 4.0.3, NEC, Japan). Since an emissivity of 1.0 for plants have been reported to induce an error of <1 °C (Jackson, 1982) and that the emissivity for plant leaves varies in the range of 0.92-0.99 (Idso et al., 1969; Rees, 2001; Sutherland, 1986), the emissivity for the cotton canopy used for this experiment was 0.97 (also used by Wittich, 1997). A rectangular area within an image was selected to enclose several leaves for the estimation of average canopy temperature. A detailed sensitivity analysis of image processing indicated that error and bias associated with the estimation of average canopy temperature in this manner was not significant (Appendix A1).

During thermal imaging the position of viewed area within the field of view was recorded separately with the help of a hand-held GPS (Model 72, Garmin, Kansas, USA) to allow measurements of spatial variation in canopy temperature within the experiment. Permanent markers were installed at the time of first measurement in order to use the same position for subsequent measurements. The GPS unit had a wide area augmentation system (WAAS) capability with an accuracy of 3 m. All measurements were not influenced by the accuracy of the GPS unit greatly because of the use of permanent field-based markers and fixed position of neutron probe access tubes at the experimental site. Since the GPS recorded the location of all measurements in latitude and longitude format (i.e. degree, minute and

second), the recorded data were converted to easting and northing by using a UTM conversion excel spread sheet (Dutch, 2007).

Evaporation is only one of the many components of the canopy energy balance that affect canopy temperature. Factors such as radiation, wind speed, air temperature, and humidity also have major effects (Jones, 1992). Without sufficient information about these factors, measurements of leaf temperature alone are not enough to determine estimates of the transpiration rate or infer the stomatal conductance. One solution is to make use of `dry' and `wet' reference surfaces, where the observed leaf temperature is compared with the temperature that the same leaves would attain under the conditions of zero and maximum transpiration when placed in the same environment (Jones et al., 1997). In earlier studies, some artificial reference surfaces were used, for example, wet and dry filter papers (Jones et al., 2002). The problem, however, is that the thermal and radiative properties of these surfaces may differ from those of the observed plants, so that their energy balance differs from the real leaves (Leinonen and Jones, 2004). Therefore, Jones et al. (2002) proposed the use of leaves sprayed with water as wet references and leaves for which all transpiration was prevented by covering in petroleum jelly as dry references. Temperature of any pixels not falling within the temperature range defined by the references could then be eliminated from the analysis on the assumption that they would not include canopy (Jones and Leinonen, 2003).

Therefore cotton leaves were sprayed with water on both sides for about 1 min to simulate the condition of a fully transpiring leaf immediately before image acquisition to estimate temperature of wet reference leaf (T_{wet}). Additional reference leaves were covered with petroleum jelly to simulate the condition of a non-transpiring leaf for estimation of dry reference leaf (T_{dry}). Images of wet and dry reference leaves were taken for each irrigation treatment at the time of image acquisition of normal leaves (Fig. 4.3).

The temperatures of wet and dry reference leaves were used in the calculation of I_G and *ICWSI* as detailed below.

The crop water stress index (I_G) is expressed as

$$I_G = \frac{T_{dry} - T_c}{T_c - T_{wet}} \ , \qquad (4.2)$$

where T_{dry} (°C) is the temperature of the leaf covered with petroleum jelly on both sides, T_c (°C) is the canopy temperature of normal leaf measured with an infrared camera and T_{wet} (°C) is the temperature of leaf sprayed with water on both sides of the leaf. A modified crop water stress index (*ICWSI*) was also derived using the following expression.

$$ICWSI = \frac{T_c - T_{wet}}{T_{dry} - T_{wet}}. \quad (4.3)$$

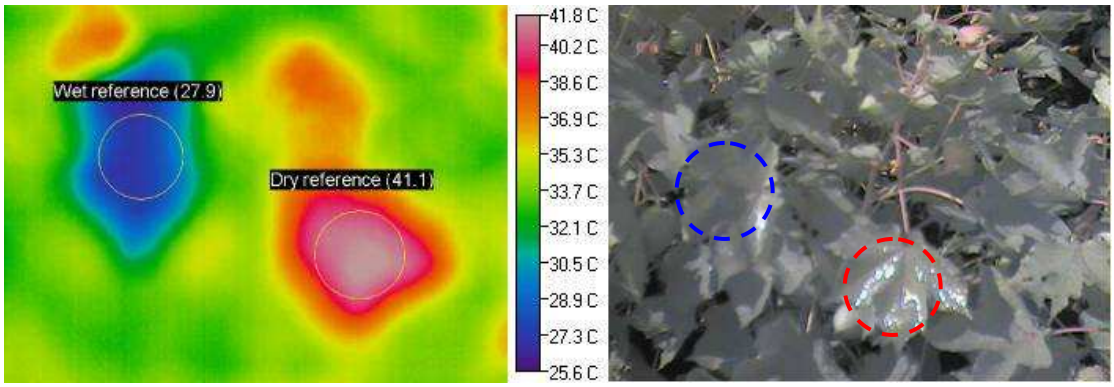

Figure 4. 3 Variation in the temperature of wet and dry reference leaves for cotton. Numbers in parenthesis are temperature (°C) for the thermal image (left) and the corresponding visual image (right). Red circle represents the leaf covered with petroleum jelly and blue circle represents the leaf sprayed with water.

It can be seen from Eqns. 4.2 and 4.3 that I_G and *ICWSI* are inversely related to each other. Grant et al. (2006) suggested that the average temperature of areas of canopies containing several leaves is more useful for distinguishing between irrigation treatments than the temperatures of individual leaves, as average temperatures over several leaves per canopy are expected to reduce the impact of variation in leaf angles.

Soil water

Soil water content was measured with the neutron probe within the access tubes (as described before) on the same day as for thermal imaging to explore interrelationships between canopy temperature (°C) and soil water content within the root zone. The effective root zone depth on the date of thermal imaging was

determined for each irrigation treatment by plotting the volumetric soil water content (θ in m^3 m^{-3}) on Y-axis and soil depth (cm) on the X-axis (Fig. 4.4). Effective rooting depth was assumed to be the soil depth nearest to the surface at which temporal variation in successive water content was negligible.

All data of measured θ was converted to mm of water for each depth of soil and then soil water was accumulated up to the effective root-zone depth on the date of thermal imaging in order to relate it with the canopy temperature (°C). Soil water measurements were taken on the date of thermal imaging as well as before and after the measurement of thermal images to determine the effective root zone depth on the date of thermal imaging. Thermal imagery measurements were taken 6 times during the entire cotton season (Table 4.1).

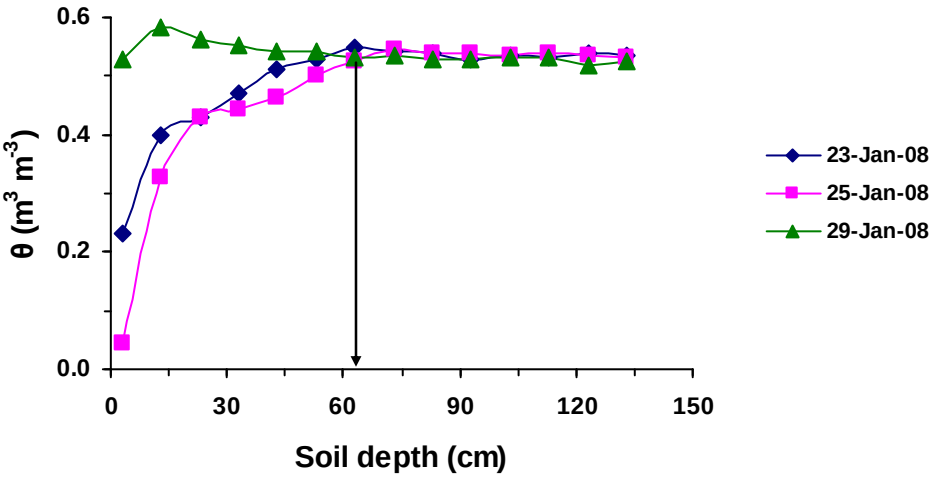

Figure 4. 4 Procedure used for the determination of effective root zone depth on the date of thermal imaging. A soil depth of 63 cm has been considered as the effective root zone depth in this example.

Table 4. 1 Timing and measurement dates of thermal imaging of cotton (2007-08) crop during the experiment.

Measurement dates (DAP)	Time of measurement
74	10.39 A.M. – 11.10 A.M.
81	2.43 P.M. – 3.32 P.M.
94	3.05 P.M. – 3.35 P.M.
135	12.25 P.M. – 1.20 P.M.
144	11.14 A.M. – 11.58 A.M.
155	10.18 A.M. – 10.49 A.M.

Leaf water potential

Since the development of pressure chamber, leaf water potential (Ψ_l) has become an important tool to assess the water status of plants (Jones, 1990b). Daily Ψ_l measured on the leaf of a plant reflects a combination of many factors: local leaf water demand, soil water availability, internal plant hydraulic conductivity and stomatal regulation (Chone et al., 2001). Therefore Ψ_l was measured with a Model 1000 pressure chamber (PMS Instrument Company, Oregon, USA) on selected occasions to assist interpretation of water deficit within the plant (Fig. 4.5). Ψ_l was measured on 2 occasions (74 and 94 DAP) during the cotton 2007-08 season after midday (i.e. 12 P.M.). For this measurement, the third leaf from the top of the plant was selected. Each leaf was cut with a thin-blade scissor and inserted into the pressure chamber as soon as possible to reduce any change in Ψ_l.

The cotton crop was harvested by hand picking during 13-16 of May 2008 and cotton yield was measured separately for each replicate plot of various irrigation treatments.

Figure 4. 5. Leaf water potential measurement for a typical cotton leaf mounted within the pressure chamber. A leaf similar to the measured leaf (not for measurement) is shown outside the pressure chamber.

4.2.4 Cotton (2008-09 season)

For this cotton season, the site and plot characteristics remained unchanged from the previous year. During this season, daily maximum and minimum air temperature was in the range of 1.1– 40.1 °C and relative humidity 16 – 100%. There was a total of 471 mm of rain received during the growing season.

All cotton seeds were sown at a depth of 5 cm on 15th November 2008. Row and plant spacing was maintained at 100 cm and 10 cm, respectively. During sowing urea was applied at a rate of 68 kg N ha^{-1}. The target planting density for the cotton crop was 17 plants m^{-1}. Most of the crop emerged 8 days after sowing and the measured planting density after emergence was 10-12 plants m^{-1}. For weed control, 1 L ha^{-1} of Glyphosate was applied to all experimental plots on 24th November 2008. Additional 1.5 L ha^{-1} of Glyphosate was applied on 15th January 2009. Urea was applied at a rate of 102 kg N ha^{-1} to all the plots at 70 days after planting (DAP). Irrigation treatment was imposed 67 DAP onward and continued until 136 DAP. All replicates of T50, T60, T70 and T85 treatments received 214, 78, 58 and 23 mm of irrigation water, respectively.

4.2.4.1 Measurements

Thermal images were taken with the infrared camera (NEC TH7800 model, NEC, Japan) for 12 plots 2 m above the ground as described for the 2007-08 season. Canopy temperature was derived from the analysis of the thermal image with the image processing software. Air temperature was also measured during the time of thermal imaging with an Omega type RTD (resistance temperature detector) probe. Images of wet (T_{wet}) and dry (T_{dry}) reference leaves were taken for each irrigation treatment at the time of image acquisition of normal leaves. Detailed specification about the infrared camera, emissivity for the cotton crop, procedure for selection of wet and dry leaves and calculation of I_G and ICWSI indices from the reference leaves remained the same as described previously for 2007-08 season. During thermal imaging the position of thermal imagery in the field was recorded separately with the help of a hand-held GPS (Model 72, Garmin, Kansas, USA) to allow measurements of spatial variation in canopy temperature within the experiment. Thermal images were measured on 6 occasions (Table 4.2).

Table 4.2 Timing and measurement dates of thermal imaging of cotton (2008-09) crop during the experiment.

Measurement dates (DAP)	Time of measurement of thermal imaging
62	9.24 A.M. – 9.40 A.M.
76	9.40 A.M. – 10.02 A.M.
88	10.40 A.M. – 11.15 A.M.
125	11.17 A.M. – 11.42 A.M.
136	10.58 A.M. – 11.26 A.M.
144	12.31 P.M. – 12.57 P.M.

Soil water content was measured with the neutron probe as described previously on matching dates as for thermal imaging to explore interrelationships between canopy temperature (°C) and soil water content within root zone. The effective root zone depth was determined on the date of thermal imaging as described in the previous section to relate to the canopy temperature (°C) with soil water (mm).

Ψ_l was measured with Model 1000 pressure chamber (PMS Instrument Company, Oregon, USA) on 4 occasions (Table 4.3) in the same manner as in the previous section. Stomatal conductance (g_s) of the leaves used for thermal imaging was measured with a PMR-5 steady-state porometer (PP Systems, Norfolk, UK) under ambient light conditions (Fig. 4.6) on 5 occasions (Table 4.3). Cotton was not harvested for this season due to severe damage of the crop from the herbicide 2, 4 D at the flowering stage.

Table 4. 3 Timing and measurement dates for leaf water potential (Ψ_l) and stomatal conductance (g_s) of cotton crop during 2008-09 season.

Measurement dates (DAP)	Time of measurement of Ψ_l	Time of measurement of g_s
62	10.00 A.M. – 11.05 A.M.	-
76	11.40 A.M. – 12.27 P.M.	10.52 A.M. – 11.29 A.M.
88	12.15 P.M. – 1.12 P.M.	11.20 A.M. – 12.05 P.M.
125	1.15 P.M. – 2.07 P.M.	12.15 P.M. – 1.07 P.M.
136	-	11.35 A.M. – 12.05 P.M.
144	-	1.30 P.M. – 2.15 P.M.

Figure 4.6. Stomatal conductance measurement for a typical cotton leaf with PMR-5 steady-state porometer.

4.2.5 Cotton (Glass house study)

The details of the soil properties, preparation of pots for growing cotton plants and irrigation treatments are given in Chapter 3. Soil used for the glasshouse experiment was identical to that used for the field experiments. As mentioned before in Chapter 3, there were altogether 28 pots in this experiment representing 7 replicates of 4 irrigation treatments. Since 12 pots (4 treatments × 3 replicates) were placed on the lysimeter system, the remaining 16 pots (4 treatments × 4 replicates) were placed on a bench adjacent to the mini-lysimeter system inside the glasshouse at the same height as the lysimeter pots. Description of lysimeter system was explained in Chapter 3. Experiment with cotton (*Gossypium hirsutum* L.) in the glass house continued from 12th December 2008 to 4th June 2009 (Fig. 4.7). Weather parameters for the experimental period of cotton have been described previously in Chapter 3. Crop and irrigation management for cotton plants inside the glasshouse was also explained previously in Chapter 3.

Figure 4. 7. Cotton growing in the glasshouse pots. The front three rows of pots are on the mini-lysimeter system.

Thermal images were taken on 6 occasions for all the irrigation treated pots with an infrared camera (Table 4.4). Detailed specification about the infrared camera, emissivity setting for the cotton crop, procedure for selection of wet and dry leaves and calculation of I_G and ICWSI indices from the reference leaves remained similar to that described for the field experiments. Canopy temperature (°C) was derived from the images with the Image Processor Pro II software (Version 4.0.3, NEC, Japan). Air temperature (°C) was also measured during the time of thermal imaging with an Omega type RTD (resistance temperature detector) probe. In order to relate the canopy temperature with soil water, the weight of the pots were taken with the balance and then gravimetric water content was estimated and multiplied with the bulk density of soil in each pot to derive volumetric soil water content for each pot. This volumetric water content was multiplied with the effective depth of soil in each pot (i.e. 19.2 cm) to estimate soil water (mm) stored in each pot at the time of thermal imaging. Stomatal conductance (g_s) of the leaves was measured with PMR-5 steady-state porometer (PP Systems, Norfolk, UK) on 3 occasions (Table 4.4). Porometer measurements were taken immediately before acquisition of thermal infrared image. The second leaf from the top of the plant was selected for stomatal conductance measurements. All cotton plants were harvested on 4th June 2009.

Table 4. 4 Timing and measurement dates for thermal imaging and stomatal conductance (g_s) of cotton crop during the glass house experiment.

Measurement dates (DAP)	Time of measurement of thermal imaging	Time of measurement of g_s
106	12.00 P.M. – 1.10 P.M.	-
111	11.40 A.M. – 12.45 P.M.	11.21 A.M. – 11.35 A.M.
119	12.40 P.M. – 1.35 P.M.	-
138	11.50 A.M. – 12.45 P.M.	11.34 A.M. – 11.48 A.M.
145	12.31 P.M. – 1.27 P.M.	12.11 P.M. – 12.23 P.M.
151	12.10 P.M. – 12.57 P.M.	-

Data collected from all experiments were analyzed with the analysis of variance recommended for randomised block designs (Snedecor and Cochran, 1989). Whenever a measured variable was found to be significantly affected by irrigation treatments ($p \leq 0.05$), mean values were compared with an estimate of least significant difference (LSD).

4.2.6 Comparison of irrigation treatments

In field experiments, irrigation treatments were based on plant available water capacity (PAWC) whereas in the glasshouse experiment, irrigation treatments were based on field capacity (FC). For determination of PAWC two parameters are required such as drainable upper limit (i.e. similar to field capacity) and crop lower limit (i.e. considered as wilting point). PAWC is the difference between DUL and CLL.

Here an example is provided to show the comparison of irrigation treatments between the field and glasshouse studies. If we consider FC = 50% and wilting point = 20%, then PAWC = 50% - 20% = 30%. In the field, for T50 treatment, we allow 50% depletion of PAWC, i.e. allowing a drop in water content of 30% × 0.5 = 15%. Therefore, volumetric soil water contnet (θ) at the time of irrigation would be 50% - 15% = 35%. Similarly, for the glasshouse experiment T50 treatment required irrigation when θ reached 50% of FC means when θ = 50% × 0.5 = 25%. Table 4.5 shows the comparison of irrigation treatments imposed in the field and glasshouse. It can be seen from Table 4.5 that θ was in order of T50>T60>T70>T85 in the field experiment, whereas it was in the order T80>T70>T50>T40 in the glasshouse experiment. Thus, T50 treatment plots in the field were most frequently irrigated

whereas T80 treatment pots were most frequently irrigated in the glasshouse. Similarly, T85 and T40 irrigation treatments were the least irrigated experimental units in the field and glasshouse experiments, respectively.

Table 4. 5 Comparison of various irrigation treatments for field and glasshouse experiments.

Field experiment			Glasshouse experiment		
Irrigation treatments	Percentage of depletion of PAWC	θ (%)	Irrigation treatments	Percentage of FC	θ (%)
T50	50	35	T40	40	20
T60	60	32	T50	50	25
T70	70	29	T70	70	35
T85	85	24.5	T80	80	40

4.3 Results and discussion

4.3.1 Field experiments

Fig. 4.8 shows a typical thermal image of plant canopy with exposed soil surface between adjacent rows of cotton in the field. Thermal image was analysed with Image processor Pro II software to derive the temperature of plant and soil surfaces separately. It can be seen from the Fig. 4.8 that soil temperature was appox. 20 °C higher than the cotton canopy temperature. Fig. 4.9 shows the temperature of the image when the processed area included both soil and plant canopy. Thus, without separate analysis of the canopy and the soil surface, the canopy temperature would be considered as 38.8 °C, which is almost 7 °C higher than the actual canopy temperature. Therefore, a bias in estimating canopy temperature would be introduced due to the background noise arising from soil.

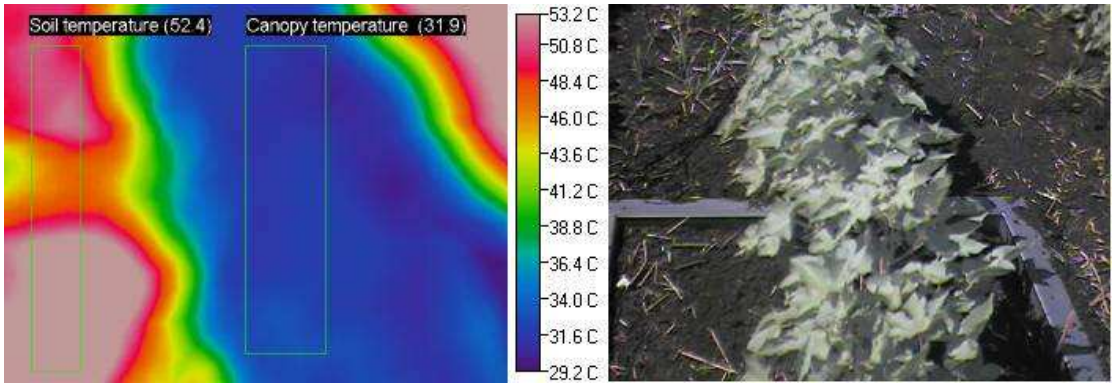

Figure 4. 8 Temperature of cotton canopy and adjacent soil within the cotton field. Numbers in parenthesis are temperatures (°C) for the thermal image (left) applied to the corresponding visual image (right). Rectangle(s) on the thermal image (left) represent pixels used for deriving average surface temperature.

Correct analysis and interpretation of the thermal image of the canopy is only possible with thermography, but not possible with infrared thermometers unless several thermometers are placed very close to the leaves.

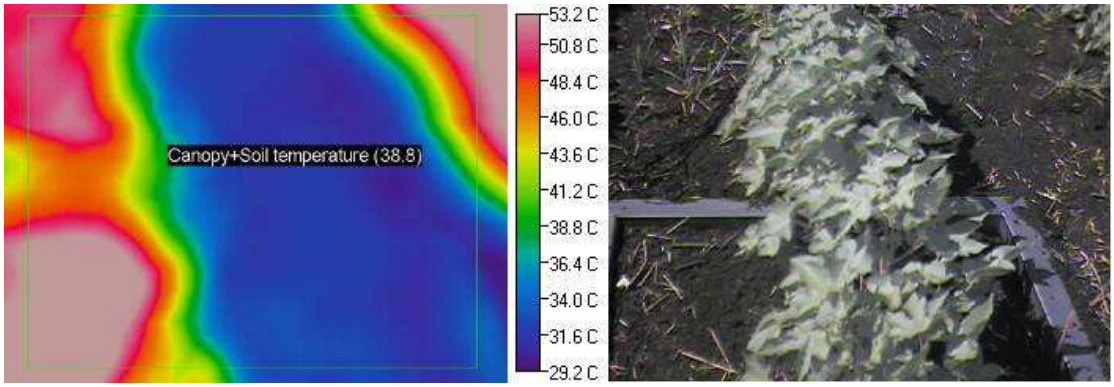

Figure 4. 9 Temperature for the combined image of canopy and soil within the cotton field. Number in the parenthesis for the thermal image (left) denotes temperature (°C) as applied to the corresponding visual image (right). Note the large rectangle on the thermal image (left) that combines leaf and soil to derive average surface temperature.

4.3.1.1 Effects of soil water on canopy temperature

Significant effects of irrigation treatments were found on canopy temperature and soil water within the root zone on 5 out of the 6 measurement occasions for both 2007-08 and 2008-09 seasons. Mean values of canopy temperature and soil water within the root zone for these measurement periods are shown in Tables 4.6, 4.7, 4.8 and 4.9. It can be observed from Tables 4.6 and 4.8 that significant variation in canopy temperature with irrigation treatments could be due to the variation in the frequency of irrigation applied. Canopy temperature in T50 irrigation treatment was consistently lower than that for T85 treatment throughout the cotton season because plants under T50 treatment were irrigated more frequently than the plants under T85 treatment. Maximum difference in canopy temperature between T50 and T85 irrigation treatment was 7.1 and 4.7 °C for 2007-08 and 2008-09 seasons respectively. Table 4.7 and 4.9 indicate that more frequently irrigated treatment (T50) had significantly higher soil water content within the root zone than the least frequently irrigated treatment (T85). Thus, plants when irrigated frequently are not expected to develop high level of internal water deficit stress as soil water availability to plants is not impaired. Lack of significant internal water deficit stress in leaves allow the plants to maintain high transpiration rate that reduces the canopy

temperature due to cooling of leaves. Figures 4.10 and 4.11 show the canopy temperature of cotton plants at 81 DAP for T50 and T85 irrigation treatments, respectively. It can be observed from these figures that the canopy temperature was lower (26.8 °C) for T50 irrigation treatment than that of T85 treatment (33.1 °C).

Table 4. 6 Effects of irrigation treatments on the canopy temperature of cotton (2007-08) in the field on selected measurement dates (indicated as days after planting, DAP). Mean values with a different superscript are significantly different (P≤0.05) when compared with the least significant difference (LSD) following analysis of variance.

Measurement	Canopy temperature (°C)				LSD
dates (DAP)	T50	T60	T70	T85	(°C)
81	26.4^{b}	32.0^{a}	32.9^{a}	33.5^{a}	1.6
94	25.6^{c}	29.1^{b}	30.9^{a}	29.9^{a}	1.7
135	28.5^{b}	28.7^{b}	28.2^{b}	33.9^{a}	2.8
144	25.1^{b}	27.9^{a}	27.3^{a}	29.1^{a}	2.1
155	26.8^{c}	30.1^{a}	28.6^{b}	31.4^{a}	1.7

Table 4. 7 Effects of irrigation treatments on soil water within root zone of cotton (2007-08) in field on selected measurement dates (indicated as days after planting, DAP). Mean values with a different superscript are significantly different (P≤0.05) when compared with the least significant difference (LSD) following analysis of variance.

Measurement	Soil water within root zone (mm)				LSD
dates (DAP)	T50	T60	T70	T85	(mm)
81	335.5^{b}	250.7^{a}	245.1^{a}	246.7^{a}	34.6
94	338.5^{b}	291.3^{a}	261.6^{a}	272.6^{a}	31.2
135	316.4^{b}	310.9^{b}	326.1^{b}	264.2^{a}	30.8
144	431.6^{b}	329.4^{a}	345.3^{a}	321.2^{a}	48.1
155	364.8^{b}	303.6^{a}	318.2^{a}	293.6^{a}	36.8

Table 4. 8 Effects of irrigation treatments on the canopy temperature of cotton (2008-09) in the field on selected measurement dates (indicated as days after planting, DAP). Mean values with a different superscript are significantly different (P≤0.05) when compared with the least significant difference (LSD) following analysis of variance.

Measurement	Canopy temperature (°C)				LSD
dates (DAP)	T50	T60	T70	T85	(°C)
76	27.4^{b}	27.6^{a}	28.2^{a}	28.4^{a}	0.6
88	27.7^{c}	29.0^{b}	29.4^{a}	31.4^{a}	1.0
125	26.2^{b}	27.9^{b}	27.1^{b}	28.3^{a}	1.4
136	25.9^{b}	27.6^{a}	26.9^{a}	27.8^{a}	1.1
144	27.1^{c}	28.3^{a}	28.0^{b}	28.4^{a}	0.8

Table 4. 9 Effects of irrigation treatments on soil water within root zone of cotton (2008-09) in field on selected measurement dates (indicated as days after planting, DAP). Mean values with a different superscript are significantly different (P≤0.05) when compared with the least significant difference (LSD) following analysis of variance.

Measurement dates (DAP)	Soil water within root zone (mm)				LSD (mm)
	T50	T60	T70	T85	
76	266.1^{b}	252.4^{a}	234.3^{a}	230.8^{a}	21.8
88	253.9^{b}	234.2^{a}	220.2^{a}	205.1^{a}	25.1
125	350.7^{b}	268.5^{b}	312.6^{b}	264.3^{a}	56.1
136	363.3^{b}	295.9^{a}	339.9^{a}	296.6^{a}	48.6
144	344.7^{b}	263.7^{a}	289.1^{a}	257.1^{a}	38.7

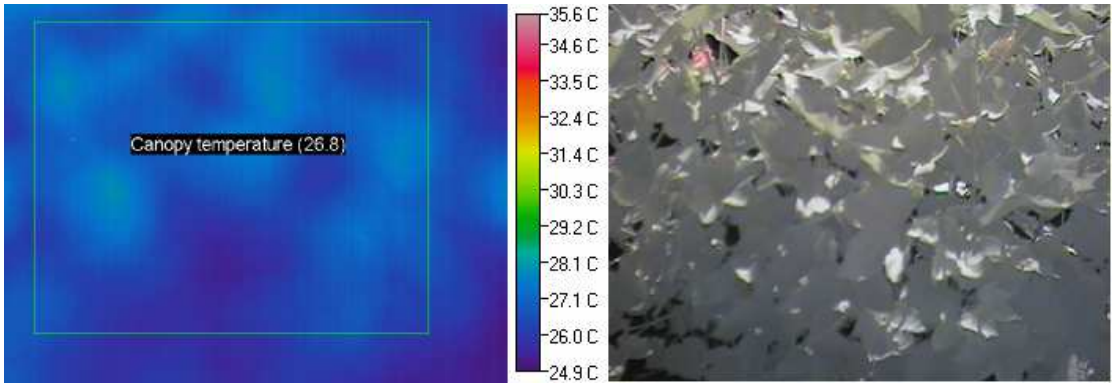

Figure 4. 10 Temperature of the canopy of cotton plants for T50 irrigation treatment at 81 DAP. Number in parenthesis on the thermal image (left) is canopy temperature (°C) for the corresponding visual image (right).

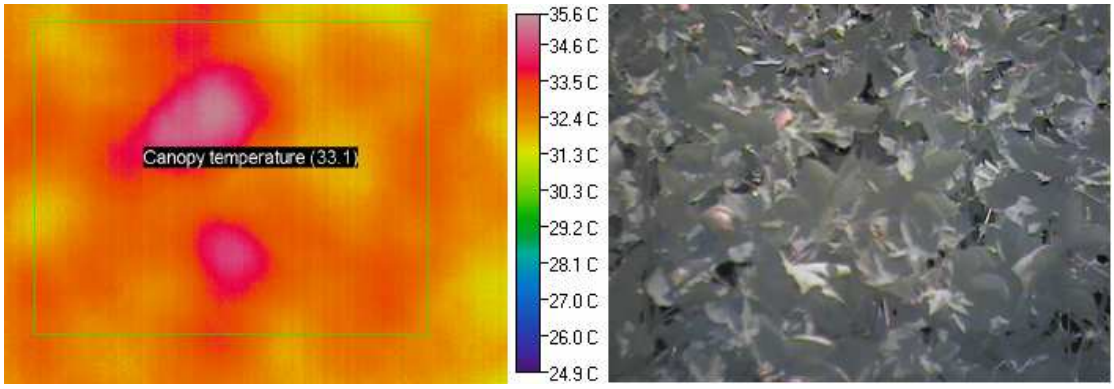

Figure 4. 11 Temperature of the canopy of cotton plants for T85 irrigation treatment on the same day as in Fig. 4.10. Number in parenthesis is the canopy temperature (°C) for the thermal image (left) that corresponds with the visual image (right).

To investigate the effect of soil water on canopy temperature for the cotton crop, canopy temperature was plotted against soil water within the root zone (Fig. 4.12). It can be concluded from Fig. 4.12 that the canopy temperature of cotton crop

decreased with an increase in soil water content within root zone. Canopy temperature varied within 24.9-31.4, 27.3-33.2, 26.4-33.5 and 27.3-35.4 °C for T50, T60, T70 and T85 treatments, respectively for the soil water range of 270.3–446.7, 219.4–347.2, 231.5–370.5 and 236.7-354.7 mm. Canopy temperature usually depends on vapour pressure deficit (VPD), which is usually estimated from air temperature and relative humidity (see p33-39, Allen et al., 1998). Due to the unavailability of relative humidity data during the measurements of canopy temperature, approximate estimates of VPD could be obtained by combining air temperature measurements with relative humidity data from the nearby weather station for the measurement dates. Average VPD values at the time of canopy temperature measurements at 74, 81, 94, 135, 144 and 155 DAP were 1.53, 2.35, 1.01, 2.27, 1.70 and 1.24 kPa, respectively for cotton 2007-08 season. Similar relationship between canopy temperature and soil water within the root zone was also found for cotton during 2008-09 season (Fig. 4.13).

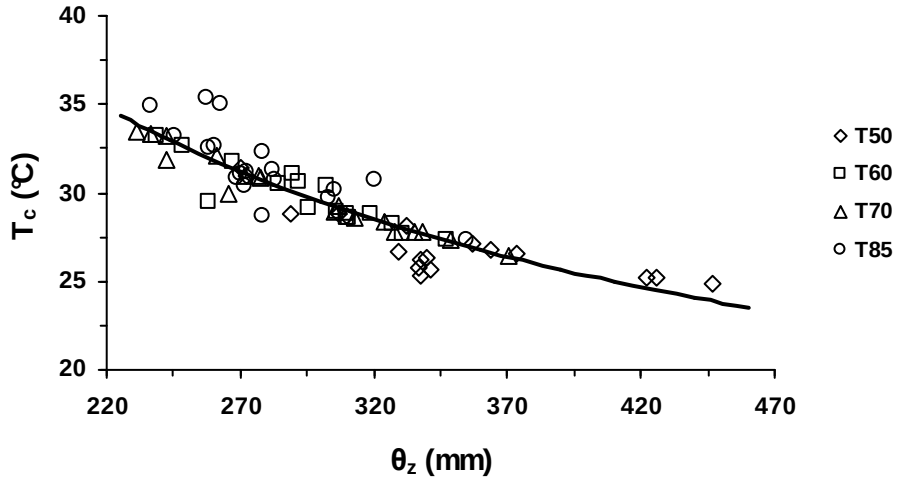

Figure 4. 12 The dependence of canopy temperature (T_c) on soil water within the root zone (θ_z) for various irrigation treatments of cotton for the 2007-08 season ($T_c = 612.13\ \theta_z^{-0.532}$, n = 72, $R^2 = 0.83$, $P \leq 0.001$).

Similarly VPD values were calculated for the cotton 2008-09 season and average VPD values were 1.69, 0.41, 3.02, 1.71, 1.25 and 1.69 kPa on 62, 76, 88, 125, 136 and 144 DAP, respectively. R^2 indicates the extent to which the variation in the plotted data is represented by the regression while the probability (P-values) of the fitted coefficients (slope and intercept terms) are obtained with the analysis of

variance to represent the degree of confidence. The equation fitted for canopy temperature against soil water within root zone was highly significant (P≤0.001) and also had high coefficients of determination (R^2) value for both the seasons. Due to the similarity in the regression equations used, an equation $T_c = 382.47\ \theta_z^{-0.416}$ can describe the variation in canopy temperature with soil water for the combined data.

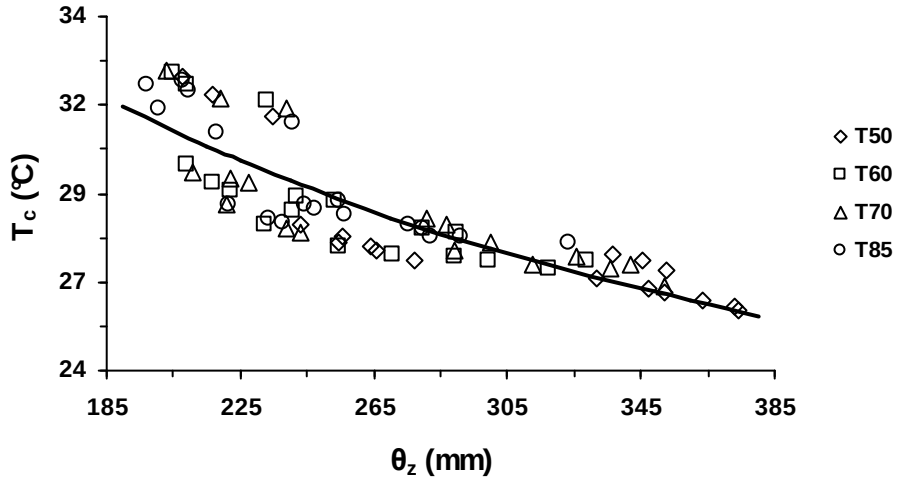

Figure 4. 13 The dependence of canopy temperature (T_c) on soil water within the root zone (θ_z) for various irrigation treatments of cotton for the 2008-09 season ($T_c = 152.81\ \theta_z^{-0.301}$, n = 72, $R^2 = 0.73$, P≤0.001).

4.3.1.2 Effects of soil water on the difference between canopy and air temperature ($T_c - T_a$)

An Omega type RTD probe was used for the measurement of air temperature during the time of thermal imaging in cotton 2008-09 season only. The difference of canopy and air temperature (T_c–T_a in °C) was plotted against soil water within the root zone (Fig. 4.14). The difference between canopy and air temperature was positive when the soil water within the root zone was low. The difference between canopy and air temperature for T50 treatment was negative at most times because of frequent irrigation keeping soil water deficit low. Low soil water deficit should allow plants to maintain a high transpiration rate reducing canopy temperature to become similar or lower than the air temperature. In case of least frequently irrigated treatment (T85), the difference between the canopy and air temperature was mostly positive indicating insufficient cooling of leaves due to reduced transpiration rate from leaves as a result of frequent shortage of water within the root zone. Greater scatter in these

data compared with similar data in Fig. 4.13 indicated an increase in errors when two separate measurements were combined.

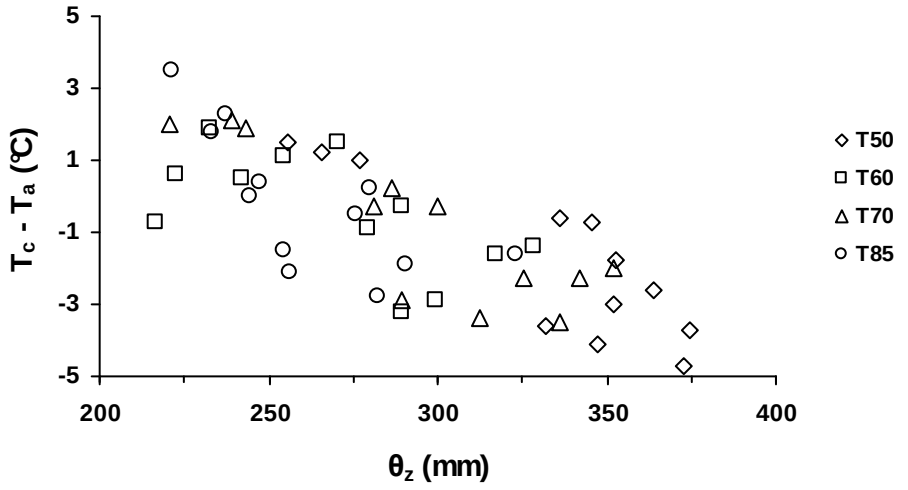

Figure 4. 14 The effects of variation in soil water within the root zone (θ_z) on the difference in canopy and air temperature ($T_c - T_a$) for various irrigation treatments of cotton during 2008-09 season.

4.3.1.3 Crop water stress indices and their implications to irrigation scheduling

Crop water stress indices (i.e. ICWSI and I_G) for the cotton crop were calculated from the canopy (T_c), wet (T_{wet}) and dry reference (T_{dry}) temperature (°C) as described in the materials and methods section of this chapter. For calculation of these crop water stress indices, T_c was measured for all the 12 plots whereas T_{wet} and T_{dry} reference temperature was measured for one replicate plot of each irrigation treatment. As the temperature of T_c, T_{wet} and T_{dry} changed with a change in irrigation treatment, more time was required for these calculations. It would be ideal to measure the wet reference temperature measurement for leaves from the wettest plot (with highest soil water content) and dry reference temperature measurement for leaves from the driest plot (with least soil water content). This would save some time and it may even cover the leaves from plots with intermediate soil water content because coefficient of variation in reference temperatures was less than 5%. In order to test the usefulness of these crop water stress indices for irrigation scheduling, ICWSI and I_G were plotted against soil water within the root zone of cotton for 2007-08 and 2008-09 seasons (Figs. 4.15, 4.16, 4.17 and 4.18). It can be concluded

from Figures 4.15 and 4.17 that ICWSI decreased with an increase in soil water within the root zone. ICWSI values varied form 0.14 to 0.88 for various irrigation treatments in 2007-08 season whereas the variation was 0.22 to 0.72 in 2008-09 season. Since ICWSI is low when crop water stress is low and vice-versa, occurrence of consistently low ICWSI in T50 treatment indicated that low canopy temperature was due to low crop water stress.

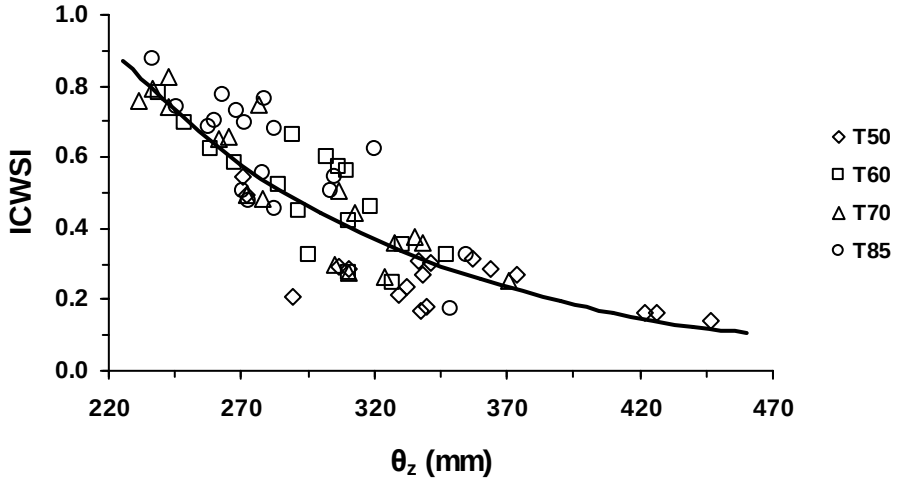

Figure 4. 15 The relationship between soil water within root zone (θ_z) and crop water deficit index, ICWSI for various irrigation treatments of cotton in 2007-08 season.

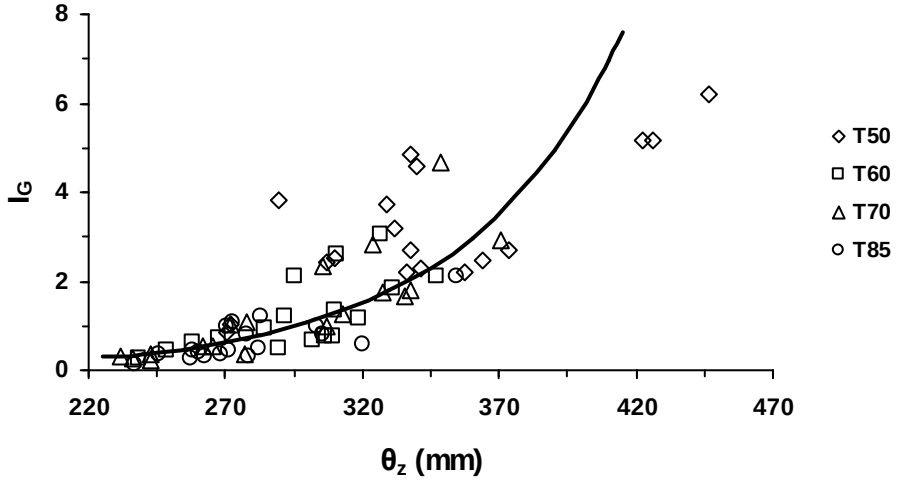

Figure 4. 16 The relationship between soil water within root zone (θ_z) and crop water deficit index, I_G for various irrigation treatments of cotton in 2007-08 season.

I_G indicated high values when the soil water within the root zone was high (Figs. 4.16 and 4.18). The magnitude of I_G was 0.83-6.22, 0.28–3.06, 0.21–4.65 and 0.14–2.10 for T50, T60, T70 and T85 treatments, respectively for cotton during the 2007-08 season and 1.29–3.62, 0.43–2.05, 1.10–2.76 and 0.38–1.94 during the 2008-09 season. Values of I_G were generally higher for T50 than T85 treatment because of increased frequency of irrigation.

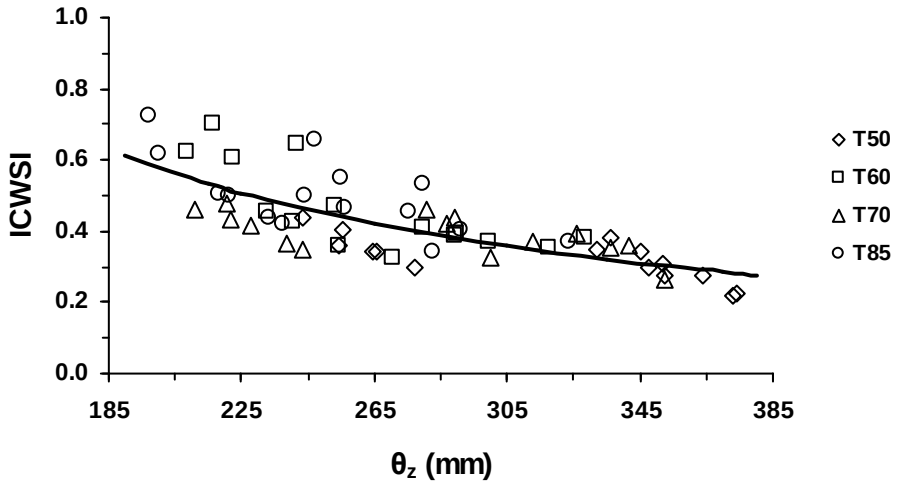

Figure 4. 17 The relationship between soil water within root zone (θ_z) and crop water deficit index, ICWSI for various irrigation treatments of cotton in 2008-09 season.

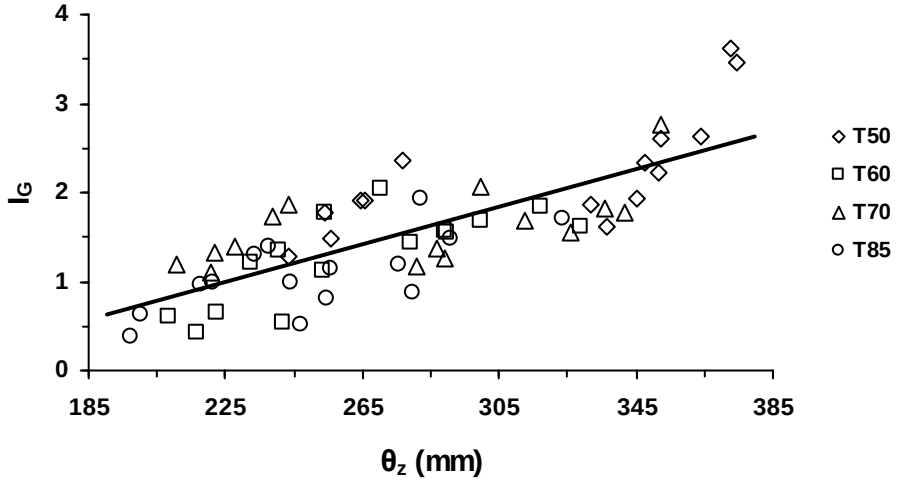

Figure 4. 18 The relationship between soil water within root zone (θ_z) and crop water deficit index, I_G for various irrigation treatments of cotton in 2008-09 season.

Fitted regression equations of ICWSI and I_G against soil water within the root zone are presented in Table 4.10. All the fitted values for these regression equations were highly significant ($P \leq 0.001$). Coefficients of determination (R^2) values for these regressions were higher for cotton during 2007-08 season than 2008-09 season. Although both indices relate significantly ($P \leq 0.001$) with soil water within the root zone, ICWSI is thought to be superior than I_G for irrigation scheduling as it varies within 0 to 1, whereas I_G does not have an upper limit to its variation. Most crop water stress indices based on canopy temperature tend to relate water deficit in leaves in response to atmospheric VPD. Little previous efforts have been made to relate crop water stress indices with soil water deficit. Both ICWSI and I_G estimated in this work are the indicator of internal water deficit in leaves not water deficit in soil. No universal relationship between soil and plant water deficit exists due to the variable resistance to water flow with transport of water from soil to root, root to stem and stem to leaf. Thus, these indices have limited advantage as they are based on resistance to water flow between leaf and atmosphere only.

Table 4. 10 Regression equations and coefficient of determination (R^2) for the relationships between *ICWSI* and I_G (dimensionless) and soil water within root zone (θ_z, mm) for various irrigation treatments of cotton during 2007-08 and 2008-09 seasons. No. of data points (n) used for each regressions was 72 and $P \leq 0.001$.

Cotton season	Thermal index	Regression equation	R^2
2007-08	ICWSI	$ICWSI = 6.603\ e^{-0.009\theta z}$	0.72
	I_G	$I_G = 0.006\ e^{0.017\theta z}$	0.71
2008-09	ICWSI	$ICWSI = 248.64\ \theta_z^{-1.144}$	0.60
	I_G	$I_G = 0.0.01\ \theta_z - 1.4$	0.61

4.3.1.4 Effect of leaf water potential and stomatal conductance on canopy temperature

Fig. 4.19 illustrates the plotted values of leaf water potential against canopy temperature for the 2007-08 cotton season. LWP varied from -1.37 to -2.90 MPa for a canopy temperature range of 25.3 to 33.3 °C for cotton during 2007-08 season. When the canopy temperature of leaves was low, the value of Ψ_l was high (less negative) indicating low internal water deficit in the leaves of cotton. Likewise, variation in canopy temperature with leaf water potential (Ψ_l) for the 2008-09 season was represented by Fig. 4.20. Since the slopes and intercepts in these equations are

very similar, the relationship between canopy temperature and leaf water potential for cotton changed very little between the two seasons.

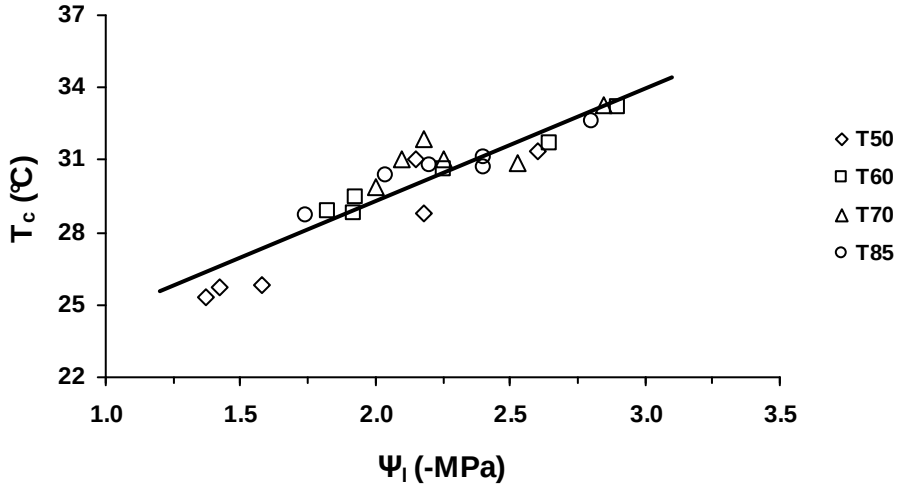

Figure 4. 19 Relationship between canopy temperature (T_c) and leaf water potential (Ψ_l) for various irrigation treatments combined for the period 74 and 94 DAP of cotton in 2007-08 season ($T_c = 4.7\ \Psi_l + 19.8$, n = 24, $R^2 = 0.84$, $P \leq 0.001$).

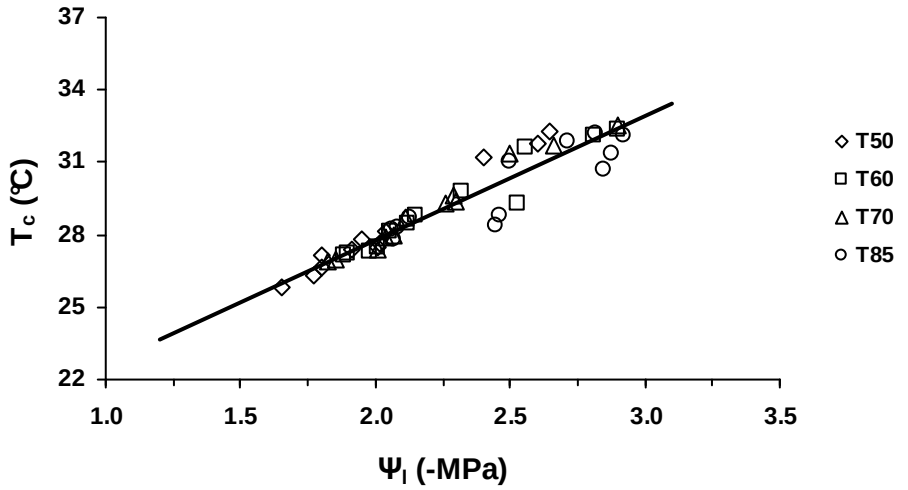

Figure 4. 20 Relationship between canopy temperature (T_c) and leaf water potential (Ψ_l) for various irrigation treatments combined for the period 62-125 DAP of cotton in 2008-09 season ($T_c = 5.2\ \Psi_l + 17.4$, n = 48, $R^2 = 0.90$, $P \leq 0.001$).

Fig. 4.21 shows the plotted values of canopy temperature (T_c) against stomatal conductance (g_s) for cotton leaves during the 2008-09 season. Canopy temperature of cotton decreased nonlinearly with an increase in stomatal

conductance. During the measurement period as stomatal conductance approximately doubled from 25 to 49 mmol m^{-2} s^{-1}, canopy temperature dropped by 6 °C from 32 to 26 °C. Since transpiration of a leaf is directly proportional to stomatal conductance, these measurements clearly indicate that high values of g_s in frequently irrigated cotton (e.g. T50 treatment) allows sufficient leaf cooling to reduce canopy temperature.

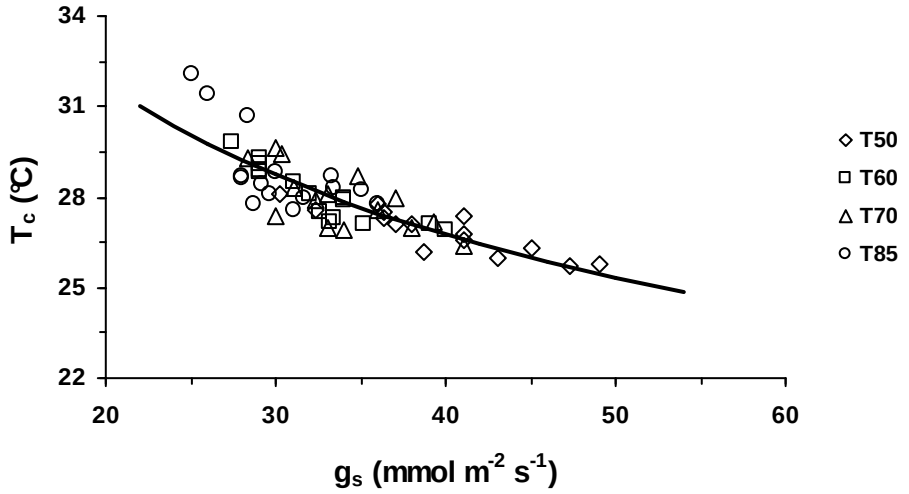

Figure 4. 21 Relationship between canopy temperature (T_c) and stomatal conductance (g_s) for various irrigation treatments of cotton (2008-09) crop (T_c = 67.04 $g_s^{-0.249}$, n = 60, R^2 = 0.72, P≤0.001).

4.3.1.5 Relationship between crop water stress indices and stomatal conductance

To investigate the effect of stomatal conductance (g_s) on crop water stress indices, stomatal conductance was plotted against ICWSI and I_G (Figs. 4.22 and 4.23). It can be seen from Fig. 4.22 that an increase in stomatal conductance decreases the magnitude of ICWSI. As low values of ICWSI are associated with low water stress in plants, an increase in g_s and transpiration rate is responsible for a decrease in ICWSI. The other water stress index I_G increased linearly with an increase in stomatal conductance (Fig. 4.23). I_G varied from 0.38 to 3.62 when stomatal conductance ranged within 25 to 49 mmol m^{-2} s^{-1}. It can be observed from Fig. 4.23 that I_G values were lower under least frequently irrigated treatment (T85) compared

with the most frequently irrigated treatment (T50) due to the difference in soil water deficit.

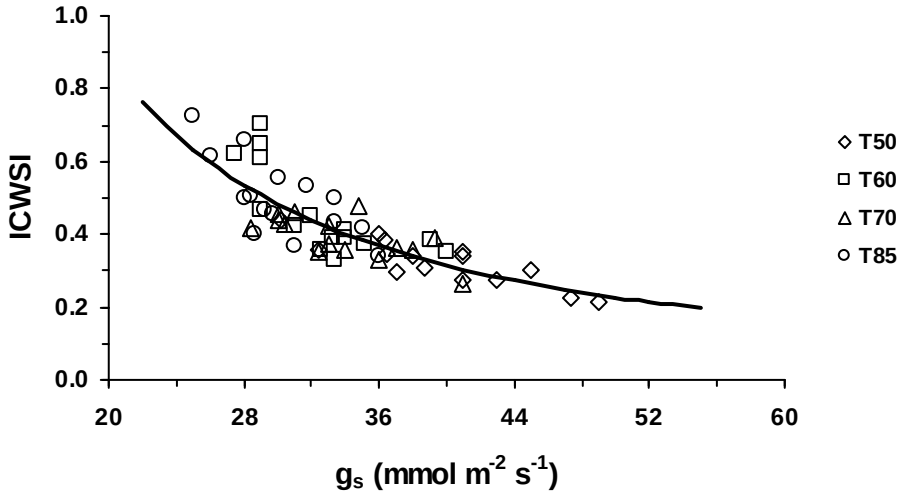

Figure 4. 22 Relationship between ICWSI and stomatal conductance (g_s) for various irrigation treatments of cotton during 2008-09 season ($ICWSI = 75.22\ g_s^{-1.485}$, n = 60, R^2 = 0.73, P≤0.001).

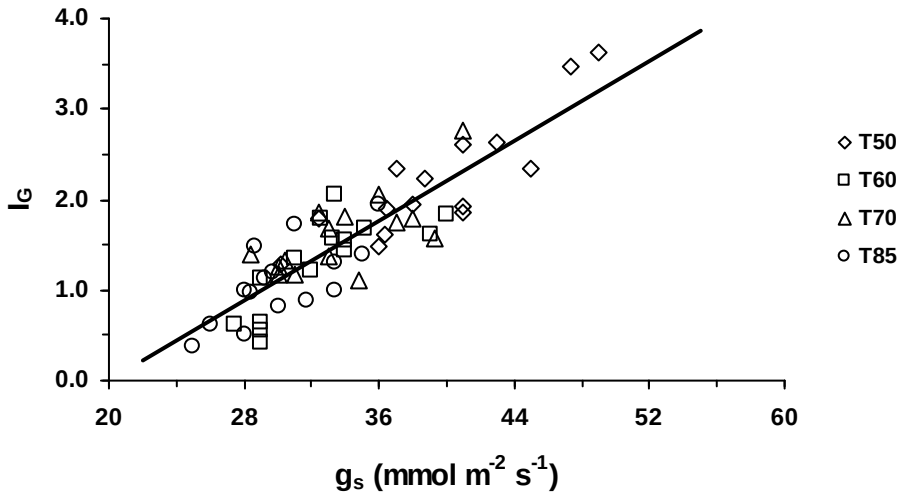

Figure 4. 23 Relationship between I_G and stomatal conductance (g_s) for various irrigation treatments of cotton during 2008-09 season ($I_G = 0.11\ g_s - 2.2$, n = 60, R^2 = 0.76, P≤0.001).

4.3.1.6 Spatial variation in soil water and canopy temperature

Spatial variation in canopy temperature (°C) and soil water (mm) within the root zone for all the 12 plots of cotton during 2007-08 and 2008-09 seasons are shown in Figs. 4.24, 4.25, 4.26 and 4.27. Measurement location for each plot is represented by a filled circle with the label denoting the irrigation treatment and the replicate plot. Dark blue areas within the field show occurrence of low canopy temperature in Figs. 4.24 and 4.26 and are also used to denote areas of high soil water content within the root zone in Figs. 4.25 and 4.27. Similarly, lighter shade of blue represents high canopy temperature and low soil water within the root zone for these figures. As areas of the field with T50 and T85 treatments respectively indicate areas of highest and lowest soil water content, frequent mapping of canopy temperature can be useful in identifying those areas of relative soil water deficit on which to apply variable quantities of water within the field to reduce soil water deficit and practice precision irrigation.

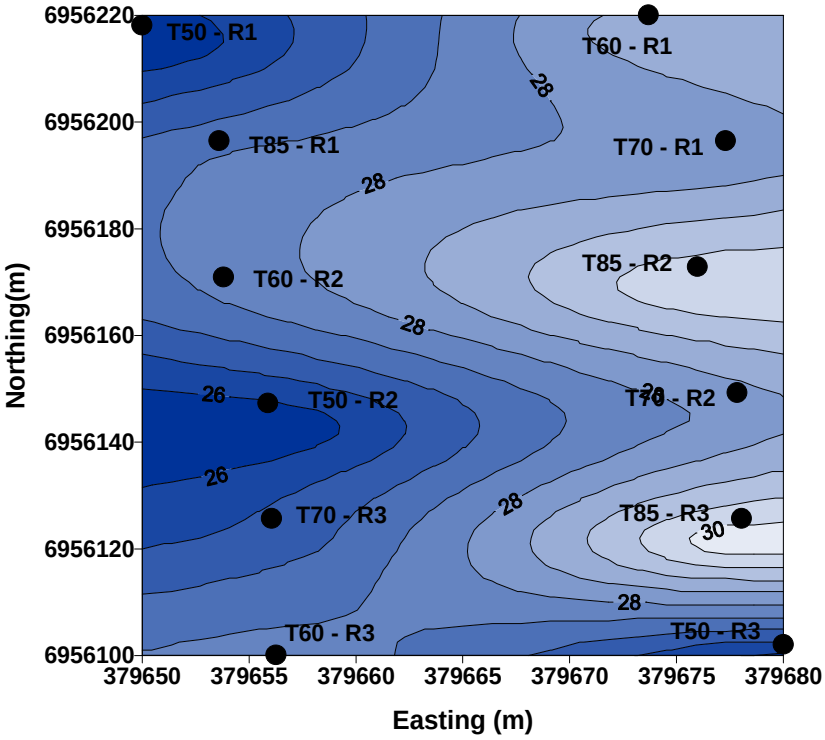

Figure 4. 24 Spatial variation in canopy temperature at the irrigation experiment site at 144 days after planting cotton during the 2007-08 season. Filled circles indicate the position of measurement for irrigation treatments T50, T60, T70 and T85 and replicates R1, R2 and R3 of each irrigation treatment. The contour lines show the values of canopy temperature in °C.

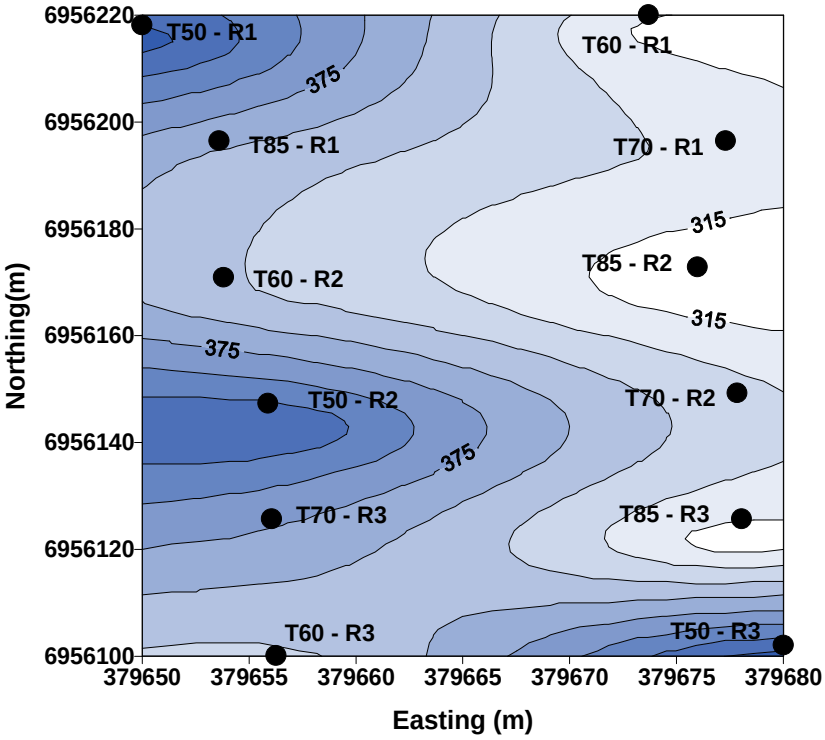

Figure 4. 25 Spatial variation in soil water within root zone at the irrigation experiment site at 144 days after planting cotton during the 2007-08 season. Filled circles indicate the position of measurement for irrigation treatments T50, T60, T70 and T85 and replicates R1, R2 and R3 of each irrigation treatment. The contour lines show the values of soil water within the root zone in mm.

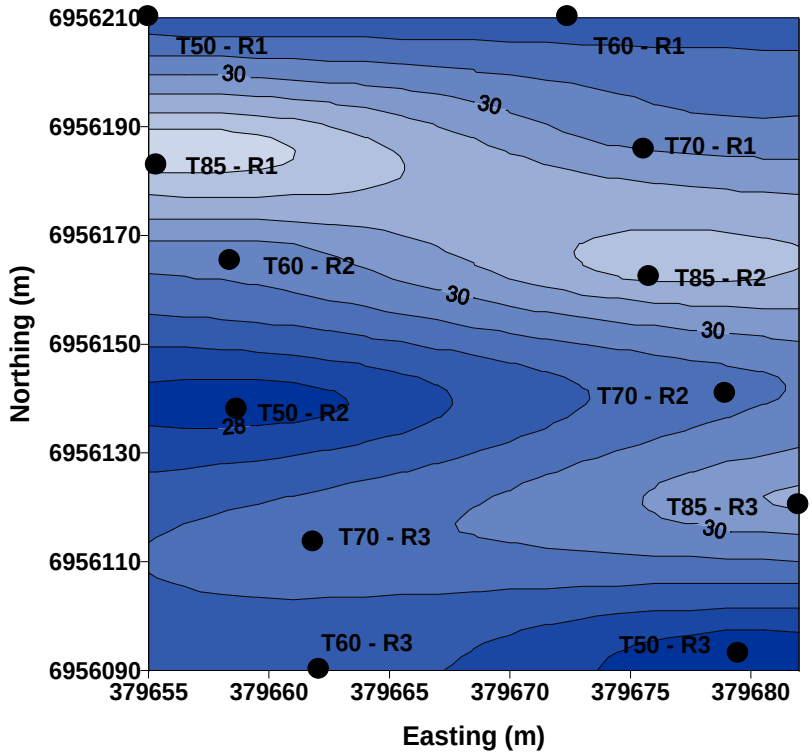

Figure 4. 26 Spatial variation in canopy temperature at the irrigation experiment site at 88 days after planting cotton during the 2008-09 season. Other explanations are as for Fig. 4.24.

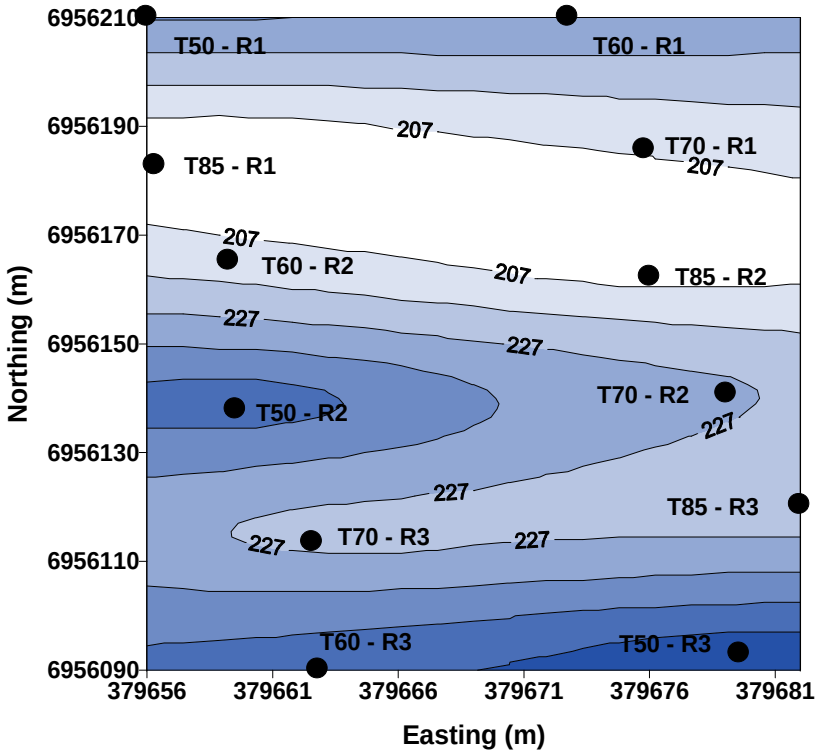

Figure 4. 27 Spatial variation in soil water within root zone at the irrigation experiment site at 88 days after planting cotton in 2008-09 season. Other explanations are as for Fig. 4.25.

4.3.2 Glasshouse experiment

4.3.2.1 Effect of stored soil water on canopy temperature

Significant effects of irrigation treatments on canopy temperature and stored soil water (or soil water storage) were found on all measurement occasions in the glasshouse experiment. Mean values of canopy temperature and stored soil water for various irrigation treatments at each measurement period are presented in Tables 4.11 and 4.12. It can be seen from Table 4.11 that the canopy temperature remained significantly higher over time for the least frequently irrigated treatment (T40) than for the most frequently irrigated treatment (T80). Maximum difference in canopy temperature between the T40 and T80 irrigation treatments was 1.8 °C that was much lower than the difference in canopy temperature observed for the most frequently and least frequently irrigated treatments in the field experiment. These differences could be due to the range of variation in soil water content and atmospheric deficits observed for these experimental locations. In the glasshouse experiment stored soil water for the T80 treatment was higher than that of T40 treatment on most occasions due to higher frequency of irrigation (Table 4.12).

Table 4. 11 Effects of irrigation treatments on the canopy temperature of cotton on 6 measurement dates (indicated as days after planting, DAP) in the glasshouse experiment. Mean values with a different superscript letter indicate significantly different irrigation treatment (P≤0.05) when compared by using the least significant difference (LSD) derived following an analysis of variance.

Measurement dates (DAP)	Canopy temperature (°C) T80	T70	T50	T40	LSD (°C)
106	27.6^{c}	28.3^{b}	27.4^{c}	29.2^{a}	0.3
111	25.7^{c}	26.8^{b}	26.9^{b}	27.5^{a}	0.3
119	28.3^{a}	27.5^{c}	28.0^{b}	28.4^{a}	0.2
138	25.3^{c}	27.3^{a}	25.1^{c}	26.3^{b}	0.3
145	25.5^{b}	25.0^{c}	26.3^{a}	26.1^{a}	0.2
151	25.9^{b}	24.9^{c}	26.5^{a}	26.3^{a}	0.2

Table 4. 12 Effects of irrigation treatments on soil water storage for 6 measurement dates (indicated as days after planting, DAP) in the glasshouse experiment with cotton. Mean values with a different superscript indicate significantly different treatments (P≤0.05) when compared with the least significant difference (LSD).

Measurement dates (DAP)	Stored soil water (mm) T80	T70	T50	T40	LSD (mm)
106	102.8^{a}	78.3^{b}	103.1^{a}	57.8^{c}	2.7
111	90.3^{a}	77.0^{b}	71.9^{c}	51.7^{d}	2.5
119	81.3^{b}	90.6^{a}	83.1^{b}	79.1^{c}	2.7
138	105.6^{a}	76.1^{d}	104.9^{b}	98.6^{c}	2.8
145	101.4^{b}	106.8^{a}	74.7^{d}	82.1^{c}	2.4
151	89.2^{b}	107.2^{a}	60.7^{d}	68.8^{c}	2.3

Values of canopy temperature were plotted against stored soil water to test the usefulness of thermal imaging for irrigation scheduling inside the glasshouse (Fig. 4.28). Canopy temperature decreased with an increase in stored soil water although the degree of scatter in these data was greater than in the field. Although the regression fitted to these data was significant (P≤0.001), the coefficient of determination (R^2) was low (0.3) which questions the suitability of thermal imaging for irrigation scheduling of glasshouse grown plants when the measurements for the entire growing season are considered. Thus, simple linear regression was used to test the effectiveness of thermal imaging for irrigation scheduling using data for each measurement occasion separately. These regression equations and R^2 values for six measurement occasions are presented in Table 4.13.

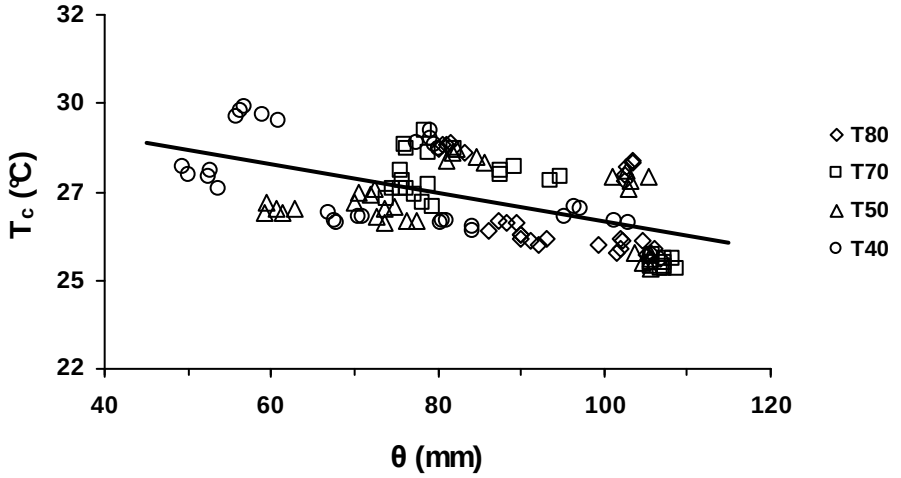

Figure 4. 28 The dependence of canopy temperature (T_c) on stored soil water (θ) under various irrigation treatments for cotton in the glasshouse experiment (T_c = -0.04 θ + 30.2, n = 120, R^2 = 0.30, P≤0.001).

Table 4. 13 Regression equations and coefficient of determination (R^2) for the relationship between canopy temperature (T_c, °C) and stored soil water (θ, mm) for various irrigation treatments on six measurement dates (indicated as days after planting, DAP). The ranges of stored soil water and canopy temperature are also shown. No. of data points (n) used was 20 and P≤0.001.

Measurement dates (DAP)	Range Soil water (mm)	Canopy temperature (°C)	Regression equation	R^2
106	56 – 105	27.1 – 29.4	T_c = -0.036 θ + 31.2	0.91
111	49 – 92	25.5 – 27.7	T_c = -0.040 θ + 29.7	0.83
119	78 – 95	27.3 – 28.7	T_c = -0.072 θ + 34.1	0.85
138	75 – 107	24.8 – 27.6	T_c = -0.068 θ + 32.5	0.85
145	73 – 109	24.7 – 26.5	T_c = -0.037 θ + 29.0	0.89
151	59 – 107	24.9 – 26.7	T_c = -0.032 θ + 28.5	0.88

Since all the fitted regression equations were highly significant (P≤0.001) with high R^2 values, it may be appropriate to use thermal imaging for irrigation scheduling for glasshouse grown plants on the day of measurement rather than combining all measurements over the entire season. Other opportunities for glasshouse grown plants are also explored in the later part of this section.

4.3.2.2 Effect of soil water storage on $T_c - T_a$

The difference between the temperature of canopy (T_c) and air (T_a) was plotted against stored soil water (Fig. 4.29). It is evident from Fig. 4.29 that higher values of

T_c-T_a were observed when stored soil water was low. T_c - T_a values were positive on most occasions for the least irrigated treatment (T40) because the plant canopy was warmer than air suggesting low transpiration of cotton with the possibility of high internal water deficit in leaves. Likewise, T_c –T_a values were negative for cotton canopies in the most frequently irrigated treatment (T80) possibly because plants were able to maintain a high transpiration rate.

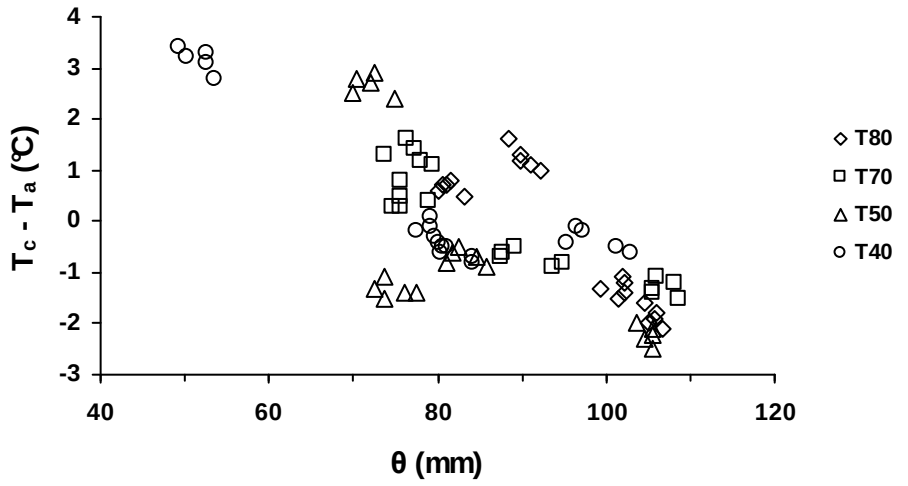

Figure 4. 29 The dependence of canopy and air temperature difference (T_c – T_a) on soil water storage (θ) for various irrigation treatments of cotton in the glasshouse experiment.

4.3.2.3 Crop water stress indices and their implications to irrigation scheduling in the glasshouse

ICWSI and I_G indices were estimated from the measurements of canopy (T_c), wet (T_{wet}) and dry (T_{dry}) reference temperatures similar to that for the field experiments. Crop water stress indices were plotted against stored soil water to test the usefulness of these indices for irrigation scheduling of glasshouse-grown plants (Figs. 4.30 and 4.31). ICWSI decreased linearly with an increase in stored soil water (Fig. 4.30). ICWSI values varied form 0.23 to 0.57 for a variation in stored soil water in the range of 49 to 109 mm for various irrigation treatments. It can be seen from Fig. 4.30 that ICWSI values were mostly lower in T80 treatment than T40 treatment because of the differences in irrigation frequency that affects temporal variation in soil water deficit.

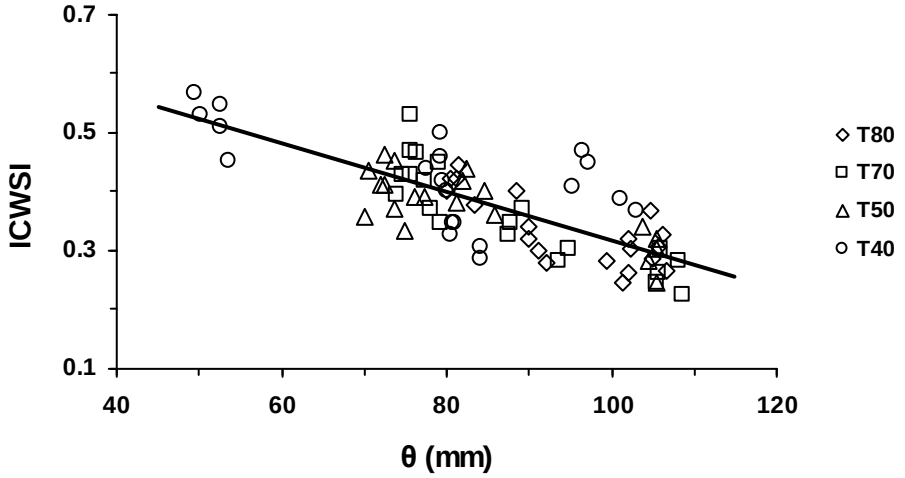

Figure 4. 30 The relationship between soil water storage (θ) and crop water deficit index, ICWSI, for various irrigation treatments of cotton in the glasshouse (*ICWSI* = -0.004 θ + 0.7, n = 80, R^2 = 0.60, P≤0.001).

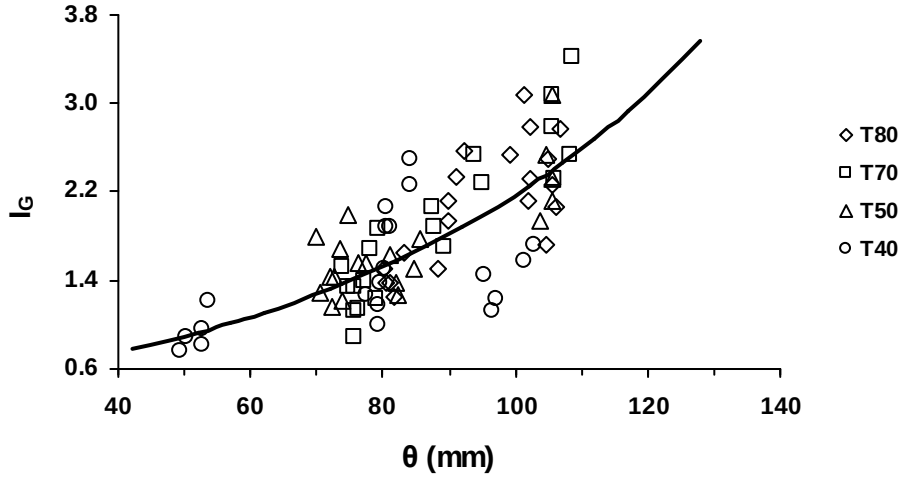

Figure 4. 31 The relationship between soil water storage (θ) and crop water deficit index, I_G for various irrigation treatments of cotton in the glasshouse experiment (I_G = 0.366 e $^{0.018\theta}$, n = 80, R^2 = 0.60, P≤0.001).

Since the relationship between ICWSI and stored soil water in Fig. 4.30 is much better than the relationship between T_c–T_a and soil water (Fig. 4.29), therefore use of T_c –T_a is not recommended for irrigation scheduling of glasshouse grown plants, but should be based on the temperature of reference leaves (T_{wet} and T_{dry}) which are used to estimate ICWSI. ICWSI also improves the scope for using canopy

temperature data for the entire season of a crop to obtain information on soil water storage rather than using canopy temperature data for the day of measurement that was suggested earlier on the basis of Fig. 4.28. I_G values varied exponentially with an increase in stored soil water (Fig. 4.31). It can be observed from Fig. 4.31 that low values of I_G were associated with T40 irrigation treatment in which soil water storage was low due to infrequent irrigation. Since I_G does not have a definite upper limit, its use for irrigation scheduling is more limited than ICWSI.

4.3.2.4 Effects of stomatal conductance on canopy temperature

Fig. 4.32 shows the plotted values of canopy temperature against stomatal conductance for various irrigation treatments for the glasshouse-grown cotton crop.

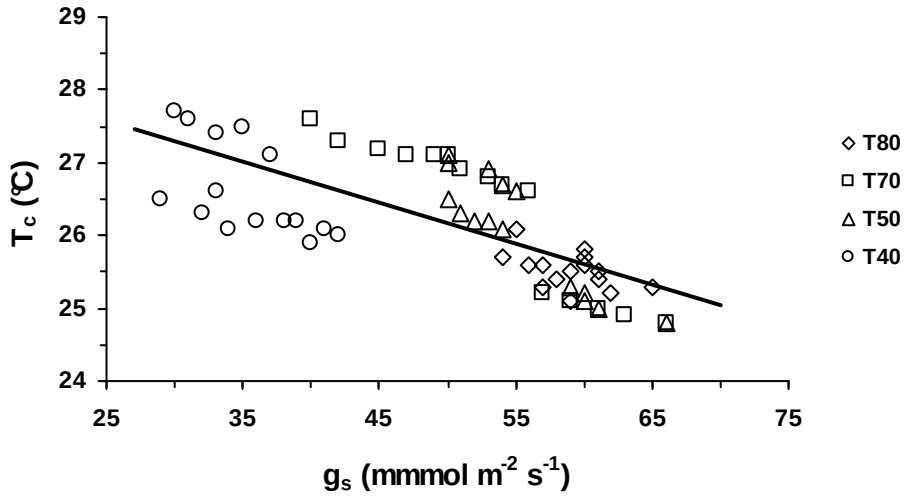

Figure 4. 32 Relationship between canopy temperature (T_c) and stomatal conductance (g_s) for various irrigation treatments of cotton crop inside the glasshouse (T_c = -0.056 g_s + 29.0, n = 80, R^2 = 0.51, P≤0.001).

It can be seen from Fig. 4.32 that low values of g_s and high values of canopy temperature mostly occurred in least frequently irrigated plants from T40 treatment due to water shortage within these plants reducing their transpiration rates. There was also a greater degree of scatter in these data compared with similar data for field experiments and that reduces confidence in the relationship between canopy temperature and stomatal conductance.

4.3.2.5 Relationship between crop water stress indices and stomatal conductance

Stomatal conductance (g_s) was plotted against crop water stress indices to determine the influence of g_s on crop indices (Figs. 4.33 and 4.34). It can be observed in Fig. 4.33 that low values of stomatal conductance were associated with high values of ICWSI in plants from T40 irrigation treatment due to increased water deficit in plants of this treatment. ICWSI values varied from 0.23 to 0.57 when stomatal conductance ranged within 29 to 66 mmol m^{-2} s^{-1}. Although the trend in these data was statistically significant, there was a greater degree of scatter when g_s was less than 45 mmol m^{-2} s^{-1}.

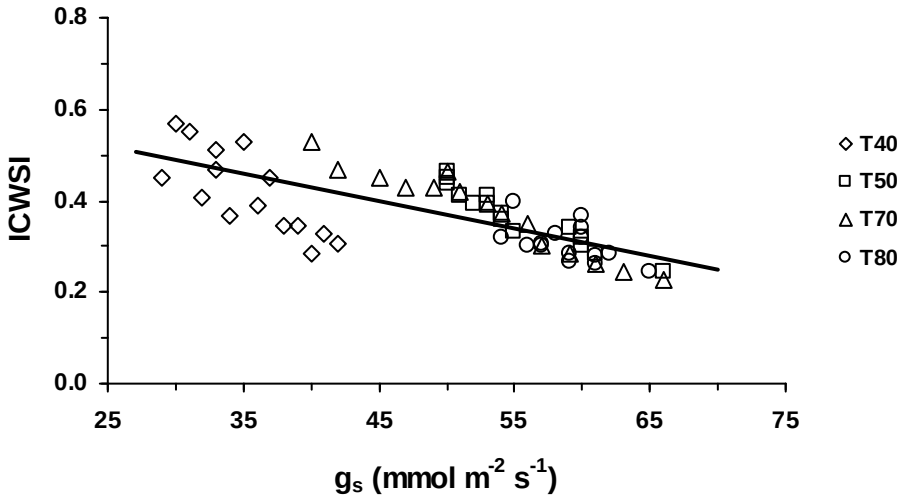

Figure 4. 33 Relationship between ICWSI and stomatal conductance (g_s) for various irrigation treatments of cotton in the glasshouse (*ICWSI* = -0.006 g_s + 0.7, n = 60, R^2 = 0.54, P≤0.001).

It can be observed from Fig. 4.34 that I_G increased linearly with an increase in stomatal conductance. High values of I_G and g_s were found for plants in T80 irrigation treatment because these plants were irrigated most frequently. As suggested earlier, frequent irrigation tends to maintain a high transpiration rate in plants due to greater number of stomata remaining open and that increases stomatal conductance in plants. Maintenance of high transpiration rate in leaves is important to sustain plant growth that is expected to increase plant productivity.

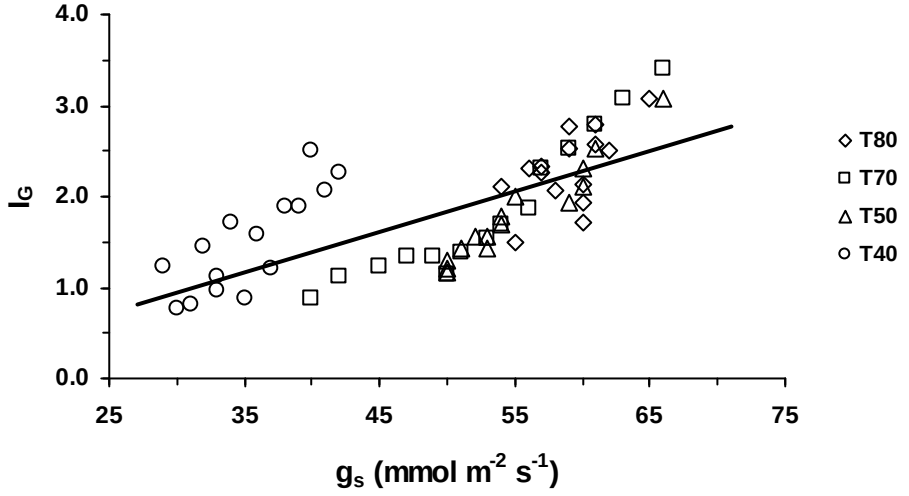

Figure 4. 34 Relationship between I_G and stomatal conductance (g_s) for various irrigation treatments of cotton in the glasshouse ($I_G = 0.045\ g_s - 0.4$, n = 60, $R^2 = 0.52$, $P \leq 0.001$).

4.4 Concluding remarks

The response of irrigated cotton crop to systematic variation in soil water deficit with various irrigation treatments described in this chapter indicates that thermal imagery or thermography is quite reliable in distinguishing most frequently irrigated (T50) and least irrigated treatment (T85) areas in the field. Strong dependency of canopy temperature on soil water within the root zone of cotton over two seasons (2007-08 and 2008-09) observed in the field suggests that this technique can be useful in mapping soil water deficit in the field. Crop water stress indices (i.e. ICWSI and I_G) have been developed as scaling variables so that these can be applied to a range of climates and crops. Although these relate well with soil water content or deficit within the root zone in the field, ICWSI is considered to be better suited for irrigation scheduling than I_G. Thermal imagery was also found to be suitable in the glasshouse experiment with cotton. Since thermography-derived canopy temperature relates well with soil water on the day of measurement rather than for the entire season, use of crop water stress indices is recommended for glasshouse-grown plants. Similarities in the pattern of spatial variation in canopy temperature and soil water over the entire cotton field reported in this chapter indicate that thermography

can be used as a rapid and convenient method for measurement of crop water deficit stress in commercial crops to predict soil water deficit such that precise quantity of water can be delivered in specific parts of a field to reduce crop water deficit stress.

Chapter 5

MONITORING WATER DEFICIT IN WHEAT WITH INFRARED THRMOGRAPHY

5.1 Introduction

Wheat is the fourth most important food and agricultural commodities in the world following sugarcane, maize and rice (FAO, 2007). Australia is placed as the 14th country with regard to wheat production in the world. Wheat is the second most important crop in Australia in terms of production (FAO, 2007). However, dwindling water resources in recent years has placed most crops including wheat under great pressure due to a possible future reduction in water yields imminent from climate change and escalating water demand due to population explosion on a global scale (Kijne et al., 2003). More efficient use of water in irrigated agriculture, in particular at the field scale, where it is related to irrigation scheduling, can be achieved from improved understandings of crop response to water deficit stress. The estimation of water stress in plants is of great importance since it can be used to monitor vegetation and predict primary productivity. A detailed knowledge of the variation in crop water status in space and time would improve the management of water resources through appropriate application and distribution of water to a crop when and where it is more vital for crop development (Mendez-Barroso et al., 2008).

Although many factors can reduce the yield of a crop, the major limiting factor is plant water deficit caused by insufficient supply and availability of water (Wanjura & Upchurch, 2000). Plant stress sensing might be considered as an ideal approach in regulating water supply to plants because the plant is a good integrator of the soil, water and climatic parameters (Gontia and Tiwari, 2008). When a crop plant transpires, water loss from its leaves cools the leaf surface such that the leaf temperature can sometimes drop below the ambient air temperature. Transpiration is an inevitable physiological process that is coupled with photosynthesis affecting growth and productivity of plants. As a crop plant continues to transpire, internal water deficit can occur starting from leaves but extending to other plant parts unless internal water supply meets the plant water demand. Any internal imbalance between

demand and supply of water in a plant leads to water deficit which may accumulate over time to translate to water stress reducing transpiration. Reduced transpiration rates reduce leaf cooling allowing leaf temperature to equilibrate to ambient temperature and may even surpass the air temperature (Jackson, 1982). Although there are additional factors that may contribute to development of internal water deficit in leaves and whole plants, leaf temperature is considered as one of the most important indicators of plants experiencing water stress (Petersen et al., 1992). Thus, canopy temperature has been used for several decades as an important indicator of water stress since development of infrared thermometers, which made this measurement possible without physically contacting the plant (Ehrler et al., 1978).

Most of the past studies on detection of water stress in plants have been based on infrared thermometry which involves acquisition of a thermal signal from the plant and the atmosphere surrounding the plant (Alderfasi and Nielsen, 2001; Gontia and Tiwari, 2008). However, measurement of foliage temperature is difficult with hand- held infrared thermometers in partially vegetated fields and most airborne and satellite based infrared sensors can limit the potential application of this technique (Rodriguez et al., 2005). In contrast, thermography (also known as infrared thermography) with greater capability allows acquisition of the thermal image of an area that can be controlled and later manipulated through post-image analysis by the user. The potential advantage of thermography over point measurements with infrared thermometers is the ability of the image to cover a large number of individual leaves and plants at one time at a high spatial resolution. Recent development and commercial availability of portable thermal imagers and the associated image analysis software has overcome the problems associated with infrared thermometers. It is possible to identify areas of varying levels of water stress in crop fields due to water or other factors affecting stomatal closure in leaves (also coincides with zero transpiration) using thermal imaging technologies (Fitzgerald et al., 2006).

Estimation of crop water status using thermal indices (derived from leaf/canopy temperature) has been shown to be very robust (Idso et al., 1981; Jackson et al., 1981) and could provide a way to map water status of plants in a field. Rodriguez et al. (2005) developed a canopy physiological stress index with spatial resolution corresponding with the needs of site specific management. Fitzgerald et

al. (2006) used both spectral and thermal sensing to detect nitrogen and water status for rainfed and irrigated wheat. Lenthe et al.'s (2007) study explained the usefulness of an infrared thermography to monitor the canopy health of wheat. Estimation of evapotranspiration for a wheat crop by using thermal infrared images and ground based radiometers was described by French et al. (2006). Rigorous testing of thermal imaging against more traditional physiological techniques of measuring water status of plants under field conditions is still required to determine the correspondence between thermal emission characteristics and physiological response of plants to water deficit (Grant et al., 2006). Earlier studies which have used infrared methods for irrigation scheduling are able to indicate stomatal closure or transpiration rate but they give no information on the amount of soil water available or that needs to be supplemented via irrigation at that time (Jones, 2004b). Therefore, experiments were conducted both in the field and glasshouse with wheat to test:

- whether thermal imaging can be used as an irrigation scheduling technique for wheat crops growing under various irrigation treatments;
- the effectiveness of crop water stress indices (e.g. I_G and ICWSI described in previous chapters) in estimating soil water status.
- the effects of plant physiological measures of plant water status on the canopy temperature and their relationship with crop water stress indices.

5.2 Materials and Methods

Two experiments were conducted on wheat (*Triticum aestivum* L., cv Lang) in 2008. The first experiment was a field experiment at the Queensland Primary Industries and Fisheries (now referred to as Department of Employment, Economic development and Innovation) experimental station near Kingsthorpe (27°30'44"S, 151°46'55"E, and 431 m elevation). The other experiment was conducted in the glass house of the University of Southern Queensland. Full details of the soil properties used for the field site were given in Chapter 4. The experimental design used was similar to that used for cotton. Soil used for the glasshouse experiment was as for the previous chapter.

5.2.1 Field experiment with wheat

This field experiment consisted of four irrigation treatments with three replications using a randomized block design. Irrigation treatments and plot layout were as detailed in Chapter 4. In this experiment with wheat, T85 treatment plots were not subdivided into solid and skip row planting as in case of cotton. Wheat was planted on 6th June 2008 and harvested on 11th November 2008. During the experimental period, daily minimum and maximum air temperature varied from -5.3 to 36.6 °C and the relative humidity between 17% and 100%. Total rainfall during the experimental period was 212 mm. Wheat seedlings emerged within 10 days after planting of seeds at a depth of 50-75 mm on 6th June 2008. At the time of planting, 100 kg N ha^{-1} of urea and 230 kg ha^{-1} of mono-ammonium phosphate was applied to all the experimental plots. Although planting density was aimed to maintain 200 plants m^{-2}, the measured planting density was 220 plants m^{-2} with a row spacing of 25 cm. For weed control, Starane 200 was initially applied at 0.5 l ha^{-1} on 1st July 2008 with a subsequent application of 1 l ha^{-1} on 22nd July 2008. At 63 DAP, when the first node of wheat appeared, an additional amount of N-fertilizer (100 kg N ha^{-1}) was applied. Each replicate plot was irrigated with bore water using a hand-shift sprinkler system (Fig. 5.1).

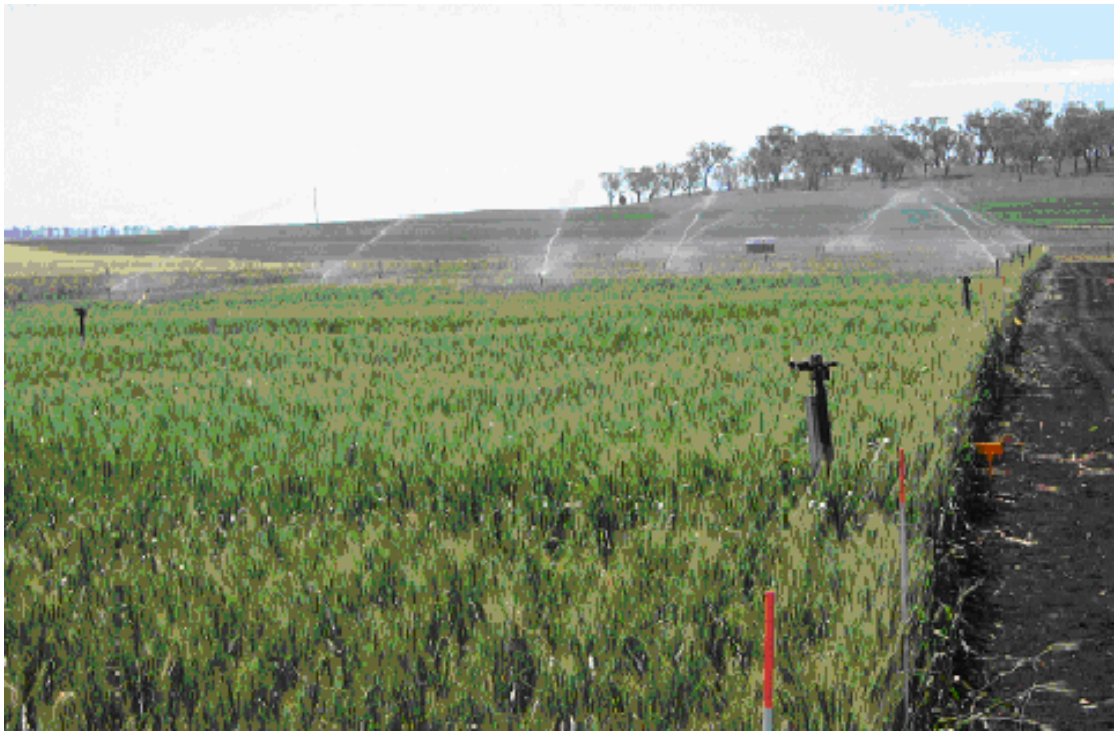

Figure 5. 1 Hand shift solid sprinkler system used for application of irrigation water to the wheat crop.

Irrigation treatments in various plots were imposed on 64 DAP and continued up to 130 DAP. All replicates of T50, T60, T70 and T85 treatments were supplied with 203, 152, 79 and 73 mm irrigation water, respectively. For T50, T60, T70 and T85 irrigation treatments, 1 neutron probe access tube was installed in each replicate plot to monitor the soil water distribution over the growing season. A neutron probe (503DR Hydroprobe, Campbell Pacific Nuclear Inc., Martinez, CA, USA) was used to measure soil water content from the surface to a depth of 1.33 m at 0.1 m depth increments. Calibration process for the neutron probe was as described previously in Chapter 4.

5.2.2 Measurements in the field

Thermal images of wheat plants were taken with an infrared camera (NEC TH7800 model, NEC, Japan) for 12 plots 2 m above the ground as described for the cotton crop in Chapter 4. Canopy temperature (°C) was derived for leaves only by analysis and processing of the thermal image with the software Image Processor Pro II (Version 4.0.3, NEC, Japan). Air temperature was also measured at the time of thermal imaging with an Omega type RTD (resistance temperature detector) probe. Images of wet and dry reference leaves were taken for each irrigation treatment at the time of image acquisition of normal leaves to derive corresponding reference surface temperatures (T_{wet} and T_{dry}). Assuming an emissivity of 1.0 for plants has been reported to induce an error of <1°C (Jackson, 1982) as emissivity for plant leaves usually varies from 0.92-0.99 (Idso et al., 1969; Rees, 2001; Sutherland, 1986). Emissivity of wheat crop selected for this experiment was 0.98 (as reported by Chen & Zhang, 1989; Husband & Monteith, 1986; Wang et al., 1994). Detailed specification of the infrared camera, procedure for selection of wet and dry leaves and estimation of crop water stress indices such as I_G and ICWSI from the reference leaves remained the same as described in Chapter 4.

Following thermal imaging, the position of image objects in the field was recorded separately with the help of a hand-held GPS (Model 72, Garmin, Kansas, USA) to examine spatial variation in canopy temperature within the experiment. Since the GPS recorded the location of all measurements in latitude and longitude format (i.e. degree, minute and second), the recorded data were converted to easting and northing by using a UTM conversion excel spread sheet (Dutch, 2007). Table

5.1 shows the timing and measurement dates of thermal imaging. Soil water content was measured with the neutron probe on the same day as for thermal imaging to explore the interrelationships between canopy temperature (°C) and soil water content within the root zone of the crop. The effective root zone depth was determined for the day of thermal imaging as described in Chapter 4 that allowed estimation of soil water (θ_z, mm).

Table 5. 1 Timing and measurement dates of thermal imaging of wheat crop during the experiment.

Measurement dates (DAP)	Time of measurement
63	10.50 A.M. – 11.10 A.M.
70	2.10 P.M. – 2.25 P.M.
105	9.30 A.M. – 10.10 A.M.
112	9.40 A.M. – 10.15 A.M.
119	9.40 A.M. – 10.10 A.M.
131	9.35 A.M. – 10.10 A.M.

Leaf water potential (Ψ_l) was measured with a Model 1000 pressure chamber (PMS Instrument Company, Oregon, USA) on five occasions (Table 5.2) as described in the previous chapter. Wheat leaves were sampled from the area used for thermal imaging to measure stomatal conductance of leaves (g_s) with a PMR-5 steady state porometer (PP Systems, Norfolk, UK) under ambient light conditions on 3 occasions (Table 5.2). Finally, wheat was harvested by harvester on 11th November 2008 and grain yield was measured separately for each replicate plot of various irrigation treatments.

Table 5.2 Timing and measurement dates of leaf water potential and stomatal conductance of wheat crop during the experiment.

Measurement dates (DAP)	Time of measurement of Ψ_l	Time of measurement of g_s
70	2.30 P.M. – 3.35 P.M.	-
105	12.00 P.M. – 1.35 P.M.	10.35 A.M. – 11.45 A.M.
112	10.25 A.M. – 11.35 A.M.	11.40 A.M. – 12.45 P.M.
119	10.30 A.M. – 11.40 A.M.	11.10 A.M. – 12.40 P.M.
131	10.15 A.M. – 11.30 A.M.	-

5.2.3 Glasshouse experiment

An irrigation experiment with wheat (*Triticum aestivum* L., cv. Lang) was conducted within the glasshouse from 31st July 2008 to 5th December 2008 (Fig. 5.2). The experiment consisted of 28 pots that represented 7 replicates of 4 irrigation treatments, all arranged in a randomised block design. The details of the properties of soil used for the experiment, method of preparation of pots and irrigation treatments have been explained in Chapter 3. As mentioned in Chapter 3, 12 of the 28 pots (4 treatments × 3 replicates) were placed over the mini-lysimeter system for continuous monitoring of water loss from pots at short time intervals. The remaining 16 pots (4 treatments × 4 replicates) were placed on a bench adjacent to the mini lysimeter system inside the glasshouse at the same height as the lysimeter pots. Detailed description of the mini-lysimeter system and weather parameters during the growth period of wheat have been previously given in Chapter 3. Detailed information on the crop and irrigation management aspects for wheat in this experiment is also given in Chapter 3.

Figure 5. 2 Wheat growing in pots in the glasshouse experiment. Front three rows of pots are placed over the mini-lysimeter system.

Thermal images of plants were taken on 6 occasions (Table 5.3) for all replicates of irrigation treated pots with the infrared camera as for the field experiment. Images of reference leaves (i.e. T_{wet} and T_{dry}) were taken on 4 occasions (73, 81, 84 and 91 DAP) in the same way as for the field experiment. Details of the infrared camera, procedure for selection of wet and dry leaves and calculation of I_G and ICWSI indices from the reference leaves was as described in Chapter 4. Emissivity for wheat crop inside the glasshouse remained the same as for the field experiment. Canopy temperature (°C) was derived from analysis of thermal images with the Image Processor Pro II software (Version 4.0.3, NEC, Japan). Air temperature (°C) was also recorded during the time of thermal imaging with Omega type RTD (resistance temperature detector) probe. In order to relate the canopy temperature with soil water, stored soil water (θ, mm) in each pot during thermal imaging was calculated according to the procedure as described previously in Chapter 4. Leaf water potential (Ψ_l) was measured with the Model 1000 pressure chamber (PMS Instrument Company, Oregon, USA) following thermal imaging on four occasions (Table 5.3).

All wheat plants were harvested on 5th December 2008. At harvest, whole plants above the soil level were excised and then the total weights of plants along with grains were measured with an electronic platform balance. After that plants and grains were dried inside the oven at 65° C for three days and the weight of plant and grain was measured after drying.

Table 5. 3 Timing and measurement dates for thermal imaging and leaf water potential of wheat plants in the glasshouse experiment.

Measurement dates (DAP)	Time of thermal imaging	Time of measurement of Ψ_l
69	12.10 P.M. – 12.50 P.M.	-
73	12.00 P.M. – 12.40 P.M.	-
81	11.00 A.M. – 12.00 P.M.	12.05 P.M. – 12.35 P.M.
84	11.50 A.M. – 12.40 P.M.	12.50 P.M. – 1.20 P.M.
91	1.00 P.M. – 2.00 P.M.	2.10 P.M. – 2.40 P.M.
98	12.10 P.M. – 12.55 P.M.	1.05 P.M. – 1.35 P.M.

5.3 Results and Discussion

5.3.1 Wheat experiment

5.3.1.1 Effects of soil water on canopy temperature

Analysis of variance of the measured field data indicated significant effects of irrigation treatments on canopy temperature and soil water within the root zone for 4 of the 6 measurement occasions. Mean values of canopy temperature and soil water within the root zone for these measurement periods are shown in Tables 5.4 and 5.5. It can be seen from Table 5.4 that canopy temperature for T50 irrigation treated wheat plants remained consistently lower than the T85 treated wheat plants throughout the season because plants under T50 treatment were irrigated more frequently than the plants under T85 treatment. Soil water within the root zone of wheat in Table 5.5 indicated that more frequently irrigated treatment (T50) also remained consistently wetter than the least irrigated treatment (T85).

Table 5. 4 Effects of irrigation treatments on the canopy temperature of wheat in the field on selected measurement dates (indicated as days after planting, DAP). Mean values with a different superscript are significantly different (P≤0.05) when compared with the least significant difference (LSD).

Measurement dates (DAP)	Canopy temperature (°C) T50	T60	T70	T85	LSD (°C)
105	25.6^{b}	29.1^{a}	26.4^{b}	29.2^{a}	2.4
112	22.5^{b}	24.5^{a}	23.3^{b}	24.5^{a}	1.0
119	25.9^{b}	30.3^{a}	29.9^{a}	30.1^{a}	0.5
131	24.6^{b}	29.7^{a}	29.3^{a}	30.3^{a}	2.1

Table 5. 5 Effects of irrigation treatments on soil water within root zone of wheat in the field on selected measurement dates (indicated as days after planting, DAP). Mean values with a different superscript are significantly different (P≤0.05) when compared using LSD as for the previous table.

Measurement dates (DAP)	Soil water within root zone (mm) T50	T60	T70	T85	LSD (mm)
105	320.6^{a}	287.5^{c}	303.6^{b}	294.1^{bc}	14.5
112	343.8^{a}	311.5^{c}	327.2^{b}	316.3^{bc}	12.3
119	387.3^{a}	309.8^{b}	325.4^{b}	313.5^{b}	29.5
131	443.5^{a}	352.8^{b}	349.5^{b}	330.4^{b}	45.7

To investigate the effects of soil water on canopy temperature for the wheat crop, canopy temperature was plotted against soil water within the root zone (Fig. 5.3). An equation fitted to these data is $T_c = 0.667\ \theta_z^{0.629}$, (n = 72, R^2 = 0.49, P≤0.001), where T_c = canopy temperature in °C and θ_z = soil water within the root zone in mm. It can be seen from Fig. 5.3 that the canopy temperature of the wheat crop appeared to increase with increase in soil water content. In this case, a combined analysis of the data tends to contradict the general notion that canopy temperature should be low at high soil water content as increased water supply in root zone of a plant should allow it to maintain adequate transpiration and cooling of leaves. Since the resistance to water flow from soil via root and stem to leaf is not constant over time (see discussion in Section 4.3.1.3 in Chapter 4), the variation of canopy temperature (as an indicator of the resistance to water flow from leaf to atmosphere) with variation in soil water for cotton (Figs. 4.12, 4.13 and 4.28) over the entire growing season was quite different from wheat (Fig. 5.3). Additional differences in the relationship between canopy temperature and soil water for the two crops could be also due to the wider variation in soil water over all irrigation treatments for cotton (Tables 4.7 and 4.9) compared with wheat (Table 5.6) and the differences in weather conditions at the time of canopy temperature measurements.

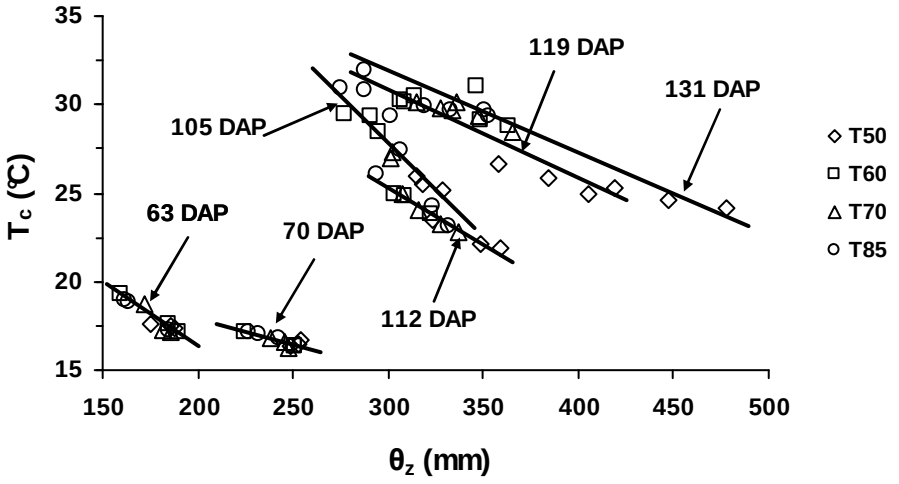

Figure 5. 3 Variation in canopy temperature (T_c) with soil water within the root zone (θ_z) for various irrigation treatments of wheat in the field. Six solid lines within this graph show a local decreasing trend in canopy temperature with increasing soil water within the root zone for the specific date of measurement shown as days after planting (DAP).

Further explanation to apparent contradictory situation in Fig. 5.3 arising as a result of the differences in weather conditions is as follows. Cooling of leaves usually occur in relation to the ambient temperature as heat is exchanged between the leaf surface and the surrounding air during transpiration. As the capacity of stomata to control transpiration from leaves varies with species and cultivars, a hydraulic feedback within the control system of stomata (Jones, 1998) may limit the maximum conductance and transpiration rate when weather conditions (e.g. atmospheric vapour pressure deficit, VPD) differ substantially during the measurements of canopy temperature. VPD is usually estimated from air temperature and relative humidity (see p33-39, Allen et al., 1998). Due to the unavailability of relative humidity data during the measurements of canopy temperature, approximate estimates of VPD could be obtained by combining air temperature measurements with relative humidity data from the nearby weather station for some of the measurement dates. Average VPD values at the time of canopy temperature measurements on 63, 105, 112 and 119 DAP were 0.88, 2.33, 1.51 and 1.66 kPa, respectively.

It can be seen from Fig. 5.3 that the slope of the linear relationships between T_c and θ_z suggested for various dates (DAP) tend to increase with an increase in VPD. This distinctive nature of the physiological response of wheat to water deficit has been used to develop a canopy stress index that combines T_c (derived from thermography) with air temperature (T_a) and VPD (Rodriguez et al., 2005). One of the possible reasons for the dependency of canopy temperature-soil water relationship on weather conditions (VPD) for wheat is due to a distinct seasonal change expected during the growth period. In this experiment, wheat was planted in winter and harvested towards the beginning of summer and that contributed to a substantial variation in ambient temperature during the season. The solid lines shown in Fig. 5.3 describing the linear trend in data for various DAP was derived by fitting regression equations to the data for individual dates of measurement (Table 5.6).

All regression equations shown in Table 5.6 were highly significant ($P \leq 0.001$) with high R^2 values and all indicated that canopy temperature decreases with an increase in soil water within the root zone for a given day of measurement. Ranges of soil water and canopy temperature observed for selected measurement dates are also shown in this table to which the fitted regressions apply. These analyses indicate

that the general plant response of linear decrease in canopy temperature with increasing soil water may apply uniformly for the whole cropping season of cotton (Chapter 4) but not for wheat (this chapter).

Table 5. 6 Regression equations and coefficient of determination (R^2) for the relationship between canopy temperature (T_c, °C) and soil water within root zone (θ_z, mm) for various irrigation treatments on 6 measurement dates (indicated as days after planting, DAP), range of soil water and canopy temperature. No. of data points (n) used for each measurement date was 12 and $P \leq 0.001$.

Measurement dates (DAP)	Range Soil water (mm)	Range Canopy temperature (°C)	Regression equation	R^2
63	160 – 190	17.1 – 19.3	$T_c = -0.071\ \theta_z + 30.6$	0.91
70	225 – 254	16.2 – 17.2	$T_c = -0.029\ \theta_z + 23.7$	0.77
105	275 – 329	24.9 – 30.9	$T_c = -0.107\ \theta_z + 59.9$	0.76
112	294 – 359	21.9 – 26.1	$T_c = -0.065\ \theta_z + 44.8$	0.95
119	288 – 419	25.3 – 30.8	$T_c = -0.050\ \theta_z + 45.8$	0.91
131	288 – 477	24.2 – 31.9	$T_c = -0.046\ \theta_z + 45.7$	0.90

5.3.1.2 Effects of soil water on the difference between canopy and air temperature difference ($T_c - T_a$)

Air temperature (T_a) was measured with an Omega type RTD probe on 4 occasions (ie. 63, 105, 112 and 119 DAP) at the time of thermal imaging. The difference in canopy (T_c) and air temperature was estimated and has been plotted against the soil water within the root zone (Fig. 5. 4). This figure shows considerable improvement in the dependency of T_c over θ_z as it incorporates the seasonal variation in T_a. In case of T50 treatment (the most frequently irrigated) the difference between canopy and air temperature was negative most of the time possibly because plants were able to maintain a high transpiration rate throughout the season. This supports early assertions by Jackson (1982) that the canopy temperature should be similar or lower than the air temperature when water availability to plants is adequate. In case of least irrigated treatment (T85) the canopy temperature remained higher than the air temperature indicating lower water availability or persistence of some degree of water deficit in wheat in this experiment.

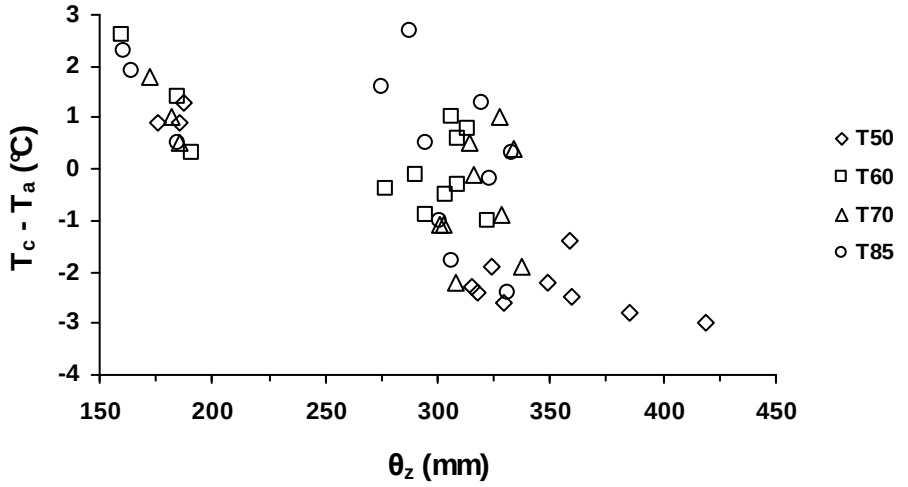

Figure 5. 4 The dependence of canopy and air temperature difference ($T_c - T_a$) on soil water within the root zone (θ_z) for various irrigation treatments of wheat in the field.

5.3.1.3 Crop water deficit indices and their implications to irrigation scheduling

Crop water deficit indices such as ICWSI and I_G were calculated from the measurements of canopy, wet and dry reference temperature as described previously in Chapter 4. Estimation of these indices was time consuming because at any measurement occasion, there were 12 plots (three replicate plots of four irrigation treatments) for which each canopy temperature measurement was supplemented with dry and wet reference temperature measured for leaves from each replicate plot. For rapid estimation and practical use of these thermal indices for irrigation scheduling, it may be possible to derive the wet reference temperature from the plot with the highest soil water content (most frequently irrigated treatment) and the dry reference temperature from the plot with the least soil water content (least frequently irrigated plot) since the coefficient of variation in reference temperatures was small (<8%). It is expected that these reference temperatures would help with the scaling of canopy temperature for wheat leaves at the intermediate levels of soil water (other irrigation treatments). Fig. 5.5 shows the plotted values of ICWSI against soil water within the root zone for the entire wheat season as well as fitted values for these parameters separately on each measurement date.

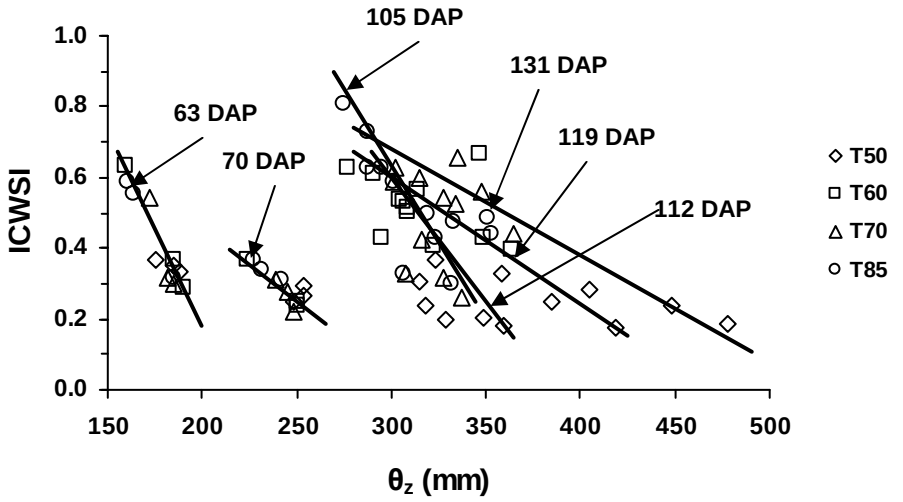

Figure 5. 5 Variation in crop water deficit index ICWSI with soil water within the root zone (θ_z) for various irrigation treatments of wheat in the field. Six solid lines within this graph show a local decreasing trend in ICWSI with increasing soil water within the root zone for specific date of measurement shown as days after planting (DAP)

The water stress index ICWSI commonly varies from 0 to 1 with 0 value indicating plants under no water stress to 1 for plants under maximum water stress. No systematic pattern of dependence between the plotted variables can be seen in Fig. 5.5 when all the measurements of ICWSI and soil water within the root zone of wheat crop are considered. The variation in the data appears to be similar to that in Fig. 5.3. ICWSI values in Fig. 5.5 ranged from 0.18 to 0.37 for T50, 0.22 to 0.67 for T60 and T70 and 0.30 to 0.81 for T85 treatments when all the measurements for ICWSI and soil water within the root zone of wheat were taken into consideration. Low ICWSI value (<0.4) on most occasions for T50 indicates little internal water deficit in wheat due to frequent irrigation.

In a similar manner, high values of ICWSI (>0.7) or high internal water deficit in wheat was observed in least frequently irrigated treatment of T85. Due to the overlap in values of ICWSI and soil water within root zone, no unique relationship between the plotted variables can be seen in Fig. 5.5. Therefore, fitted values of ICWSI against soil water within root zone for each measurement date are also shown separately in Fig. 5.5. It can be observed from Fig. 5.5 that ICWSI values decreased with increase in soil water within root zone for each individual date of measurement.

Fig. 5.6 shows plotted values of I_G against soil water within root zone for the entire wheat season as well as fitted values for these parameters separately on each measurement date. The major difference between these two indices is that, unlike ICWSI, I_G is usually high when the soil water within the root zone is high. I_G values varied from 1.71 to 4.67 for T50 treatment, 0.50 and 3.53 for intermediate irrigation treatments (i.e. T60 and T70) and 0.24 to 2.24 for T85 treatment, respectively. Since a general trend did not exist for the data in Figs. 5.5 and 5.6, regression equations for these variables were checked to judge their suitability for irrigation scheduling for the day of measurement. The regression equations, R^2 values and range of crop water deficit indices and soil water for these regressions are presented in Tables 5.7 and 5.8.

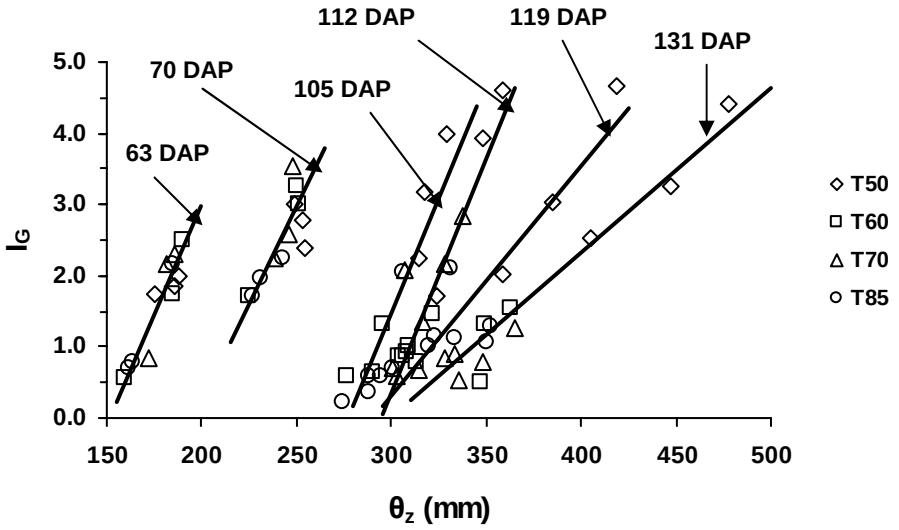

Figure 5. 6 Variation in crop water deficit index I_G with soil water within the root zone (θ_z) for various irrigation treatments of wheat in the field. Six solid lines within this graph show an increase in I_G with increasing soil water within the root zone for individual date of measurement (shown as DAP).

The coefficient of determination **(**R^2) of all the fitted regressions varied from 0.76 – 0.95 in case of ICWSI and 0.73 – 0.92 for I_G and were highly significant ($P \leq 0.001$). ICWSI may be considered more appropriate for irrigation scheduling than I_G, because there is no fixed range of variation for this index where as ICWSI varied form 0 to 1. Thus, on a given day of measurement, ICWSI can be used for irrigation scheduling when it reaches a critical value (e.g. 0.4), as mentioned earlier, so that crop plants will not experience high water stress. These indices were developed to

examine whether plants are experiencing internal water deficit. Their variation against environmental factors particularly VPD is well established in situations when the crops are well watered or fully water stressed (Idso et al., 1981). A crop that is growing in a normal condition, these indices are expected to indicate a systematic pattern of variation when plotted against VPD (Idso et al., 1981), but their pattern of variation against soil water content or deficit is unknown.

Table 5. 7 Regression equations and coefficient of determination (R^2) for the relationship between *ICWSI* and soil water within root zone (θ_z, mm) for various irrigation treatments on six measurement dates (indicated as days after planting, DAP), range of soil water and ICWSI. No. of data points (n) used for each DAP was 12 and P≤0.001.

Measurement dates (DAP)	Range		Regression equation	R^2
	Soil water (mm)	ICWSI		
63	160 – 190	0.29 – 0.63	$ICWSI = -0.011\ \theta_z + 2.4$	0.91
70	225 – 254	0.22 – 0.37	$ICWSI = -0.004\ \theta_z + 1.3$	0.77
105	275 – 329	0.20 – 0.81	$ICWSI = -0.010\ \theta_z + 3.7$	0.76
112	294 – 359	0.18 – 0.63	$ICWSI = -0.007\ \theta_z + 2.7$	0.95
119	288 – 419	0.18 – 0.63	$ICWSI = -0.004\ \theta_z + 1.7$	0.91
131	288 – 477	0.19 – 0.73	$ICWSI = -0.003\ \theta_z + 1.6$	0.81

Table 5. 8 Regression equations and coefficient of determination (R^2) for the relationship between I_G and soil water within root zone (θ_z, mm) for various irrigation treatments on six measurement dates (indicated as days after planting, DAP), range of soil water and I_G. No. of data points (n) used for each DAP was 12 and P≤0.001.

Measurement dates (DAP)	Range		Regression equation	R^2
	Soil water (mm)	I_G		
63	160 – 190	0.58 – 2.50	$I_G = 0.061\ \theta_z - 9.3$	0.89
70	225 – 254	1.72 – 3.53	$I_G = 0.054\ \theta_z - 10.7$	0.79
105	275 – 329	0.24 – 4.00	$I_G = 0.061\ \theta_z - 16.9$	0.73
112	294 – 359	0.60 – 4.60	$I_G = 0.065\ \theta_z - 19.2$	0.91
119	288 – 419	0.60 – 4.67	$I_G = 0.032\ \theta_z - 9.3$	0.91
131	288 – 477	0.37 – 4.40	$I_G = 0.023\ \theta_z - 6.9$	0.92

5.3.1.4 Effect of leaf water potential and stomatal conductance on canopy temperature

Fig. 5.7 describes the relationship between canopy temperature (T_c) and leaf water potential (Ψ_l) measured on selected occasions. Ψ_l varied from -2.3 to -3.65 MPa when canopy temperature varied within 16-32 °C. The canopy temperature of the wheat crop increased when Ψ_l decreased (or became more negative) due to increased

internal water deficit within the wheat leaves. Fig. 5.8 shows plotted values of canopy temperature against stomatal conductance for the wheat crop.

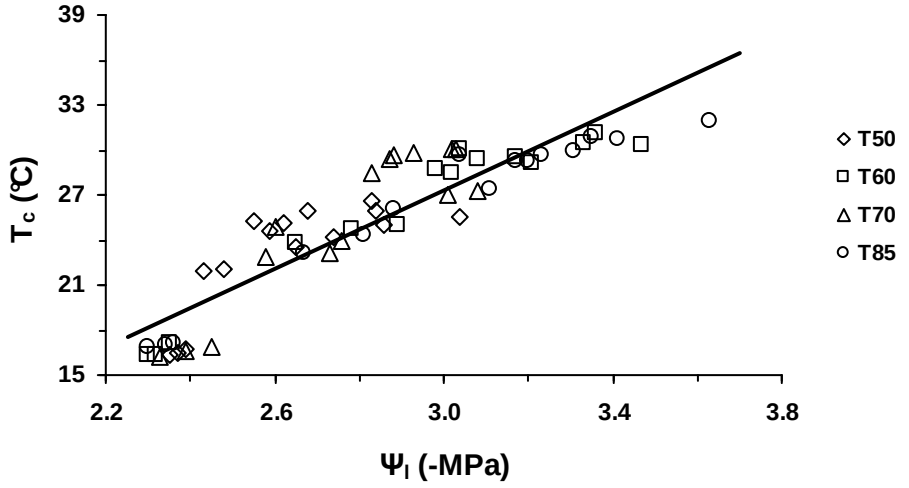

Figure 5. 7 The relationship between canopy temperature (T_c) and leaf water potential (Ψ_l) for various irrigation treatments given to the wheat crop (T_c = 13.04 Ψ_l – 11.8, n = 60, R^2 = 0.83, P≤0.001).

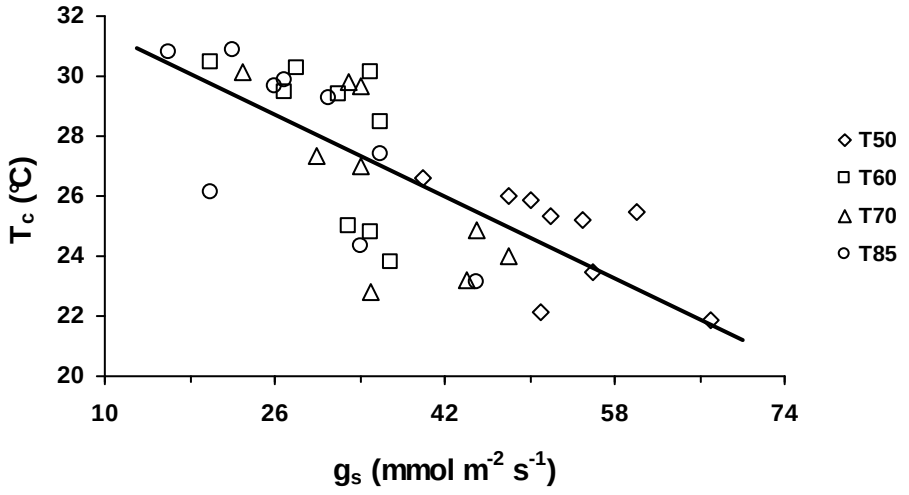

Figure 5. 8 The relationship between canopy temperature (T_c) and stomatal conductance (g_s) for various irrigation treatments given to the wheat crop (T_c = -0.17 g_s + 33.1, n = 36, R^2 = 0.53, P≤0.001).

Canopy temperature of wheat increased with a decrease in stomatal conductance of the leaves. Since high values of g_s and low values of T_c were observed mostly for plants from the T50 treatment in Fig. 5.8, it can be concluded that frequent irrigation of crops increases canopy transpiration due to an increase in stomatal conductance of leaves which may be the main reason for the reduction in canopy temperature.

5.3.1.5 Relationship between crop water deficit indices and stomatal conductance

Figs. 5.9 and 5.10 show variation in crop water deficit indices (i.e. ICWSI and I_G) with stomatal conductance of wheat leaves. It can be seen from these figures that values of g_s were 3-4 times higher for the frequently irrigated plants (T50 treatment) than the least irrigated plants (T85 treatment). It can be observed from Fig. 5.9 that canopies with high stomatal conductance have low ICWSI values. Since I_G and ICWSI are inversely related, I_G values were high when stomatal conductance was also high (Fig. 5.10).

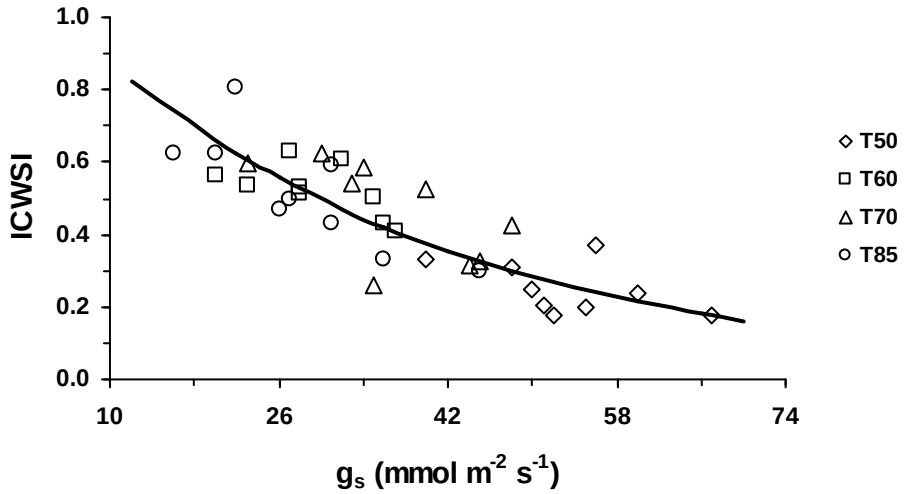

Figure 5. 9 The relationship between ICWSI and stomatal conductance (g_s) for various irrigation treatments given to the wheat crop ($ICWSI$ = 1.148 e $^{-0.028\ gs}$, n = 36, R^2 = 0.72, P≤0.001).

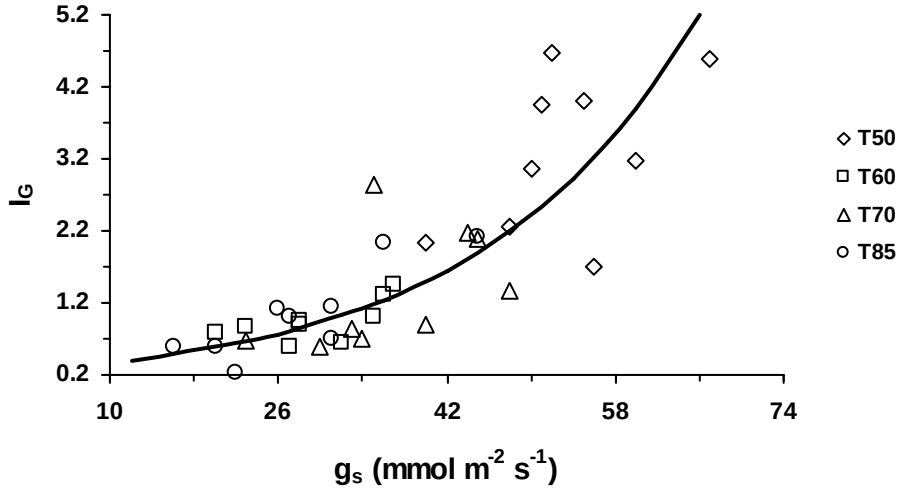

Figure 5. 10 The relationship between I_G and stomatal conductance (g_s) for various irrigation treatments given to the wheat crop ($I_G = 0.222\ e^{0.048\ gs}$, n = 36, $R^2 = 0.71$, $P \leq 0.001$).

5.3.1.6 Spatial variation in soil water and canopy temperature

Figures 5.11 and 5.12 show the spatial variation in canopy temperature and soil water within the root zone for all the 12 plots of the irrigation experiment with wheat. Filled circles on these maps represent the measurement location for each plot with labels denoting irrigation treatments (T50…T85) and replicates (R1…R3). Zones within these maps with a darker shade of blue indicate low value of canopy temperature which coincided with a similar location in the field of high soil water within the root zone. In a similar way, areas of lighter shade of blue (almost white) represent high canopy temperature and low soil water within the root zone. Since areas of the field with T50 and T85 treatments respectively indicate areas of lowest and highest soil water deficit, frequent mapping of canopy temperature can be used as an estimator of relative soil water deficit in a field so that the appropriate quantity of irrigation water can be applied to reduce variation in canopy temperature and soil water deficit in a wheat field.

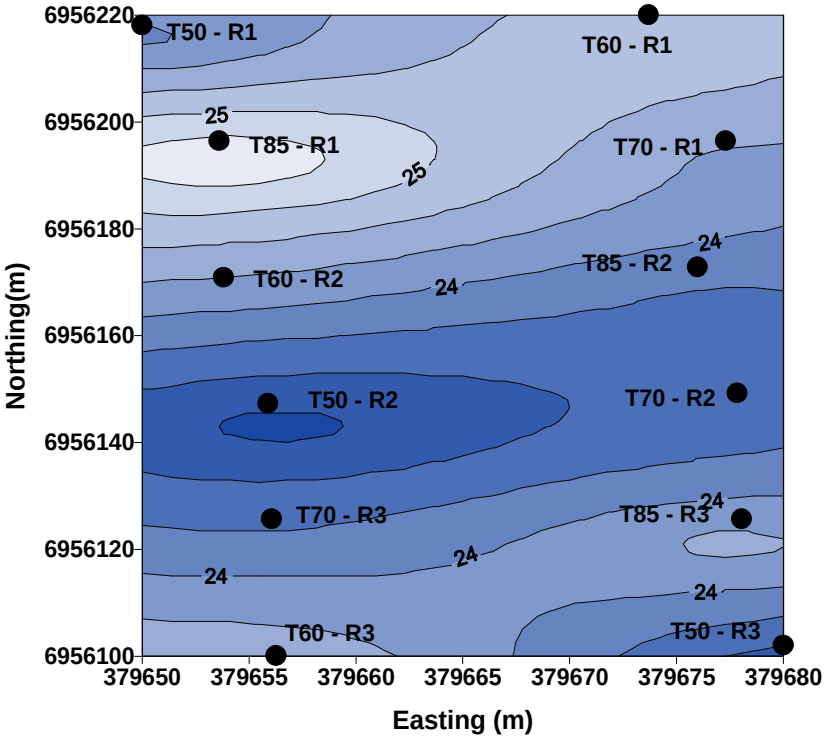

Figure 5. 11 Spatial variation in canopy temperature at the irrigation experiment site at 112 days after planting wheat. Filled circles indicate the position of measurement for irrigation treatments T50, T60, T70 and T85 and replicates R1, R2 and R3 of each irrigation treatment. The contour lines show the values of canopy temperature in °C.

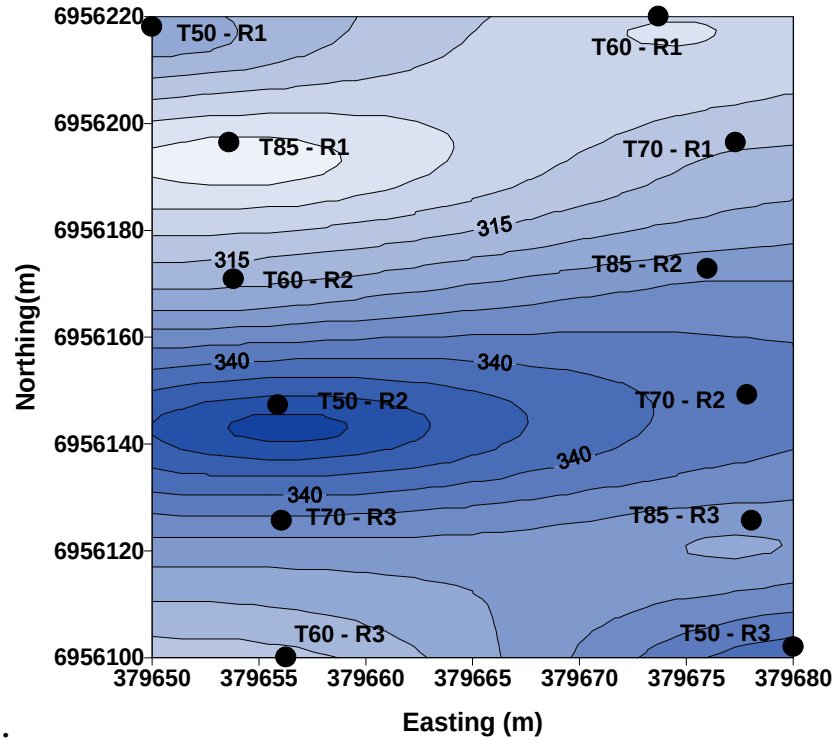

.

Figure 5. 12 Spatial variation in soil water within root zone at the irrigation experiment site at 112 days after planting wheat. Filled circles indicate the position of measurement for irrigation treatments T50, T60, T70 and T85 and replicates R1, R2 and R3 of each irrigation treatment. The contour lines show the values of soil water within the root zone in mm.

5.3.2 Glasshouse experiment

5.3.2.1 Effect of stored soil water on canopy temperature

Significant effects of irrigation treatments on canopy temperature and soil water storage (stored soil water) were detected on all six measurement occasions. Soil water stored following a given irrigation (and any drainage shortly afterward) is a function of water deficit present in the soil at the time of irrigation (arising from ET losses from the previous irrigation) and the water that could be retained by the soil following an irrigation and drainage. Due to the small volume of root zone limited by the size of pot, all stored soil water can be considered as available to the plant for evapotranspiration.

Mean values of canopy temperature and stored soil water for these measurement periods are shown in Tables 5.9 and 5.10. It can be seen from Table 5.9 that the canopies of plants growing under T40 irrigation treatment were significantly warmer than under T80 treatment at most times during the experiment, except at 73 days after planting. This is because irrigation was given to plants under T40 treatment a few days before (at 70 DAP) that increased θ for the T40 treatment to increase over the θ for T80 treatment (Table 5.10). Data on soil water storage in Table 5.10 indicated that more frequently irrigated treatment (T80) also remained consistently wetter than the least irrigated treatment (T40), except at 73 DAP as explained above. The maximum difference in canopy temperature between the least irrigated and frequently irrigated treatment was 2.7 °C during the crop growth period.

Table 5. 9 Effects of various irrigation treatments on the canopy temperature of wheat on selected measurement dates (indicated as days after planting, DAP) inside the glasshouse. Mean values with a different superscript are significantly different (P≤0.05) when compared with the least significant difference (LSD) given.

Measurement dates (DAP)	Canopy temperature (°C) T80	T70	T50	T40	LSD (°C)
69	28.4^{c}	28.6^{c}	30.6^{b}	31.1^{a}	0.3
73	28.7^{c}	29.5^{b}	30.6^{a}	28.0^{d}	0.4
81	33.6^{b}	32.7^{c}	34.8^{a}	34.8^{a}	0.2
84	31.8^{b}	30.8^{d}	31.1^{c}	32.7^{a}	0.2
91	34.7^{c}	35.8^{a}	34.9^{bc}	35.1^{b}	0.3
98	36.4^{c}	36.4^{c}	38.3^{a}	37.7^{b}	0.2

Table 5. 10 Effects of various irrigation treatments on water stored within soil on selected measurement dates (indicated as days after planting, DAP) in the glasshouse experiment with wheat. Mean values with a different superscript are significantly different (P≤0.05) when compared with the least significant difference (LSD) given.

Measurement dates (DAP)	Stored soil water (mm) T80	T70	T50	T40	LSD (mm)
69	106.2^{a}	94.4^{b}	66.8^{c}	51.1^{d}	2.6
73	92.2^{b}	81.3^{c}	62.9^{d}	102.4^{a}	4.6
81	80.9^{b}	91.2^{a}	64.7^{c}	63.8^{c}	3.5
84	85.1^{c}	104.1^{a}	96.9^{b}	52.5^{d}	3.4
91	103.4^{a}	75.7^{c}	94.9^{b}	97.5^{b}	4.3
98	106.0^{a}	106.3^{a}	58.2^{c}	73.7^{b}	4.2

In order to test the effectiveness of thermal imaging for irrigation scheduling for glasshouse-grown wheat, values of canopy temperature were plotted against stored soil water (Fig. 5.13).

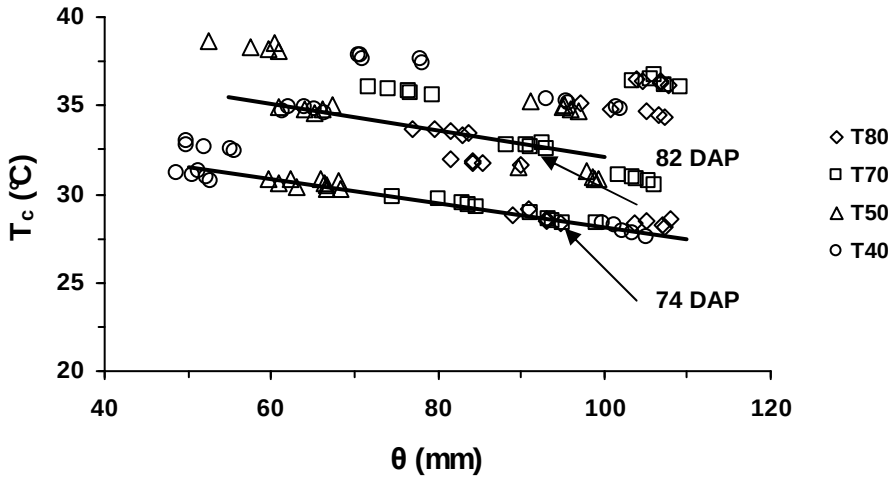

Figure 5. 13 The dependence of canopy temperature (T_c) on stored soil water (θ) for various irrigation treatments given to the wheat crop in the glasshouse. Two solid lines within this graph show a decrease in canopy temperature with increase in stored soil water for selected date of measurement.

Canopy temperature did not appear to be strongly influenced by soil water due to considerable scatter in the data. The slope of the two solid lines fitted for canopy temperature against soil water for selected measurement dates (i.e. 73 and 81 DAP) were relatively flat. Thus, thermal imaging appears to be less suitable for irrigation scheduling of crop plants in the glasshouse, especially those crops with

narrow leaves (e.g. wheat), because of the nature of variability of the combined data. There may be a possibility that wheat plants were able to adjust canopy temperature in relation to available water and/or timing of irrigation that reduced the dependence of canopy temperature on stored soil water.

However regression equations, coefficient of determination (R^2) relating canopy temperature and stored soil water for six measurement occasions are given in Table 5.11. High values of R^2 (0.92-0.98) indicated that all the fitted regression models were highly significant ($P \leq 0.001$). Thus it is possible to use thermal imaging as an aid to irrigation scheduling by considering a single day's measurement to determine relative soil water storage instead of considering the data for the entire wheat season.

Table 5. 11 Regression equations and coefficient of determination (R^2) for the relationship between canopy temperature (T_c, °C) and soil water storage (θ, mm) for various irrigation treatments on six measurement dates (indicated as days after planting, DAP). Ranges of stored soil water and canopy temperature are also given. No. of data points (n) used for each regression was 20 and $P \leq 0.001$.

Measurement dates (DAP)	Range Soil water (mm)	Range Canopy temperature (°C)	Regression equation	R^2
69	49 – 107	28.1 – 31.3	$T_c = -0.055\ \theta + 34.0$	0.95
73	60 – 105	27.6 – 30.9	$T_c = -0.067\ \theta + 34.8$	0.97
81	61 – 93	32.5 – 35.0	$T_c = -0.075\ \theta + 39.6$	0.96
84	50 – 106	30.5 – 33.0	$T_c = -0.036\ \theta + 34.6$	0.94
91	72 – 107	34.4 – 36.0	$T_c = -0.041\ \theta + 38.9$	0.92
98	53 – 109	36.1 – 38.6	$T_c = -0.041\ \theta + 40.7$	0.98

5.3.2.2 Effect of soil water storage on $T_c – T_a$

In this experiment, air temperature (T_a) was measured with an Omega type RTD probe during the time of thermal imaging. The difference between canopy (T_c) and air temperature was plotted against stored soil water (Fig. 5. 14). $T_c – T_a$ was positive when θ was low; particularly for wheat plants in the T40 treatment (least frequently irrigated pots). Positive values of $T_c – T_a$ indicate insufficient heat loss from leaves as a result of low transpiration rate. In case of frequently irrigated treatment (T80) the canopy temperature remained lower than the air temperature due to high storage and availability of soil water allowing a high transpiration from wheat leaves.

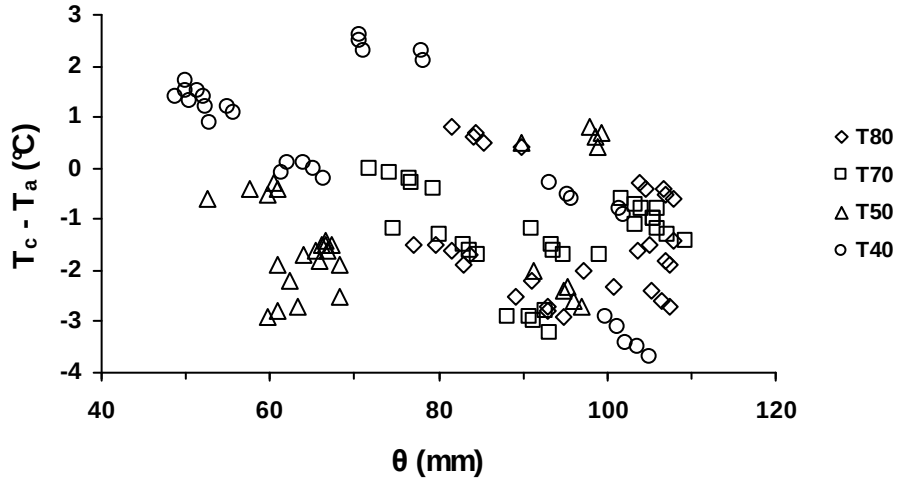

Figure 5. 14 The dependence of canopy and air temperature difference ($T_c - T_a$) on soil water storage (θ) for various irrigation treatments of wheat in the glasshouse.

5.3.2.3 Crop water deficit indices and their implications to irrigation scheduling

Crop water deficit indices, such as ICWSI and I_G were calculated as described previously for field studies. ICWSI and I_G were plotted against soil water storage (Figs. 5.15 and 5.16).

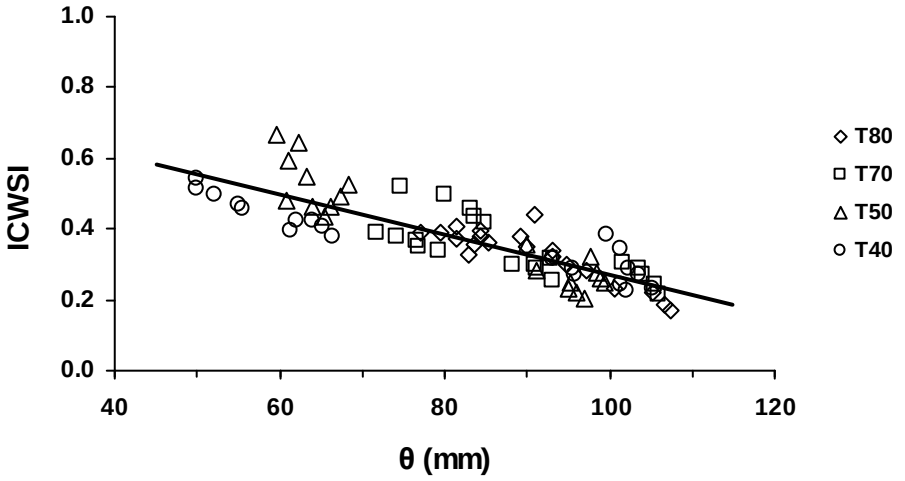

Figure 5. 15 The relationship between soil water storage (θ) and crop water deficit index, ICWSI, for various irrigation treatments of wheat in the glasshouse (*ICWSI* = -0.006 θ + 0.84, n = 80, R^2 = 0.73, P≤0.001).

ICWSI ranged from 0.17 to 0.67 when stored soil water varied within 50 to 107 mm. Low values of ICWSI indicated plants to be under low plant water deficit stress and vice versa. I_G values varied from 0.50 to 4.82 when stored soil water varied in the range of 50 to 107 mm. A high value of I_G corresponded with a high value of stored soil water. Since ICWSI is a scaled variable that ranges between 0-1 compared with I_G with no upper limit to its variation, ICWSI may be considered more appropriate for irrigation scheduling than I_G. The fitted equation for ICWSI against stored soil water in this experiment was slightly better due to the higher value of R^2. Although no systematic pattern of dependence was found between ICWSI and soil water within the root zone of the wheat crop in the field, when data for the entire season were combined, ICWSI related well with stored soil water inside the glasshouse.

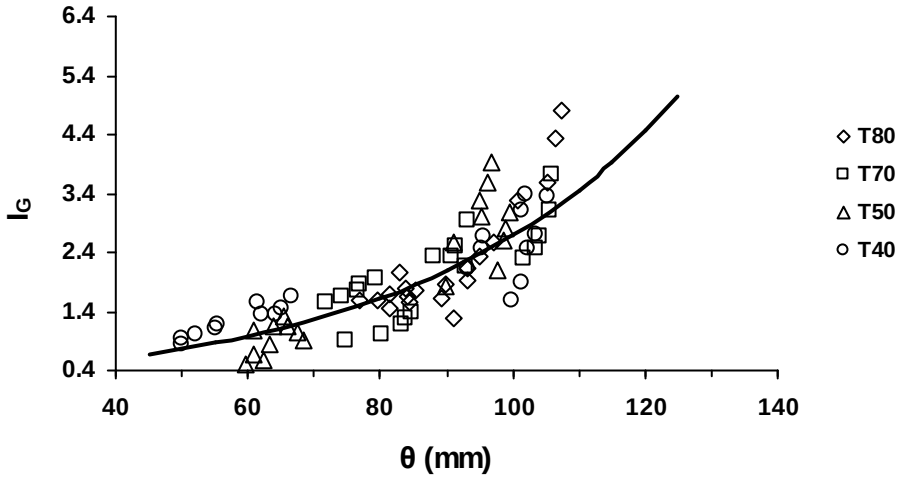

Figure 5. 16 The relationship between stored soil water (θ) and crop water deficit index, I_G for various irrigation treatments of wheat in the glasshouse ($I_G = 0.217\ e^{0.025\,\theta}$, n = 80, R^2 = 0.72, P≤0.001).

Linear regressions were also used to fit ICWSI against stored soil water on specific measurement dates to check the suitability of ICWSI index as an aid to irrigation scheduling when a single day's measurement is available. The fitted regression equations, R^2 values and range of variation in soil water and ICWSI for selected measurement dates are given in Table 5.12. For all the fitted regression models, R^2 varied within 0.87-0.93 and found to be highly significant (P≤0.001). Therefore, ICWSI index based on a single day of measurement can also be used for

irrigation scheduling of plants in the glasshouse in the same way as shown for the field experiment.

Table 5. 12 Regression equations and coefficient of determination (R^2) for the relationship between *ICWSI* (*y*) and stored soil water (θ, mm) for various irrigation treatments on 4 measurement dates (indicated as days after planting, DAP), range of stored soil water and ICWSI. No. of data points (n) for each regression was 20 and P≤0.001.

Measurement dates (DAP)	Range		Regression equation	R^2
	Soil water (mm)	ICWSI		
73	60 – 105	0.23 – 0.67	*ICWSI* = -0.007 θ + 1.1	0.91
81	61 – 93	0.25 – 0.49	*ICWSI* = -0.005 θ + 0.8	0.79
84	50 – 106	0.21 – 0.54	*ICWSI* = -0.005 θ + 0.7	0.93
91	72 – 107	0.17 – 0.39	*ICWSI* = -0.006 θ + 0.8	0.87

5.3.2.4 Effects of leaf water potential on canopy temperature

A plot of canopy temperature against leaf water potential (Ψ_l) is shown in Fig. 5.17. Ψ_l varied from -1.2 to -3.2 MPa for a variation in canopy temperature of 30.5 to 38.5 °C.

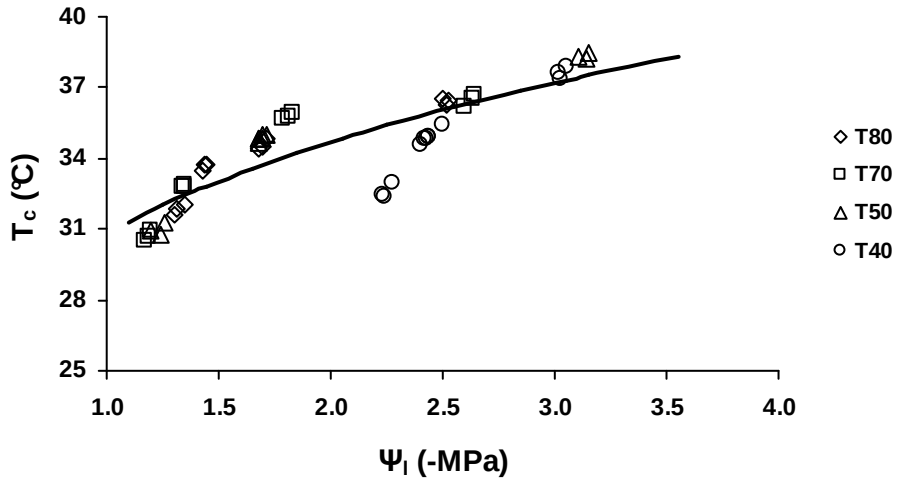

Figure 5. 17 The relationship between canopy temperature (T_c) and leaf water potential (Ψ_l) for various irrigation treatments of wheat in the glasshouse (T_c = 30.801 $\Psi_l^{0.172}$, n = 48, R^2 = 0.73, P≤0.001).

Under field conditions, canopy temperature of wheat varied linearly with leaf water potential whereas inside the glasshouse the relationship between canopy

temperature and Ψ_l was nonlinear. From the plotted data it can be seen that there was a slight nonlinearity in the overall increase in canopy temperature as leaf water potential decreased (becoming more negative).

5.4 Concluding remarks

In this and other Chapters, a number of linear and nonlinear regression models were used to describe the relationship between variables with the purpose to apply these in other experiments with similar sites and crops. Nonlinear regression equations can be useful to describe direct plant response (e.g. stomatal conductance) and indirect plant response (e.g. crop water deficit index) to variation in soil water within the root zone in the field or for the whole soil volume within pots. Specific forms of exponential, nonlinear equations have certain mathematical properties that may limit their use for predictions when *x* and *y* variables are switched. For an equation of the type $y = a \times e^{-bx}$; when $x = 0$, $y = a$, but when $y = 0$, x becomes an undefined quantity. In this situation, although *x* can be estimated for a small value of y (~0.001), a different type of nonlinear equation or a linear equation is preferred. Since nonlinear equations represent complex processes better than linear equations, a departure from linearity suggests that there may be additional physical or physiological processes involved in the soil-water-plant interaction shown by the measured data that is not yet clearly understood.

Chapter 6

MONITORING SPATIAL VARIATION OF SOIL WATER IN CROP FIELDS WITH EM38

6.1 Introduction

Increasing interest in precision agriculture in recent years has led to a need for soil maps that are more detailed and accurate than those traditionally produced (Batte, 2000). Grid mapping is generally regarded as one of the more accurate ways to map a field in detail (Buol et al., 1997). However, grid mapping is time consuming and expensive because of the time and labour involved to create accurate grids in the field (Brevik et al., 2003), making it desirable to find other, more rapid means of obtaining information for detailed soil mapping. In-situ measurement of apparent electrical conductivity (EC_a) in the field has generated considerable interest over time as a potential technique in many soil applications, as EC_a can be used as a surrogate variable to infer other soil properties. Electromagnetic induction (EMI) is a non-invasive technique that allows measurement of apparent soil electrical conductivity (EC_a) by inducing an electrical current in the soil. A transmitter located at one end of the electromagnetic (electrical conductivity) instrument induces circular eddy current loops in the soil. The magnitude of these loops is directly proportional to the conductivity of the soil in the vicinity of that loop. Each current loop generates a secondary electromagnetic field which is proportional to the value of the current flowing within the loop. A fraction of the secondary induced electromagnetic field from each loop is intercepted by the receiver coil and the sum of these signals is amplified and formed into an output voltage which is linearly related to depth-weighted soil EC_a (Rhoades, 1992). EMI has several, known advantages over other methods which include avoidance of use of radioactive sources (e.g. use of a neutron source in a neutron moisture meter) and speed and ease of use due to its portability and non-invasive nature (Reedy and Scanlon, 2003). For these reasons, EMI technique was developed to enable rapid and repetitive monitoring of a large number of sites over an extended period in both fallow and cropped fields.

Measurements of EC_a of soil with EM38 (based on the EMI technique) have received considerable interests from the precision agriculture community (Corwin and Lesch, 2005; Fritz et al., 1999). The parameters which dominantly influence EC_a are soil salinity, clay content and clay mineralogy, soil moisture and soil temperature (Friedman, 2005; James et al., 2000; McNeill, 1980a). EC_a data can be used to indirectly estimate soil properties if the contributions of the other soil properties affecting the EC_a measurement are known or can be estimated. Previous studies have found good correlation between clay content and soil electrical conductivity measurements with EM38 (Dalgaard et al., 2001; Hedley et al., 2004; Triantafilis and Lesch, 2005). This technique has been also used to study variations in soil depth (Bork et al., 1998), soil type (Greve and Greve, 2004), salinity (Rhoades et al., 1989; Triantafilis et al., 2000), and the risk of deep drainage of water (Triantafilis et al., 2004). Spatial measurement of EC_a has been reported as a potential measurement for predicting variation in crop production caused by soil water differences (Heermann et al., 2000; Jaynes et al., 1995). Various aspects of soil water content and its relationship with EC_a have been studied at various spatial scales (Kachanoski et al., 1988; Kachanoski et al., 1990; Khakural et al., 1998; Morgan et al., 2000), but few studies have attempted temporal variation in water content. At a given location, EC_a can vary with changes in soil moisture content (Brevik et al., 2006). Brevik and Fenton (2002) found soil moisture to be the single most important edaphic factor among others (e.g., soluble salts, clay content and soil temperature) that influenced EC_a determination. The study reported here was conducted to identify:

- the effects of variation in soil water content on apparent electrical conductivity of soil (EC_a) measured with EM38 in both vertical and horizontal mode;
- the effects of placing EM38 at various heights above the ground on EC_a;.
- the effects of variation in air and soil temperature on EC_a.

6.2 Materials and Methods

This study was conducted in an experimental field with cotton (*Gossypium hirsutum* L.) and wheat (*Triticum aestivum* L.) under various irrigation treatments at Kingsthorpe Research Station of the Queensland Primary Industries and Fisheries

(now referred to as the Department of Employment, Economic development and Innovation) near Kingsthorpe (27°30'44"S, 151°46'55"E, and 431 m elevation). Details of the soil properties at the experimental site, crop and irrigation management for each crop were described in previous chapters.

6.2.1 Measurements

EM38 survey was done during the 2008 wheat growing season and 2008-09 cotton crop. The EM38 (Geonics Limited, Mississauga, Ontario, Canada) instrument used in this experiment was based on a spacing of 1 m between a transmitting coil located at one end of the instrument and a receiver coil at the other end, and operated at a frequency of 14.6 kHz. EM38 could be operated in one of the two measurement modes. In the vertical mode (VM), the measured values of EC_a are known to be a function of the soil properties within a depth of about 1.5 m. while in the horizontal mode (HM), EC_a corresponds with soil properties within 0.75 m depth (McNeill, 1980b). EM38 has considerably greater application for agricultural purposes because the depth of measurement corresponds roughly with the root zone of most agricultural crops when the instrument is placed in the VM configuration (Corwin and Lesch, 2005). EM38 survey was done in both VM (Fig. 6.1) and HM (Fig. 6.2) at the centre of each plot (i.e. 3 m from the neutron access tubes) on the ground for 12 occasions (i.e. 13, 19, 28, 35, 56, 63, 70, 80, 105, 112, 131 and 145 DAP) during the wheat season. Similarly an EM38 survey was conducted on 7 occasions (62, 76, 88, 125, 136, 144 and 159 DAP) for the cotton season in both VM and HM.

On all occasions, EM38 was first calibrated and nulled according to the manufacturer's instruction before starting a measurement. Continuous proximal sensing, often referred to the electromagnetic induction sensing of soil electrical conductivity, together with precise global positioning systems (GPS) have enabled accurate mapping of within-field soil variability to help site specific management (Plant, 2001). This requires location of each EM38 measurement in the field to be recorded with a hand held GPS. The location of each EM38 measurement was recorded at the time of first measurement with the GPS unit (mentioned in earlier chapters). Wooden pegs were driven into the ground at those measurement locations as permanent to minimise positional errors arising from the accuracy of GPS used. Since the GPS recorded the location of all measurements in latitude and longitude

format (i.e. degree, minute and second), the recorded data were converted to easting and northing by using a UTM conversion excel spread sheet (Dutch, 2007).

Figure 6. 1 Operation of EM38 in vertical mode (VM) at the soil surface in the field.

Figure 6. 2 Operation of EM38 in horizontal mode (HM) at the soil surface in the field.

As it has been reported that ambient temperature can influence EC_a readings collected with the EM38 equipment (Sudduth et al., 2001), air temperature was recorded with an Omega type RTD probe during the EM38 survey of each experimental plot. Some studies have shown that changes in temperature over a time period of several weeks to months can significantly influence EC_a readings of EM38 (Brevik and Fenton, 2002; Nugteren et al., 2000; Sudduth et al., 2001). This is due to the dependency of soil electrical conductivity on soil temperature that varies seasonally due to the variation in air temperature (Huth and Poulton, 2007). Variation in soil temperature is usually greater near the soil surface (i.e. at shallow depths of 5 and 10 cm) than at greater depths (e.g. 30 cm) with little or no change at depths below 60 cm (Jury et al., 1991). Therefore soil temperature was measured with the RTD probe at 5, 10 and 25 cm depths by pushing the tip of the temperature probe to the appropriate soil depth (Fig. 6.3). These depths were chosen primarily to represent temporal variation in soil temperature in the field during EM38 measurement. Measurement of soil temperature at shallow depths (i.e. 5 and 10 cm) was time consuming because the probe required a longer time period (2 to 3 min) for readings to stabilise than for measurement of soil temperature at 25 cm depth.

Figure 6. 3 Soil temperature measurement in the field with Omega RTD probe (meter on the left, RTD sensor on right pushed to 25 cm depth).

When the soil was dry, it was difficult to push the temperature probe into the ground. A stainless steel rod with a conical tip was first pushed into the ground to make a pilot hole to a depth of few mm lower than the desired depth. The temperature probe was then inserted to the desired depth to measure soil temperature. Both soil temperature at 5, 10 and 25 cm depths and air temperature were measured on 10 occasions (i.e. 13, 19, 28, 35, 56, 63, 70, 105, 131 and 145 DAP) during the wheat season and on 5 occasions (88, 125, 136, 144 and 159 DAP) for cotton season. Variation of soil temperature at 5, 10 and 25 cm depths and the air temperature over time for various irrigation treatments is shown in Fig. 6.4 for wheat season.

It can be observed from Fig. 6.4 that air temperature was consistently higher than soil temperature at various depths (i.e. 5, 10 and 25 cm) for various irrigation treatments for wheat season. The trend in variation in soil temperature at 5, 10 and 25 cm depths was similar for 4 irrigation treatments, which indicates that there was no effect of irrigation on the soil temperature in the wheat field. The data for soil and air temperature for the cotton season is given in Table 6.1. It can be concluded from this table that there was not much variation in air and soil temperature at various depths for various irrigation treatments in the cotton field.

Table 6. 1 Variation of soil temperature at 5, 10 and 25 cm depth, and air temperature for T50, T60, T70 and T85 irrigation treatments of cotton season.

Irrigation treatments	Range of Air temp. (°C)	Range of soil temp. at 5 cm depth (°C)	Range of soil temp. at 10 cm depth (°C)	Range of soil temp. at 25 cm depth (°C)
T50	26.1 – 32.3	23.5 – 37.2	21.2 – 30.0	22.1 – 27.7
T60	26.8 – 32.7	25.4 – 38.7	22.6 – 30.8	22.7 – 28.0
T70	26.9 – 33.0	26.1 – 38.9	22.7 – 30.9	22.9 – 28.3
T85	27.0 – 33.2	26.3 – 39.1	23.1 – 31.3	23.1 – 28.2

It has been shown previously that EC_a measurements with the EM38 are strongly influenced by the distance of EM38 probe from the ground level, i.e. when EM38 is placed at some height above the ground (Sudduth et al., 2001).

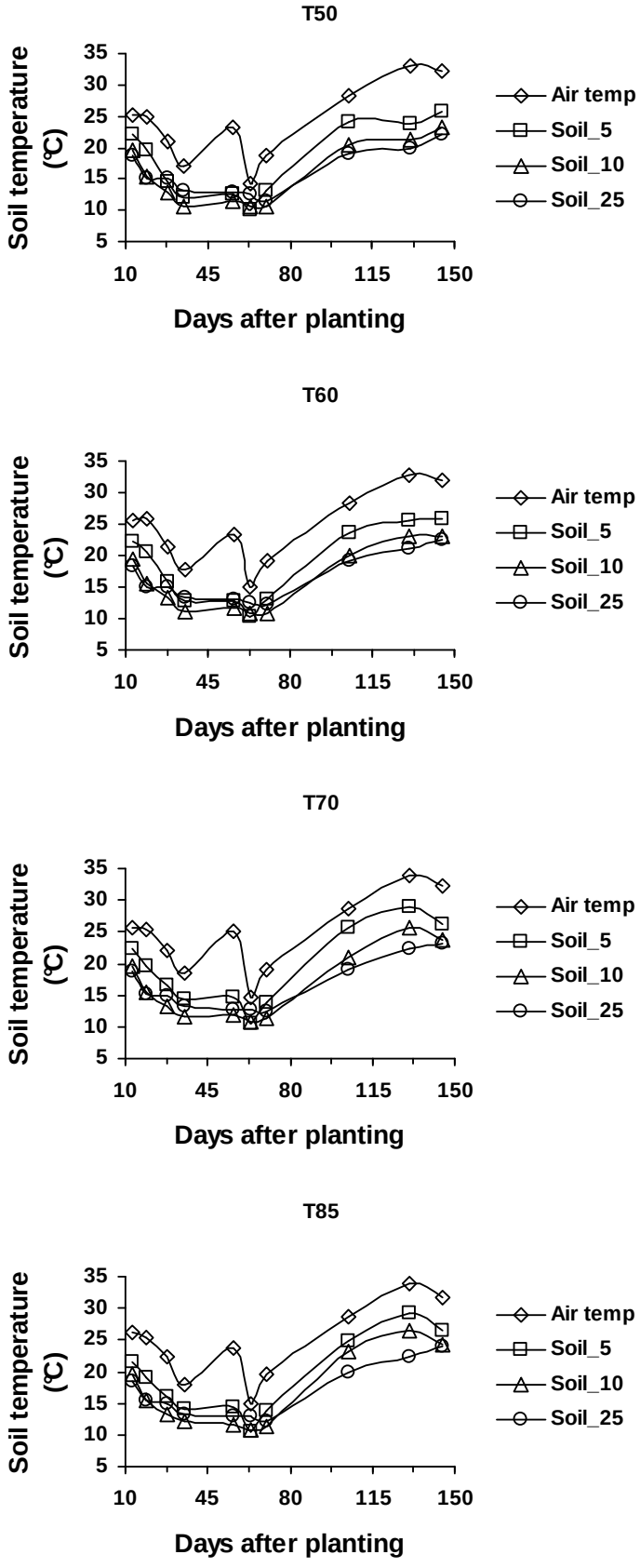

Figure. 4 Temporal variation of soil temperature at 5, 10 and 25 cm depth, and air temperature for T50, T60, T70 and T85 irrigation treatments during the wheat season.

To gain further insight into the response of EM38 to variation in soil water content at various depths, additional measurements with the EM38 were taken in both VM and HM at 0.1 and 0.4 m height above the ground at the same locations as for previous measurements, but limited to only 7 occasions (i.e. 56, 63, 70, 105, 131 and 145 DAP) for wheat and 7 occasions (62, 76, 88, 125, 136, 144 and 159 DAP) for cotton. To facilitate the EM38 measurement at desired heights above the ground a wooden frame with a platform was used (Fig. 6.5) because EM38 readings are not influenced by non-metallic material, such as wood.

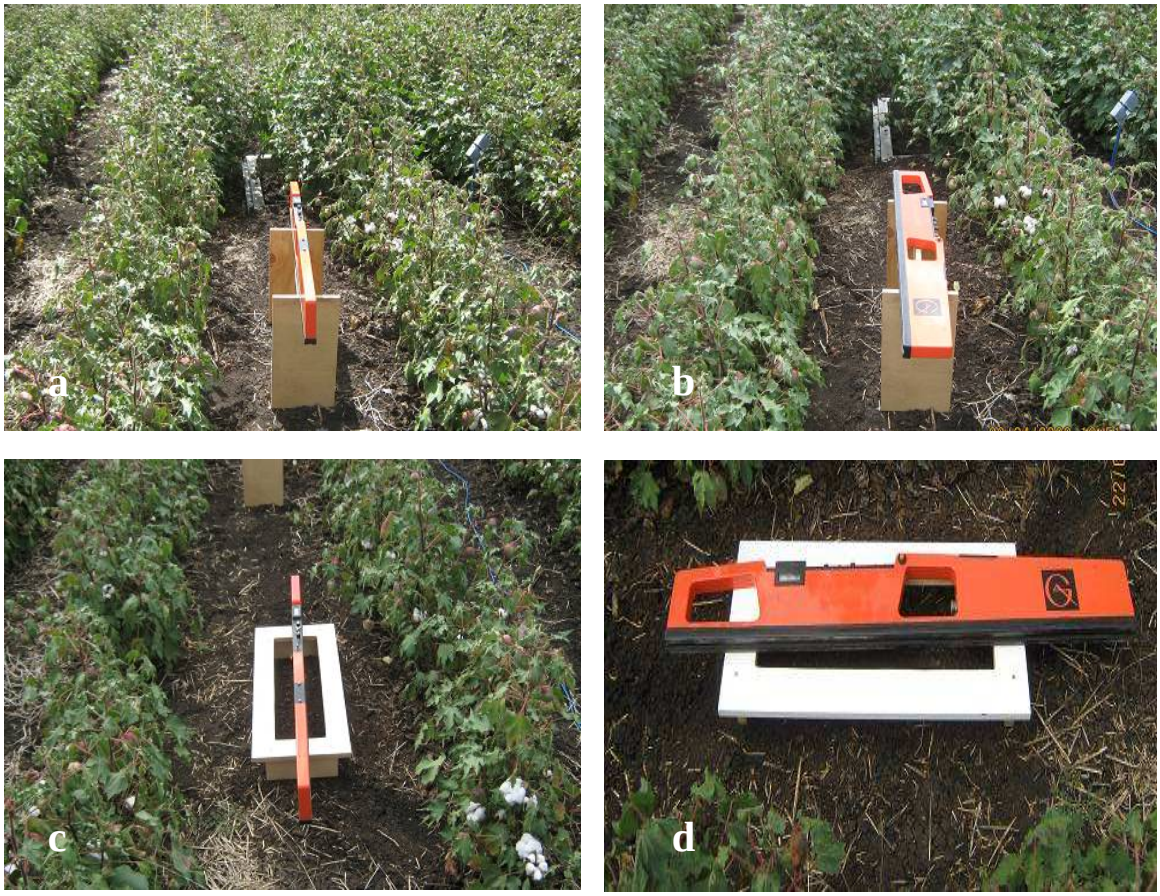

Figure 6. 5 EM38 measurements in the field at various heights above the ground shown for a cotton field. (a) VM – 0.4 m height, (b) HM – 0.4 m, (c) VM – 0.1 m and (d) HM – 0.1 m.

Raising the EM38 above the ground is equivalent to shunting or lowering of the EM38 depth-response function, i.e. in VM, an EM38 reading at 0.1 m above the ground is expected to represent EC_a within1.4 m of soil depth and at 0.4 m above the ground within 1.1 m of soil depth. In a similar way, measurements in the HM at 0.1

and 0.4 m height above the ground, the effective soil depth of measurement could be reduced to 0.65 and 0.35 m, respectively. A neutron probe was used to measure soil water content from the surface to a depth of 1.33 m at 0.1 m depth increments on the same day as all EM38 measurements. Details of the neutron probe calibration are given in Chapter 4. The volumetric moisture content was converted to mm of water for each depth and then accumulated to a depth close to the effective depth of sensing of EM38 probe. Measurements for five soil depths (i.e. 0.33, 0.63, 0.73, 1.13, and 1.33 m) were used to relate EC_a (mS m^{-1}) measured with EM38 with the estimated soil water content (mm). Since soil water content was measured to a maximum depth of 1.33 m, EM38-measured values of EC_a were correlated with this water content in VM at the ground level as well as at 0.1 m height above the ground.

6.3 Results and Discussion

6.3.1 Wheat experiment

6.3.1.1 Effects of soil water content on EC_a

Variation in EC_a with variation in soil water within the top 1.33 m of soil is shown for combined irrigation treatments of wheat in Fig. 6.6 for the VM measurements of EM38. EC_a generally increased with increase in soil water content.

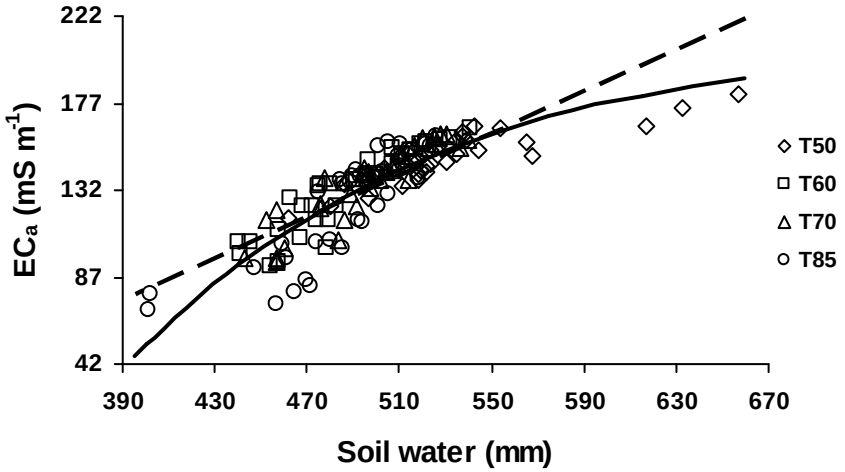

Figure 6. 6 The relationship between water content within the top 1.33 m of soil and EC_a measured in the vertical mode for various irrigation treatments.

A dashed line has been used to represent the linear regression equation for these data as $y = 0.54\ x - 135.54$ (n = 144, $R^2 = 0.70$, $P \leq 0.001$), where $y = EC_a$ (mS m^{-1}) measurement of EM38 in VM and x = soil water (mm) within 1.33 m depth of soil. It can be seen from Fig. 6.6 that this linear regression equation did not fit well to these data for wet soil conditions when soil water > 550 mm, possibly because the effective response depth of EM38 in VM is 1.50 m and that did not match well with soil water represented within 1.33 m soil depth. Therefore, a nonlinear equation was fitted to these data (represented by a solid line in Fig. 6.6) as $y = 211.76\ [1 - 16.01\ e^{-0.007x}]$ (n = 144, $R^2 = 0.77$, $P \leq 0.05$), that represented the data better than the linear regression.

Soil water within 1.33 m depth for various irrigation treatments was in the range of 460 – 660 mm for T50, 440 – 540 mm for T60 and T70, and 400 – 525 mm for T85. All plots under T50 were irrigated most frequently and T85 least frequently. Although the depths used for soil water content and EC_a with EM38 were different, in Fig. 6.6, these trends suggest that a departure from linearity in the response of EM38 may occur for very wet soils or fields receiving more frequent irrigation to maintain low soil water deficit. Similar measurements of EC_a with EM38 in HM also showed an increase in EC_a with increase in soil water within 0.73 m depth (Fig. 6.7).

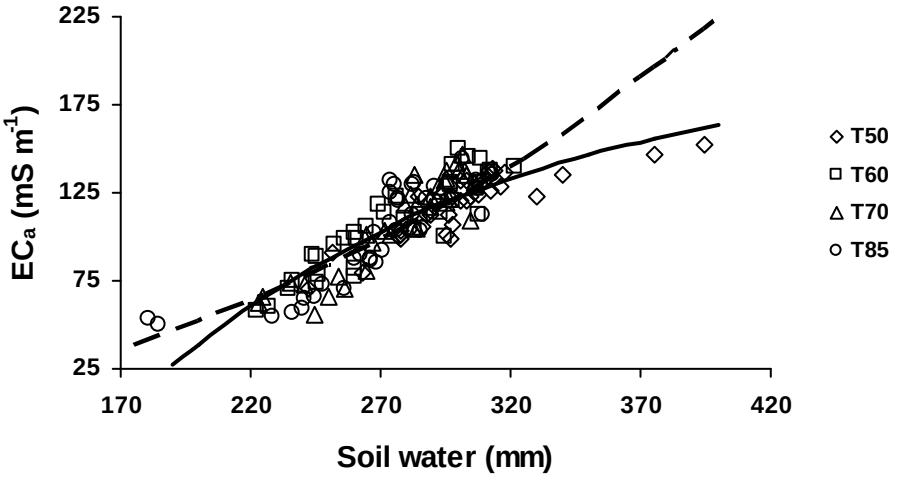

Figure 6. 7 The relationship between water content within the top 0.73 m of soil and EC_a measured in horizontal mode for various irrigation treatments.

An equation $y = 0.0007\ x^{2.116}$, (n = 144, $R^2 = 0.78$, $P \leq 0.001$) fitted to these data is shown as a dashed line in Fig. 6.7, where $y = EC_a$ (mS m^{-1}) measurement of

EM38 in HM and x = soil water (mm) within 0.73 m depth of soil. Note that the data range when relating EC_a in HM with soil water content was less than that shown in Fig. 6.6, as EC_a responds to soil water within a shallower depth of 0.75 m. Although EC_a measured in the HM increased with increase in soil water content, the dashed line did not appear to represent the data well at high soil water content as in case of VM of EM38. These data could be best represented with a nonlinear equation of the type $y = 202.46\ [1 - 3.369\ e^{-0.007x}]$ ($n = 144$, $R^2 = 0.76$, $P \leq 0.05$).

Brevik et al. (2006) found that soil water content has a significant influence on the soil EC_a measurement with EM38 and also indicated that the potential of EC_a techniques for soil mapping were best in the field when the soils exhibited a wide range of EC_a. Huth and Poulton (2007) have also indicated the effectiveness of EMI techniques in monitoring variation in soil moisture in response to its extraction by crops and trees in an agroforestry system. Since studies on the effects of soil water content on EC_a measurement with EM38 are limited for irrigated crops, the experiment reported here was conducted to investigate the effects of soil water on EC_a.

In order to study the variation in EC_a in response to variation in soil water content when EM38 is placed at some height above ground, values of EC_a for VM at 0.1 and 0.4 m height above the ground were plotted against soil water in the top 1.33 and 1.13 m (Figs. 6.8 and 6.9). Although variation in soil water was similar to that in Fig. 6.6, a change in the range of EC_a values obtained (57-172 mS m^{-1}) compared with 70-182 mS m^{-1} obtained for VM of EM38 earlier showed a linear increase in EC_a with increased soil water content. These results suggest that EC_a measured in VM at 0.1 m height above the ground represented soil water within 1.33 m depth much closely with a higher degree of precision. Similar linear relationships were also found with measurements of EC_a in VM of EM38 when the instrument was placed at 0.4 m height above the ground (Fig. 6.9), although the range of soil water content (320-575 mm) and EC_a (50 to 140 mS m^{-1}) were both reduced considerably due to a reduction in the effective response depth of the EM38.

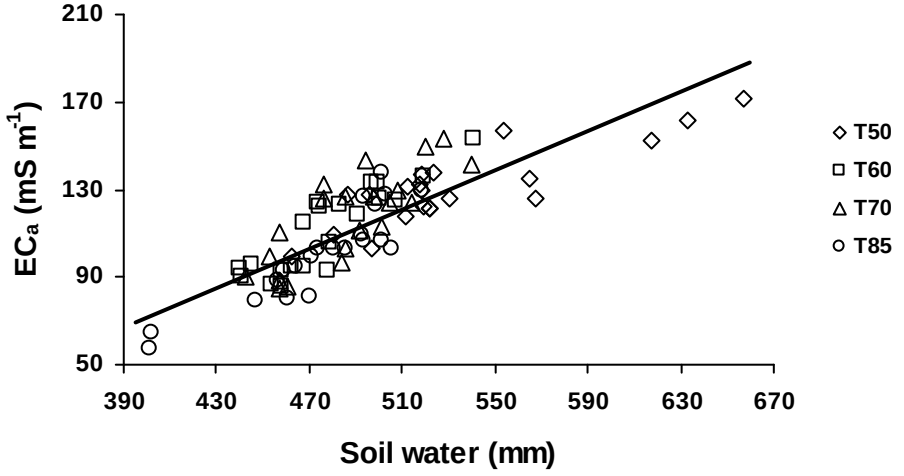

Figure 6. 8 The relationship between water content within the top 1.33 m of soil and EC_a measured in vertical mode at 0.1 m height above the ground for various irrigation treatments.

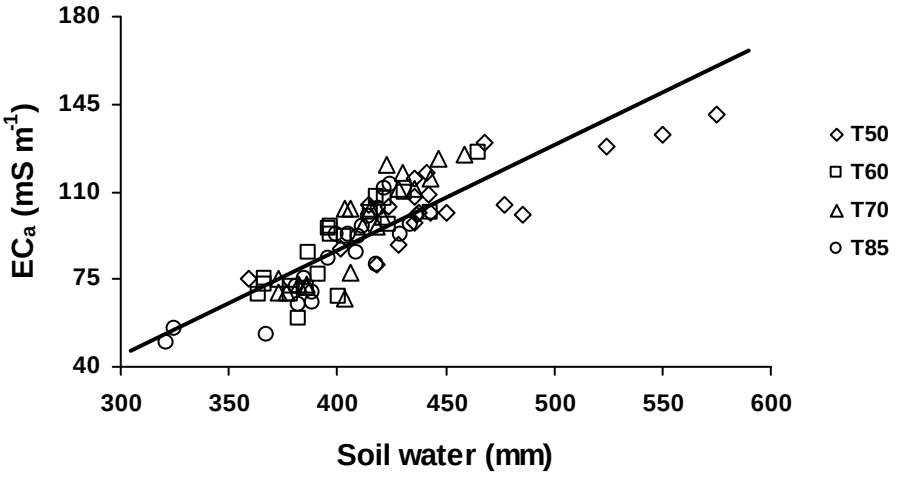

Figure 6. 9 The relationship between water content within the top 1.13 m of soil and EC_a measured in vertical mode at 0.4 m height above the ground for various irrigation treatments.

These results collectively indicate that by placing the EM38 at various heights above the ground, it is possible to estimate and/or predict soil water content for a range of soil depths within the maximum sensing depth of the EM38 in VM. These results suggest that it is possible to predict soil water content at much shallower depths (i.e. 0.3-0.6 m) by selecting appropriate heights above the ground in HM of EM38. The statistics for the regression equations representing the general

relationship between the plotted variables in these figures (Figs. 6.8, 6.9, 6.10 and 6.11) are given in Table 6.2. The coefficient of determination (R^2) indicates the extent to which the variation in the plotted data is represented by the regression while the probability (P-values) of the fitted coefficients (slope and intercept terms) are obtained with the analysis of variance to represent the degree of confidence.

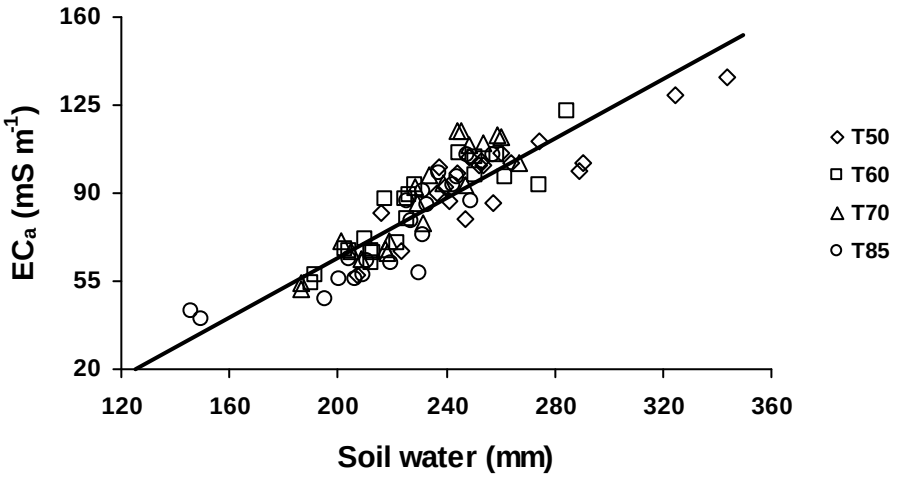

Figure 6. 10 The relationship between water content within the top 0.63 m of soil and EC_a measured in HM at 0.1 m height above the ground for various irrigation treatments.

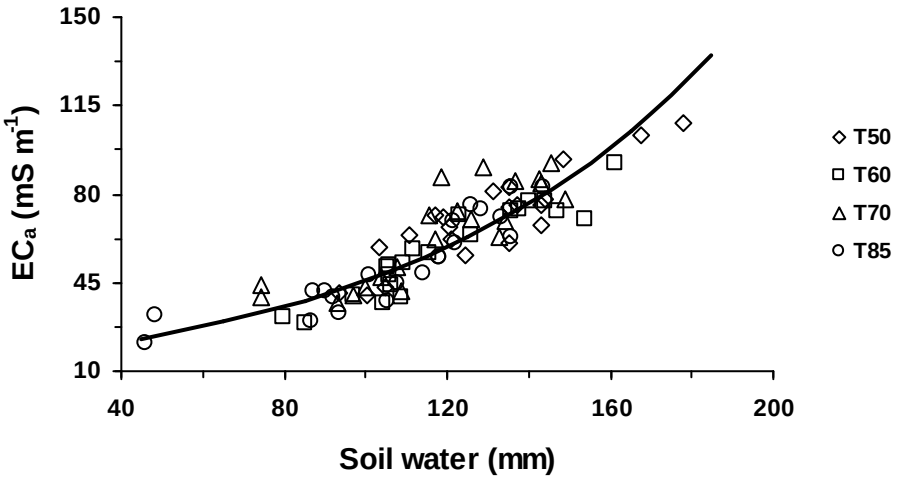

Figure 6. 11 The relationship between water content within the top 0.33 m of soil and EC_a measured in horizontal mode at 0.4 m height above the ground for various irrigation treatments.

Data in Table 6.2 indicated R^2-values to be higher with EC_a measured in HM than in VM. Improvements in regression with HM over VM could be due to the higher contribution of upper soil layers near the surface to measured values of EC_a than the lower soil layers that supports the earlier assertion of McNeill (1992) that contribution of various soil layers to EC_a decrease exponentially within the effective soil depth of 0.75 m. Therefore, EM38 readings would be expected to be more strongly and closely related with soil water content near the surface than at deeper soil layers.

Table 6. 2 Regression equations and coefficient of determination (R^2) for the relationships between EC_a (y, mS m^{-1}) and soil water (x, mm) for various irrigation treatments in VM and HM of EM38 at 0.1 and 0.4 m above the ground for wheat. No. of data points (n) used for each regression model was 84 and $P \leq 0.001$.

Height above ground (m)	Mode of operation	Regression equation	R^2
0.1	VM	$y = 0.45\,x - 108.67$	0.70
	HM	$y = 0.59\,x - 53.47$	0.78
0.4	VM	$y = 0.42\,x - 81.77$	0.71
	HM	$y = 12.916\ e^{0.013x}$	0.81

The ability of the EM38 to predict soil water near the soil surface with high accuracy as observed in this study suggests that EM38 in HM will allow good representation of temporal changes in soil water content in the surface soil layers of irrigated crop fields, where most changes are likely to occur due to irrigation and evapotranspiration. Overall, there was a significant effect ($P \leq 0.001$) of soil water on EC_a. Sudduth et al. (2001) used an EM38 sensor for mobile data collection in the field and also investigated the sensitivity of EC_a to detect variation in soil depth under grassed conditions. They found that raising the EM38 above ground reduced EC_a to a much greater extent in HM of EM38 than in VM. This differential response in the operational modes of the EM38 has enabled sensing of soil water in the shallower soil zones than that has been possible in previous studies.

6.3.1.2 Effects of temperature on EC_a

Soil temperature is another important factor that influences EC_a. In this study soil temperature was averaged over all the measurement depths (i.e. 5, 10 and 25 cm depths) and plotted against measured EC_a in both vertical and horizontal modes of EM38 (Figs. 6.12 and 6.13). Similar data obtained for EC_a measured in the

horizontal mode of EM38 were plotted against average soil temperature in Fig. 6.13. It can be concluded from these figures that with an increase in soil temperature, values of EC_a mostly decreased from a maximum value of 15.3 and 15.1 °C, respectively.

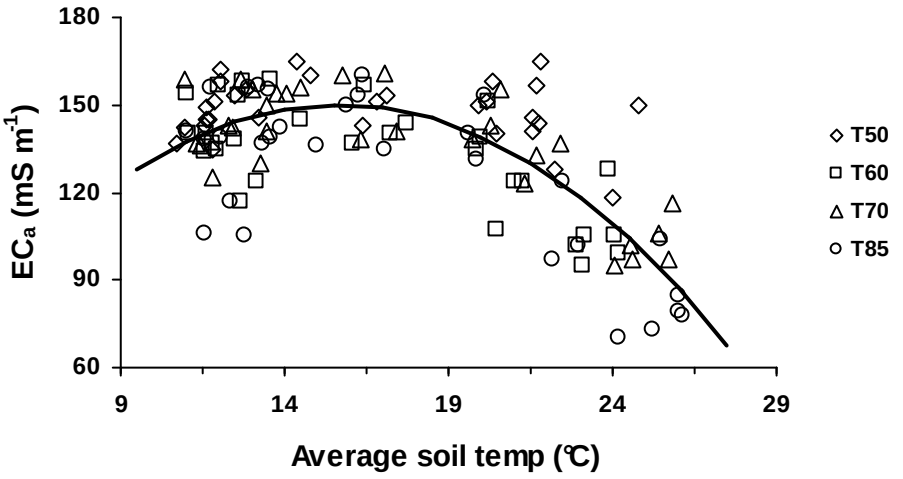

Figure 6. 12 The relationship between average soil temperature within 5 - 25 cm depth of soil and EC_a measured in vertical mode for various irrigation treatments (y = 6.5 + 18.4 x – 0.6 x^2, n = 120, R^2 = 0.57, P≤0.001).

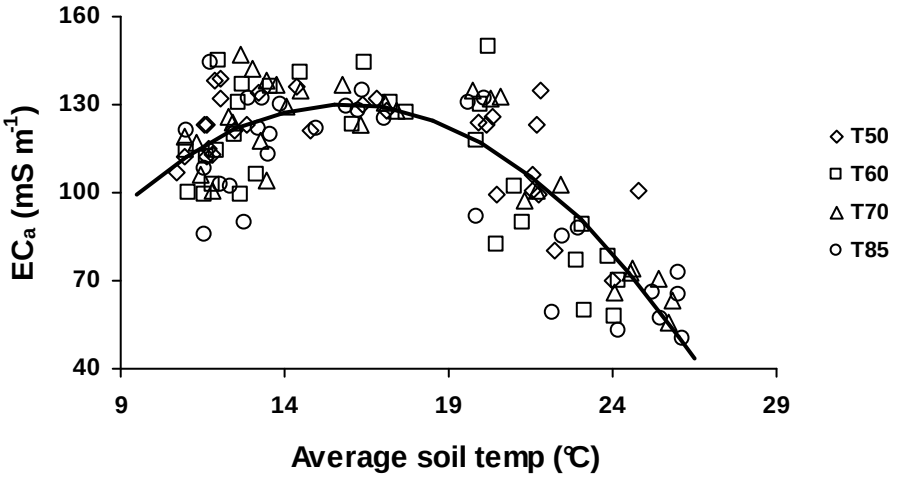

Figure 6. 13 The relationship between average soil temperature within 5 - 25 cm depth of soil and EC_a measured in horizontal mode for various irrigation treatments (y = -61.9 + 24.2 x – 0.8 x^2, n = 120, R^2 = 0.68, P≤0.001).

Since all electrical conductivity (EC) measurements in soil are influenced by temperature, EC is generally expressed at a standard temperature of 25 °C. In order to relate EC_a measurements with soil temperature, a correction factor is often used to extrapolate EC_a measured at a known temperature to EC_a at 25 °C. Huth and Poulton (2007) suggested using correction factor developed by Richards (1954) as

$$EC' = EC/ [1+0.0191(T-25)], \quad (6.1)$$

where EC' and EC are respectively corrected and uncorrected values of EC of soil solutions and T is the soil temperature (°C). This correction scheme usually applied to EC measurements when there is substantial amount of water in the surrounding soil as in case of EC measurements at a soil-water ratio of 1:2 or greater in the laboratory. Actual EC_a correction for soil temperature in the field could be quite complex due to simultaneous variation in depth sensing range of EM38 and variation in soil-water ratio due to variation in soil water content. The observed trends in Figs. 6.12 and 6.13 indicate that actual EC in the field reached maximum at 15.1 to 15.3 °C, but not 25 °C as suggested in Eq. 6.1. Thus, the trends of EC_a in Figs. 6.12 and 6.13 are consistent with the type of variation in EC of soil solutions expected with solution temperature as in Eq. 6.1, but are unlikely to peak at 25 °C because of the variation caused by soil-water ratio.

Since EC generally declines with increase temperature, simple linear regression models were used to determine the effects of air and soil temperature at 5, 10 and 25 cm depths separately on EC_a measurement for both vertical and horizontal mode of EM38. Regression equations and associated values of R^2 for both VM and HM of EM38 are given in Tables 6.3 and 6.4. Although all the fitted regression equations have negative slope indicating a decrease in EC_a with increase in temperature and were all highly significant ($P \leq 0.001$), this could be due to the amount of data (n = 120) used. Low R^2 values (0.27-0.36 for VM and 0.29-0.43 for HM) obtained with these regression models suggest that the contribution of temperature to EC_a was much smaller due to a higher dependence of EC_a on soil water. Previous studies on the use of EM38 to determine the effects of soil temperature on EC_a on a wide range of landscapes are limited for irrigated condition (Brevik and Fenton, 2002; Nugteren et al., 2000; Sudduth et al., 2001) due to the complex interaction of EC_a with soil water and temperature described above.

Table 6. 3 Regression equations and coefficient of determination (R^2) for the relationship between EC_a (y, mS m^{-1}) and temperature (both soil and air, x, °C) for various irrigation treatments in VM of EM38 for wheat. No. of data points (n) used for was 120 and $P \leq 0.001$.

Temperature	Regression equation	R^2
Air	y = -1.95 x + 182.73	0.27
Soil – 5 cm	y = -2.05 x + 173.45	0.31
Soil – 10 cm	y = -2.55 x + 176.69	0.37
Soil – 25 cm	y = -3.48 x + 192.17	0.36

Table 6. 4 Regression equations and coefficient of determination (R^2) for the relationship between EC_a (y, mS m^{-1}) and temperature (both soil and air, x, °C) for various irrigation treatments in HM of EM38 for wheat. No. of data points (n) used was 120 and $P \leq 0.001$.

Temperature	Regression equation	R^2
Air	y = -2.31 x + 166.40	0.29
Soil – 5 cm	y = -2.46 x + 156.12	0.34
Soil – 10 cm	y = -3.14 x + 161.36	0.43
Soil – 25 cm	y = -4.36 x + 181.68	0.43

6.3.1.3 Spatial variation in soil water and EC_a

Since the position of all measurements remained fixed over time, as determined by the GPS records for all EM38 and water content measurements and as shown in previous sections that there was a strong dependency of EC_a on soil water content, it is possible now to compare EC_a maps with soil water maps on a given day of measurement to gain additional confidence on the usefulness of EC_a and its ability to predict soil water content. Figures 6.14 and 6.15 show the spatial variation in EC_a measurement in VM and soil water for all the 12 plots of the wheat irrigation experiment. Filled circles on these maps represent the measurement location for each plot with label denoting irrigation treatment (T50…T85) and replicate (R1…R3). Areas within these maps with a darker shade of blue indicate a relatively high value of EC_a that coincides with a similar location in the field of high soil water content within the depth-response range of EM38 (Figs 6.14 and 6.15). In a similar way, areas of lighter shade of blue (almost white) depict low EC_a and soil water content. Since areas of the field with T50 and T85 treatments, indicate areas of lowest and highest soil water deficit respectively, frequent mapping of EC_a can be used to apply variable quantities of water to minimise differences in water content and to reduce soil water deficit for the practice of precision irrigation.

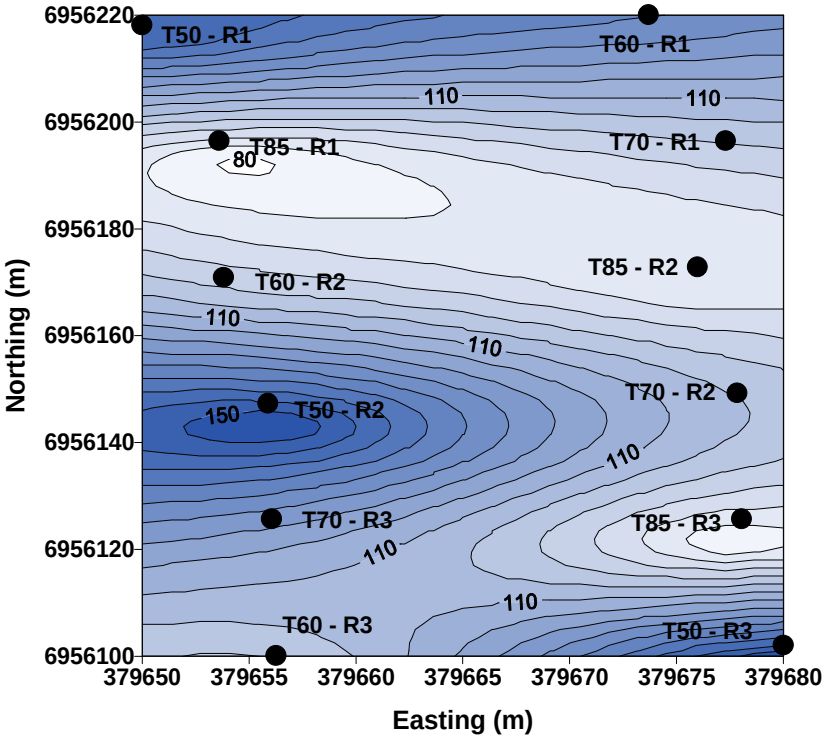

Figure 6. 14 Spatial variation in EC_a at the irrigation experiment site at 131 days after planting wheat. Filled circles indicate the position of measurement for irrigation treatments T50, T60, T70 and T85 and replicates R1, R2 and R3 of each irrigation treatment. The contour lines show values of EC_a in mS m^{-1}.

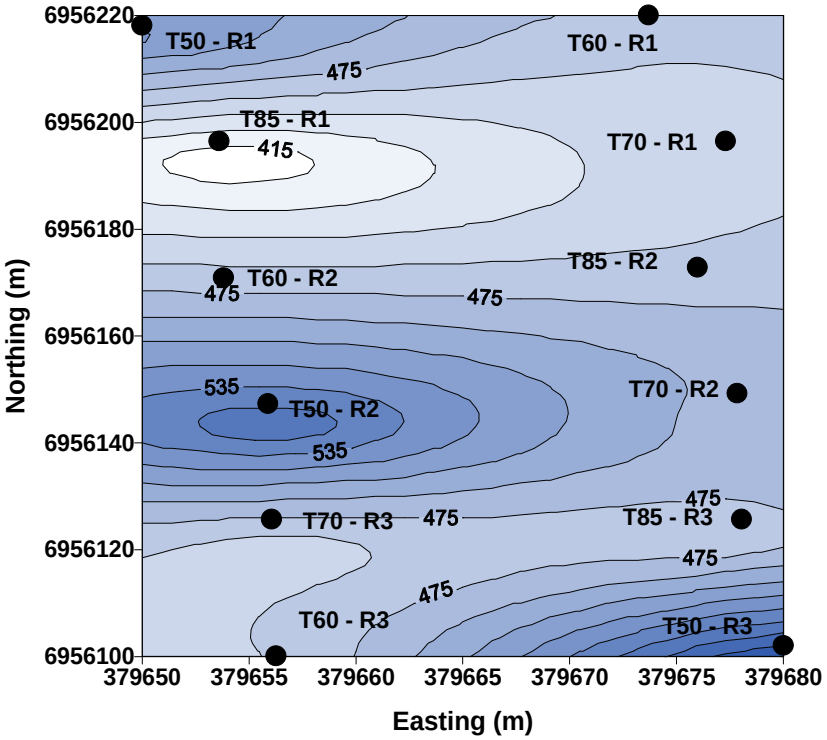

Figure 6. 15 Spatial variation in soil water content within 1.33 m depth for the irrigation experiment at 131 days after planting wheat. Filled circles indicate the position of measurement for each plot of the entire field. T50, T60, T70 and T85 are irrigation treatments and R1, R2 and R3 are replicates of each treatment. The contour lines show the values of soil water in mm within the depth sensing range of EM38.

6.3.2 Cotton experiments

6.3.2.1 Effects of soil water content on EC_a

Fig. 6.16 shows variation in EC_a in VM of EM38 against variation in soil water within the top 1.33 m of soil for various irrigation treatments of cotton. It can be observed form Fig. 6.16 that value of EC_a increased exponentially with increase in soil water within the top 1.33 m of soil. The relationship between EC_a measured in VM of EM38 and soil water was non linear because the effective response depth of EM38 in VM is 1.50 m and that did not match well with soil water represented within 1.33 m soil depth. Value of EC_a measurement in VM of EM38 varied from 71 to 153 mS m^{-1} for a range of 335 to 575 mm of soil water (within 1.33 m depth) for various irrigation treatments. Values of EC_a were higher for T50 irrigation treatment than T85 because T50 was frequently irrigated while T85 was least irrigated.

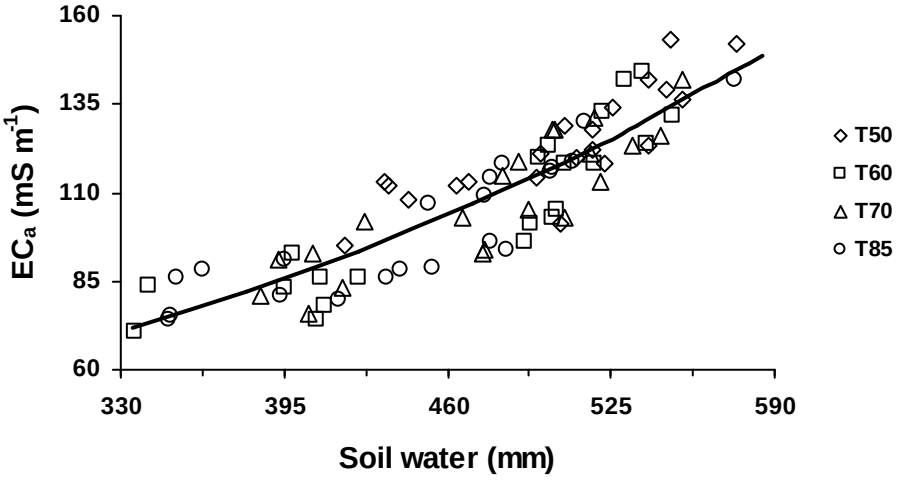

Figure 6. 16 The relationship between water content within the top 1.33 m of soil and EC_a measured in the vertical mode for various irrigation treatments of cotton season (y = 27.289 $e^{0.003x}$, n = 84, R^2 = 0.79, P≤0.001).

Similarly variations of soil water within 0.73 m depth have been plotted against measurements of EC_a in HM of EM38 (Fig. 6.17). It can be concluded from Fig. 6.17 that both soil water and EC_a values were lower for HM in comparison with VM values because the effective response depth in HM was 0.75 m.

Values of EC_a measured in the VM at 0.1 and 0.4 m height above the ground were plotted against soil water within 1.33 and 1.13 m depths respectively to study the effect of soil water on variation in EC_a when the EM38 was placed at a certain height above the ground (Figs. 6.18 and 6.19).

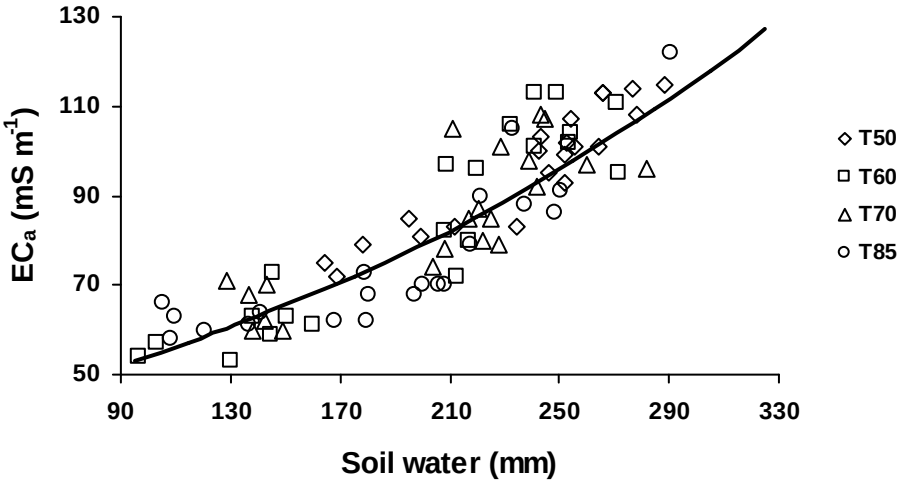

Figure 6. 17 The relationship between water content within the top 0.73 m of soil and EC_a measured in the horizontal mode for various irrigation treatments of cotton season (y = 34.913 e $^{0.004x}$, n = 84, R^2 = 0.81, P≤0.001).

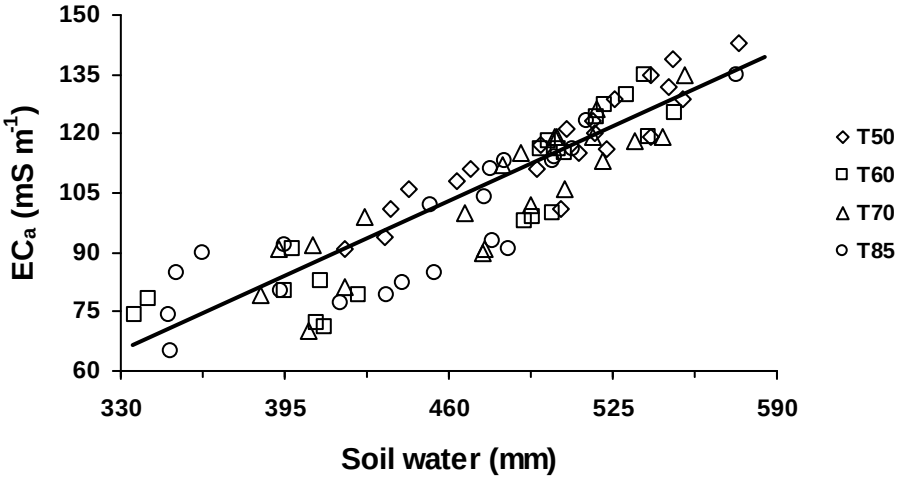

Figure 6. 18 The relationship between water content within the top 1.33 m of soil and EC_a measured in vertical mode at 0.1 m height above the ground for various irrigation treatments of cotton season.

It can be observed from Fig. 6.18 that although the soil water range was same (i.e. 335-575 mm) as for the VM of EM38 on the ground surface, EC_a values were much lower (i.e. 65 to 143 mS m^{-1}). A similar linear relationship was also found between EC_a and soil water when the EM38 was placed at 0.4 m height above the ground (Fig. 6.19). In this case both soil water (255 to 493 mm) and EC_a (57 to 133 mS m^{-1}) values were lower than that observed in the VM of EM38 measurements. This decrease was due to a reduction in the effective response depth of EM38 to 1.10 m. These results suggest that soil water can be predicted well in the field by placing the EM38 at various heights above the ground in VM.

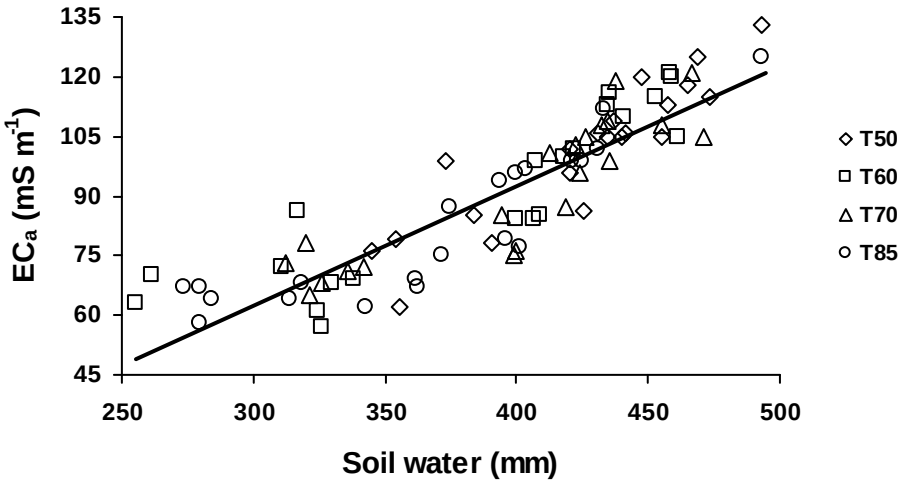

Figure 6. 19 The relationship between water content within the top 1.13 m of soil and EC_a measured in vertical mode at 0.4 m height above the ground for various irrigation treatments of cotton season.

Figs. 6.20 and 6.21 show the plotted values of EC_a at 0.1 and 0.4 m height above the ground in HM against soil water within 0.63 and 0.33 m depth respectively. EC_a values varied from 53 to 122 mS m^{-1} for variation in soil water in the range of 100 to 290 mm when the EM38 was placed at 0.1 m height above ground in HM. Both EC_a (36 to 98 mS m^{-1}) and soil water (25 to 146 mm) values decreased considerably when EM38 was used at 0.4 m height above the ground in HM, because the effective response depth was reduced to 0.35 m. Thus, it is possible to predict soil water at shallow soil depths (i.e. 0.3 – 0.6 m) by placing the EM38 at various heights above the ground in HM.

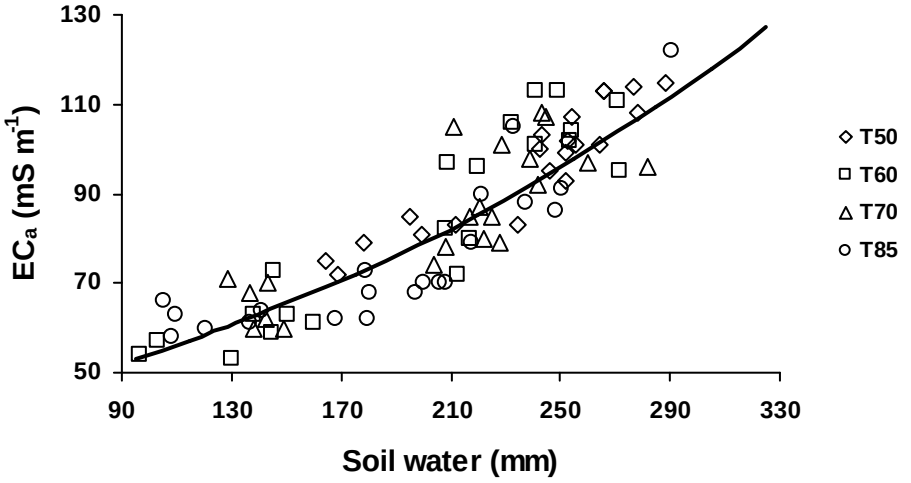

Figure 6. 20 The relationship between water content within the top 0.63 m of soil and EC_a measured in HM at 0.1 m height above the ground for various irrigation treatments of cotton season.

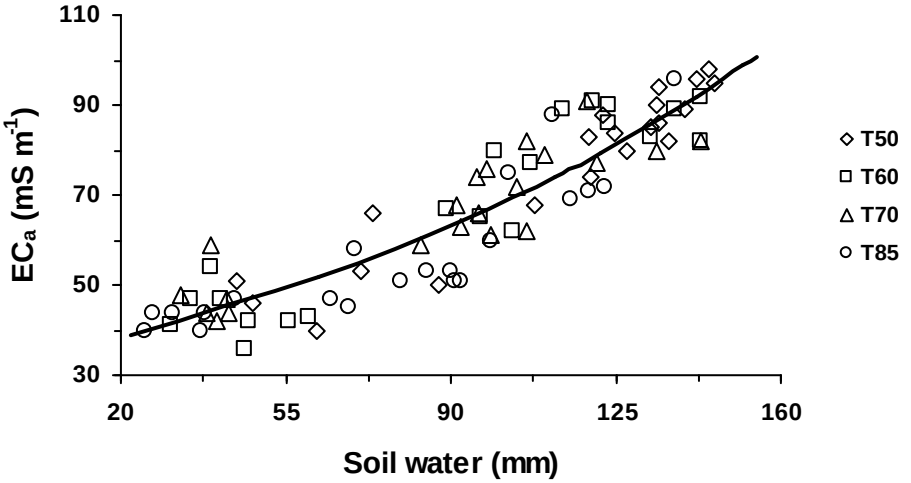

Figure 6. 21 The relationship between water content within the top 0.33 m of soil and EC_a measured in HM at 0.4 m height above the ground for various irrigation treatments of cotton season.

The statistics of the regression equations representing the general relationship between the plotted variables in these figures (Figs. 6.18, 6.19, 6.20 and 6.21) are given in Table 6.5. Data in Table 6.5 indicated R^2-values to be higher with EC_a measured in HM than in VM similar to that observed for wheat. Significant effects ($P \leq 0.001$) of soil water on EC_a were found for all these measurements.

Table 6. 5 Regression equations and coefficient of determination (R^2) for the relationships between EC_a (y, mS m^{-1}) and soil water (x, mm) for various irrigation treatments in VM and HM of EM38 at 0.1 and 0.4 m above the ground for cotton. No. of data points (n) used was 84 and $P \leq 0.001$.

Height above ground (m)	Mode of operation	Regression equation	R^2
0.1	VM	$y = 0.29\ x - 32.97$	0.80
	HM	$y = 37.049\ e^{0.004x}$	0.84
0.4	VM	$y = 0.30\ x - 27.55$	0.78
	HM	$y = 33.028\ e^{0.007x}$	0.84

6.3.2.2 Effect of temperature on EC_a

Simple linear regression models were used to determine the effects of air and soil temperature at 5, 10 and 25 cm depths separately on EC_a measured in both vertical and horizontal modes of EM38. Regression equations and associated values of R^2 for both VM and HM of EM38 are given in Tables 6.6 and 6.7. Low R^2 values (0.16-0.27 for VM and 0.08-0.20 for HM) obtained with these regression models suggest that the contribution of temperature to EC_a was much smaller than that due to the variation in soil water.

Table 6. 6 Regression equations and coefficient of determination (R^2) for the relationship between EC_a (y, mS m^{-1}) and temperature (both soil and air, x, °C) for various irrigation treatments in VM of EM38 for cotton. No. of data points (n) used was 60 and $P \leq 0.001$.

Temperature	Regression equation	R^2
Air	$y = 4.45\ x - 26.07$	0.27
Soil – 5 cm	$y = 1.56\ x + 57.10$	0.16
Soil – 10 cm	$y = 3.08\ x + 22.40$	0.22
Soil – 25 cm	$y = 5.34\ x - 31.98$	0.28

Table 6. 7 Regression equations and coefficient of determination (R^2) for the relationship between EC_a (y, mS m^{-1}) and temperature (both soil and air, x, °C) for various irrigation treatments in HM of EM38 for cotton. No. of data points (n) used was 60.

Temperature	Regression equation	R^2	P
Air	$y = 3.37\ x - 13.56$	0.18	≤ 0.001
Soil – 5 cm	$y = 1.00\ x + 54.95$	0.08	≤ 0.05
Soil – 10 cm	$y = 2.18\ x + 27.32$	0.13	≤ 0.005
Soil – 25 cm	$y = 4.22\ x - 22.17$	0.20	≤ 0.001

6.3.2.3 Spatial variation in soil water and EC_a

Spatial variation in EC_a measurement in VM of EM38 and soil water within 1.33 m depth is shown in Figs. 6.22 and 6.23 for all the 12 plots of various irrigation treatments for the cotton crop. Filled circles on these maps represent the measurement location for each plot with label denoting irrigation treatment (T50…T85) and replicate (R1…R3). Dark blue areas indicate the higher value of EC_a and soil water within 1.33 m depth in Figs. 6.22 and 6.23. Similarly lighter shade of blue (almost white) within these maps represent low value of EC_a that matches with a similar location in the field of low soil water within 1.33 m depth. Since areas of the field with T50 and T85 treatments indicate areas of lowest and highest soil water deficit respectively, frequent mapping of EC_a can be used to apply the difference in the quantities of water to reduce soil water deficit as a strategic move towards precision irrigation.

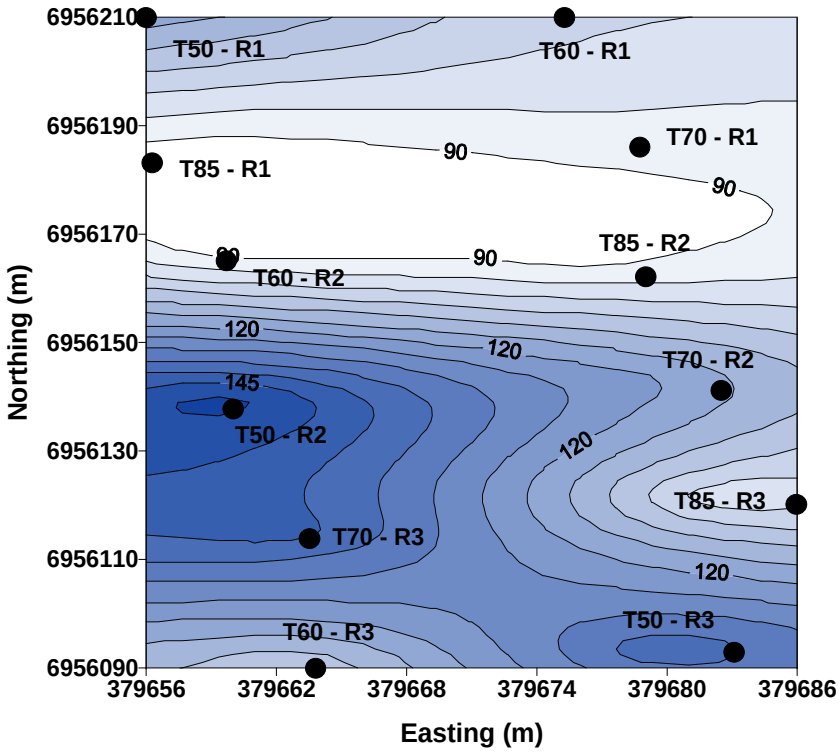

Figure 6. 22 Spatial variation in EC_a at the irrigation experiment site at 125 days after planting cotton. Filled circles indicate the position of measurement for irrigation treatments T50, T60, T70 and T85 and replicates R1, R2 and R3 of each irrigation treatment. The contour lines show values of EC_a in mS m^{-1}.

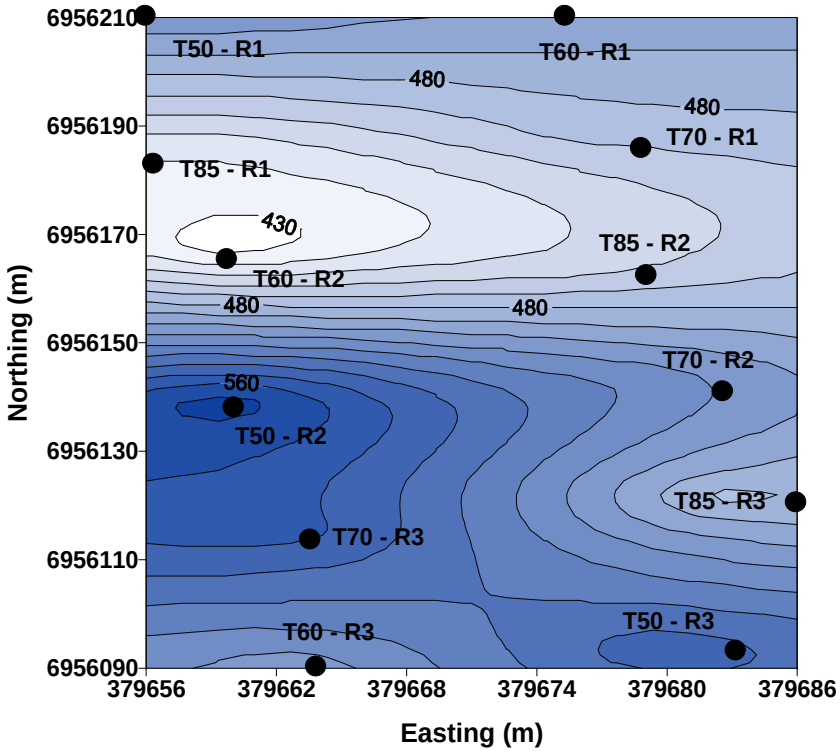

Figure 6. 23 Spatial variation in soil water content within 1.33 m depth for the irrigation experiment at 125 days after planting cotton. Filled circles indicate the position of measurement for each plot of the entire field. T50, T60, T70 and T85 are irrigation treatments and R1, R2 and R3 are replicates of each treatment. The contour lines show the values of soil water in mm.

6.3.3 Prediction of soil water from EC_a measurements

For wheat and cotton experiments, EC_a measurements with EM38 in VM near the surface and also above the ground (i.e. at 0.1 and 0.4 m height) correlated well with soil water within the effective sensing depth of EM38. For this reason, it should be possible to predict spatial variation in soil water from the measurements of EC_a during the growth period of both crops by using the regression equations developed to describe EC_a-soil water relationships. These predictive equations required switching the dependency of variables as common with various measurements, e.g. most spectroscopic measurements and measurement of soil water with neutron moisture meter.

Soil water predicted from EC_a measurements for the growing seasons of the wheat and cotton crops is shown in Fig. 6.24. Although it can be seen that for Figs 6.24b and 6.24c, the trends are close enough due to the possibility of considerable overlap of 95% confidence limit (not shown in these figures), the agreement between

the cropping seasons was relatively poor in Fig. 6.24a. Predicted soil water within 1.33 m depth was higher for wheat than cotton when the value of EC_a was <100 mS m^{-1} and lower for cotton than wheat when EC_a was within 100-155 mS m^{-1}. These difference in predicted soil water for both crops could be due to (a) incorrect matching of soil-water depth (1.33 m) with the effective sensing depth of EM38 (1.5 m), (b) temperature differences during measurements, (c) effects of residual fertilizer from the previous crop and (d) timing of fertilizer application relative to EC_a measurements during the growing season. Since in the predictive mode, soil water within a depth of 1.1–1.3 m can be predicted reasonably well by placing the EM38 at various heights above the ground (Figs. 6.24b and c), some limitations of EC_a measurements in the VM of EM38 can be easily avoided.

Similar measurements of EC_a with the EM38 in HM near the surface as well as above the ground (i.e. at 0.1 and 0.4 m heights) were also used to predict soil water within 0.33-0.73 m depth for wheat and cotton. These comparisons are shown in Fig. 6.25. It can be seen that there was a greater degree of disagreement between cropping seasons when both soil water and EC_a were low due to simultaneous reduction in soil depth (for accumulation of water) and effective sensing depth of EM38. Thus, soil water can be predicted at a high degree of confidence and precision using EM38 when the soil has a high EC_a and is moderately moist. However, when the soil has a low EC_a and/or the ground appears relatively dry due to lack of adequate soil depth to hold sufficient water or due to low clay content, EM38 would be useful to determine effective soil depth or to distinguish one soil type from another.

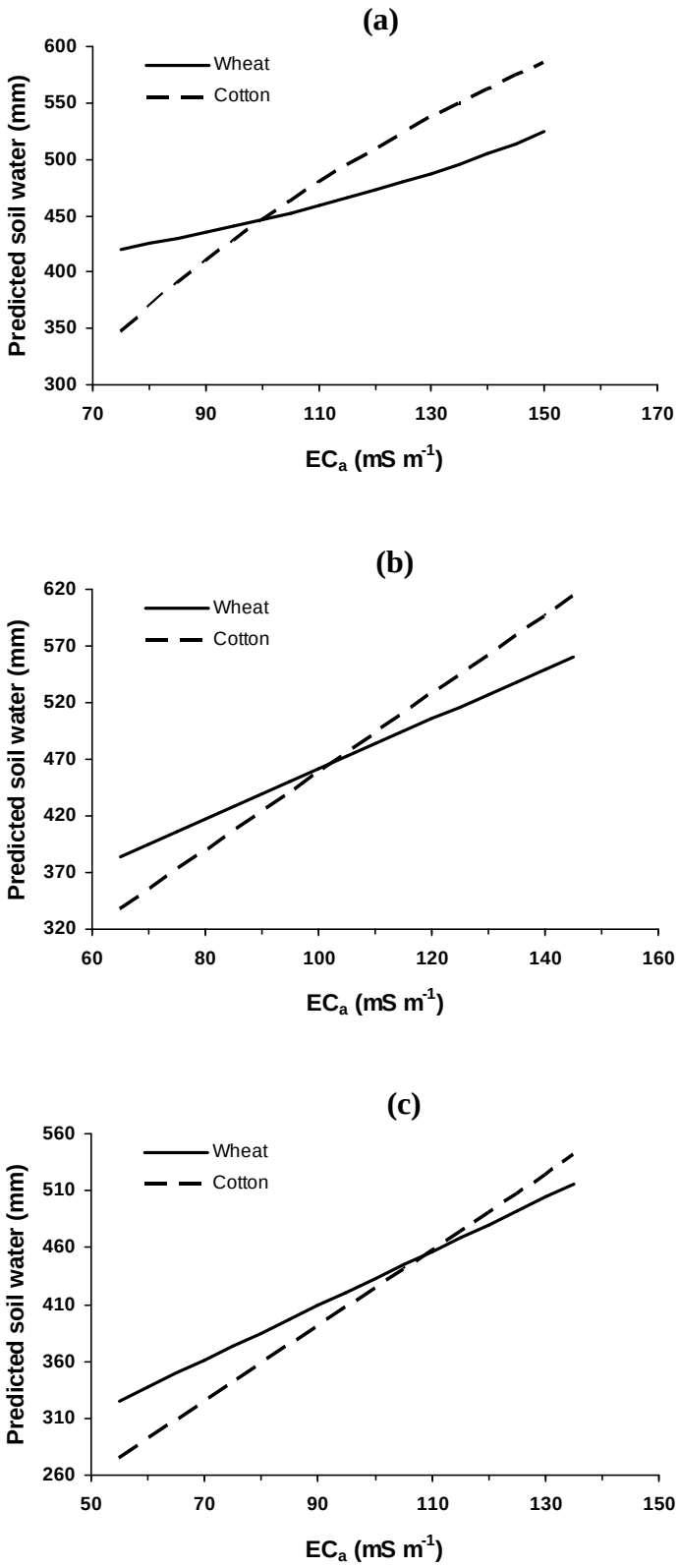

Figure 6. 24 A comparison of predicted soil water from EC_a during the wheat and cotton seasons. (a) VM near the surface, relating to 1.33 m depth of soil water, (b) VM at 0.1 m height above the ground, relating to 1.33 m depth of soil water and (c) VM at 0.4 m height above the ground, relating to 1.13 m depth of soil water.

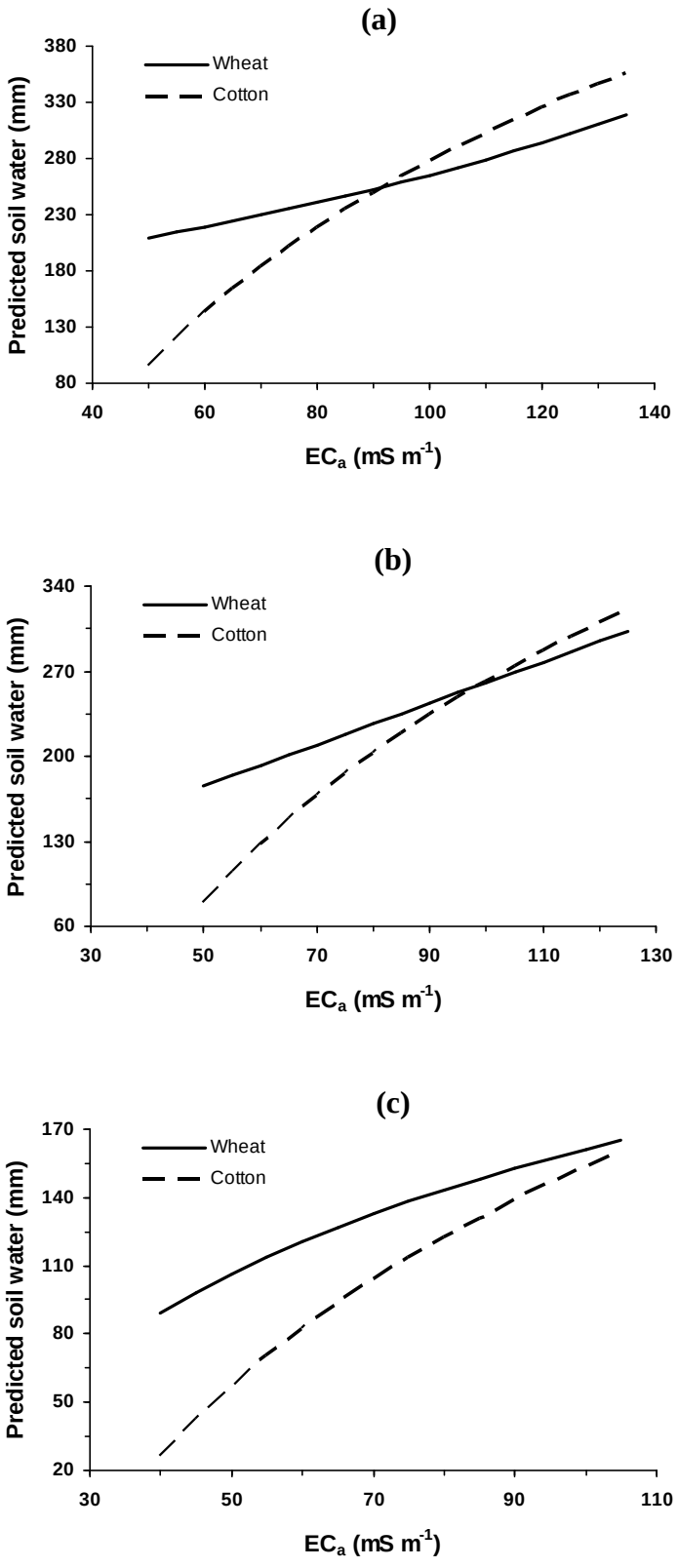

Figure 6. 25 A comparison of predicted soil water from EC_a during the wheat and cotton seasons. (a) HM near the surface, relating to 0.73 m depth of soil water, (b) HM at 0.1 m height above the ground, relating to 0.63 m depth of soil water and (c) HM at 0.4 m height above the ground, relating to 0.33 m depth of soil water.

6.4 Concluding remarks

Simultaneous measurements of soil water content and EC_a measured with EM38 in the field have indicated that for soils of high clay content the EM38 measured EC_a can be used for prediction of soil water within the root zone of a range of crops by combining vertical and horizontal modes of measurement at ground level and supplementing these measurements by placing the EM38 at various heights above the ground. Since EMI techniques used for the measurement of EC_a can provide a large amount of spatial information relatively quickly and economically when compared with direct but invasive measurements of soil water content with neutron probe or other soil water sensors, it would be desirable to use this technique with mobile irrigation application systems. Seasonal variation in temperature can influence EC_a significantly, but its overall effects are relatively small. Maps of EC_a can be used to gain information on soil water to apply precision irrigation when spatial variability in EC_a in a field is largely due to the variation in soil water content. If the spatial variation in EC_a in a field is due to the spatial variation of a soil property that does not contribute to variation in soil water content, then EC_a maps should not be used to predict soil water in that situation. In those situations, it may be used for the determination of soil depth or to distinguish various types of soils.

Chapter 7
GENERAL DISCUSSION AND CONCLUSIONS

Spatial variability is a common feature of all landscapes although certain features of the landscape (e.g. terrain) might appear uniform. Most simple theories developed on physical, chemical and biological processes in soil and plant sciences tend to treat soil and plant material as uniform and homogeneous. Sustainable irrigation practices developed to optimise crop growth and yield on spatially variable landscapes also had little success in identifying and quantifying spatial variability in soil properties which are relevant to irrigation application (e.g. soil water content) and in accommodating its variation in controlling timing and amount of irrigation water application on landscapes.

These deficiencies in irrigation science have led to examining the hypothesis in this work that crop growth in a field is nonuniform due to uneven crop water deficit present in the field. This can be quantified with measurements of water potential and stomatal conductance of leaves as both influence loss of water from leaves via transpiration. When plants transpire, loss of water vapour affects their energy balance due to emission of heat during transpiration. As it is possible to measure heat emission from leaves with infrared thermometers or thermography, spatial variation in crop water deficit in a field can be assessed with measurements of leaf/canopy temperature in various parts of the field.

When soil is relatively dry, plants may experience water stress due to high internal water deficit causing partial to full stomatal closure in leaves during the day time. Since stomatal closure reduces heat emission from plant canopies, measurement of canopy temperature can be used as an indicator of thermal sensing of stomatal closure. Accumulation of crop water deficit of variable magnitude over time in a field is expected to influence growth and yield. Thus, spatial variation in crop yield can be related to spatial variation in soil water deficit that is influenced by the amount and frequency of rainfall and irrigation.

Experiments have been undertaken with cotton and wheat in the field and glasshouse to meet the objectives described above and as stated in Chapter 1. Spatial variation in soil water deficit in the field and in glasshouse pots was introduced using

various irrigation treatments that allowed control of timing and frequency of irrigation. Accurate estimates of soil water content and crop water deficit with a calibrated mini-lysimeter system was described in Chapter 3. Spatial variation in crop properties (e.g. stomatal conductance, leaf water potential and canopy temperature) due to the arrangement of irrigation treatments in the field are described for cotton and wheat in Chapters 4 and 5. In-situ measurements of apparent electrical conductivity (EC_a) in the field experiments with EM38 was undertaken at various times to measure spatial variation in soil water content as an alternative approach to thermal imaging of crop plants as it is independent of crop plants.

This chapter provides a synthesis of the main findings of those chapters to indicate overall outcomes (conclusions) and the direction for future research in this area. Since both soil water content and canopy temperature for all studied crops varied spatially due to random allocation of irrigation treatments to various parts of the field, the relationship between crop and soil properties are explored below.

7.1 Relationships between soil and plant water status

Both soil and plant water status can be expressed in two ways: either as water content or as water potential. Soil and plant water deficit are also expressed using the same conventions that are used for water status. Here deficit implies a reduced value of water status below maximum. The zero water deficit condition for soil usually coincides with field capacity, whereas for plants it coincides with full turgor. In order to relate plant water status with soil water, there is a need to acknowledge that water generally moves from soil through plant towards the atmosphere due to loss of water from leaves via transpiration. A gradient of water content (water potential) occurs within the flow path of water as water tends to move in the direction of low water status. Water status or deficit in the atmosphere can be expressed as vapour pressure deficit (VPD) which is a function of temperature and relative humidity of the atmosphere. When relative humidity is 100%, VPD = 0.

In most experiments described in this thesis, soil water was measured within the root zone of crops in volumetric form (θ) and on some occasions, it was integrated over the root zone (z) as θ_z. Since plant water status measured in volumetric form is not sensitive to the flow of water through soil-plant-atmosphere

continuum, leaf water potential (Ψ_l) was measured as an indicator in these experiments. When leaves are fully turgid, theoretically leaf water potential reaches maximum and is close to zero. Such high values of leaf water potential usually occur before sunrise as plants gain turgidity due to absence of transpiration during the night. As photosynthesis and transpiration in plant leaves occur during the day and in adjoining cells of leaves, both processes stop during the night due to the absence of any photosynthetically active radiation (PAR, expressed as quantum flux density within 0.4-0.7 μm wavelength of solar radiation).

Plants can regulate leaf water potential to reduce transpiration rate (T_r) of leaves by controlling water inflow into leaf and water outflow from leaves by partial to full closure of stomata which affects stomatal conductance (g_s). The extent to which a plant is able to adjust leaf water deficit via modification of T_r, Ψ_l and g_s in response to fluctuations in soil water or atmospheric water status on a given day or throughout the growing season is probably a characteristic feature of the plant (expressed through genetic × environment interaction) and relates to the plant's sensitivity to drought. This is illustrated for cotton and wheat in both field and glasshouse experiments (Figs. 7.1a-c) using the relationship between soil water status (θ or θ_z) and leaf water potential (Ψ_l) gathered from various experiments described in Chapters 4 and 5. It can be seen from Fig. 7.1a that seasonal variation in θ_z-Ψ_l was uniform and well coordinated for cotton whereas such behaviour was absent for wheat (Figs. 7.1b-c). In field experiments (Fig. 7.1b), when wheat plants were young (at 70-105 DAP) and exposed to dry soil ($\theta_z \leq 260$ mm), Ψ_l was mostly below -2.5 MPa but varied considerably in the range of -2.5 to -3.7 MPa when soil was moderately wet. These data indicate that wheat plants can maintain higher water flow rate to leaves compared to cotton by increasing the magnitude of Ψ_l and adjusting it within 1 MPa to suit local environmental condition at a given level of soil water deficit. Adjustment of Ψ_l was even greater in glasshouse experiments although the range of variation in Ψ_l was relatively smaller than that which was observed in the field experiment with wheat.

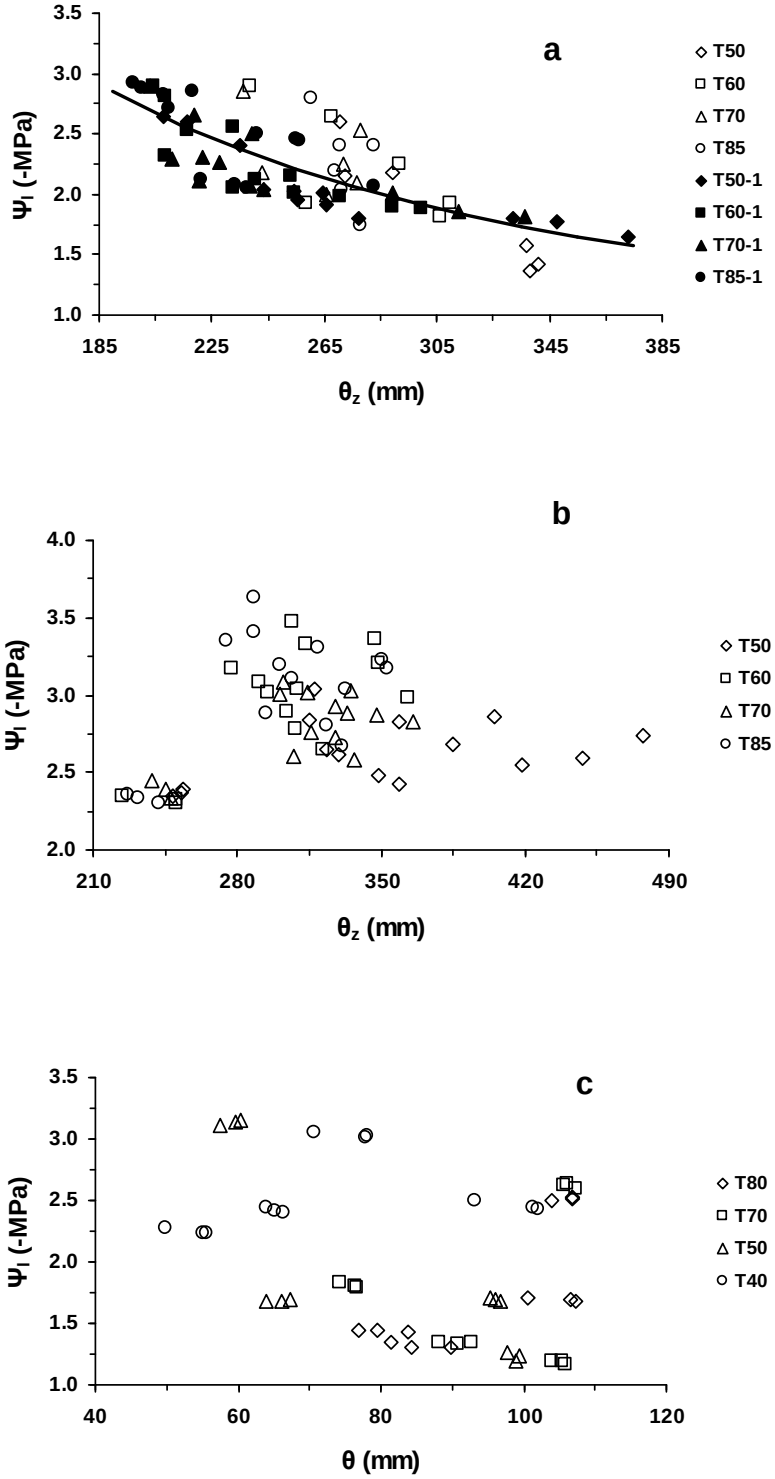

Figure 7. 1 Relationship between soil water within the root zone (θ_z or θ) and leaf water potential (Ψ_l) for (a) cotton under various irrigation treatments during the field experiment in 2007-08 and 2008-09 seasons (b) wheat under various irrigation treatments in the field experiment and (c) wheat under various irrigation treatments in the glasshouse experiment.

When soil water within the root zone of a crop changes over time but within a certain limit (as with irrigation treatments given in a number of experiments in this

work), a linear increasing trend in stomatal conductance (g_s) with increase soil water (θ or θ_z) was evident on most occasions (Fig. 7.2). Since g_s is an instantaneous measure of stomatal conductance of single leaves, it is strongly influenced by atmospheric conditions at the time of measurement, especially vapour pressure deficit (VPD) and radiation (PAR). Thus the degree of scatter observed in Fig. 7.2 could be partly due to the timing and the ambient weather conditions for these measurements. In the glasshouse experiment with cotton (Fig. 7.2b), g_s remained low and was relatively insensitive to θ for the least frequently irrigated treatment T40. This suggests that the stomata in cotton leaves remained partially closed at most measurement times in T40 treatment throughout the season. Since photosynthesis and transpiration are jointly influenced by stomatal conductance (Jarvis and Davies, 1998), low values of g_s may have an adverse effect on crop growth.

Water loss from leaves via transpiration is an inevitable process that allows plants to assimilate CO_2 as plants tend to optimise water loss and photosynthesis by regulating g_s (Jones, 1998). Therefore leaf temperature is maintained within an optimal range and a given change in g_s on transpiration can influence g_s itself through a feedback mechanism (Jarvis and Davies, 1998). Due to the complex relationship between transpiration and stomatal conductance, transpiration rate (T_r) of single leaves may be dependent on leaf temperature, but spatial variability of T_r (refers to leaf to leaf variation at various positions within the canopy) can be substantial due to the spatial variability of g_s (Jones, 1999a). Simultaneous measurements of g_s and T_r made with the porometer showed a general decline in transpiration rate with an increase in leaf temperature (data not shown). T_r of a leaf tends to decrease due to partial stomatal closure causing an increase in leaf temperature. Variation of T_c with T_r (Fig. 7.3) showed a reduction in canopy temperature (T_c, obtained as an average estimate of temperature of several leaves with the infrared thermography) with increased transpiration rate measured for single leaves with the porometer. At low conductance and low transpiration rate, T_c not only increases but its variability is also usually high (Fuchs, 1990; Leinonen and Jones, 2004). This reduces the sensitivity of T_c as a measure of transpiration rate of whole canopy and is a characteristic of plant species (detailed in Chapters 4 and 5).

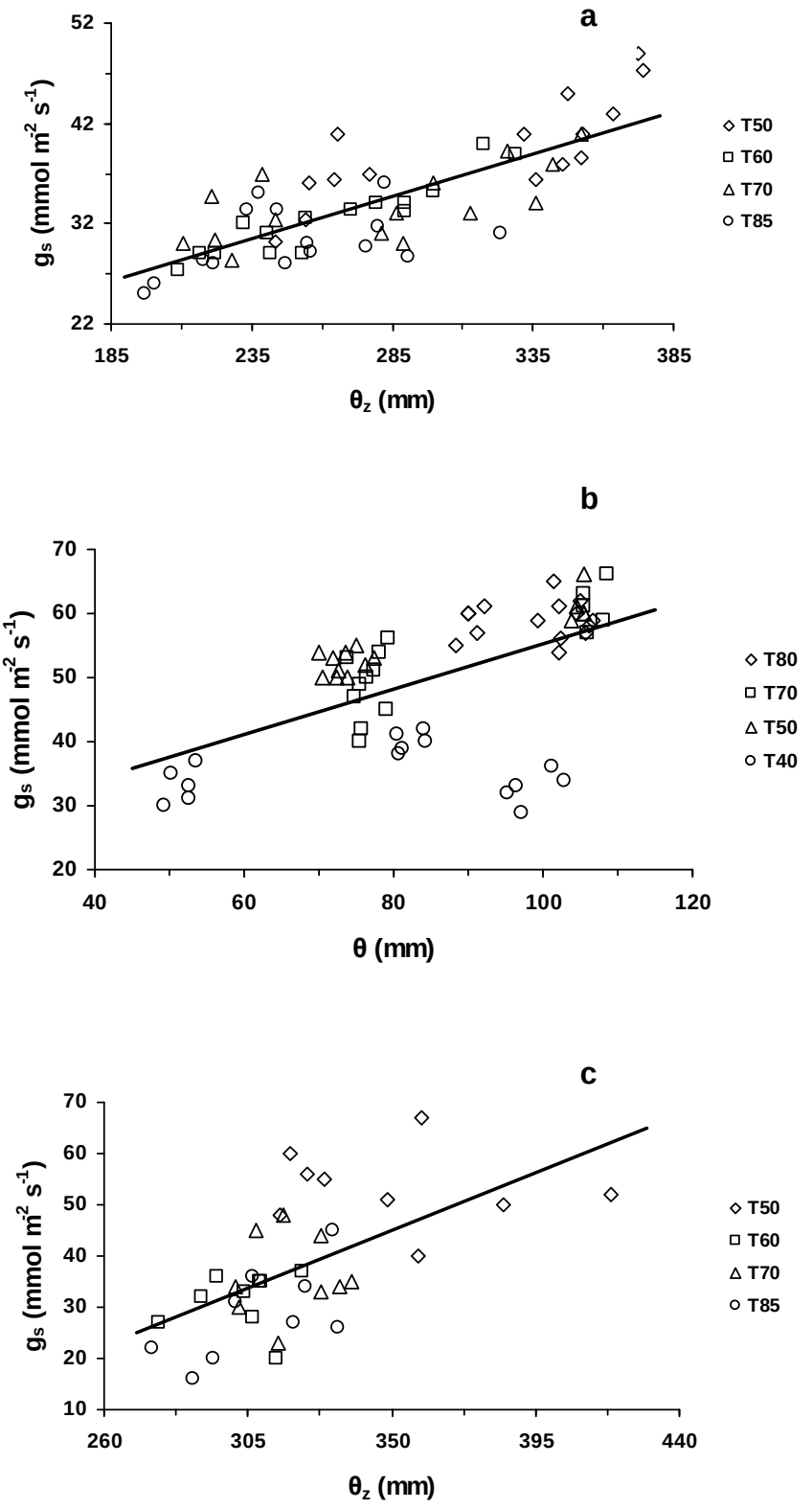

Figure 7. 2 The effect of soil water within root zone (θ_z or θ) on stomatal conductance (g_s) for various irrigation treatments of (a) cotton in the field during 2008-09 season, (b) cotton in the glasshouse experiment and (c) wheat in the field experiment.

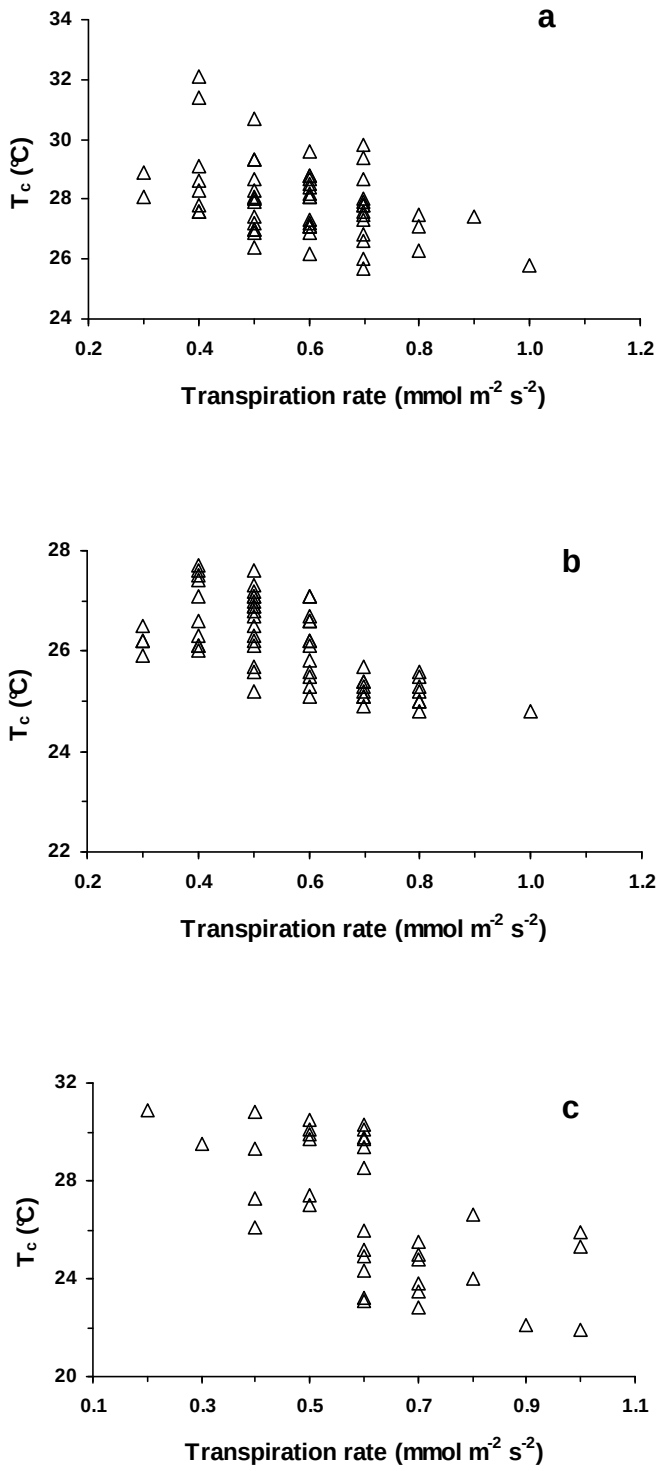

Figure 7. 3 The effect of transpiration rate of single leaves (T_r) on canopy temperature (T_c) for various irrigation treatments of (a) cotton in the field during 2008-09 season, (b) cotton in the glasshouse experiment and (c) wheat in the field experiment.

7.2 Performance of EM38 in assessing soil water status

It has been shown in Chapter 6 that apparent electrical conductivity (EC_a) measured with the EM38 equipment can be used to obtain information on the spatial distribution of soil water content. Since EC_a is a complex function of several soil properties including soil temperature, accurate prediction of the absolute quantity of soil water at a given position in a crop field is difficult. Application of fertilizers to a growing crop can also introduce error since the primary response of EM38 is highly dependent on ions in the soil solution. In order to determine the extent to which EC_a data of EM38 would be useful in assessing spatial distribution of soil water in the field, two scenarios (best- and worst-case) are examined.

The best-case scenario refers to the Fig. 6.24c in Chapter 6 where prediction of soil water within 1.13 m depth from EC_a (in vertical mode of EM38 at 0.4 m above the ground) agreed well in wheat and cotton crops. Measured data of spatial distribution of water content within the top 1.13 m depth on a given day in the cotton field (Fig. 7.4) is compared with predicted water content using the prediction model (θ_z-EC_a relationship) for cotton and EM38 data on the same day in the same field (Fig. 7.5) and using the same EM38 data for cotton but using the prediction model for wheat (Fig. 7.6).

Focussing on white areas on the map (dry areas in the field) with contour intervals of 10 mm water shows that the position of these areas agreed reasonably well (i.e. they are all located within 6956150-6956170N) although the size of dry areas differed a little. Predicted water content using the data and model for cotton in (Figs 7.4 and 7.5) showed that the predicted water content within the dry area was underestimated by 20 mm (measured = 350 mm and predicted = 330 mm) while using cotton data with the wheat model (Figs. 7.4 and 7.6) water content was overestimated by 10 mm (measured = 350 mm and predicted = 360 mm). Focussing on the dark blue areas on these maps (wet areas in the field) shows that the position and size of these areas were even better matched than for the dry areas. Predicted water content in these areas differed from the measured water content by 20 mm (Fig. 7.6) and 40 mm (Fig. 7.5). Thus, this best case scenario analysis suggests that the EM38 data in the vertical mode (VM) can be used to distinguish wet and dry areas in a field with 20-40 mm accuracy irrespective of the growing crop.

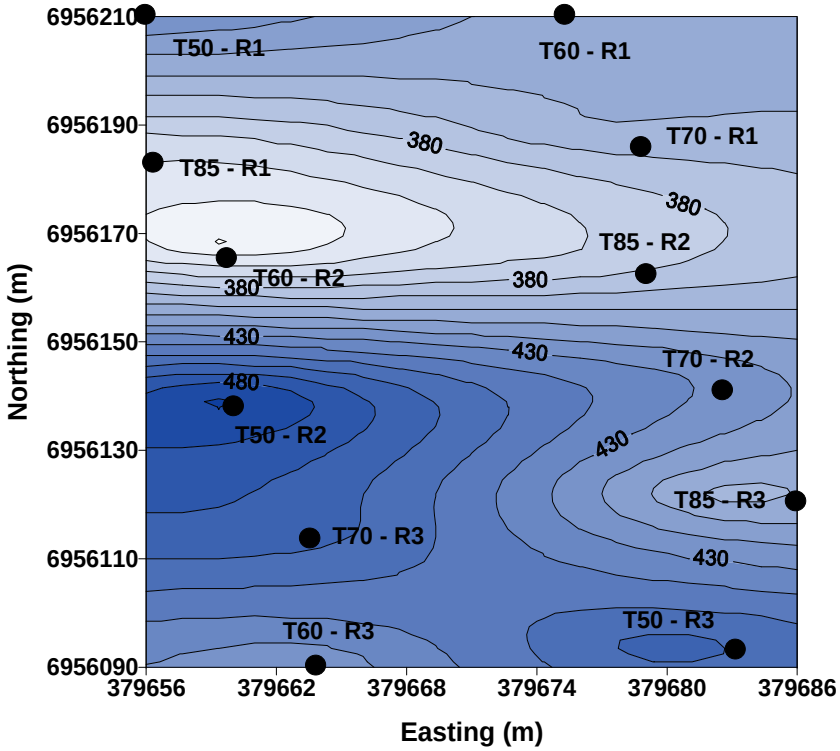

Figure 7. 4 Spatial variation in measured soil water content (θ_z) within 1.13 m depth for the irrigation experiment at 125 days after planting cotton. Filled circles indicate the position of replicate plots (R1, R2 and R3) of irrigation treatments (T50, T60, T70 and T85). Contour lines show measured values of soil water (θ_z) within 1.13 m depth (in mm).

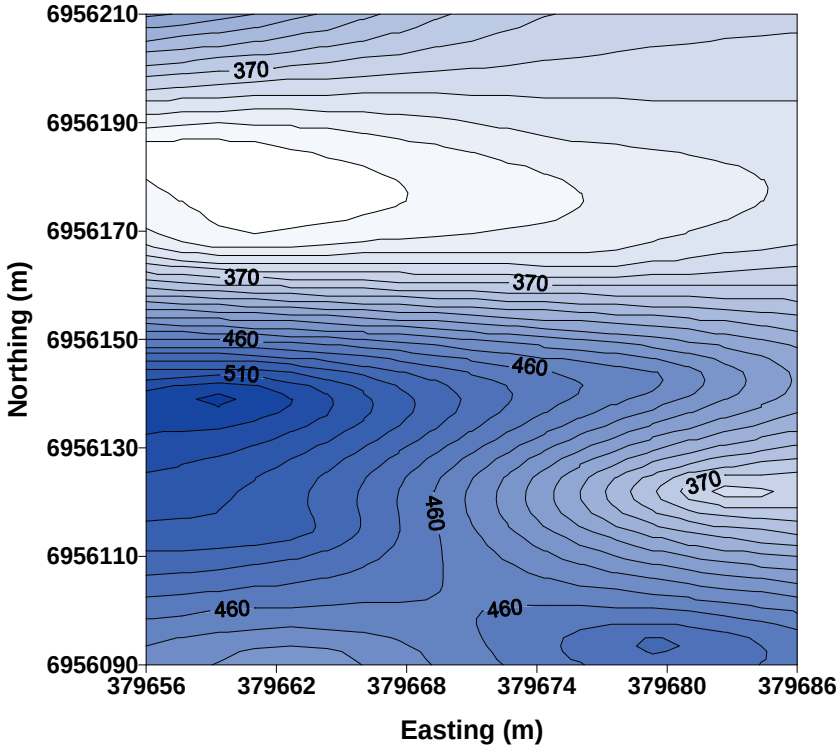

Figure 7. 5 Spatial variation of predicted soil water content (θ_z) within 1.13 m depth for the irrigation experiment at 125 DAP cotton from EM38 data measured in VM at 0.4 m height above ground in the cotton field and using the θ_z-EC_a relationship for cotton.

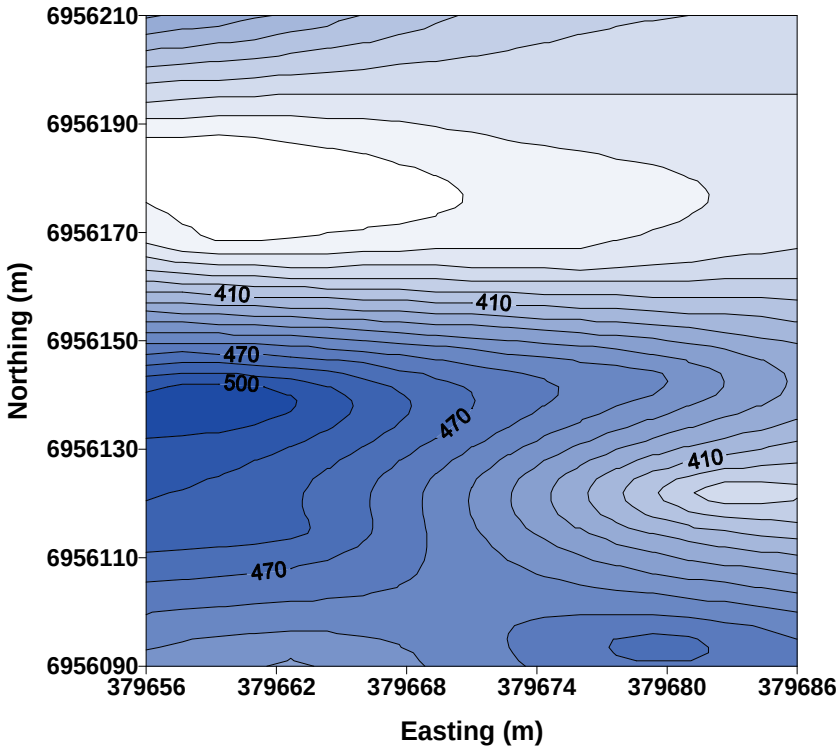

Figure 7. 6 Spatial variation of predicted soil water content (θ_z) within 1.13 m depth for the irrigation experiment at 125 DAP cotton from EM38 data measured in VM at 0.4 m height above ground in the cotton field and using the θ_z-EC_a relationship for wheat.

The worst-case scenario refers to the Fig. 6.25c in Chapter 6 where prediction of soil water within 0.33 m depth from EC_a (in HM of EM38 at 0.4 m above the ground) differed substantially between wheat and cotton, especially when the field was dry and EC_a values were low. Measured data of spatial distribution of water content within the top 0.33 m depth on a given day in the cotton field (Fig. 7.7) is compared with predicted water content using the prediction model (θ_z-EC_a relationship) for cotton and EM38 data on the same day in the same field (Fig. 7.8) and using the same EM38 data for cotton but using prediction model for wheat (Fig. 7.9).

Focussing on white areas on the map (dry areas in the field) with contour intervals of 10 mm water shows that the positions of these areas are displaced by about 20 m in the south direction (i.e. from 6956190N to 6956170N). Predicted water content for dry areas using data and model for cotton in Figs 7.7 and 7.8 showed that water content was underestimated by 35 mm (measured = 75 mm and predicted = 45 mm) while using cotton data with the wheat model (Figs. 7.7 and 7.9)

water content was overestimated by 25 mm (measured = 75 mm and predicted = 100 mm).

Focussing on the dark blue areas on these maps (wet areas in the field) shows that the position of wet areas was slightly better matched than the dry areas but not size. Predicted water content in these areas differed from the measured water content by only 10 mm (Figs. 7.7-7.9). Thus, prediction of water content within shallow soil layers with HM of EM38 reduces accuracy since there is little water within the shallow depth and that reduces the sensitivity of the EM38.

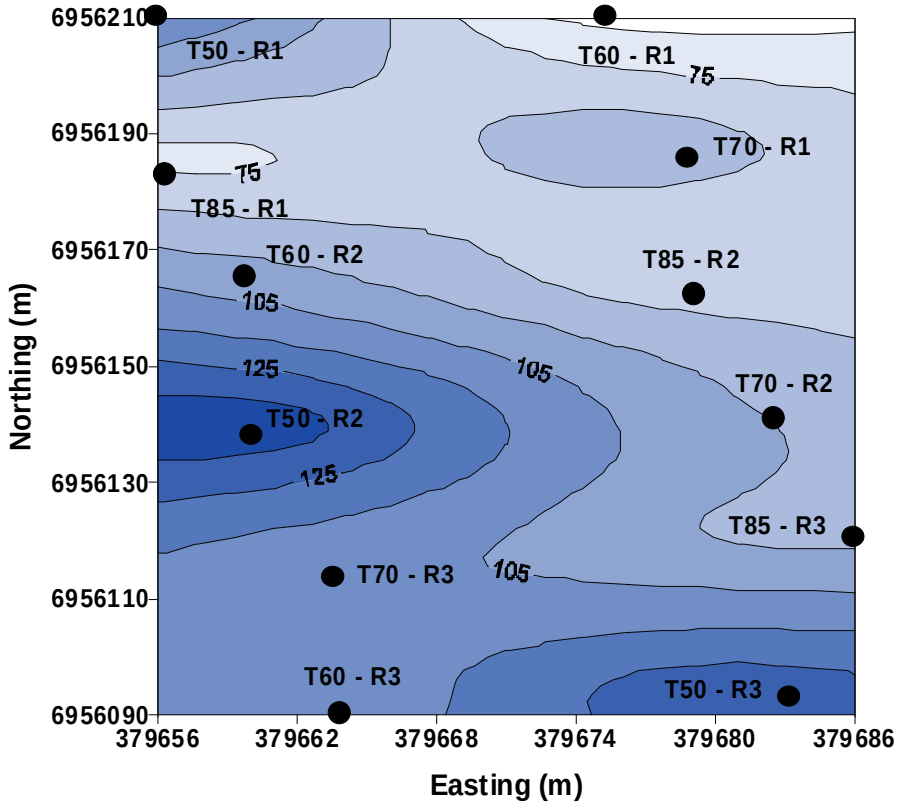

Figure 7. 7 Spatial variation in measured soil water content (θ_z) within 0.33 m depth for the irrigation experiment at 125 days after planting cotton. Filled circles indicate the position of replicate plots (R1, R2 and R3) of irrigation treatments (T50, T60, T70 and T85). Contour lines show measured values of soil water (θ_z) within 0.33 m depth (in mm).

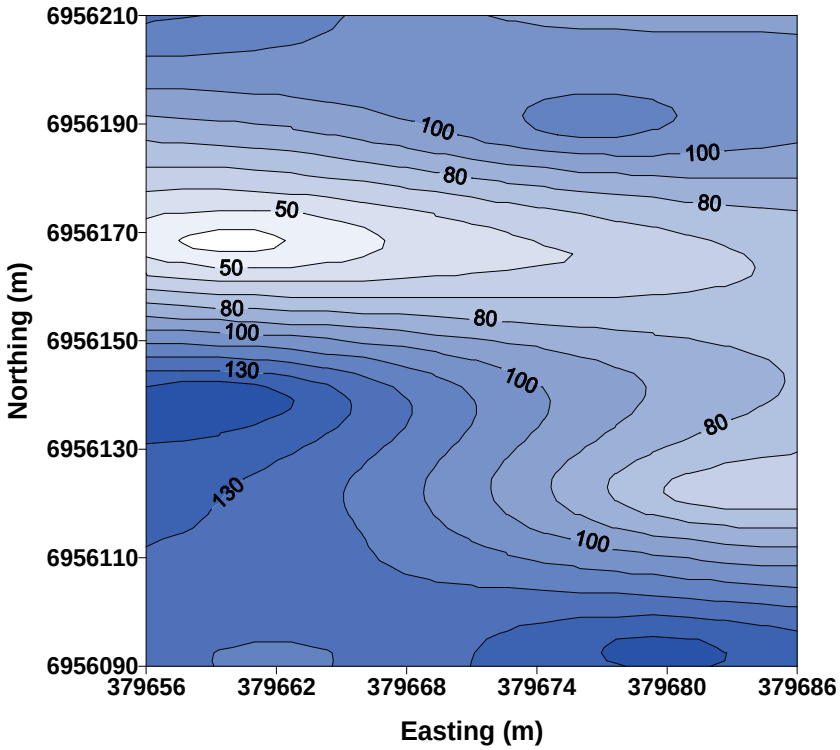

Figure 7. 8 Spatial variation of predicted soil water content (θ_z) within 0.33 m depth for the irrigation experiment at 125 DAP cotton from EM38 data measured in HM at 0.4 m height above ground in the cotton field and using the θ_z-EC_a relationship for cotton.

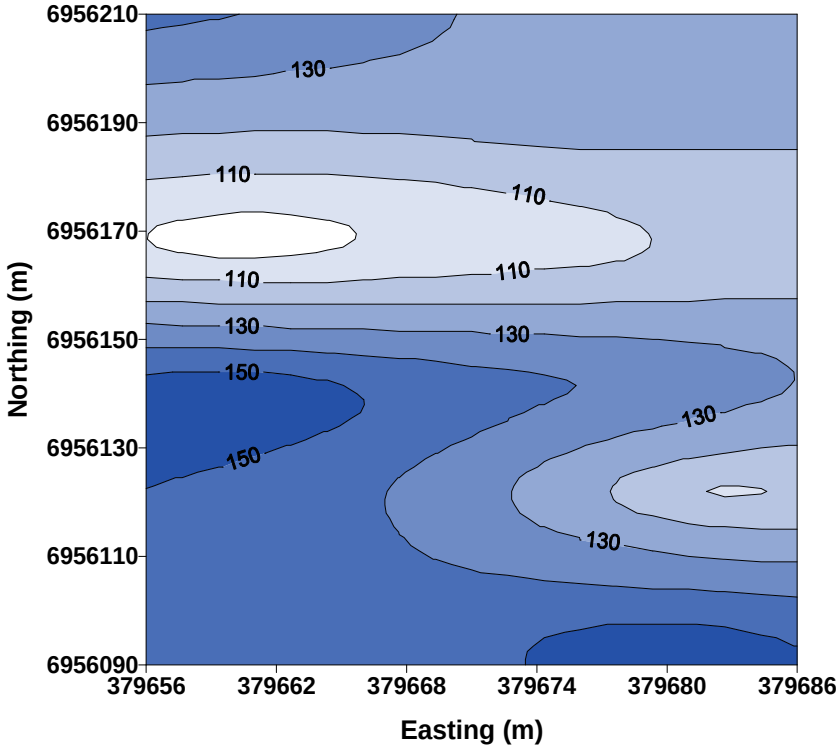

Figure 7. 9 Spatial variation of predicted soil water content (θ_z) within 0.33 m depth for the irrigation experiment at 125 DAP cotton from EM38 data measured in HM at 0.4 m height above ground in the cotton field and using the θ_z-EC_a relationship for wheat.

7.3 Effective irrigation strategies

Irrigation strategies involving timing and quantity of irrigation to crop fields that accommodates spatial variation in soil water content (as a characteristic feature of in-situ variation in soil properties or associated with water application system) can only be considered effective if the strategy maintains a sustainable level of crop growth and yield. For this purpose, the data on above-ground crop biomass as an indicator of growth and yield of economic product (grain or fibre) were analysed together with the data on seasonal water use (expressed as ET for the period from planting to harvest). ET was estimated for all field and glasshouse experiments using a soil water balance equation that assumed zero runoff and zero drainage (for field experiments only) beyond the root zone for all irrigation and rainfall events.

For field experiments, ET (mm) was estimated as:

$$ET = \sum_{i=1}^{n} P_{i,i+1} + I_{i,i+1} + (\theta_i - \theta_{i+1}) \qquad (7.1)$$

and for the glasshouse experiments,

$$ET = \sum_{i=1}^{n} I_{i,i+1} - D_{i,i+1} + (\theta_i - \theta_{i+1}), \qquad (7.2)$$

where $P_{i,i+1}$, $I_{i,i+1}$ and $D_{i,i+1}$ were rainfall, irrigation and drainage, respectively in mm during two consecutive measurement occasions (denoted as i and i+1) and θ_i and θ_{i+1} were soil water content (mm) measured within the top 1.33 m of soil in the field or for the entire volume of soil in the pot during the same measurement period. The number (n) used in Eqns. 7.1 and 7.2 exceeded the maximum number of irrigations given to the most frequently irrigated treatment that carried the least soil water deficit. Since both dry matter production and yield in each experiment was expressed in kg ha^{-1} and ET in mm, water use efficiency (WUE) could be estimated as the ratio yield or biomass and ET.

Biomass and yield data for both crops in the field and glasshouse experiments are given in Tables 7.1 and 7.2. These data indicate that yield and biomass for both crops were highest with the most frequently irrigated treatment T50 in the field experiments and T80 in the glasshouse experiments. Similarly, lowest

yield and biomass for both crops were obtained with the least frequently irrigated treatments T85 and T40, in the field and glasshouse experiments respectively.

Table 7. 1 Effects of irrigation treatments on above ground biomass and yield of cotton (2007-08) and wheat (2008) in field experiments. Within a row of values, mean biomass or yield with a different superscript letter indicate significant difference at P≤0.05 when compared with the least significant difference (LSD). NS indicates P>0.5.

Crops	Biomass (kg ha^{-1}) for irrigation treatments				LSD (kg ha^{-1})
	T50	T60	T70	T85	
Cotton	13736.4^{a}	10499.4^{a}	11335.5^{a}	8378.1^{b}	3031.2
Wheat	13469.3^{a}	12317.3^{a}	9445.3^{b}	8448.0^{b}	2943.1
	Yield (kg ha^{-1})				
Cotton	1355.7	1258.9	1217.5	1292.5	NS
Wheat	3894.0^{a}	3581.5^{a}	2010.8^{b}	1775.2^{b}	454.0

Table 7. 2 Effects of irrigation treatments on above ground biomass and yield of cotton (2008-09) and wheat (2008) in glasshouse experiments. Within a row of values, mean biomass or yield with a different superscript letter indicate significant difference at P≤0.05 when compared with the least significant difference (LSD).

Crops	Biomass (kg ha^{-1}) for irrigation treatments				LSD (kg ha^{-1})
	T80	T70	T50	T40	
Cotton	9374.1^{a}	8260.6^{b}	8144.1^{b}	6298.7^{c}	914.3
Wheat	7326.1^{a}	6759.6^{b}	5912.5^{c}	4853.8^{d}	438.8
	Yield (kg ha^{-1})				
Cotton	3286.6^{a}	2656.7^{b}	2750.9^{b}	2044.9^{c}	164.2
Wheat	2605.0^{a}	2558.8^{a}	2112.4^{b}	1559.0^{c}	251.7

An irrigation strategy can be considered as effective if it does not cause significant yield reduction and results in the highest possible water use efficiency to be achieved. Water use efficiency estimated for these experiments (Table 7.3) shows that water use efficiency declines with increased frequency of irrigation. However, the irrigation treatment T60 in the field experiment caused neither significant decline in biomass or yield (Table 7.1) nor any significant decrease in water use efficiency (Table 7.3) for both cotton and wheat. In the glasshouse experiments, irrigation treatment T70 can be considered ideal for both wheat and cotton on the basis of yield and water use efficiency (Tables 7.2 and 7.3). A detailed comparison of irrigation treatments given in Table 4.5 of Section 4.2.6 shows that T60 in the field and T70 in

the glasshouse refer to volumetric soil water content of 32 and 35% respectively. Thus, an effective irrigation strategy for cotton and wheat should aim to apply irrigation when soil water content within the root zone drops to 32-35%.

Table 7. 3 Effects of irrigation treatments on water use efficiency of cotton and wheat in field and glasshouse experiments. Within a row of values, mean values with a different superscript letter indicate significant difference at P≤0.05 when compared with the least significant difference (LSD). NS indicates P>0.5.

Experiment	Crops	Water use efficiency (kg ha^{-1} mm^{-1})				LSD (kg ha^{-1})
		T50	T60	T70	T85	
Field	Cotton	1.94	2.21	2.27	2.49	NS
Field	Wheat	10.02^{a}	9.54^{a}	7.92^{b}	5.97^{c}	0.98
		T80	T70	T50	T40	
Glasshouse	Cotton	3.91^{a}	3.30^{b}	3.93^{a}	3.50^{b}	0.28
Glasshouse	Wheat	5.12	5.75	5.61	5.84	NS

If a field consists of clay soil similar to that used in this experiment and exhibits spatial variability in water content then irrigation should be applied to maintain the critical water content of 32-35% throughout the field during crop growth. When soil water content approaches this critical limit, irrigation should be applied up to the drained upper limit or field capacity if there are no salinity hazards in the field. Whether a field is uniform or exhibits spatial variability in water content due to in-situ variation in soil properties, soil water content and its distribution can be estimated with either thermal imagery or EM38 measurements. Since soil water can be assessed in the field using canopy temperature (T_c) (Chapters 4 and 5) or EC_a (Chapter 6), it is possible to apply the precise quantity of irrigation water on time in crop fields.

7.4 Conclusions

On the basis of the results presented in this work and implications discussed, the following conclusions are reached.

1. It is possible to measure evapotranspiration (ET) and water use of crops economically at a resolution of 0.027 mm of water with the mini-lysimeter system described in Chapter 3. The equipment and measurement technique described in this chapter has allowed measurement of temporal variation in soil water and ET at short

time intervals (~10 min) which is ideal for studying spatial and temporal variability in growth and performance of irrigated crops.

2. Proximal thermal sensing of crop plants with a thermal infrared camera (thermography) has been found to be an ideal tool for evaluating water deficit stress in crop plants. Studies on cotton and wheat indicated that the canopy temperature – soil water relationship is influenced by the extent to which stomata control transpiration, which may differ with crop species. However, it is still possible to predict soil water status and deficit in crop fields with a reasonable degree of confidence using thermal images of canopy temperature. Spatial variation in canopy temperature and soil water for a crop field (presented as maps) is remarkably well correlated. Therefore, it is possible to differentiate well-irrigated areas (low canopy temperature and high soil water) from water stressed areas (high canopy temperature and low soil water) within crop fields with thermal imagery. Since thermal imagery based water stress indices (ICWSI and I_G) require additional measurements, thermal images of a crop field on a given day can be used directly for soil water assessment. The use of ICWSI is mostly recommended for glasshouse grown plants.

3. Spatial distribution of soil water content and water deficit stress in crop fields can also be derived from measurements of apparent electrical conductivity (EC_a) with EM38 (an equipment based on the electromagnetic induction method). Since EC_a is a complex function of several variables including temperature, absolute quantities of soil water can be predicted in crop fields with moderate accuracy, with regions of wet and dry areas within the field being easily identified.

4. On clay soils, a volumetric soil water content corresponding with the irrigation treatments T60 (field) or T70 in (glasshouse) is recommended as an effective irrigation strategy because it does not cause significant yield reduction in cotton or wheat, while allowing the highest possible water use efficiency to be achieved. Since soil water content and its spatial distribution can be estimated with either thermal imagery or EM38 measurements, it is possible to apply irrigation precisely to achieve the desired value of soil water content.

REFERENCES

ABS (2006). *Water Account Australia 2004-05, Cat. No. 4610.0*. Australian Bureau of Statistics, Canberra.

Aboukhaled, A., Alfaro, A. & Smith, M. (1982). *Lysimeters*. Food and Agricultural Organisation Irrigation and drainage paper no. 39, Rome.

Alderfasi, A. A. & Nielsen, D. C. (2001) Use of crop water stress index for monitoring water status and scheduling irrigation in wheat. *Agricultural Water Management,* 47**,** 69-75.

Al-Karadsheh, E., Sourell, H. & Krause, R. (2002) Precision Irrigation: New strategy irrigation water management. *Conference on International Agricultural Research for Development.* October, 9-11, Witzenhausen, Germany.

Allen, R.G., Pereira, L.S., Raes, D. & Smith, M. (1998). *Crop evapotranspiration-guidelines for computing crop water requirements*. Food and Agricultural Organisation Irrigation and drainage paper no. 56, Rome.

Ashktorab, H., Pruitt, W. O. & Paw, U. K. T. (1994). Partitioning of evapotranspiration and micro-Bowen-Ratio system. *Journal of Irrigation and Drainage Engineering,* 120**,** 450-464.

Baldocchi, D. D. (2003). Assessing the eddy covariance technique for evaluating carbon dioxide exchange rates of ecosystems: past, present and future. *Global Change Biology,* 9, 1-14.

Baldocchi, D. D., Law, B. E. & Anthoni, P. M. (2000). On measuring and modeling energy fluxes above the floor of a homogeneous and heterogeneous conifer forest. *Agricultural and Forest Meteorology,* 102**,** 187-206.

Banton, O., Seguin, M. K. & Cimon, M. A. (1997). Mapping field-scale physical properties of soil with electrical resistivity. *Soil science society of America Journal,* 61**,** 1010-1017.

Batte, M. T. (2000). Factors influencing the profitability of precision farming systems. *Journal of Soil and Water Conservation*, 55, 12–18.

Bausch, W. C. & Bernard, T. M. (1992). Spatial averaging Bowen ratio system: Description and lysimeter comparison. *Transactions of the ASAE,* 35(1)**,** 121-128.

Bennett, A. J. (2000). Environmental consequences of increasing production: some current perspectives. *Agriculture, Ecosystems and Environment,* 82**,** 89-95.

Bork, E. W., West, N. E., Doolittle, J. A., & Boettinger, J. L. (1998). Soil depth assessment of sagebrush grazing treatments using electromagnetic induction. *Journal of Rangeland Management*, 51, 469–474.

Bowen, I. S. (1926). The ratio of heat losses by conduction and by evaporation from any water surface. *Physical Review,* 27**,** 779-787.

Brevik, E. C. & Fenton, T. E. (2002). The relative influence of soil water content, clay, temperature, and carbonate minerals on soil electrical conductivity readings taken with an EM-38 along a Mollisol Catena in Central Iowa. *Soil survey horizons,* 43**,** 9-13.

Brevik, E. C., Fenton, T. E., & Jaynes, D. B. (2003). Evaluation of the accuracy of a central Iowa soil survey and implications for precision soil management. *Precision Agriculture*, 4, 323–334.

Brevik, E.C., Fenton, T.E. and Lazari, A. (2006). Soil electrical conductivity as a function of soil water content and implications for soil mapping. *Precision Agriculture*, 7: 393-404.

Bullock, D. S. & Bullock, D. G. (2000). From agronomic research to farm management guidelines: A primer on the economoics of information and precision technology. *Precision Agriculture,* 2**,** 71-101.

Buol, S. W., Hole, F. D., McCracken, R. J., & Southard, R. J. (1997). *Soil genesis and classification, 4th edn*. Iowa State University Press, Ames, USA.

Burt, C. M., Mutziger, A. J., Allen, R. G. & Howell, T. A. (2005). Evaporation Research: Review and Interpretation. *Journal of Irrigation and Drainage Engineering,* 131**,** 37-58.

Cambouris, A. N., Nolin, M. C., Zebarth, B. J. & Leverdiere, M. R. (2006). Soil management zones delineated by electrical conductivity to characterize spatial and temporal variations in Potato yield and in soil properties. *American Journal of Potato Research,* 83, 381-395.

Chaerle, L. & Van Der Straten, D. (2000). Imaging techniques and early detection of plant stress. *Trends in Plant Science,* 5**,** 495-501.

Chen, J. M. & Zhang, R. H. (1989). Studies on the measurements of crop emissivity and sky temperature. *Agricultural Forest Meteorology,* 49**,** 23-34.

Chone, X., Van Leewen, C., Dubourdieu, D., & Gaudillere, J. P. (2001). Stem water potential is a sensitive indicator of grapevine water status. *Annals of Botany*, 87, 477-483.

Clawson, K. L. & Blad, B. L. (1982). Infrared thermometry for scheduling irrigation of corn. *Agronomy Journal,* 74**,** 311-316.

Cohen, Y., Alchanatis, V., Meron, M., Saranga, Y. & Tsipris, J. (2005). Estimation of leaf water potential by thermal imagery and spatial analysis. *Journal of Experimental Botany,* 56**,** 1843-1852.

Corwin, D. L. & Lesch, S. M. (2003). Application of soil electrical conductivity to precision agriculture: Theory, principles and guidelines. *Agronomy Journal,* 95**,** 445-471.

Corwin, D. L. & Lesch, S. M. (2005). Apparent soil electrical conductivity measurements in agriculture. *Computers and Electronics in Agriculture,* 46**,** 11-43.

Corwin, D. L., Lesch, S. M., Shouse, P. J., Soppe, R. & Ayars, J. E. (2003). Identifying soil properties that influence cotton yield using soil sampling directed by apparent soil electrical conductivity. *Agronomy Journal,* 95**,** 352-364.

Dalgaard, M., Have, H., & Nehmdahl, H. (2001). Soil clay mapping by measurement of electromagnetic conductivity. *Third European Conference on Precision Agriculture*. June, 18-20, Montepelier, France, pp.367-372.

De Azevedo, P. V., Soares, J. M., Da Silva, V. D. P. R., Da Silva, B. B. & Nascimento, T. (2008). Evapotranspiration of superior grapevines under intermittent irrigation. *Agricultural Water Management,* 95**,** 301-308.

DeTar, W. R. (2008). Yield and growth characteristics for cotton under various irrigation regimes on sandy soil. *Agricultural Water Management,* 95**,** 69-76.

Detar, W. R., Penner, J. V. & Funk, H. A. (2006). Airborne remote sensing to detect plant water stress in full canopy cotton. *Transactions of the ASABE,* 49(3)**,** 655-665.

Doolittle, J. A., Sudduth, K. A., Kitchen, N. R. & Indorante, S. J. (1994). Estimating depths to claypans using electromagnetic induction methods. *Journal of Soil and Water Conservation,* 49**,** 572-575.

Dowling, D. (2009).Water on the brain: 2008–2009 Australian Cotton Production Estimates. The Australian Cottongrower, *Cotton Yearbook 2009,* pp. 4.

Dugas, W. A., Fritschen, L. J., Gay, L. W., Held, A. A., Matthias, A. D., Reicosky, D. C. & Steiner, J. L. (1991). Bowen ratio, eddy correlation, and portable chamber measurements of sensible and latent heat flux over irrigated spring wheat. *Agricultural and Forest Meteorology,* 56**,** 1-20.

Dutch, S. (2007). Converting UTM to Latitude and Longitude (Or Vice versa). http://www.uwgb.edu/dutchs/UsefulData/UTMFormulas.htm. Viewed on 29.10.2007.

Ehlert, D., Schmerler, J. & Schuetze, S. (2001). Sensor-based real-time application of late N-fertiliser in winter wheat. *Third European Conference on Precision Agriculture*. June 18-20, Montepelier, France, pp.911-916.

Ehrler, W. L., Idso, S. B., Jackson, R. D. & Reginato, R. J. (1978). Wheat canopy temperature: Relation to plant water potential. *Agronomy journal,* 70**,** 251-256.

Evans, D.E., Sadler, E.J., Camp, C.R. & Millen, J.A. 2000. Spatial canopy temperature measurements using central pivot mounted IRTs. *In: Proceedings of the fifth international conference on precision agriculture*, Minnesota, USA.

Evett, S. R., Howell, T. A., Schneider, A. D., Upchurch, D. R. & Wanjura, D. F. (1996). Canopy temperature based automatic irrigation control. IN CAMP, C. R., SADLER, E. J. & YODER, R. E. (Eds.) *Evapotranspiration and irrigation scheduling. Proceedings of international conference.* San Antonio.

Evett, S. R., Mazahrih, N. T., Jitan, M. A., Sawalha, M. H., Colaizzi, P. D. & Ayars, J. E. (2009). A weighing lysimeter for crop water use determination in the Jordan valley, Jordan. *Transactions of the ASABE,* 52(1)**,** 155-169.

FAO (2002). *Deficit irrigation scheduling based on plant growth stages showing water stress tolerance by C. Kirda*. Water report No. 22. Food and Agricultural Organisation, Rome.

FAO (2007). *Food and agricultural commodities production*. http://faostat.fao.org/site/339/default.aspx. Viewed on 01.07.2009.

Fereres, E. & Soriano, M. A. (2007). Deficit irrigation for reducing agricultural water use. *Journal of Experimental Botany,* 58**,** 147-159.

Fitzgerald, G. J., Rodriguez, D., Christensen, L. K., Belford, R., Sadras, V. O. & Clarke, T. R. (2006). Spectral and thermal sensing for nitrogen and water status in rainfed and irrigated wheat environments. *Precision Agriculture,* 2006**,** 233-248.

Foley, J. L. & Harris, E. (2007). Field calibration of ThetaProbe (ML2x) and ECHO probe (EC-20) soil water sensors in a Black Vertosol. *Australian Journal of Soil Research,* 45**,** 233-236.

French, A. N., Hunsaker, D. J., Clarke, T. R., Fitzgerald, G. J., Luckett, W. E. & Jr. Pinter, P. J. (2006). Energy balance estimation of evapotranspiration for wheat grown under variable management practices in central Arizona. *Transactions of the ASABE,* 50(6)**,** 2059-2071.

Friedman, S. P. (2005). Soil properties influencing apparent electrical conductivity: A review. *Computers and Electronics in Agriculture,* 46**,** 45-70.

Fritschen, L. J. & Simpson, J. R. (1989). Surface energy and radiation balance sysytems: General description and improvements. *Journal of Applied Meterology,* 28**,** 680-689.

Fritz, R. M., Malo, D. D., Schumacher, T. E., Clay, D. E., Carlson, C. G., Ellsbury, M. M. & Dalsted, K. J. (1999). Field comparison of two soil electrical conductivity measurement systems. In: Robert, P. C., Rust, R. H., Larson, W. E. (eds). *Proceedings of the fourth international conference on precision agriculture,* pp. 1210-1217. ASA, CSSA, SSSA, Madison, USA.

Fuchs, M. (1990). Infrared measurements of canopy temperature and detection of plant water stress. *Theoritical and Applied Climatology,* 42**,** 253-261.

Fuchs, M. & Tanner, C. B. (1966). Infrared thermometry of vegetation. *Agronomy Journal,* 58**,** 597-601.

Fuentes, S. (2005). Precision irrigation for grapevines (Vitis Vinifera L.) under RDI and PRD. Sydney, University of Western Sydney.

Fuentes, S., Conroy, J., Collins, M., Kelly, G. & Mora, R. (2004). A soil-plant-atmosphere approach to evaluate PRD on grapevines (Vitis Vinifera L. var Shiraz). *The Australian & New Zealand Grapegrower and Winemaker***,** 54-58.

Gardner, E.A. (1985). *Identification of Soils and Interpretation of Soil Data, Chapter: Soil Water,* Australian Society of Soil Science Inc, Qld Branch, Brisbane. pp. 197-234.

Gardner, B. F., Blad, B. L. & Watts, D. G. (1981). Plant and air temperatures in diffrentially irrigated corn. *Agricultural Meteorology,* 25**,** 207-217.

Gates, D. M. (1964). Leaf temperature and transpiration. *Agronomy Journal,* 56**,** 273-277.

Ghadiri, H., Connell, D. & Parker, R. (1999). Sorption-desorption and column leaching of strychnine with soil. *Australian Journal of Soil Research,* 38**,** 603-616.

Godwin, D. C., Jones, C. A., Ritchie, J. T., Vlek, P. L. G. & Youngdahl, L. G. (1984). The water and nitrogen components of the CERES models. *International Symposium on Minimum Data Sets for Agrotechnology Transfer.* Patancheru, India.

Gontia, N. K. & Tiwari, K. N. (2008). Development of crop water stress index of wheat crop for scheduling irrigation using infrared thermometry. *Agricultural water management,* 95**,** 1144-1152.

Grant, O. M., Tronina, L., Jones, H. G. & Chaves, M. M. (2006). Exploring thermal imaging variables for the detection of stress responses in grapevine under different irrigation regimes. *Journal of Experimental Botany,* 58**,** 815-825.

Greve, M. H., & Greve, M. B. (2004). Determining and representing width of soil boundaries using electrical conductivity and MultiGrid. *Computers & Geosciences*, 30, 569–578.

Hartsock, N. J., Mueller, T. G., Thomas, G. W., Barnhisel, R. I., Wells, K. L. &. Shearer, S. A. (2001). Soil electrical conductivity variability. In P.C. Robert et al. (ed.) *Proceedings of 5th International. Conference on Precision Agriculture,* Bloomington, MN. 16-19 July 2000. ASA, CSSA, and SSSA, Madison, WI.

Hatfield, J. L. (1990). *Methods of estimating evapotranspiration. In Irrigation of Agricultural Crops,* 435-474. eds. B. A. Stewart and D. R. Nielsen. Madison, American Society of Agronomy.

Havlin, J., Beaton, J., Tisdale, S. & Nelson, W. (Eds.) (1999). *Soil Fertility and Fertilizers,* New Jersey, USA, Prentice Hall.

Hedley, C. B., Yule, I. Y., Eastwood, C. R., Shepherd, T. G., & Arnold, G. (2004). Rapid identification of soil textural and management zones using electromagnetic induction sensing of soils. *Australian Journal of Soil Research,* 42(4), 389–400.

Heermann, D. F., Hoeting, J., Duke, H. R., Westfall, D. G., Buchleiter, G. W., Westra, P., Peairs, F. B. & Fleming, K. (2000). Irrigated Precision Farming for Corn Production. *Proceedings of Second International Conference on Geospatial Information in Agriculture and Forestry*, pp. 144-151, Lake Buena Vista, Florida.

Hipps, L. E., Ashrar, G. & Kanemasu, E. T. (1985). A theoritically based normalization of the environmental effects on foliage temperature. *Agricultural and Forest Meteorology,* 35**,** 113-122.

Hoffer, A. M. (1978). *Biological and physical considerations in applying computer-aided analysis techniques to remote sensor data, in Remote Sensing: The Quantitative Approach,* P.H. Swain and S.M. Davis (Eds), McGraw-Hill Book Company, pp.227-289.

Houghton, J. T., Ding, Y., Griggs, D. J., Noguer, M., van der Linden, P. J., Dai, X., Maskell, K. & Johnson, C. A. (2001). *Climate change 2001: the scientific basis*. Cambridge: Cambridge University Press.

Howell, T. A., Schneider, A. D. & Tolk, J. A. (1991). Sprinkler evaporation losses and efficiency. *In proceedings Central plains irrigation short course.* Manhattan.

Hsiao, T. C., Steduto, P. & Fereres, E. (2007). A systematic and quantitative approach to improve water use efficiency in agriculture. *Irrigation Science,* 25**,** 209-231.

Hunt, P. G., Bauer, P. J. & Matheny, T. A. (1997). Crop production in a wheat-cotton doublecrop rotation with conservation tillage. *Journal of Production Agriculture,* 10**,** 462-465.

Husband, N. D. S. & Monteith, J. L. (1986). Radiative surface temperature and energy balance of a wheat canopy. 1. Comparison of radiative and aerodynamic canopy temperature. *Boundary Layer Meteorology,* 36**,** 1-17.

Huth, N. I. & Poulton, P. L. (2007). An electromagnetic induction method for monitoring variation in soil moisture in agroforestry systems. *Australian Journal of Soil Research,* 45**,** 63-72.

Idso, S. B. (1982). Non water stressed baselines: A key to measuring and interpreting plant water stress. *Agricultural Meteorology,* 27**,** 59-70.

Idso, S. B., Jackson, R. D., Ehrler, W. L. & Mitchell, S. T. (1969). A method for determination of infrared emittance of leaves. *Ecology,* 50**,** 899-902.

Idso, S. B., Jackson, R. D. & Reginato, R. J. (1977). Remote sensing of crop yields. *Science,* 196.

Idso, S. B., Jackson, R. D., Pinter, P. J. J., Reginato, R. J. & Hatfield, J. L. (1981). Normalising the stress-degree-day parameter for environmental variablility. *Agricultural Meteorology,* 24**,** 45-55.

Isbell, R. F. (1996). *The Australian Soil Classification*. Collingwood, Victoria, CSIRO Publishing.

Jackson, R. D. (1982). Canopy temperature and crop water stress. *Advances in Irrigation,* 1**,** 43-80.

Jackson, R. D., Idso, S. B., Reginato, R. J. & Pinter, P. J. J. (1981). Canopy temperature as a drought stress indicator. *Water Resources Research,* 17**,** 1133-1138.

Jackson, R. D., Reginato, R. J. & Idso, S. B. (1977). Wheat canopy temperature: A practical tool for evaluating water requirements. *Water Resources Research,* 13**,** 651-656.

James, I. T., Waine, T. W., Brandley, R. I., Godwin, R. J. & Taylor, J. C. (2000). *A comparison between traditional methods and EMI scanning for determining soil textural boundaries*. Agenda 2000, Warwick, paper no. 00-PA-014.

Jarvis, A. J. & Davies, W. J. (1998). The coupled response of stomatal conductance to photosynthesis and transpiration. *Journal of Experimental Botany,* 49**,** 399-406.

Jaynes, D. B., Colvin, T. S., & Ambuel, J. (1995). Yield mapping by electromagnetic induction. In: Robert, P. C., Rust, R. H., Larson, W.E. (Eds.). *Proceedings of the Second International Conference on Site-specific Management for Agricultural Systems*, pp. 383–394. ASA-CSSA-SSSA, Madison, USA.

Johnson, C. K., Doran, J. W., Duke, H. R., Wienhold, B. J., Eskridge, K. M. & Shanahan, J. F. (2001). Field-scale electrical conductivity mapping for delineating soil condition. *Soil science society of America Journal,* 65**,** 1829-1837.

Jones, H. G. (1990a). Plant water relations and implications for irrigation scheduling. *Acta Horticulturae,* 278**,** 67-76.

Jones, H. G. (1990b). Physiological aspects of the control of water status in horticultural crops. *Horticultural science,* 25**,** 19-26.

Jones, H. G. (Ed.) (1992). *Plants and Microclimate*, Cambridge, Massachusetts, Cambridge University Press.

Jones, H. G. (1998). Stomatal control of photosynthesis and transpiration. *Journal of Experimental Botany,* 49**,** 387-398.

Jones, H. G. (1999a). Use of thermography for quantitative studies of spatial and temporal variation of stomatal conductance over leaf surfaces. *Plant, Cell and Environment,* 22**,** 1043-1055.

Jones, H. G. (1999b). Use of infrared thermometry for estimation of stomatal conductance as a possible aid to irrigation scheduling. *Agricultural and Forest Meteorology,* 95**,** 139-149.

Jones, H. G. (2004a). Irrigation scheduling: advantages and pitfalls of plant-based methods. *Journal of Experimental Botany,* 55**,** 2427-2436.

Jones, H. G. (2004b). Application of thermal imaging and infrared sensing in plant physiology and ecophysiology. *Advances in botanical research,* 41**,** 108-155.

Jones, H. G. & Leinonen, I. (2003). Thermal imaging for the study of plant water relations. *Journal of Agricultural Meteorology,* 59**,** 205-217.

Jones, H. G. & Schofield, P. (2008). Thermal and other remote sensing of plant stress. *General and applied plant physiology,* 34**,** 19-32.

Jones, H. G., Aikman, D. A. & Mcburney, T. (1997). Improvements to infrared thermometry for irrigation scheduling. *Acta Horticulturae* 449**,** 259-266.

Jones, H. G., Stoll, M., Santos, T., De Sousa, C., Chaves, M. M. & Grant, O. M. (2002). Use of infrared thermography for monitoring stomatal closure in the field: application to grapevine. *Journal of Experimental Botany,* 53**,** 2249-2260.

Jury, W. A., Gardner, W. R. and Gardner, W. H. (1991). *Soil Physics, 5th edn* (John Wiley and Sons, Inc.).

Kachanoski, R. G., Gregorich, E. G. & Van Wesenbeck, I. J. (1988). Estimating spatial variations of soil water content using non contacting electromagnetic inductive methods. *Canadian Journal of Soil Science,* 68**,** 715-722.

Kachanoski, R. G., De Jong, E. & Van Wesenbeck, I. J. (1990). Field scale patterns of soil water storage from non-contacting measurements of bulk electrical conductivity. *Canadian Journal of Soil Science,* 70**,** 537-541.

Karam, F., Lahoud, R., Massad, R., Kabalan, R., Breidi, J., Chalita, C. & Rouphael, Y. (2007). Evapotranspiration, seed yield and water use efficiency of drip irrigated sunflower under full and deficit irrigation conditions. *Agricultural Water Management,* 90**,** 213-223.

Khakural, B. R., Robert, P. C. & Hugins, D. R. (1998). Use of non-contacting electromagnetic inductive method for estimating soil moisture across a landscape. *Communications in soil science and plant analysis,* 29 (11-14)**,** 2055-2065.

Kijne, J. W., Barker, R. & Molden, D. (2003). *Water Productivity in Agriculture: Limits and Opportunities for Improvements*. Comprehensive Assessment of Water Management in Agriculture Series, No. 1. CABI Publishing: Wallingford, UK.

King, J. A. & Dampney, P. M. R. (2000). Electro-Magnetic Induction for measuring soil properties. *Aspects of Applied Biology, Remote sensing in agriculture,* 60**,** 247-252.

King, J. A., Dampney, P. M. R., Lark, M., Mayr, T. R. & Bradley, R. I. (2001). Sensing soil spatial variability by electromagnetic induction (EMI): It's potential in

precision farming. *Third European Conference on Precision Agriculture*. June, 18-20, Montepelier, France, pp.419-424.

Kirda, C., Moutonnet, P., Hera, C. & Nielsen, D. R. (Eds.) (1999). *Crop yield response to deficit irrigation*, Kluwer academic publishers.

Kirda, C. (2000). *Deficit irrigation scheduling based on plant growth stages showing water stress tolerance*. Deficit Irrigation Practices, Food and Agricultural Organisation Water Reports 22.

Kitchen, N. R., Sudduth, K. A. & Drummond, S. T. (1999). Soil electrical conductivity as a crop productivity measure for claypan soils. *Journal of Production Agriculture,* 12**,** 607-617.

Kitchen, N. R., Sudduth, K. A., Myers, D. B., Drummond, S. T. & Hong, S. Y. (2005). Delineating productivity zones on claypan soil fields using apparent soil electrical conductivity. *Computers and Electronics in Agriculture,* 46, 285-308.

Kizer, M. A., Elliott, R. L. & Stone, J. F. (1990). Hourly ET model calibration with eddy flux and energy balance data. *Journal of Irrigation and Drainage Engineering,* 116**,** 172-181.

Ko, J. & Piccinni, G. (2009). Corn yield responses under crop evapotranspiration-based irrigation management. *Agricultural Water Management,* 96**,** 799-808.

Kravchenko, A. N., Omonode, R., Bollero, G. A. & Bullock, D. G. (2002). Quantitative mapping of soil drainage classes using topographical data and soil electrical conductivity. *Soil science society of America Journal,* 66**,** 235-243.

Lee, X. (1998). On micrometerological observations of surface air exchange over all vegetation. *Agricultural and Forest Meteorology,* 91**,** 39-49.

Leinonen, I. & Jones, H. G. (2004). Combining thermal and visible imagery for estimating canopy temperature and identifying plant stress. *Journal of Experimental Botany,* 55**,** 1423-1431.

Leinonen, I., Grant, O. M., Tagliavia, C. P. P., Chaves, M. M. & Jones, H. G. (2006). Estimating stomatal conductance with thermal imagery. *Plant, Cell and Environment,* 29**,** 1508-1518.

Lenthe, J. H., Oerke, E. C. & Dehne, H. W. (2007). Digital infrared thermography for monitoring canopy health of wheat. *Precision Agriculture,* 8**,** 15-26.

Lesch, S. M. (2005). Sensor-directed response surface sampling designs for characterizing spatial variation in soil properties. *Computers and Electronics in Agriculture,* 46**,** 153-179.

Lesch, S. M., Corwin, D. L. & Robinson, D. A. (2005). Apparent soil electrical conductivity mapping as an agricultural management tool in arid zone soils. *Computers and Electronics in Agriculture,* 46, 351-378.

Li, S., Kang, S., Zhang, L., Li, F., Zhu, Z. & Zhang, B. (2008). A comparison of three methods for determining vineyard evapotranspiration in the arid desert regions of northwest China. *Hydrological processes,* 22**,** 4554-4564.

Liddiard, K. C. (2004). *The active microbolometer: a new concept in infrared detection.*. Proc. SPIE 5274, 227, Perth, Australia.

Liu, W. Z., Hunsaker, D. J., Li, Y. S., Xie, X. Q. & Wall, G. W. (2002). Interrelations of yield, evapotranspiration, and water use efficiency from marginal analysis of water production functions. *Agricultural Water Management,* 56**,** 143-151.

Mahan, J. R. & Yeater, K. Y. (2008). Agricultural applications of a low-cost infrared thermometer. *Computers and Electronics in Agriculture,* 64**,** 262-267.

Malone, R. W., Stewardson, D. J., Bonta, J. V. & Nelsen, T. (1999). Calibration and quality control of the Coshocton weighing lysimeters. *Transactions of the ASABE,* 42**,** 701-712.

Marek, T., Piccinni, G., Schneider, A., Howell, T. A., Jett, M. & Dusek, D. (2006). Weighing lysimeters for the determination of crop water requirements and crop coefficients. *Applied Engineering in Agriculture,* 22(6)**,** 851 - 856.

Martin, E. C., De Oliviera, A. S., Folta, A. D., Pegelow, E. J. & Slack, D. C. (2001). Development and testing of a small weighable lysimeter system to assess water use by shallow-rooted crops. *Transactions of the ASAE,* 44**,** 71-78.

Massman, W. J. (2000). A simple method for estimating frequency response corrections for eddy covariance systems. *Agricultural and Forest Meteorology,* 104**,** 185-198.

Massman, W. J. & Lee, X. (2002). Eddy covariance flux corrections and uncertainties in long term studies of carbon and energy exchanges. *Agricultural and Forest Meteorology,* 113**,** 121-144.

Mcbride, R. G. (2003). Relationships between soil properties and yield variability and the potential for establishing management zones for site-specific management in North Carolina. *Soil Science.* North Carolina, North Carolina State University.

Mckenzie, R. C., Chomistek, W. & Clark, N. F. (1989). Conversion of electromagnetic inductance readings to saturated paste extract values in soils for different

temperature, texture and moisture conditions. *Canadian Journal of Soil Science,* 69**,** 25-32.

McNeill, J. D. (1980a). *Electrical conductivity of soil and rocks*. Technical Note TN-5 (Geonics Ltd., Mississauga, Ontario, Canada).

McNeill, J. D. (1980b). *Electromagnetic terrain conductivity measurement at low induction numbers*. Technical Note TN-6 (Geonics Ltd., Mississauga, Ontario, Canada).

McNeill, J. D. (1992). Rapid, accurate mapping of soil salinity by electromagnetic ground conductivity meters. *In: Advances in Measurements of Soil Physical Properties: Bringing Theory into Practice*. SSSA Special Publication 30 (ASA, CSSA, SSSA, Madison, WI, USA), pp. 209–229.

Mendez-Barroso, L. A., Garatuza-Payan, J. & Vivoni, E. R. (2008). Quantifying water stress on wheat using remote sensing in the Yaqui valley, Sonora, Mexico. *Agricultural Water Management,* 95**,** 725-736.

Monteith, J. L. & Unsworth, M. (Eds.) (1990). *Principles of environmental physics*.

Morgan, C. L. S., Norman, J. M., Wolkowski, R. P., Lowery, B., Morgan, G. D., & Schuler, R. (2000). Two approaches to mapping plant available water: EM-38 measurements and inverse yield modeling. In: Robert, P. C., Rust, R. H., Larson, W.E. (Eds.). *Proceedings of the 5th International Conference on Precision agriculture*, p. 14. ASA, CSSA, SSSA, Madison, USA.

Morgan, C. L. S., Norman, J. M. & Lowery, B. (2003). Estimating plant available water across a field with an inverse yield model. *Soil science society of America Journal,* 67**,** 620-629.

Nugteren, W. A., Malo, D. D., Schumacher, T. E., Schumacher, J. A., Carlson, C. G., Clay, D. E., Clay, S. A. and Dalsted, K. J. (2000). Hillslope chronosequence of electromagnetic induction readings as influenced by selected soil properties. *In: Proceedings of the 5th International Conference on Precision Agriculture,* edited by P. C. Roberts, R. H. Rust and W. E. Larson (ASA, CSSA, SSSA, Madison, WI, USA), Published on CD-ROM, p. 8.

Payero, J. O. & Irmak, S. (2008). Construction, installation and performance of two repacked weighing lysimeters. *Irrigation Science,* 26**,** 191-202.

Paw U, K. T., Qiu, J., Su, H. B., Watanabe, T. and Brunet, Y. (1995). Surface renewal analysis: A new method to obtain scalar fluxes without velocity data. *Agricultural and Forest Meteorology*, 74(1-2), 119-137.

Paz, J. O., Batchelor, W. D., Colvin, T. S., Logsdon, S. D., Kaspar, T. C. & Karlen, D. L. (1998). Analysis of water stress effects causing spatial yield variability in soybeans. *Transactions of the ASAE,* 41(5)**,** 1527-1534.

Paz, J. O., Batchelor, W. D., Tylka, G. L. & Hartzler, R. G. (2001). A modelling approach to quantify the effects of spatial soybean yield limiting factors. *Transactions of the ASAE,* 44(5)**,** 1329-1334.

Petersen, K. L., Fuchs, M., Moreshet, S., Cohen, Y. & Sinoquet, H. (1992). Computing transpiration of sunlit and shaded cotton foliage under variable water stress. *Agronomy Journal,* 84**,** 91-97.

Pinter Jr, P. J., Fry, K. E., Guinn, G. & Mauney, J. R. (1983). Infrared thermometry: A remote sensing technique for predicting yield in water-stressed cotton. *Agricultural Water Management,* 6**,** 385-395.

Plant, R. E. (2001). Site-specific management: the application of information technology to crop production. *Computers and Electronics in Agriculture,* 30**,** 9-29.

Prueger, J. H., Hatfield, J. L., Aase, J. K. & Pikul, J. L. (1997). Bowen-ratio comparisons with lysimeter evapotranspiration. *Agronomy journal,* 89**,** 730-736.

Ratliff, L. F., Ritchie, J. T. & Cassel, D. K. (1983). A survey of field-measured limits of soil water availability and related to laboratory-measured properties. *Soil science society of America journal,* 47**,** 770-775.

Reedy, R. C. & Scanlon, B. R. (2003). Soil water content monitoring using electromagnetic induction. *Journal of Geotechnical and Geoenvironmental Engineering,* 129**,** 1-12.

Rees, W. G. (Ed.) (2001). *Physical Principles of Remote Sensing,* Cambridge, Mass, Cambridge University Press.

Remorini, D. & Massai, R. (2003). Comparison of water status indicators for young peach trees. *Irrigation Science,* 22**,** 39-46.

Rhoades, J. D., Manteghi, N. A., Shouse, P. J. & Alves, W. J. (1989). Soil electrical conductivity and soil salinity: New formulations and calibrations. *Soil science society of America Journal,* 53**,** 433-439.

Rhoades, J. D. (1992). Instrumental field methods of salinity appraisal. *In: Advances in Measurements of Soil Physical Properties: Bringing Theory into Practice*. SSSA Special Publication 30 (ASA, CSSA, SSSA, Madison, WI, USA), pp. 231–248.

Rhoades, J. D., Chanduvi, F. & Lesch, S. M. (1999a). *Soil salinity assessment: methods and interpretation of electrical conductivity measurements.* FAO Irrigation and

Drainage Paper no. 57. Food and Agriculture Organization of the United Nations, Rome, Italy, 1–150.

Rhoades, J. D., Corwin, D. L. & Lesch, S. M. (1999b). *Geospatial measurements of soil electrical conductivity to assess soil salinity and diffuse salt loading from irrigation*. p. 197–215. *In* D.L. Corwin (ed.) Assessment of non-point source pollution in the vadose zone. Geophysical Monogr. 108. Am. Geophysical Union, Washington, DC.

Richards, L. A. (Ed.) (1954). *Diagnostic and improvement of saline and alkali soils*. U.S. Dept of Agriculture Handbook No. 60. (U.S. Govt. Print. Office: Washington, DC).

Ritchie, J. T. (1981). Soil water availability. *Plant and Soil,* 58**,** 81-96.

Rodriguez, D., Sadras, V. O., Christensen, L. K. & Belford, R. (2005). Spatial assessment of the physiological status of wheat crops as affected by water and nitrogen supply using infrared thermal imagery. *Australian Journal of Agricultural Research,* 56**,** 983-993.

Sanders, J., Jim, H., Kvien, C. & Stuart, P. (2000). Analysis of the benefits of precision irrigation in South Georgia. http://nespal.cpes.peachnet.edu/agwateruse/initiative/pivot analysis.pdf. Viewed on 10.7.2006.

Sela, E., Cohen, Y., Alchanatis, V., Saranga, Y., Cohen, S., Moller, M., Meron, M., Bosak, A., Tsipris, J. & Orolov, V. (2007). Thermal imaging for estimating and mapping crop water stress in cotton. In: J. V. Stafford (ed.), *European Conference in Precision Agriculture 2007*, Skiathos, Greece, pp. 365-371.

Sheets, K. R. & Hendrickx, J. M. H. (1995). Noninvasive soil water content measurement using electromagnetic induction. *Water Resources Research,* 31**,** 2401-2409.

Sinclair, T. R., Tanner, C. B. & Bennett, J. M. (1984). Water-use efficiency in crop production. *BioScience,* 34, 36-40.

Snedecor, G. W. & Cochran, W. G. (1989). *Statistical Methods*. Iowa State University Press, Ames, Iowa, USA, pp. 503.

Snyder, R. L., Spano, D., Duce, P., Paw U, K. T. & Rivera, M. (2008). Surface renewal estimation of pasture evapotranspiration. *Journal of Irrigation and Drainage Engineering,* 134(6), 716-721.

Sudduth, K., Kitchen, J. & Drummond, S. (1999). Soil conductivity sensing on clay pan soils: Comparison of Electromagnetic Induction and direct methods. *Proc 4th International conference on Precision Agriculture*. pp. 979-990. ASA, CSSA and SSSA, Madison, USA.

Sudduth, K. A., Drummond, S., T. & Kitchen, N. R. (2001). Accuracy issues in electromagnetic induction sensing of soil electrical conductivity for precision agriculture. *Computers and Electronics in Agriculture,* 31**,** 239-264.

Sullivan, D. G., Fulton, J. P., Shaw, J. N. & Bland, G. (2007). Evaluating the sensitivity of an unmanned thermal infrared aerial system to detect water stress in a cotton canopy. *Transactions of the ASABE* 50(6)**,** 1955-1962.

Sutherland, R. A. (1986). Broadband and spectral emissivities (2-18 mm) of some natural soils and vegetation. *Journal of Atmospheric and Ocean Technology,* 3**,** 199-202.

Tennakoon, S. B. & Hulugalle, N. R. (2006). Impact of crop rotation and minimum tillage on water use efficiency of irrigated cotton in a vertisol. *Irrigation science,* 25**,** 45-52.

Tennakoon, S. B. & Milroy, S. P. (2000). Evaluation of crop water use efficiency and farm level irrigation efficiency of irrigated cotton farms in northern NSW and southern Queensland. IN CONNELLAN, G. J. (Ed. *Irrigation Association of Australia.* Melbourne, Victoria, Australia.

Tolk, J. A., Howell, T. A. & Evett, S. R. (2005). An evapotranspiration research facility for soil- plant-environment interactions. *Applied Engineering in Agriculture,* 21(6)**,** 993-998.

Torre-Neto, A., Schueller, J. K. & Haman, D. (2001). Automated system for variable rate micro-sprinkler irrigation in citrus: A demonstration unit. *Third European Conference on Precision Agriculture*. June, 18-20, Montpelier, France, pp.725-730.

Triantafilis, J., & Lesch, S. M. (2005). Mapping clay content variation using electromagnetic induction techniques. Computers and Electronics in Agriculture, 46, 203–237.

Triantafilis, J., Laslett, G. M. & McBratney, A. B. (2000). Calibrating an electromagnetic induction instrument to measure salinity in soil under irrigated cotton. *Soil Science Society of America Journal*, 64, 1009–1017.

Triantafilis, J., Odeh, I. O. A., Jarman, A. L., Short, M. G. & Kokkoris, E. (2004). Estimating and mapping deep drainage risk at the district level in the lower Gwydir and Macquarie valleys, Australia. *Australian Journal of Experimental Agriculture*, 44, 893–912.

Tyagi, N. K., Sharma, D. K. & Luthra, S. K. (2000). Determination of evapotranspiration and crop coefficient of rice and sunflower with lysimeter. *Agricultural Water management*.

Van Bavel, C. H. M. (1961). Lysimetric measurements of evapotranspiration rates in the eastern United States. *Soil Science Society of America Journal,* 25**,** 138-141.

Waine, T. W., Blackmore, B. S. & Godwin, R. J. (2000). Mapping available water content and estimating soil textural class using electromagnetic induction. *European Society of Agricultural Engineers Paper No. 00-SW-044*, AgEng2000 Warwick, UK.

Wang, H., Yi, X., Huang, G., Xiao, J., Li, X. and Chen, S. (2004). IR microbolometer with self-supporting structure operating at room temperature. *Infrared Physics and Technology,* 45(1), 53-57.

Wang, X., Horiguchi, I. & Machimura, T. (1994). Emissivities in the window region for plant canopies and the effects of plant cover ratio and others. *Journal of Agricultural Meteorology,* 50**,** 177-183.

Wanjura, D. F. & Upchurch, D. R. (2000). Canopy temperature characterizations of corn and cotton water status. *Transactions of the ASAE,* 43(4)**,** 867-875.

Wanjura, D. F. & Upchurch, D. R. (2002). Water status response of corn and cotton to altered irrigation. *Irrigation science,* 21**,** 45-55.

Wanjura, D. F., Upchurch, D. R. & Mahan, J. R. (2006). Behavior of temperature-based water stress indicators in Biotic-controlled irrigation. *Irrigation science,* 24**,** 223-232.

Williams, B. G. & Hoey, D. (1987). The use of electrical induction to detect the spatial variabilty of the salt and clay contents of soils. *Australian Journal of Soil Research,* 25**,** 21-27.

Wittich, K.-P. (1997). Some simple relationships between land -surface emissivity, greenness and the plant cover fraction for use in satellite remote sensing. *International Journal of Biometeorology,* 41**,** 58-64.

Xu, C. Y. & Chen, D. (2005). Comparison of seven models for estimation of evapotranspiration and groundwater recharge using lysimeter measurement data in Germany. *Hydrological processes,* 19**,** 3717-3734.

Young, M. H., Wierenga, P. J. & Mancino, C. F. (1997). Monitoring near surface soil water storage in Turfgrass using time domain reflectometry and weighing lysimetry. *Soil Science Society of America Journal,* 61**,** 1138-1146.

Yuan, G., Luo, Y., Sun, X. & Tang, D. (2004). Evaluation of a crop water stress index for detecting water stress in winter wheat in the North China Plain. *Agricultural Water Management,* 64**,** 29-40.

Appendix A1

Sensitivity analysis of thermal image processing

In various chapters of this thesis, each thermal image was analysed with the help of Image Processor Pro II software to derive average canopy temperature. The purpose of this appendix is to undertake a sensitivity analysis to determine if the method of image processing used introduces any bias in the determination of canopy temperature from the thermal image. For this sensitivity analysis, two methods have been used for both cotton and wheat. For method 1, a large rectangular area (~49447 pixels) was chosen within the thermal image to derive the average canopy temperature for the entire thermal image. For method 2, five smaller rectangular areas (~3290 pixels) were selected within the large rectangle used for method 1 to derive average canopy temperature for each rectangle. Average canopy temperature from each of the five rectangular areas was then averaged to obtain the average canopy temperature for the whole thermal image. With both methods, visual image were consulted in deciding the size of rectangular area for the analysis to exclude areas of thermal image that may include non-plant material or other background objects. Average canopy temperature was estimated with each method on five separate occasions (as replicates) for both cotton and wheat.

Detailed information on selection of area within the image with both methods and crops are shown in Figures A1.1 and A1.2. Average canopy temperatures obtained with both methods for cotton and wheat are given in Table A1.1. Paired t-test used to compare two methods of image analysis showed that the difference between the two methods was small (0.1-0.3 °C) although for cotton method 1 significantly gave slightly higher canopy temperature than method 2. On the basis of this sensitivity analysis it is concluded that small differences may exist between various methods of image analysis, but it is unlikely influence average canopy temperature significantly.

Table A1. 1 Comparison of average canopy temperature obtained with two methods of image analysis for cotton and wheat in the field.

Crop	Average canopy temperature (°C)	
	Method 1	Method 2
Cotton	31	30.6
	25.2	25.0
	30.2	29.9
	28.6	28.4
	28.3	28.0
Mean	28.7	28.4
Wheat	16.7	16.6
	17.5	17.0
	27	27.1
	22.8	22.6
	26.6	26.6
Mean	22.1	22.0

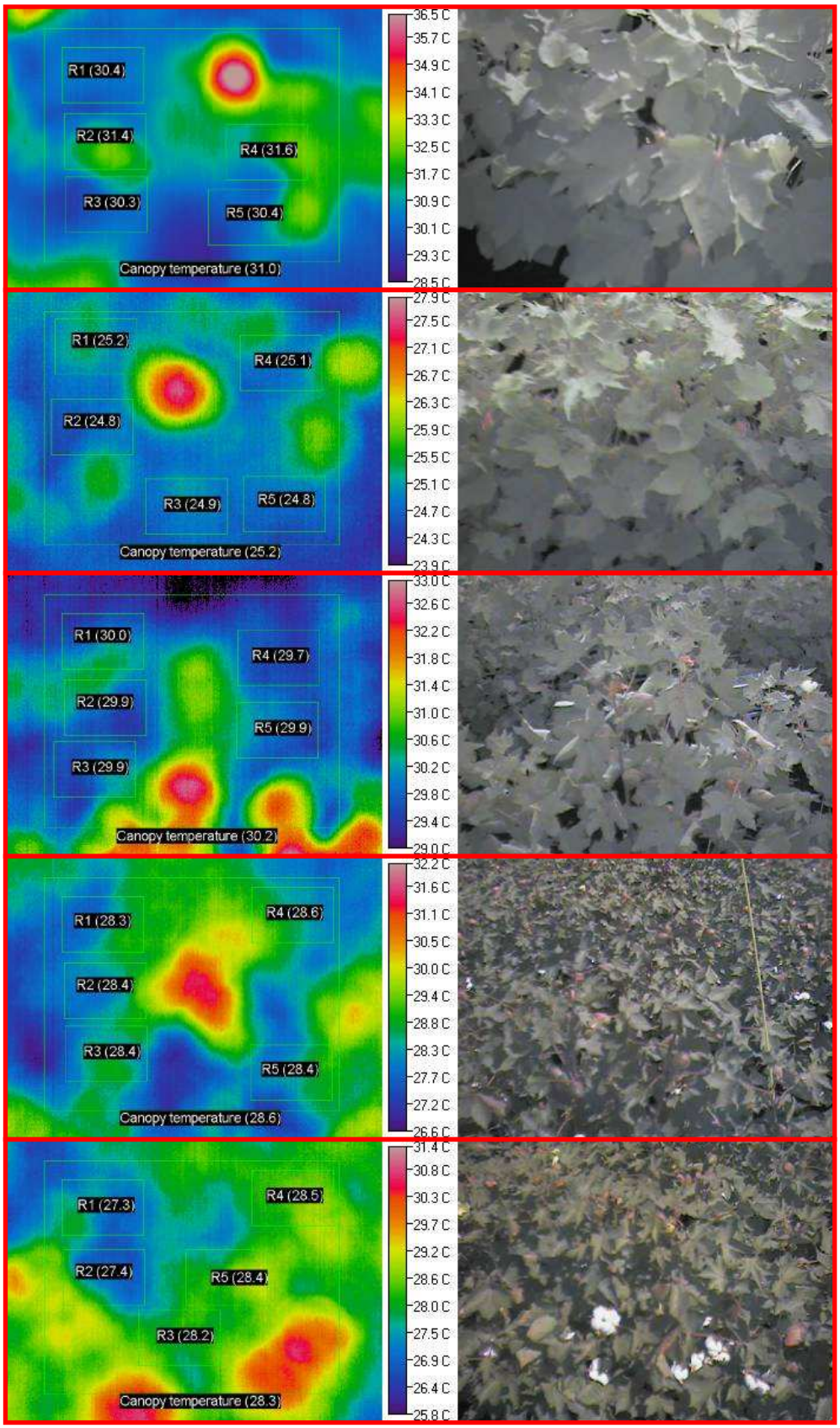

Figure A1. 1 Derivation of average canopy temperature for cotton from processing of thermal images with two different methods on five separate occasions. Numbers in parenthesis are temperature (°C) for one large and five small rectangles selected within the thermal image (left). Visual image corresponding with the thermal image is shown on right.

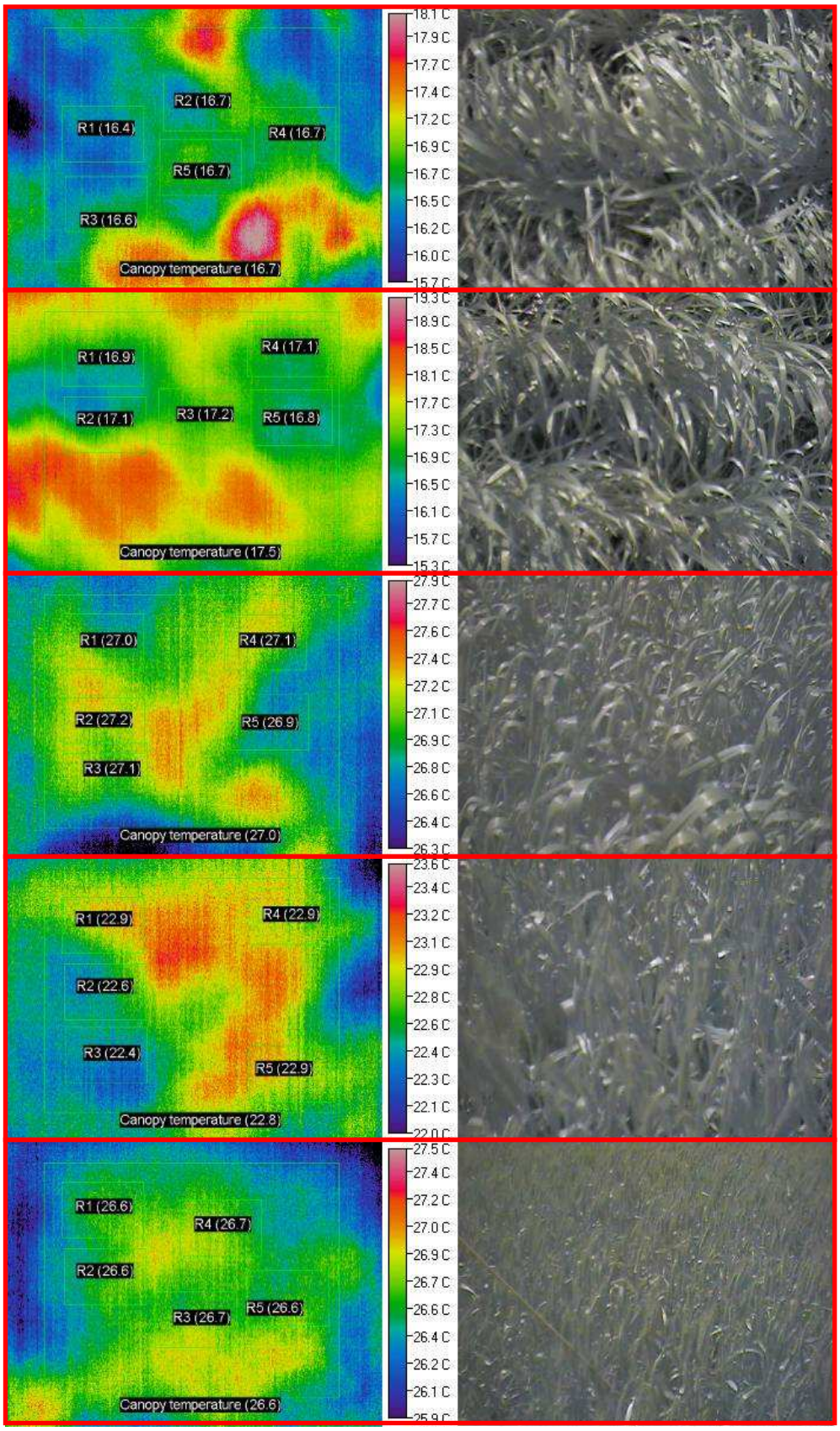

Figure A1. 2 Derivation of average canopy temperature for wheat from processing of thermal images with two different methods on five separate occasions. Numbers in parenthesis are temperature (°C) for one large and five small rectangles selected within the thermal image (left). Visual image corresponding with the thermal image is shown on right.